Arthritis & Rheumatology

An Official Journal of the American College of Rheumatology
www.arthritisrheum.org and wileyonlinelibrary.com

Arthritis & Rheumatology

An Official Journal of the American College of Rheumatology
www.arthritisrheum.org and wileyonlinelibrary.com

VOLUME 74 • October 2022 • NO. 10

Systemic Lupus Erythematosus

Sjögren's Syndrome

Corrigendum

Autoimmunity

Letters

Cover image: The figure on the cover (from Xu et al, pages 1699–1705) shows submandibular salivary gland biopsy results in NOD/Ltj mice that received combined anti-CD4 antibody and self antigen peptide Ro480. Hematoxylin and eosin staining shows that mice treated with anti-CD4 antibody and Ro480 had much fewer and smaller infiltrations in the inflamed salivary glands.

In this Issue

Highlights from this issue of *A&R* | **By Lara C. Pullen, PhD**

Walking for Exercise Benefits Individuals with Knee Osteoarthritis

In this issue, Lo et al (p. 1660) report that, in individuals with knee osteoarthritis (OA), walking for exercise was associated with less frequent development of knee pain. The observed changes included those that were consistent with both structural modifications and symptom improvements. This study is the first to explore the effects of walking stratified by knee static alignment, and researchers found that walkers with varus alignment developed new frequent knee pain less frequently when compared to non-walkers in this group.

p. 1660

The observational study included 1,212 self-selected walkers (73% of whom reported walking for exercise) ages 50 years and older with radiographic knee OA (45% male). The mean ± SD age was 63.2 ± 7.9 years, and the mean ± SD body mass index was 29.4 ± 4.6 kg/m². The study retrospectively ascertained walking exposure but did not address other exercise.

The researchers documented Kellgren/Lawrence radiographic knee OA severity grades of 2 (64% of participants), 3 (29% of participants), and 4 (7% of participants). Two-thirds of participants had some medial joint space narrowing (JSN), and one-third reported having frequent knee symptoms. In participants who walked, odds of new frequent knee pain had decreased 40% when compared to non-walkers, with an adjusted odds ratio of 0.6 (95% CI 0.4–0.8). Progression of medial JSN was less common in those who walked for exercise compared to non-walkers.

Current guidelines advocate walking as beneficial for individuals with knee OA. The new findings offer further hope that walking may serve as an inexpensive intervention for this most common type of arthritis. The authors conclude that health care providers should encourage patients with knee OA to walk for exercise. They also suggest that future studies should evaluate whether walking for exercise could be disease-modifying.

Machine Learning Identifies Common Signature for Anti–SSA/Ro 60 Antibody Expression

In this issue, Foulquier et al (p. 1706) report that anti–Ro 60+ patients present with a specific inflammatory signature regardless of their disease type. The team used dimensionality reduction approaches to machine learning and high throughput multiomics data to extract this robust signature specific to anti–Ro 60+ patients and found that the identified signature remained stable over time and was not influenced by treatment. The investigators reported that anti–Ro 60+ patients presented with hypergammaglobulinemia and an association with other autoantibodies (anti–Ro 52, anti-SSB, and rheumatoid factor). Their analysis revealed a significant difference in interferon Z scores between anti–Ro 60+ patients and anti–Ro 60- patients with SS, SLE, and undifferentiated connective tissue disease. Also, in all diseases studied, the transcript Z scores of 3 genes (*ATP10*, *MX1*, and

p. 1706

PARP14) were clearly higher in anti–Ro 60+ patients compared to anti–Ro 60− patients. All observed differences were significant except for patients with mixed connective tissue disease. This difference meant these 3 transcripts constituted a clear signature. Moreover, the signature carried by *ATP10A* appeared to be specific to anti–Ro 60+ patients.

To control the interferon signature in anti–Ro 60+ patients with autoimmune diseases, rheumatologists must break the continual turnover of Ro 60–specific clones that seem to drive lifelong Ro 60 humoral autoimmunity. When the researchers performed a reactome pathway analysis of the 33 differentially expressed and methylated genes, they found a link between anti–Ro 60+ antibodies and interferon signature, cytokine secretions, and interferon regulatory factor 7, which were associated with Toll-like receptor signaling. The new findings suggest that clinicians should consider a dual therapeutic approach

Figure 1. Venn diagram showing gene overlap according to the different omics data analyses conducted using machine learning (RNA-Seq, DNA methylation, and single-nucleotide polymorphisms [SNPs]) to discriminate anti–Ro 60+ patients from anti–Ro 60– patients.

that targets both Ro-associated RNAs and anti–Ro 60 autoantibodies.

No Malignancy Increase with Tofacitinib in Real-World Setting

Tofacitinib inhibits JAK1 and JAK3, both enzymes involved in the activation of the JAK/signal transducer and activator of transcription signaling pathway. The ORAL Surveillance trial, a large phase IIIb and IV post-marketing trial required by the US Food and Drug Administration, indicated that twice daily dosages of tofacitinib at both 5 mg and 10 mg were associated with an increased risk of malignancy, excluding nonmelanoma skin cancer (NMSC). In contrast, a meta-analysis of 6 phase II, 6 phase III, and 2 long-term extension studies found that the incidence rate of malignancies, excluding NMSC, among patients treated with tofacitinib was consistent with the expected range of patients with moderate-to-severe rheumatoid arthritis (RA).

p. 1648

In this issue, Khosrow-Khavar et al (p. 1648) report that their analysis of RA patients treated in a real-world setting revealed no evidence of an increased risk of malignancy development with tofacitinib therapy, compared to tumor necrosis factor inhibitor therapy. The authors note, however, that since the mean follow-up time in their study was <1 year, their results cannot rule out the possibility of an increase in risk that might accrue with a longer duration of treatment with tofacitinib.

The investigators analyzed data from 3 US insurance claims databases encompassing RA patients. The large multi-database cohort study included 83,295 patients, 10,504 of whom received treatment with tofacitinib. The authors note that the difference in findings between the ORAL Surveillance trial and the current study may stem from the fact that the current study documented cancer rates in a real-world evidence cohort that included all RA patients treated in routine care. In contrast, the ORAL Surveillance trial focused on patients ≥50 years of age who had ≥1 risk factor for cardiovascular disease as well as a history of treatment with methotrexate.

Journal Club

A monthly feature designed to facilitate discussion on research methods in rheumatology.

The Relationship of Pain Reduction with Prevention of Knee Replacement Under Dynamic Intervention Strategies

Jafarzadeh et al, *Arthritis Rheumatol* 2022;74:1668–1675

Knee replacement rates have been increasing exponentially in the US and are straining the Medicare budget. In this issue, Jafarzadeh et al asked whether new effective treatments for OA would reduce these rates and, if so, by how much? Effects of new treatments on knee replacement rates usually cannot be estimated accurately from trial data. Trials require a large sample size to detect clinically meaningful changes in the risk of a knee replacement and are often too costly to conduct. Further, trials tend to incorporate only short-term follow-up, and knee replacements are long-term outcomes. They usually study static interventions, in which participants are assumed to follow their assigned treatment. Changing disease status or patient characteristics may require treatment modification so that baseline treatment assignment may not adequately represent later treatment. The authors sought an approach that enables study of a dynamic intervention strategy, e.g., when knee pain level reaches or exceeds a threshold. Advances in causal inference methodology can address the effects of changing treatments on such outcomes as knee replacement in an analysis of longitudinal data from observational studies.

In an analysis of data from the Osteoarthritis Initiative (OAI), the investigators used a novel method that measures causal effect of a longitudinal time-varying intervention strategy, quantified by a measure referred to as the modified treatment policy (an alternative measure to average treatment effect), to accommodate realistic dynamic interventions that adapt to a patient's evolving characteristics. Modified treatment policy measures the difference in mean or probability of an outcome occurrence if a participant receives a series of treatments based on his/her evolving characteristics, compared to no treatment. This method allows for emulation of a sequence of trials as if randomization is repeated at every OAI study visit, reassigning participants to a different treatment most appropriate to their evolved characteristics.

Findings from this emulated longitudinal trial suggest that a dynamic intervention strategy in which reducing knee pain by 1 unit (0–20 scale) whenever knee pain level reached or exceeded 5 on the WOMAC Index pain subscale resulted in reducing the risk of knee replacement from 6.3% to 5.8% in painful knees.

Questions

1. What are the challenges of studying long-term outcomes in chronic conditions?

2. Why is it necessary to consider a dynamic intervention strategy rather than a static intervention strategy?

3. What are the advantages of post-baseline reassignment of participants to a different treatment level that are made possible by this approach?

4. What are the advantages and disadvantages of estimating treatment effect by using a modified treatment policy, compared to approaches that estimate an average treatment effect for static treatments?

A12

In this Issue

Highlights from this issue of *A&R* | By Lara C. Pullen, PhD

Walking for Exercise Benefits Individuals with Knee Osteoarthritis

In this issue, Lo et al (p. 1660) report that, in individuals with knee osteoarthritis (OA), walking for exercise was associated with less frequent development of

p. 1660

knee pain. The observed changes included those that were consistent with both structural modifications and symptom improvements. This study is the first to explore the effects of walking stratified by knee static alignment, and researchers found that walkers with varus alignment developed new frequent knee pain less frequently when compared to non-walkers in this group.

The observational study included 1,212 self-selected walkers (73% of whom reported walking for exercise) ages 50 years and older with radiographic knee OA (45% male). The mean ± SD age was 63.2 ± 7.9 years, and the mean ± SD body mass index was 29.4 ± 4.6 kg/m^2. The study retrospectively ascertained walking exposure but did not address other exercise.

The researchers documented Kellgren/Lawrence radiographic knee OA severity grades of 2 (64% of participants), 3 (29% of participants), and 4 (7% of participants). Two-thirds of participants had some medial joint space narrowing (JSN), and one-third reported having frequent knee symptoms. In participants who walked, odds of new frequent knee pain had decreased 40% when compared to non-walkers, with an adjusted odds ratio of 0.6 (95% CI 0.4–0.8). Progression of medial JSN was less common in those who walked for exercise compared to non-walkers.

Current guidelines advocate walking as beneficial for individuals with knee OA. The new findings offer further hope that walking may serve as an inexpensive intervention for this most common type of arthritis. The authors conclude that health care providers should encourage patients with knee OA to walk for exercise. They also suggest that future studies should evaluate whether walking for exercise could be disease-modifying.

Machine Learning Identifies Common Signature for Anti–SSA/Ro 60 Antibody Expression

In this issue, Foulquier et al (p. 1706) report that anti–Ro 60+ patients present with a specific inflammatory signature regardless of their disease type. The team used

p. 1706

dimensionality reduction approaches to machine learning and high throughput multiomics data to extract this robust signature specific to anti–Ro 60+ patients and found that the identified signature remained stable over time and was not influenced by treatment. The investigators reported that anti–Ro 60+ patients presented with hypergammaglobulinemia and an association with other autoantibodies (anti–Ro 52, anti-SSB, and rheumatoid factor). Their analysis revealed a significant difference in interferon Z scores between anti–Ro 60+ patients and anti–Ro 60- patients with SS, SLE, and undifferentiated connective tissue disease. Also, in all diseases studied, the transcript Z scores of 3 genes (*ATP10*, *MX1*, and

PARP14) were clearly higher in anti–Ro 60+ patients compared to anti–Ro 60− patients. All observed differences were significant except for patients with mixed connective tissue disease. This difference meant these 3 transcripts constituted a clear signature. Moreover, the signature carried by *ATP10A* appeared to be specific to anti–Ro 60+ patients.

To control the interferon signature in anti–Ro 60+ patients with autoimmune diseases, rheumatologists must break the continual turnover of Ro 60–specific clones that seem to drive lifelong Ro 60 humoral autoimmunity. When the researchers performed a reactome pathway analysis of the 33 differentially expressed and methylated genes, they found a link between anti–Ro 60+ antibodies and interferon signature, cytokine secretions, and interferon regulatory factor 7, which were associated with Toll-like receptor signaling. The new findings suggest that clinicians should consider a dual therapeutic approach
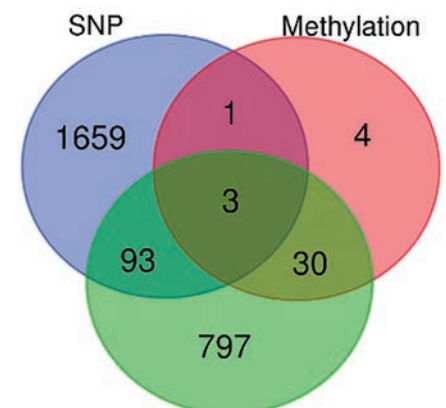

Figure 1. Venn diagram showing gene overlap according to the different omics data analyses conducted using machine learning (RNA-Seq, DNA methylation, and single-nucleotide polymorphisms [SNPs]) to discriminate anti–Ro 60+ patients from anti–Ro 60– patients.

that targets both Ro-associated RNAs and anti–Ro 60 autoantibodies.

No Malignancy Increase with Tofacitinib in Real-World Setting

Tofacitinib inhibits JAK1 and JAK3, both enzymes involved in the activation of the JAK/signal transducer and activator of transcription signaling pathway. The ORAL

p. 1648 Surveillance trial, a large phase IIIb and IV post-marketing trial required by the US Food and Drug Administration, indicated that twice daily dosages of tofacitinib at both 5 mg and 10 mg were associated with an increased risk of malignancy, excluding nonmelanoma skin cancer (NMSC). In contrast, a meta-analysis of 6 phase II, 6 phase III, and 2 long-term extension studies found that the incidence rate of malignancies, excluding NMSC, among patients treated with tofacitinib was consistent with the expected range of patients with moderate-to-severe rheumatoid arthritis (RA).

report that their analysis of RA patients treated in a real-world setting revealed no evidence of an increased risk of malignancy development with tofacitinib therapy, compared to tumor necrosis factor inhibitor therapy. The authors note, however, that since the mean follow-up time in their study was <1 year, their results cannot rule out the possibility of an increase in risk that might accrue with a longer duration of treatment with tofacitinib.

The investigators analyzed data from 3 US insurance claims databases encompassing RA patients. The large multi-database cohort study included 83,295 patients, 10,504 of whom received treatment with tofacitinib. The authors note that the difference in findings between the ORAL Surveillance trial and the current study may stem from the fact that the current study documented cancer rates in a real-world evidence cohort that included all RA patients treated in routine care. In contrast, the ORAL Surveillance trial focused on patients ≥50 years of age who had ≥1 risk factor for cardiovascular disease as well as a history of treatment with methotrexate.

Journal Club

A monthly feature designed to facilitate discussion on research methods in rheumatology.

The Relationship of Pain Reduction with Prevention of Knee Replacement Under Dynamic Intervention Strategies

Jafarzadeh et al, *Arthritis Rheumatol* 2022;74:1668–1675

Knee replacement rates have been increasing exponentially in the US and are straining the Medicare budget. In this issue, Jafarzadeh et al asked whether new effective treatments for OA would reduce these rates and, if so, by how much? Effects of new treatments on knee replacement rates usually cannot be estimated accurately from trial data. Trials require a large sample size to detect clinically meaningful changes in the risk of a knee replacement and are often too costly to conduct. Further, trials tend to incorporate only short-term follow-up, and knee replacements are long-term outcomes. They usually study static interventions, in which participants are assumed to follow their assigned treatment. Changing disease status or patient characteristics may require treatment modification so that baseline treatment assignment may not adequately represent later treatment. The authors sought an approach that enables study of a dynamic intervention strategy, e.g., when knee pain level reaches or exceeds a threshold. Advances in causal inference methodology can address the effects of changing treatments on such outcomes as knee replacement in an analysis of longitudinal data from observational studies.

In an analysis of data from the Osteoarthritis Initiative (OAI), the investigators used a novel method that measures causal effect of a longitudinal time-varying intervention strategy, quantified by a measure referred to as the modified treatment policy (an alternative measure to average treatment effect), to accommodate realistic dynamic interventions that adapt to a patient's evolving characteristics. Modified treatment policy measures the difference in mean or probability of an outcome occurrence if a participant receives a series of treatments based on his/her evolving characteristics, compared to no treatment. This method allows for emulation of a sequence of trials as if randomization is repeated at every OAI study visit, reassigning participants to a different treatment most appropriate to their evolved characteristics.

Findings from this emulated longitudinal trial suggest that a dynamic intervention strategy in which reducing knee pain by 1 unit (0–20 scale) whenever knee pain level reached or exceeded 5 on the WOMAC Index pain subscale resulted in reducing the risk of knee replacement from 6.3% to 5.8% in painful knees.

Questions

1. What are the challenges of studying long-term outcomes in chronic conditions?

2. Why is it necessary to consider a dynamic intervention strategy rather than a static intervention strategy?

3. What are the advantages of post-baseline reassignment of participants to a different treatment level that are made possible by this approach?

4. What are the advantages and disadvantages of estimating treatment effect by using a modified treatment policy, compared to approaches that estimate an average treatment effect for static treatments?

Clinical Connections

In Vivo Generation of SSA/Ro Antigen–Specific Regulatory T Cells Improves Experimental Sjögren's Syndrome in Mice

CORRESPONDENCE
Wanjun Chen, MD: wchen@mail.nih.gov
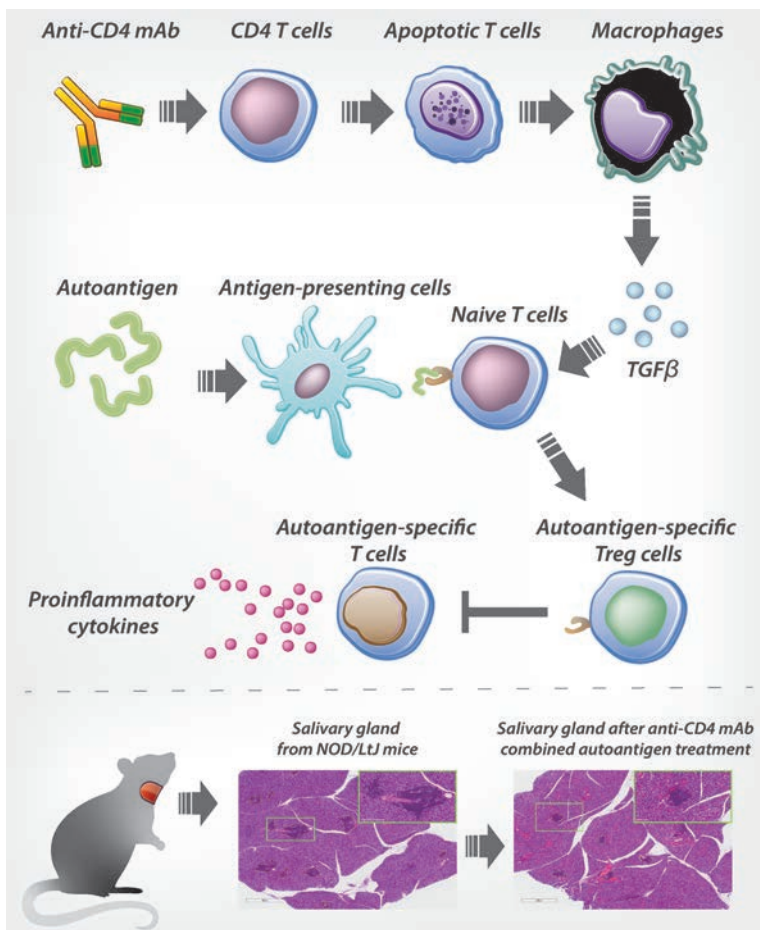
SUMMARY

Sjögren's syndrome (SS) is a systemic autoimmune disease with impaired Treg cells and large numbers of activated T cells, which contribute to the initiation and perpetuation of the disease. In this study, Xu et al used a combination of CD4 T cell depletion together with administration of SS-specific autoantigen peptide Ro480 to induce antigen-specific Treg cells in the NOD/LtJ mice with SS-like disease. This was achieved mechanistically by the presence of autoantigens and transforming growth factor β (TGFβ) produced by phagocytes upon taking up apoptotic CD4+ T cells. This treatment successfully suppressed interferon-γ (IFNγ) production of CD4+ T cells and inflammation infiltration in the salivary glands of SS-like NOD/LtJ mice and blocked the development of SS. This work further supports the concept that antigen-specific Treg cell generation can be accomplished in mice with ongoing and established autoimmune diseases. These findings could advance the path to the development of similar therapy for human patients with autoimmune diseases, including SS.

KEY POINTS

- A single dose of anti-CD4 monoclonal antibodies (mAb) can efficiently deplete CD4+ T cells, and the apoptotic T cells trigger phagocytes to produce TGFβ in vivo.

- Combination of anti-CD4 mAb and peptide Ro480 generates Ro480 antigen–specific Treg cells in vivo in NOD/LtJ mice with SS-like disease.

- Anti-CD4 mAb and Ro480 treatment reduces IFNγ in CD4+ T cells in salivary glands and suppresses SS-like symptoms in NOD/LtJ mice.

Dynamics of Methylation of SLE-Associated CpG Suites in Relation to SLE Subtypes in a Longitudinal Cohort

CORRESPONDENCE
Cristina M. Lanata, MD: Cristina.lanata@nih.gov
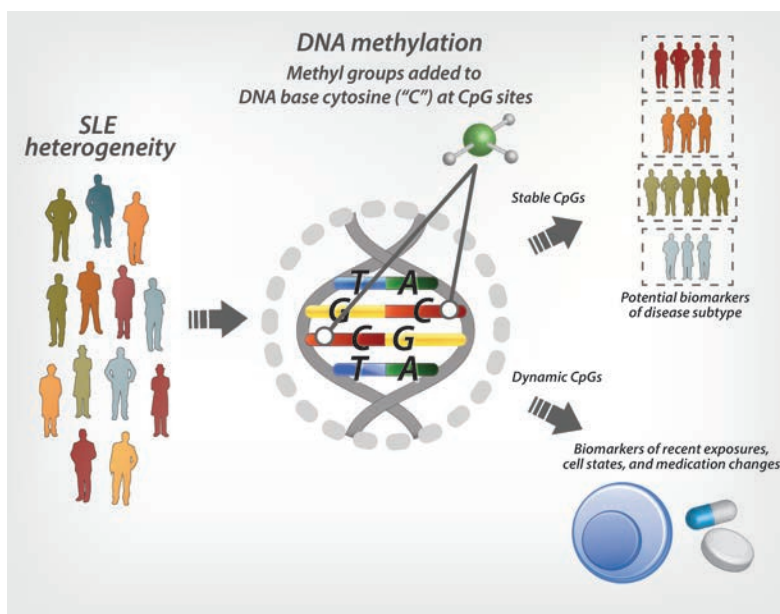
KEY POINTS

- DNA methylation is a chemical modification in DNA that regulates gene expression. Differences in whole-blood DNA methylation have been associated with SLE subtypes in previous cross-sectional studies.

- Longitudinal studies offer insight into what DNA methylation marks could be studied as stable biomarkers of SLE disease subtype.

- Some methylation marks seem to vary with time, medication use, and changes in cell proportion.

SUMMARY

One of the biggest challenges in the diagnosis and treatment of patients with systemic lupus erythematosus (SLE) is the molecular and clinical heterogeneity of the disease itself. There are many efforts to discover biomarkers that could be used successfully to target patients with the most appropriate therapeutic approach. In this issue, Lanata et al highlight how one biomarker, DNA methylation, can be leveraged to examine SLE heterogeneity. DNA methylation is an epigenetic mechanism used to regulate gene expression. When measured, DNA methylation can provide information on biological pathways being repressed or activated in circulating immune cells. However, DNA methylation is not a static measurement, and it can vary with age, smoking status, medication use, and environmental exposures.

Previously, Lanata et al reported on 256 CpGs that were differentially methylated according to disease subtypes in a cohort of 332 SLE patients. In the current issue, the authors reexamined how stable this finding was after 2 years. This study revealed that the majority of the previously reported CpG sites remained stable (185 CpGs; 72.3%). A selection of 20 CpGs with the most variance across subtypes that did not change over time were proposed as potential biomarkers of disease subtypes to be validated in future prospective studies. These include CpGs in *TNK2*, *RABGAP1L*, *IRF7*, *IFI44L*, *TRIM22*, and many interferon-responsive genes. The authors also found that although the majority of SLE subtype–associated CpGs were stable, the remaining CpGs changed at a higher proportion compared to background genome-wide methylation. In addition, changes in cell proportion were associated with changes at 67 CpGs ($P < 2.70 \times 10^{-5}$), and 15 CpGs had ≥1 significant association with the use of an immunosuppressive medication. These data suggest that some CpGs are reflective of environmental changes while other CpGs remain stable.

AMERICAN COLLEGE
of RHEUMATOLOGY
Empowering Rheumatology Professionals

EDITORIAL

Three Months of Glucocorticoids in Rheumatoid Arthritis: A Bridge Too Short?

Maarten Boers (iD)

Since their invention, glucocorticoids (GCs) have always been regarded as special. Hailed as a "miracle drug" after Philip S. Hench demonstrated astonishing effects in a patient with severe rheumatoid arthritis (RA) in 1948, pioneering physicians quickly realized that extended therapy with high doses carried a high risk of adverse events (AEs). Hench received his Nobel prize only 2 years later [1], and in his acceptance lecture he enumerated a comprehensive list of AEs before proposing a sensible approach and introducing low-dose therapy:

> "Physicians who would use these hormones should become familiar with these possible side effects and with certain measures devised for their prevention, modification or control. Because of their potential effects, cortisone or adrenocorticotropic hormone should be used with caution in the following: hypertensive cardiovascular disease, diabetes mellitus, tuberculosis, old rheumatic carditis with decompensation, latent or frank psychoses, marked osteoporosis associated with senility or with rheumatoid arthritis, and peptic ulcers. Certain measures have been devised to prevent or modify some of the undesirable effects. These include […] early reduction of the initial suppressive doses to lower 'maintenance doses' in all cases in which use of the hormones is prolonged. […] During the past few months we have been using smaller suppressive and smaller maintenance doses than we used previously; results have been generally quite satisfactory and will be reported elsewhere." [1]

Research on GCs has also made it a special drug. Bradford Hill is widely credited with the invention of the modern randomized trial (on streptomycin in tuberculosis) [2], but few people know that he also helped design a set of high-quality trials that documented the usefulness of low-dose GCs in RA between 1950 and 1960 [3,4]. However, physicians and patients in many countries clamored for access, so already in 1952 (without proper research, documentation, or guidelines on dosing), the US Food and Drug Administration approved the drug for use by all US physicians [5]. This resulted in uncontrolled use by physicians uneducated by experts such as Hench, in a period when effective alternatives were scarce or unavailable. It is highly likely that adverse experiences led to backlash and the widely held view among rheumatologists that GCs were "evil" drugs, only to be used briefly and as a last resort to combat flares. Such use was often unsatisfactory, because the disease would flare again after the drug was stopped. Curiously enough, the drug was blamed for such flares, suggesting that GCs should continue to work even when discontinued. In the meantime, internists started to use high-dose GCs for many systemic diseases and malignancies. Harms were readily apparent but accepted in the face of serious and life-threatening disease. In rheumatology, efforts turned to the development and study of nonsteroidal antiinflammatory drugs in the hope these would be safer, with alternatives such as sulfasalazine and methotrexate.

It took over 30 years for the focus to return to GCs as a cotreatment for RA. Kirwan et al showed benefits of low-dose GCs on structural damage [6], step-down GC combination therapy was found to be safe and beneficial for disease activity and damage (as demonstrated in the Combinatietherapie Bij Reumatoïde Artritis [COBRA] study [7]), and the trial experience with alternative combinations of GCs and other conventional and biologic disease-modifying antirheumatic drugs was almost uniformly positive [8,9]. This included trials that continued therapy for up to 2 years. Very recently, the pragmatic Glucocorticoid Low-dose Outcome in Rheumatoid Arthritis (GLORIA) trial compared the results of 2 years of prednisolone (5 mg/day) or placebo added to optimized standard care in senior patients with established RA (disease duration ≥11 years, age ≥65 years) [10]. Even at this low dose, prednisolone reduced disease activity and joint

Maarten Boers, MD, PhD, MSc: Department of Epidemiology & Data Science, Amsterdam University Medical Center, Vrije Universiteit, Amsterdam, The Netherlands.

Author disclosures are available at https://onlinelibrary.wiley.com/action/downloadSupplement?doi=10.1002%2Fart.42249&file=art42249-sup-0001-Disclosureform.pdf.

Address correspondence to Maarten Boers, MD, PhD, MSc, Department of Epidemiology & Data Science, Amsterdam University Medical Center, Vrije Universiteit, Amsterdam, The Netherlands. Email: eds@amsterdamumc.nl.

Figure 1. Initial step-down glucocorticoid (GC) dosing schedules from the study by Krause et al and other trials. The original Combinatietherapie Bij Reumatoïde Artritis (COBRA) trial kept the methotrexate (MTX) dose to 7.5 mg/week, but more recent studies have allowed increases as required. S.C. = subcutaneous; SSZ = sulfasalazine.

techniques. For example, a relative risk (or odds ratio) that is "adjusted" for disease activity (as a marker of disease severity) statistically compares the risk of GC exposure to nonexposure in patients with the same level of disease activity. However, this procedure ignores the fact that a patient currently receiving GCs who has the same disease activity as a patient not receiving GCs would flare to a higher level of disease activity if the GCs were withdrawn. In other words, the underlying RA severity of the patient receiving GC treatment is worse than that of the patient not receiving GC treatment. To date, I have not seen a study that overcorrects to compensate for this problem.

These conflicting findings from studies continue to confuse experts and clinicians. Most guideline committees now follow a Grading of Recommendations Assessment, Development and Evaluation (GRADE) procedure or something similar to create evidence-based guidelines, but GCs form a special category. Until 2021, the American College of Rheumatology did not address the potential role of GCs in its treatment guidelines for RA, and now it does but "conditionally advises against" GC therapy in RA (12). The European Alliance of Associations for Rheumatology offers a more liberal approach but advises no more than bridge therapy and to cease treatment as soon as possible (13). So in the case of GCs, academic societies deviate from GRADE, preferring tradition and the evidence of observational studies above that of trials. However, practicing rheumatologists have been ignoring these guidelines for many years: trials and observational studies consistently show that a substantial proportion (30–70%, 50% in trial populations) of patients with established RA are receiving chronic low-dose GCs, even patients who also receive highly effective targeted therapy.

In this issue of *Arthritis & Rheumatology*, Krause et al describe a large placebo-controlled trial examining the potential benefit of short-term GC bridge therapy on structural damage in RA (14). The study was adequately powered for a difference of 2 Sharp/van der Heijde units and was meticulously conducted, but it was unable to show benefit of up to ~1,400 mg oral prednisolone over 12 weeks. Measurement of disease activity showed strong benefits of GCs in the first 12 weeks that disappeared upon discontinuation. Bridge therapy was also shown to be safe. Caveats include the finding of minimal (but clinically irrelevant) trends in favor of GCs, and the fact that the placebo group more frequently received intraarticular GCs as comedication. Also, in the subsequent 40 weeks, physicians were allowed to administer GCs, and they did in all treatment groups. Oral prednisolone was given in a mean cumulative dose of 764 mg, which equates to 2.7 mg/day (if all patients were treated); and patients received a mean of 2.5 intraarticular injections. This may have contaminated the comparison and contributed to the overall very low mean progression rate of 1 unit.

Even though this is a negative study, it is welcome, because it helps make GCs more "normal," i.e., a drug that needs to be given at a certain dose for a certain period of time before it can

damage progression, with the tradeoff of a 24% increased risk of an AE of special interest, mostly nonsevere infections.

These trial findings are in stark contrast to those of observational studies. There is a huge and ever-growing body of evidence that shows that exposure to even low-dose GCs is associated with a higher risk of a wide spectrum of AEs. How is that possible? Most likely, at least part of the explanation is that observational findings are biased through strong confounding by indication: with the strongly negative opinion about GCs, only patients with relatively severe RA are likely to receive GCs, but severe RA by itself can cause many of the AEs attributed to GCs (11). In this way, GC exposure is (also) a marker for severe RA and its consequences, rather than the cause of all AEs. Although most recent studies try to limit confounding, strong confounding by indication (disease severity) cannot be corrected by statistical

exert its effects, and also one that stops working upon discontinuation. The study confirms that physicians who favor brief treatment with GCs to bridge the period before other therapies start to work can expect rapid effects on disease activity that wane as soon as GCs are discontinued. However, even substantial doses of GCs will not slow radiographic progression of damage if given for only 3 months. The high-dose GC group received a treatment schedule reminiscent of the original COBRA trial that showed reduction of damage progression at 6 months (7), so we could surmise that the minimum treatment period is ~6 months, and the minimum dose after step-down is 7.5 mg/day, for a cumulative dose of 2,300 mg in 6 months. However, for damage at 1 year, both COBRA-light (step-down from 30 to 7.5 mg/day, cumulative dose at 6 months 1,800 mg) (15) and COBRA-slim (step-down from 30 to 5 mg/day, cumulative dose at 6 months 1,300 mg) (16) were noninferior to COBRA (Figure 1). This suggests that the benefit of GCs on damage might be obtained with a lower cumulative dose than applied in the trial by Krause et al, if applied in a step-down schedule in which low-dose GC therapy is continued for ≥6 months.

These findings may also be useful to consider for those who champion the use of a biologics-first approach in RA patients with a poor prognosis. The suggestion is that biologics can be rapidly tapered and stopped as soon as the disease is under control. Most likely, biologics also need to be given at a certain dose for a certain period of time (6 months?) before they can reduce damage progression. These findings also need to be viewed in light of the improved prognosis of current RA patients; the extent of damage at initial presentation and progression of such damage have strongly decreased over the last 2 decades, as the authors document in their discussion. This was confirmed in the GLORIA trial, in which it was observed that damage progression in 2 years was 0.3 units in the prednisolone group and 1.9 in the placebo group (10), similar to the rates in the Krause trial.

So, what's next? In my view, recent studies on GCs have substantially enlarged the body of evidence and redefined GCs as a normal drug, with advantages and disadvantages like any other. This study shows the benefits but also the limitations of bridge therapy. Other studies (including GLORIA) suggest that there is a place for chronic low-dose GC add-on therapy in RA.

AUTHOR CONTRIBUTIONS

Dr. Boers drafted the article, revised it critically for important intellectual content, and approved the final version to be published.

REFERENCES

1. Hench PS. Nobel Lecture, 1950. URL: https://www.nobelprize.org/uploads/2018/06/hench-lecture.pdf.

2. Hill AB. Suspended judgment. Memories of the British Streptomycin Trial in Tuberculosis. The first randomized clinical trial. Control Clin Trials 1990;11:77–9.

3. Copeman WS, Savage O, Bishop PM, Dodds EC, Gottlieb B, Glyn JH, et al. A study of cortisone and other steroids in rheumatoid arthritis. Br Med J 1950;2:849–55.

4. Joint Committee of the Medical Research Council and Nuffield Foundation on clinical trials of cortisone A, and other therapeutic measures in chronic rheumatic diseases. A COMPARISON of prednisolone with aspirin on other analgesics in the treatment of rheumatoid arthritis. Ann Rheum Dis 1959;18:173–88.

5. Conn DL. The story behind the use of glucocorticoids in the treatment of rheumatoid arthritis. Semin Arthritis Rheum 2021;51:15–9.

6. Kirwan JR, for the arthritis rheumatism council low-dose glucocorticosteroid study group. The effects of glucocorticosteroids on joint destruction in rheumatoid arthritis. N Engl J Med 1995;333:142–6.

7. Boers M, Verhoeven AC, Markusse HM, van de Laar MA, Westhovens R, van Denderen JC, et al. Randomised comparison of combined step-down prednisolone, methotrexate and sulphasalazine with sulphasalazine alone in early rheumatoid arthritis [see comments] [published erratum appears in Lancet 1998 Jan 17;351(9097):220]. Lancet 1997;350:309–18.

8. Graudal N, Hubeck-Graudal T, Faurschou M, Baslund B, Jürgens G. Combination therapy with and without tumor necrosis factor inhibitors in rheumatoid arthritis: a meta-analysis of randomized trials. Arthritis Care Res (Hoboken) 2015;67:1487–95.

9. Kirwan JR, Bijlsma JW, Boers M, Shea BJ. Effects of glucocorticoids on radiological progression in rheumatoid arthritis. Cochrane Database Syst Rev 2007:CD006356.

10. Boers M, Hartman L, Opris-Belinski D For the GLORIA Trial consortium, et al. Low dose, add-on prednisolone in patients with rheumatoid arthritis aged 65+: the pragmatic randomised, double-blind placebo-controlled. Ann Rheum Dis 2022;81:925–36.

11. Boers M. Observational studies on glucocorticoids are harmful! Lupus Sci Med 2017;4:e000219.

12. Fraenkel L, Bathon JM, England BR, St Clair EW, Arayssi T, Carandang K, et al. 2021 American College of Rheumatology guideline for the treatment of rheumatoid arthritis. Arthritis Rheumatol 2021;73:1108–23.

13. Smolen JS, Landewe RB, Bijlsma JW, Burmester GR, Dougados M, Kerschbaumer A, et al. EULAR recommendations for the management of rheumatoid arthritis with synthetic and biological disease-modifying antirheumatic drugs: 2019 update. Ann Rheum Dis 2020;79:685–99.

14. Krause D, Mai A, Klaassen-Mielke R, Timmesdeld N, Trampisch U, Rudolf H, et al. The efficacy of short-term bridging strategies with high- and low-dose prednisolone on radiographic and clinical outcomes in active early rheumatoid arthritis: a double-blind, randomized, placebo-controlled trial. Arthritis Rheum 2022;74:1629–38.

15. Ter Wee MM, den Uyl D, Boers M, Kerstens P, Nurmohamed M, van Schaardenburg D, et al. Intensive combination treatment regimens, including prednisolone, are effective in treating patients with early rheumatoid arthritis regardless of additional etanercept: 1-year results of the COBRA-light open-label, randomised, non-inferiority trial. Ann Rheum Dis 2015;74:1233–40.

16. Verschueren P, De Cock D, Corluy L, Joos R, Langenaken C, Taelman V, et al. Effectiveness of methotrexate with step-down glucocorticoid remission induction (COBRA Slim) versus other intensive treatment strategies for early rheumatoid arthritis in a treat-to-target approach: 1-year results of CareRA, a randomised pragmatic open-label superiority trial. Ann Rheum Dis 2017;76:511–20.

EDITORIAL

Is Rheumatoid Arthritis a Causal Factor in Cardiovascular Disease?

S. Louis Bridges Jr ,[1] Timothy B. Niewold,[1] and Tony R. Merriman[2]

As much as 60% of the risk of developing rheumatoid arthritis (RA) is attributable to inherited genetic variants (1). It has long been recognized that risk of cardiovascular disease (CVD) is substantially increased in many rheumatic diseases, including RA, systemic lupus erythematosus, and gout (2,3). One obvious explanation for the link between RA and CVD is that clinical risk factors for CVD, such as hypertension, dyslipidemia, and obesity, are more common in RA than in the general population (4). Similarly, environmental exposures such as smoking are associated with both conditions (Figure 1). Drugs commonly used in RA, such as nonsteroidal antiinflammatory drugs and glucocorticoids, also elevate the risk of CVD (2). The JAK inhibitor tofacitinib is the latest drug reported to increase risk of CVD in RA (5). Importantly, traditional risk factors for CVD do not fully explain the elevated risk in RA. The pathogenic process of RA per se may be causal for CVD in the presence or RA (6). However, it is not possible to determine a causal relationship from epidemiologic studies, even those that are optimally designed.

In this issue of *Arthritis & Rheumatology*, Yuan et al address the question of whether the pathogenesis of RA is causally related to CVD (7). The genetic epidemiologic Mendelian randomization (MR) technique allows this question to be addressed. Analogous to a randomized clinical trial, MR exploits alleles of genetic variants randomly inherited at conception as a surrogate for "exposure" to a phenotype and tests them for association with an outcome. In this study, the exposure was RA and the outcome was CVD. Because an individual is exposed to the risk-increasing alleles from the time of conception, the influence of unmeasured and imperfectly measured confounding that is inherent in conventional epidemiology is minimized. The MR technique also avoids the vexing problems of reverse causation (when the exposure causes the risk factor rather than vice versa).

To make valid conclusions, an MR analysis must meet several assumptions: 1) relevance (the genetic variants are associated with the risk factor of interest); 2) independence (no unmeasured confounders of the associations between genetic variants and the outcome); and 3) exclusion restriction (the genetic variants affect the outcome only through their effect on the risk factor). A key way in which MR studies may violate the exclusion restriction assumption is through horizontal pleiotropy (when a genetic variant affects other traits which influence the outcome independently of the hypothesized exposure). This study appropriately used the MR-Egger and MR-PRESSO approaches. The investigators found that genetic liability (the totality of the effect of genetic factors on the development of RA) is associated with an increased risk of coronary artery disease (CAD) and intracerebral hemorrhage (ICH). This finding reveals many interesting points to consider.

What difference would be made if additional RA genetic risk factors were included?

There are at least 106 significant independent genetic associations with RA, the strongest of which is in the major histocompatibility (MHC) locus (8). In this paper, a subset of 70 single-nucleotide polymorphisms (SNPs) reproducibly associated with RA were analyzed; removing the effect of MHC region genes from the analysis did not affect the main finding. While our understanding of the role of genetics in the development of RA has improved dramatically over the last 20 years, largely due to genome-wide association studies (GWAS), it is important to note that SNPs reaching genome-wide significance ($P < 5 \times 10^{-8}$) account for only a small portion of the genetic risk of RA (9). There are likely hundreds, if not thousands, of causal variants with small effect size, not detected by GWAS (9). If these associations were able

[1]S. Louis Bridges Jr, MD, PhD, Timothy B. Niewold, MD: Hospital for Special Surgery and Weill Cornell Medicine, New York, New York; [2]Tony R. Merriman, PhD: University of Alabama at Birmingham, Birmingham, and University of Otago, Dunedin, New Zealand.

Address correspondence to S. Louis Bridges Jr, MD, PhD, Hospital for Special Surgery, 535 East 70th Street, New York, NY 10021. Email: bridgesl@hss.edu.
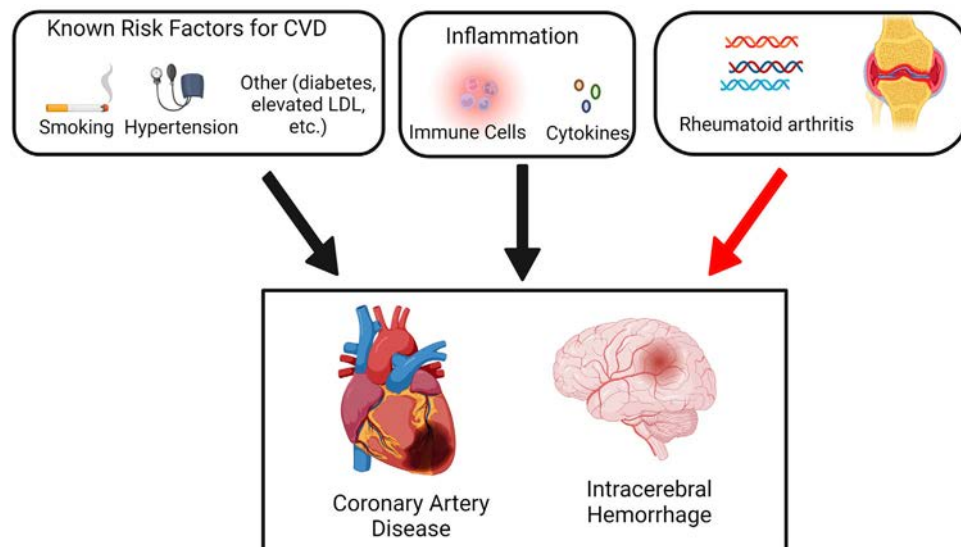
Figure 1. Rheumatoid arthritis (RA) as a causal factor in cardiovascular disease (CVD). Smoking and hypertension are causally related to CVDs such as coronary artery disease (CAD) and intracerebral hemorrhage (ICH). Smoking is thought to be associated with RA as well, while hypertension is more commonly seen in RA than in the general population. Inflammation is characteristic of both CVD and RA. Mendelian randomization analyses in the article by Yuan et al provide evidence that genetic liability to RA is causally related to CAD and ICH, independent of smoking and other risk factors (red **arrow**). LDL = low-density lipoprotein. Created with BioRender.com.

to be identified and included in the analysis, the power of the analysis would increase and the statistical evidence for association of RA with CAD and with ICH should also increase (although the effect size may not).

Although understanding the genetic underpinnings of RA was not part of this study, it is important to note that many factors play a role in its pathogenesis. These include epigenetics (changes in gene function that are not attributed to alterations of the DNA sequence), epistasis (expression of 1 gene affecting the expression of ≥1 independently inherited genes), pleiotropy (a genetic variant affecting ≥2 traits via independent biologic pathways), gene–gene interactions, and gene–environment interactions. Furthermore, the emergence of single-cell technologies has led to detailed deconvolution of cell type–specific effects of SNPs (e.g., biologic significance of the genetic variant in endothelial cells compared to T lymphocytes) (9). A common, strong, independent risk factor for CVD has recently emerged: clonal hematopoiesis of indeterminate potential (CHIP) (10). CHIP arises when somatic mutations in hematopoietic stem cells yield clonal progeny of circulating mutant leukocytes. CHIP has been reported in patients with RA (11), raising the interesting speculation that it may be involved in CVD among patients with RA.

What is the influence of ethnicity on these findings?

Because the majority of available genetic data in RA is from persons of European ancestry, this study focused on analysis of RA and CVD outcomes in this population. African Americans (12) and other populations such as Native Americans and those of Hispanic ancestry are disproportionately affected by CVD. The prevalence of RA does not appear to be significantly different between European and African populations. In addition, most common genetic risk factors associated with RA are consistent across these 2 populations (13,14), but there are some differences. For example, the index SNP of *PTPN22* has a larger effect size in European people than in African people (13), and there are subtle differences in HLA–DRB1 risk alleles between populations (15). It is important to note that genetic association and MR studies are increasingly being performed in larger cohorts of non-European populations. If this were not the case, health disparities driven by differences in participation in genetic research studies will occur.

Which characteristics of RA lead to increased risk of CAD and ICH?

Hypertension is a strong risk factor for CVD and is more common in RA patients than controls (16). Inflammation is also pivotal to the pathogenesis of both RA and CVD. The important role of inflammation in CVD is underscored by the prevention of CVD using antiinflammatory agents such as canakinumab (an interleukin-1β [IL-1β] inhibitor) and colchicine (17). Yuan et al noted an association between genetic liability to RA and increased serum levels of tumor necrosis factor (TNF) and a nearly statistically significant association with serum IL-6. It is possible that underlying factors associated with activation of specific immune-mediated inflammatory pathways in RA may explain its causal relationship with CVD.

Yuan et al also found that genetic liability to RA was also associated with serum C-reactive protein (CRP) levels. CRP is an acute-phase protein produced predominantly in the liver under the influence of IL-6 and TNF; elevated serum CRP is associated with an increased risk of CVD. The association of CAD with the genetic liability to RA was attenuated after adjustment for genetically predicted CRP levels, suggesting that CRP may at least in part mediate the association. Of note, genotype combinations of 4 SNPs in the CRP gene are associated with increased serum CRP levels but not with an increased risk of ischemic vascular disease (18). SNPs in *CRP* vary by race/ethnicity and may influence outcomes of RA (19). CRP is not thought to be causally related to CVD, but rather as a marker of cytokine activation (18).

The authors note that there were no single SNP associations that drove their findings, so no known specific RA-related pathway can be implicated in CVD risk. While it seems likely that inflammation would be the causal factor linking RA genetic risk to CVD, further work will be needed to determine the specific pathways and molecular basis for this association. It is interesting to speculate that there are factors other than inflammation by which RA may contribute to CVD, such as the presence of autoantibodies or features associated with ICH, such as subacute vasculopathy or amyloid angiopathy, or clonal hematopoiesis of indeterminate potential.

What is the clinical significance of these findings?

It is well accepted that risk factors for CVD should be actively managed in all patients with RA (2). Similarly, the goal of therapy in RA should be remission or low disease activity; a treat-to-target approach has been advocated for many years. The findings in this study provide additional support for aggressive management of RA disease activity to lower the risk of CVD.

AUTHOR CONTRIBUTIONS

Drs. Bridges, Niewold, and Merriman drafted the article, revised it critically for important intellectual content, and approved the final version to be published.

REFERENCES

1. Smolen JS, Aletaha D, Barton A, Burmeister GR, Emery P, Firestein GS, et al. Rheumatoid arthritis. Nat Rev Dis Primers 2018;4: 18001.

2. Ferguson LD, Sattar N, McInnes IB. Managing cardiovascular risk in patients with rheumatic disease. Med Clin North Am 2021;105: 247–62.

3. Avina-Zubieta JA, Thomas J, Sadatsafavi M, Lehman AJ, Lacaille D. Risk of incident cardiovascular events in patients with rheumatoid arthritis: a meta-analysis of observational studies. Ann Rheum Dis 2012;71:1524–9.

4. Navarro-Millan I, Yang S, DuVall SL, Chen L, Baddly J, Cannon GW, et al. Association of hyperlipidaemia, inflammation and serological status and coronary heart disease among patients with rheumatoid arthritis: data from the National Veterans Health Administration. Ann Rheum Dis 2016;75:341–7.

5. Ytterberg SR, Bhatt DL, Mikuls TR, Koch GG, Fleischmann R, Rivas JL, et al. Cardiovascular and cancer risk with tofacitinib in rheumatoid arthritis. N Engl J Med 2022;386:316–26.

6. Crowson CS, Liao KP, Davis JM III, Solomon DH, Matteson EL, Knutson KL, et al. Rheumatoid arthritis and cardiovascular disease [review]. Am Heart J 2013;166:622–8.

7. Yuan S, Carter P, Yang F, Burgess S, Larsson S. Genetic liability to rheumatoid arthritis in relation to coronary artery disease and stroke risk. Arthritis Rheumatol 2022;74:1639–48.

8. Okada Y, Eyre S, Suzuki A, Kochi Y, Yamamoto K. Genetics of rheumatoid arthritis: 2018 status. Ann Rheum Dis 2019;78:446–53.

9. Amariuta T, Luo Y, Knevel R, Okada Y, Raychaudhuri S. Advances in genetics toward identifying pathogenic cell states of rheumatoid arthritis. Immunol Rev 2020;294:188–204.

10. Libby P, Sidlow R, Lin AE, Gupta D, Jones LW, Moslehi J, et al. Clonal hematopoiesis: crossroads of aging, cardiovascular disease, and cancer: JACC review topic of the week [review]. J Am Coll Cardiol 2019;74:567–77.

11. Savola P, Lundgren S, Keränen MA, Almusa H, Ellonen P, Leirisalo-Repo M, et al. Clonal hematopoiesis in patients with rheumatoid arthritis. Blood Cancer J 2018;8:69.

12. Carnethon MR, Pu J, Howard G, Albert MA, Anderson CA, Bertoni AG, et al. Cardiovascular health in African Americans: a scientific statement from the American Heart Association [review]. Circulation 2017;136:e393–423.

13. Hughes LB, Reynolds RJ, Brown EE, Kelley JM, Thomson B, Conn DL, et al. Most common single-nucleotide polymorphisms associated with rheumatoid arthritis in persons of European ancestry confer risk of rheumatoid arthritis in African Americans. Arthritis Rheum 2010;62:3547–53.

14. Laufer VA, Tiwari HK, Reynolds RJ, Daniela MI, Wang J, Edberg JC, et al. Genetic influences on susceptibility to rheumatoid arthritis in African-Americans. Hum Mol Genet 2019;28:858–74.

15. Reynolds RJ, Ahmed AF, Danila MI, Hughes LB, the Consortium for the Longitudinal Evaluation of African American with Early Rheumatoid Arthritis Investigators, Gregersen PK, et al. HLA–DRB1–associated rheumatoid arthritis risk at multiple levels in African Americans: hierarchical classification systems, amino acid positions, and residues. Arthritis Rheumatol 2014;66:3274–82.

16. Jagpal A, Navarro-Millan I. Cardiovascular co-morbidity in patients with rheumatoid arthritis: a narrative review of risk factors, cardiovascular risk assessment and treatment. BMC Rheumatol 2018;2:10.

17. Boland J, Long C. Update on the inflammatory hypothesis of coronary artery disease. Curr Cardiol Rep 2021;23:6.

18. Zacho J, Tybjaerg-Hansen A, Jensen JS, Grande P, Sillesen H, Nordestgaard BG. Genetically elevated C-reactive protein and ischemic vascular disease. N Engl J Med 2008;359:1897–908.

19. Danila MI, Westfall AO, Raman K, Chen L, Reynolds RJ, Hughes LB, et al. The role of genetic variants in CRP in radiographic severity in African Americans with early and established rheumatoid arthritis. Genes Immun 2015;16:446–51.

AMERICAN COLLEGE
of RHEUMATOLOGY
Empowering Rheumatology Professionals

R E V I E W

Intracellular Sensing of DNA in Autoinflammation and Autoimmunity

Susan MacLauchlan,[1] (ID) Katherine A. Fitzgerald,[2] (ID) and Ellen M. Gravallese[1] (ID)

Evidence has shown that DNA is a pathogen-associated molecular pattern, posing a unique challenge in the discrimination between endogenous and foreign DNA. This challenge is highlighted by certain autoinflammatory diseases that arise from monogenic mutations and result in periodic flares of inflammation, typically in the absence of autoantibodies or antigen-specific T lymphocytes. Several autoinflammatory diseases arise due to mutations in genes that normally prevent the accrual of endogenous DNA or are due to mutations that cause activation of intracellular DNA–sensing pathway components. Evidence from genetically modified murine models further support an ability of endogenous DNA and DNA sensing to drive disease pathogenesis, prompting the question of whether endogenous DNA can also induce inflammation in human autoimmune diseases. In this review, we discuss the current understanding of intracellular DNA sensing and downstream signaling pathways as they pertain to autoinflammatory disease, including the development of monogenic disorders such as Stimulator of interferon genes–associated vasculopathy with onset in infancy and Aicardi-Goutières syndrome. In addition, we discuss systemic rheumatic diseases, including certain forms of systemic lupus erythematosus, familial chilblain lupus, and other diseases with established links to intracellular DNA–sensing pathways, and highlight the lessons learned from these examples as they apply to the development of therapies targeting these pathways.

Introduction

The immune system has evolved to rapidly detect and eradicate invading pathogens. Inappropriate activation of the immune system also leads to inflammatory disease. Investigation into the rare monogenic diseases resulting from dysregulated immunity has greatly informed our mechanistic understanding of innate and adaptive disease mechanisms and has influenced pharmaceutical design. Recent years have seen an explosion in the number of studies focusing on autoinflammatory diseases, establishing this burgeoning field. In particular, a wealth of clinical and basic insights has established that DNA, and the sensors that are activated by DNA, are key drivers of several autoinflammatory diseases.

Mammalian DNA is typically contained within the nucleus or mitochondria, and DNA accrual in the cytosol is perceived as a danger signal for cells. Accordingly, humans have an extensive network of enzymes and pathways dedicated to the rapid clearance of endogenous DNA from multiple cellular compartments. Detection of cytosolic DNA in particular is a trigger for mounting rapid and effective host defenses. Clinical and experimental evidence links activation of the innate immune intracellular DNA–sensing pathways to a subset of autoinflammatory diseases. Autoinflammatory diseases are distinct from autoimmune diseases as they present in periodic flares of inflammation, usually in the absence of autoantibodies or antigen-specific T lymphocytes (1,2), although the distinction between autoinflammatory and autoimmune diseases is sometimes difficult to determine due to overlapping features.

Patients with autoinflammatory disease typically develop fever and a cluster of organ- and disease-specific manifestations. These diseases arise from disruptions in the innate immune system and are subdivided into 4 main mechanistic categories (1,2):

1) inflammasomeopathies and interleukin-1β (IL-1β)–mediated autoinflammatory diseases (including familial Mediterranean fever, cryopyrin-associated periodic syndrome, hyperimmunoglobuline-mia D syndrome/mevalonate kinase deficiency, IL-1 receptor antagonist deficiency, and others); 2) autoinflammatory type I interferonopathies (including chronic atypical neutrophilic derma-tosis with lipodystrophy and elevated temperature, proteasome-associated autoinflammatory syndrome, stimulator of interferon genes [STING]–associated vasculopathy with onset in Infancy [SAVI], Aicardi-Goutières syndrome [AGS], and others) that result in excessive type 1 interferon (IFN) signaling; 3) autoinflammatory diseases mediated by the NF-κB pathway and/or aberrant tumor necrosis factor (TNF) activity; and 4) autoinflammatory diseases mediated by other pathways including the complement pathway. This review focuses on the subset of autoinflammatory type 1 interferonopathies and other inflammatory diseases that are associated with DNA sensing and type I IFN responses. We use these disease states to discuss the principles of the pathways involved, describe how rare mutations lead to disease, and review what we have learned about these pathways that may be relevant to more common rheumatic diseases. In addition, in this review we describe potential therapeutic targets in these pathways that might be leveraged for treatment.

Microbial nucleic acid–sensing pathways

The innate immune system relies on pattern-recognition receptors (PRRs) expressed in different cellular compartments that detect pathogen-associated molecular patterns (PAMPs). Engagement of the PRRs by PAMPs triggers protective antimi-crobial defenses and subsequent induction of an adaptive immune response (3). The accurate discrimination of pathogen from self DNA is critical to avoiding unintended activation of these immune pathways. Over the past few decades, the identification of PRRs and other receptors that sense microbial nucleic acids has been critical to defining the key principles of host defense. In mammalian cells, single- and double-stranded RNA, single-stranded DNA (ssDNA), and double-stranded DNA (dsDNA), RNA/DNA hybrids, and cyclic dinucleotides are all recognized as foreign, alerting the immune system to the presence of a wide array of microbial pathogens including viruses, bacteria, para-sites, and fungi (3,4).

Although certain features of nucleic acids (e.g., Toll-like receptor 9 [TLR-9] recognition of hypomethylated CpG) differ between foreign and endogenous DNA, both foreign and endog-enous nucleic acids can activate intracellular sensors. Accord-ingly, the mammalian immune system has developed several mechanisms to prevent the accumulation of endogenous nucleic acids. One such mechanism is through degradation of nucleic acids by an RNase or DNase. For DNA, DNases are either secreted (DNase I and DNase1 L3), lysosomal (DNase II), or cyto-solic (DNase III, also known as 3′ repair exonuclease 1 [TREX1])

(Figure 1A). Another mechanism of DNA degradation relates to the localization of the nucleic acid PRRs to either the endolyso-some, where the pathogen genome is degraded by exposure to low pH, or the cytosol.

The ability of RNA to elicit immune activation has been exten-sively reviewed elsewhere. This occurs in both the endolysosome (by TLRs) and cytosol (by the retinoic acid–inducible gene I [RIG-I]–like receptors, which include RIG-I and melanoma differentiation–associated protein 5 [MDA5]) (3). The endolysoso-mal TLR-9 was the first described sensor of microbial DNA, rec-ognizing unmethylated CpG dinucleotides present in bacterial and viral DNA (for review, see ref. 5). Studies in TLR-9–deficient mice highlighted the central role for TLR-9 in controlling type I IFN production from plasmacytoid dendritic cells, but key studies also revealed that TLR-9 activation accounted for only a portion of the DNA-sensing response (6). The ability of dsDNA delivered to the cytosol of macrophages to induce a type I IFN response for-mally established the existence of a TLR-9–independent intracel-lular DNA–sensing pathway (6,7). This review focuses on DNA as a potent immune stimulator and on intracellular DNA–sensing pathways.

Intracellular DNA–sensing pathways

Delivery of dsDNA to the cytosol via lipofection is an approach used to identify the receptors for cytosolic DNA. This delivery resulted in the induction of type I IFN gene transcription as well as the activation of a second pathway involving caspase 1–dependent processing of the proinflammatory cytokines IL-1β and IL-18. The receptor for this latter pathway was first defined as AIM2 (for review, see ref. 8) (Figure 1B). AIM2 forms a caspase 1–activating inflammasome that controls the proteolytic matura-tion of IL-1β and IL-18 and processing of the pore-forming protein gasdermin D, an executioner of pyroptotic cell death. AIM2 is important for protection from DNA viruses and cytosolic bacterial pathogens but does not drive the type I IFN response to dsDNA. While AIM2-dependent responses are important, induction of type I IFN and IFN-stimulated genes (ISGs) is a dominant response elicited by cytosolic dsDNA.

Cyclic GMP-AMP synthase (cGAS) was identified as a pro-tein that binds DNA, controlling the type I IFN response. Many viral pathogens, including herpes simplex viruses type 1 and 2, vac-cinia virus, and cytomegalovirus, all activate cGAS (for review, see ref. 3). In addition, bacterial pathogens including *Mycobacte-rium tuberculosis*, *Legionella*, *Listeria*, *Shigella*, *Francisella*, *Chla-mydia*, *Neisseria*, and group B *Streptococcus* engage cGAS through the sensing of pathogen DNA (3). Findings indicate that cGAS recognizes short segments of dsDNA in a sequence-independent manner. DNA binding leads to the dimerization and activation of cGAS (for review, see ref. 9) (Figure 1C). Active cGAS converts GTP and ATP to the novel second messenger cyclic GMP-AMP (cGAMP) (10). Then, cGAMP binds to the
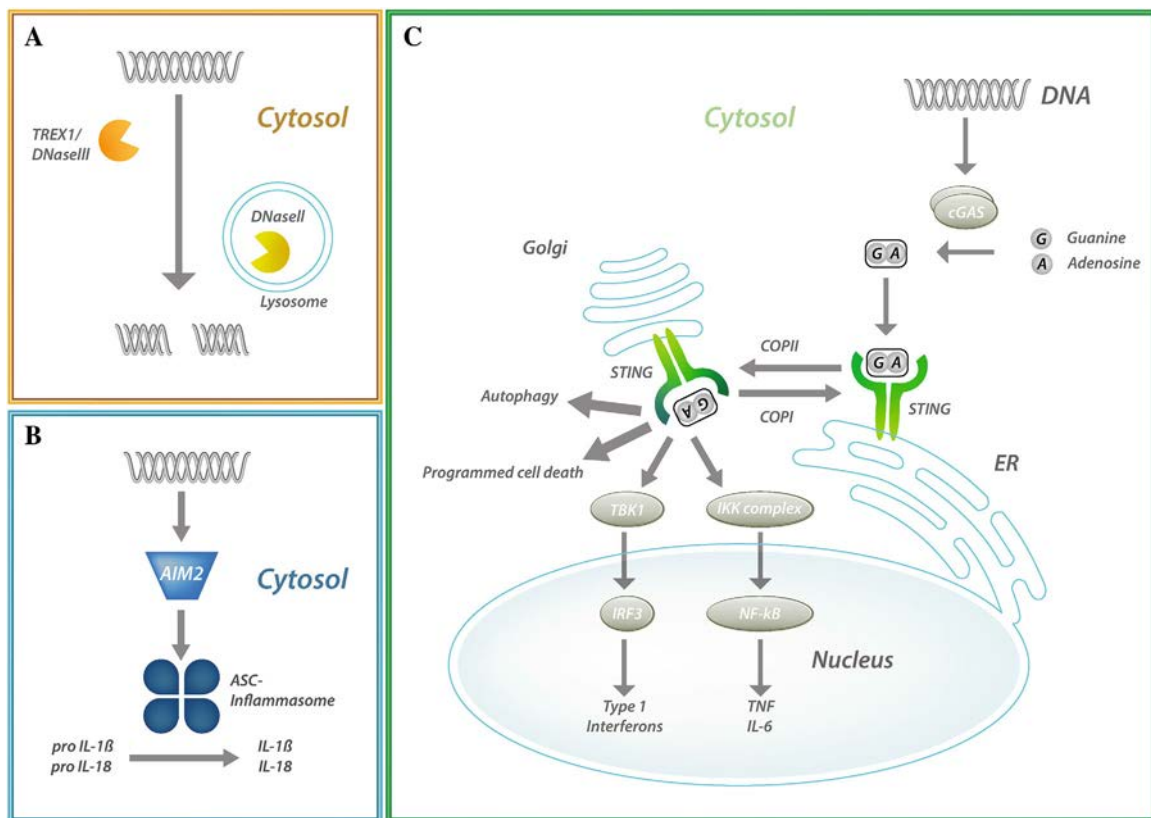
Figure 1. Schematic representation of the intracellular DNA–sensing pathways. **A**, To ensure that cytosolic DNA is effectively eliminated, several DNA-degrading enzymes (DNases) exist. These include TREX1/DNase III and the lysosomal DNase II. **B** and **C**, Intracellular DNA is recognized by two major pathways, including the Absent in Melanoma 2 (AIM2) pathway (**B**) and the cyclic GMP-AMP synthase (cGAS)/stimulator of interferon genes (STING) pathway (**C**). Detection of DNA by AIM2 leads to activation of an apoptosis-associated speck-like protein containing a CARD (ASC) inflammasome and caspase 1–mediated activation of interleukin-18 (IL-18) and IL-1β. DNA binding to cGAS leads to the production of cGAMP (GA), the ligand for STING, and cGAMP binding to STING causes homodimerization and transfer of STING to the Golgi in a process that uses the coat protein complex II (COPII). Active STING signals through TANK-binding kinase 1 (TBK1) and interferon regulatory factor 3 (IRF3) to stimulate type I interferons (IFNs), and activation of the IFN-stimulated gene IFN-α/β receptor subunit 1. STING also mediates activation of NF-κB, resulting in the production of tumor necrosis factor (TNF) and IL-6. Activation of STING can lead to pathogen clearance, autophagy, and/or programmed cell death, depending upon the context. STING is returned to the endoplasmic reticulum (ER) to down-regulate its signaling through the coat protein complex I (COPI) or is targeted for lysosomal degradation.

endoplasmic reticulum (ER)–localized adaptor protein STING (also known as MITA, ERIS, and MPYS). Upon cGAMP binding, STING homodimerizes and is trafficked to the Golgi through the ER–Golgi intermediate compartment using the cytoplasmic coat protein complex II. In the Golgi, STING interacts with the IKK-related kinase TANK-binding kinase 1 (TBK1) (11,12). STING is phosphorylated by TBK1, facilitating the binding and phosphorylation of IFN regulatory factor 3 (IRF3) by TBK1 (13). Phosphorylated IRF3 dimerizes and moves to the nucleus to induce transcription of IFNβ (14), which in turn leads to the induction of multiple ISGs.

Although induction of type I IFNs is the best studied response to STING activation, additional downstream responses include NF-κB activation of the proinflammatory cytokines TNF and IL-6, induction of autophagy, and apoptotic, necroptotic, or pyroptotic cell death (15) (Figure 1C). STING activation has been shown to lead to antigen presentation in macrophages, and to B cell apoptosis and T cell death (16,17). How these mechanisms contribute to human disease is a topic of active investigation. Deactivation of STING signaling occurs by the retrograde trafficking of STING back to the ER in a process dependent upon the coat protein complex I (COPI), or via lysosomal degradation or STING ubiquitination (15). Initially, cGAS was proposed to be localized exclusively in the cytosol where it senses DNA that gains access to that compartment. However, recent studies have shown that cGAS also localizes to the nucleus, where it is tethered to nucleosomes, the chromatin subunits of DNA packaged around histones (18,19). This binding to nucleosomes is proposed to restrain cGAS activity, preventing its activation (20). Whether cGAS recognizes endogenous DNA in the nucleus and

whether cGAS activity is limited to the cytosol are areas of ongoing research. Therefore, much remains to be learned about how cGAS is activated by cytosolic DNA.

A growing number of type I interferonopathies have been defined, several of which are associated with DNA-sensing pathways (e.g., SAVI) or with mutations in DNases or RNases (e.g., AGS) (Table 1). These diseases reveal that perturbations in DNA recognition can also result in distinct end-organ damage. In many cases, murine models of these diseases recapitulate the organ specificity of the human disease (Table 1). These observations imply that the innate immune system maintains coordinated tissue- and cell-specific responses, the nature of which are the subject of ongoing inquiry. With the mounting evidence supporting the role of DNA sensing in the pathogenesis of several autoinflammatory diseases, the longstanding question again arises as to how endogenous DNA contributes to autoimmune diseases and whether these pathways can be manipulated for therapy.

Lessons learned from monogenic mutations in the intracellular DNA–sensing pathway

Diseases involving TREX1 inactivation. The potential for DNA as a disease-causing agent was demonstrated by mutations in TREX1 (DNase III), which lead to disorders including AGS (21), familial chilblain lupus (CHBL1) (22), retinal vasculopathy with cerebral leukodystrophy (RVCL) (23,24), and a subset of patients with systemic lupus erythematosus (SLE) (25) (Figure 1A and Table 1). TREX1 is an ER-associated 3′–5′ exonuclease with high affinity both for single-stranded DNA and dsDNA (26). TREX1 mutations are frequently observed in familial cases of AGS, which are often misdiagnosed as a congenital viral infection. AGS patients have encephalopathy and severe developmental delay. TREX1 loss-of-function mutations account for a number of the AGS subsets (21), although this complex disease can also be initiated by mutations in other genes regulating RNA

Table 1. Clinical features and murine models of type I interferonopathies*

Disease	Affected protein	Effect on protein	Clinical findings	Mouse model	Murine phenotype
CHBL1	TREX1 D18N, F17S, others	Autosomal-dominant, inactivating mutation	Cutaneous form of SLE (22,29)	No animal model has been described	No mouse model recapitulates the CHBL phenotype
SLE	TREX1 D18N	Loss of function	Splenomegaly, vasculitis, renal disease (25)	TREX1 D18N	SLE-like disease, spontaneous production of autoantibodies (26)
AGS	TREX1	Loss of function	Encephalopathy, seizures, mimic of congenital viral infections (21)	TREX1 knockout	Tissue-specific inflammation targeting the heart, skeletal muscle, tongue, skin, and stomach (31,32)
RCVL	TREX1 frameshift	Carboxy-terminus mutations preserving TREX1 activity	Cerebral leukodystrophy, nonautoimmune retinal vasculopathy (23)	V235fs and D272fs	Autoantibody response to non-nuclear targets (36)
AIPCS	DNase II	Loss of function	Anti-DNA antibodies, anemia, nephritis, arthropathy (38)	DNase I–deficient DNase II/IFNAR-1 double knockout	Fatal anemia (42) Polyarthritis, ANA, splenomegaly (40,41)
SAVI syndrome	STING	Gain of function due to dimerization domain mutations V147L, V147M, N154S, V155M, and G166E	Pulmonary inflammation, cutaneous vasculopathy (46,87)	STING N153S and STING V154M	Pulmonary inflammation and fibrosis, lymphopenia, lymph node collapse, and colitis (54–57)
		Gain of function due to cGAMP-binding site mutations C206Y, R281Q, R284G	Pulmonary inflammation, cutaneous vasculopathy (47,49)	No animal model has been described	Not determined
		Gain of function due to cGAMP-binding site mutation G207E	Cutaneous vasculopathy and thyroid dysfunction (53)	No animal model has been described	Not determined
COPA syndrome	COPA	Loss of trafficking of STING out of Golgi leading to hyperactivation	Clinically similar to SAVI syndrome (60–62)	COPA E241K	Spontaneous T cell activation and T cell–mediated STING-dependent lung disease (60,88)
AGS 8/9	Biallelic mutations in LSM11 and RNU7-1	cGAS/STING activation	Encephalopathy, seizures, mimic of congenital viral infections (28)	No animal model has been described	Not determined

* CHBL1 = familial chilblain lupus; TREX1 = 3′ repair exonuclease 1; SLE = systemic lupus erythematosus; ssDNA = single-stranded DNA; dsDNA = double-stranded DNA; AGS = Aicardi-Goutières syndrome; RVCL = retinal vasculopathy with cerebral leukodystrophy; IFNAR-1 = interferon-α/β receptor subunit 1; ANA = antinuclear antibody; AIPCS = autoinflammatory-pancytopenia syndrome; SAVI = stimulator of interferon genes–associated vasculopathy with onset in infancy; STING = stimulator of interferon genes; COPA = coatomer protein subunit alpha; cGAS = cyclic GMP-AMP synthase.

degradation (27) or histone processing (28). The histone processing defects result in failure to tether cGAS to nucleosomes and downstream cGAS/STING-mediated activation of ISGs (28). The AGS-causing TREX1 mutations cluster within 1 of the 3 exonuclease domains of TREX1 or result in frame shifts that abolish TREX1 catalytic activity (21), highlighting the role of the loss of DNase activity in driving AGS. CHBL is a cutaneous form of lupus that presents with ulcerating lesions in the skin in early childhood. Patients are affected by skin changes and acral ischemia that are induced by exposure to cold. A number of inactivating mutations in TREX1 (frequently affecting Asp18) have been identified in CHBL1 patients (22,29). Noncatalytic mutations in TREX1 have been shown to result in RVCL, a fatal disease of the microvasculature that presents with reduced visual acuity and commonly also presents with neurologic, hepatic, and renal manifestations (24,30). The TREX1 mutations that give rise to RVCL are primarily frame shift mutations in the carboxy-terminus of TREX1, which preserve DNase activity but are proposed to disrupt the interaction between TREX1 and the SET complex, an ER-associated DNA repair complex containing 3 DNases that is critical for TREX1 translocation to the nucleus following oxidative stress (23).

Unlike the human diseases resulting from TREX1 mutations, TREX1-deficient mice exhibit reduced survival and tissue-specific responses in sites including the heart, skeletal muscle, skin, and stomach, while leaving other organs unaffected, suggesting that the downstream effectors of DNA detection are highly context-dependent (31,32). The myocarditis observed in the TREX1-deficient mouse is characterized by leukocyte infiltration in the myocardium, increased IFNβ levels, and production of autoantibodies to the abundant, heart-specific targets of myosin heavy chain 6 and Junctophilin-2 in mice (32,33). However, the stimulus for IFN production in the heart remains unclear and presents little phenotypic overlap with human TREX1-associated diseases (Table 1). However, consistent with the concept that DNA drives this inflammatory response, TREX1-deficient cells demonstrate accumulation of endogenous, extranuclear ssDNA, leading to chronic DNA damage and checkpoint activation (34). In mice, STING deficiency or cGAS deficiency, but not a deficiency of mitochondrial antiviral signaling protein, a key downstream mediator of RNA sensing, rescued the embryonic lethality of the TREX-deficient mouse (32,35), strengthening the link between intracellular DNA and activation of the cGAS/STING pathway in disease pathogenesis.

Murine knockin models of the human point mutations in TREX1 have led to important mechanistic insights into the pathways of disease specificity. The autosomal-dominant mutation TREX1 D18N results in SLE in mice, with spontaneous autoantibody formation to nuclear material, while 3′ frameshift mutations (V235fs and D272fs) exhibit serologic responses to non-nuclear targets [36]). Indeed, the TREX1 D18N knockin mouse, as well as the TREX1-deficient mouse,

exhibit other hallmarks of SLE, including splenomegaly, vasculitis, and renal disease (26,32,37). The disease manifestations stemming from the TREX1 D18N mutations were reversed when mutant mice were crossed with mice deficient in cGAS, including reversal of the inflammation, IFN signature, and aberrant T cell activation, also supporting a pathogenic link to the cGAS/STING pathway (37). Thus, inactivation of TREX1, resulting in superphysiologic amounts of DNA, highlights a role for excess DNA in initiating autoinflammatory disease. However, the tissue-specific reactions leading to heterogeneous downstream disease manifestations is an area needing further investigation.

DNase II and polyarthritis in mice. Like mutations in TREX1 or deficiency of TREX1, depletion of the lysosomal-associated enzyme DNase II also results in tissue-specific pathology. Patients with mutations in DNase II that result in loss of endonuclease activity develop anti-DNA antibodies, liver fibrosis, glomerulonephritis, and deforming arthropathy (38), likely due to the entry of undegraded DNA into the cytosol and the subsequent activation of intracellular DNA–sensing pathways. This disease is catergorized in the OMIM as autoinflammatory-pancytopenia syndrome (OMIM ID no. 619858). These patients also have an increased type I IFN signature and mild anemia (38). This human disease is closely phenocopied in DNase II–deficient mice, including autoantibody production, liver fibrosis, extramedullary hematopoiesis, and anemia (39–41), but these mice also develop spontaneous inflammatory arthritis. Anemia in DNase II–deficient mice leads to embryonic lethality, coincident with the onset of definitive erythropoiesis, which occurs in the liver and requires ejection of nuclei from the developing red blood cells. Presumably, DNase II–deficient macrophages are unable to adequately metabolize DNA, stimulating IFNβ production in the liver. The embryonic lethality of the DNase II–deficient mouse is reversed in mice double deficient in DNase II/interferon-α/β receptor subunit 1 (IFNAR-1) (42), which survive to adulthood. The progressive, spontaneous polyarthritis that these mice develop is driven by the proinflammatory cytokines TNF, IL-6, IL-1, and IL-18 (39–41).

To define the pathways leading to the development of polyarthritis, the DNase II/IFNAR-1–deficient mice were selectively bred to mice lacking functional intracellular DNA-dependent pathways. Specifically, these DNase II/IFNAR-1–deficient mice were bred with mice deficient in AIM2 (41,43), STING (44,45), or the endosomal TLR chaperone Unc-93 homolog B1 (Unc93B1) (41). Arthritis is reduced in mice triple deficient in AIM2 (DNase II/IFNAR-1/AIM2 deficient), due at least in part to reduced levels of IL-18 downstream of the AIM2 inflammasome. In mice triple deficient in STING (DNase II/IFNAR-1/STING deficient) there was almost complete abrogation of joint inflammation (41,43), due to reduced TNF levels and likely also IL-6 levels, both of which are produced upon activation of the STING pathway. Furthermore, STING deficiency in the context of DNase II deficiency (STING/

DNase II–deficient mice) rescued the embryonic lethality of the DNase II–deficient mouse and prevented the development of arthritis (45), demonstrating the importance of the STING pathway in disease pathogenesis in these mice. In contrast, a deficiency in Unc93B1 did not protect the DNase II/IFNAR-1– deficient mice from developing arthritis. However, antinuclear antibody (ANA) development was found to be dependent on Unc93B1 (41), but not on AIM2 or STING. Thus, AIM2 and STING are both dispensable for ANA production but contribute to arthritis pathogenesis. These data in mice highlight distinct pathways leading to specific manifestations of DNA-stimulated autoimmune disease that are independent of type I IFNs. In addition, these models highlight the role of endogenous DNA, and presumably the downstream activation of intracellular DNA sensing, in promoting certain manifestations of autoimmunity, and prompt the question of what the potential role of DNA is as an endogenous danger signal to elicit human autoimmune disease.

SAVI syndrome. In the first report of the autoinflammatory disease SAVI syndrome, 6 children with similar early-onset systemic inflammation primarily affecting cutaneous blood vessels and pulmonary vessels and parenchyma were determined to have autosomal-dominant mutations in *TMEM173*, which encodes the STING protein (46). Since that time, more than 50 patients with mutations in STING have been described (47). These mutations occur either in the STING dimerization domain (V147L, V147M, N154S, V155M, and G166E), the cGAMP-binding domain (C206Y, R281Q, R284G), or in the transmembrane linker region (H72N) (48) and result in constitutive activation of STING (47). SAVI patients present with pulmonary fibrosis, cutaneous vasculopathy, and vasculitis, but the clinical manifestations are heterogeneous. Some patients exhibit autoantibody production, while others have increased susceptibility to infection and/or neurologic or hepatic involvement (49). A newly described class of SAVI patients presenting in adulthood further broadens the spectrum of SAVI syndrome (50). These data underscore the complexity of the STING pathway and the potential importance of other STING-driven responses in disease pathogenesis. Consistent with these findings, treatment of SAVI patients using JAK inhibitors has only been partially successful, highlighting the importance of IFN-independent disease pathways (51,52).

Individual mutations in STING described in both patients and animal models appear to lead to differences in the degree of STING activation or might modulate downstream signaling in cell- and context-dependent manners, resulting in a spectrum of clinical manifestations. For instance, activating mutations, such as G207E, that lie in the cGAMP-binding domain, predominantly result in skin and thyroid manifestations (53). The crystal structure of STING, along with the confirmational changes observed during STING activation, influenced the hypothesis that manifestations of disease result from distinct activation modes by STING (48). Structure–function relationships may explain the milder lung phenotypes seen in certain patients but offers an incomplete explanation as to the heterogeneity of disease. Although it is clear that activation of STING leads to robust autoinflammation, understanding the precise mechanism by which each particular mutation results in clinical disease manifestations has remained a challenge.

With the goal of clarifying mechanisms, mice harboring the SAVI mutations present in humans were generated. Using CRISPR technology, 3 research teams created mice with the 2 most common SAVI mutations (V154M or N153S) (54–56). Homozygosity for either of these SAVI mutations results in embryonic lethality, but SAVI heterozygotes recapitulate many aspects of the human disease, including immune abnormalities and lung inflammation. These mice also develop colitis, a phenotype not described in humans to date (57). All SAVI mutant mouse strains develop lung inflammation, severe lymphopenia and lymph node collapse, as well as some induction of ISGs (54–56,58). Surprisingly, despite the IFN response being a key feature of this class of diseases and the best-studied response in STING signaling, crossing a SAVI mutant mouse with either a mouse deficient in IFNAR or IRF3, a critical transducer of IFN production, reduced the production of most ISGs (54–56,58); however, IFNAR deficiency or IRF3 deficiency failed to rescue lymphocyte dysfunction or the widespread inflammation and fibrosis in the lung (54–56,58).

Clinical manifestations in SAVI overlap with those observed in coatomer protein complex subunit A (COPA) syndrome, a rare monogenic disease arising from mutations in the WD40 domain of the COPA. COPA is a subunit of COPI, which mediates retrograde trafficking from the Golgi to the ER (Figure 1C). Like SAVI patients, COPA syndrome patients exhibit autoinflammatory disease, including interstitial lung disease and an increased expression of ISGs (59), which prompted several independent groups to seek a mechanism linking STING and COPA pathways (60–63). Retention of STING in the Golgi is sufficient for its activation, and these recent studies demonstrate that loss-of-function COPA mutations lead to accumulation of STING in the Golgi and the subsequent production of type I IFN and ISGs. These novel findings should lead to further understanding of the homeostatic regulation of STING.

Potential role of intracellular DNA–sensing pathways in autoimmune disease

Due to the strong associations between intracellular DNA sensing and autoinflammatory diseases, researchers have begun to investigate the role of endogenous DNA in autoimmune disease more broadly. It is of note that >60% of SLE patients have a type I IFN signature (64), and type I IFNs have been implicated in disease pathogenesis (65). While TLR activation likely drives this response, elevated levels of cGAMP have been detected in

peripheral blood mononuclear cells (PBMCs) from 15% of SLE patients ([66]), but not in healthy subjects or in patients with rheumatoid arthritis. Other studies have shown that sera from SLE patients strongly evoke an IFN response in macrophages, a phenomenon proposed to be due to the presence of DNA in apoptotic microvessels ([67]). DNase activity was also found to be reduced in serum samples from SLE patients ([68,69]) and a subset of SLE patients have been identified who are carriers of mutations in DNase I ([68,69]) or DNase1 L3 ([70,71]). The initially described DNase I–deficient mouse developed SLE-like disease, including autoantibody production and kidney damage in the autoimmune-susceptible 129 × C57BL/6 mouse strain, but not on a pure C57BL/6 background ([72,73]). In this mouse model, there was unintentional disruption of TNF receptor–associated protein 1 (TRAP-1)/heat shock protein 75 (HSP-75). An independently generated DNase I–deficient mouse that only targeted Dnase I and did not disrupt TRAP-1/HSP-75 also spontaneously developed an SLE-like disease and recapitulated the female bias seen in the human SLE population ([74]), underscoring the potential contribution of DNA in SLE pathogenesis.

A key question regarding the role of endogenous DNA in stimulating autoimmune disease is the source of the pathogenic, endogenous DNA. Many of the studies discussed thus far involve mutations leading to altered DNA sensing or accrual of endogenous DNA. Recent insights suggest several possible sources of endogenous DNA, including endogenous retroelements, leaked mitochondrial DNA, or uptake of extracellular DNA following tissue damage ([15]). Evidence that cGAS localizes to the nucleus introduces the possibility that nuclear DNA may be a source for cGAS activation ([18–20]). Reduced clearance of defective mitochondria via mitophagy was observed in red blood cells from SLE patients ([75]). When phagocytosed by myeloid cells, mitochondrial DNA from SLE-derived red blood cells stimulated type I IFN production in a cGAS/STING–dependent manner ([75]). In contrast, delivery of DNA or cGAMP through microparticles offers protection against disease in animal models of experimental autoimmune encephalomyelitis and type 1 diabetes ([76,77]). These studies suggest that although endogenous DNA may be a contributing factor to the pathogenesis of certain autoimmune diseases, further studies are needed to better understand its specific role in autoimmunity and the pathways involved and to determine the exact sources of the endogenous DNA at play.

Therapeutic strategies targeting STING activation

The important role that DNA detection plays in host defenses cannot be understated. Therapeutic strategies leading to the activation or inhibition of the STING pathway are in development, including those targeting cGAS, STING, and TBK1. Since these agents have been thoroughly reviewed elsewhere ([78,79]), we highlight a few intriguing STING-targeting agents. The potent

immune stimulatory activity of DNA sensing and cyclic dinucleotides is being leveraged for the treatment of viral infections. For example, 2 recent studies used small-molecule STING agonists to elicit antiviral immunity to SARS–CoV-2 infection ([80,81]). Increasingly, studies support the potential role of DNA sensing as a driver of the antitumor immune response. Accordingly, cyclic dinucleotides as well as small-molecule STING agonists are in clinical trials for the treatment of melanoma and other cancers ([82]).

The growing body of literature implicating aberrant sensing of endogenous DNA in the pathogenesis of autoinflammatory and autoimmune diseases raises the interesting possibility that limiting the activation of DNA-sensing pathways could be a therapeutic approach for the treatment of these diseases. Several small molecules that block STING signaling have been identified. A nitrofuran derivative H-151 covalently binds STING and blocks STING palmitoylation, a critical signal needed for STING trafficking ([83]). H-151 blocks IFN responses in TREX1-deficient mice ([83]). Another small-molecule inhibitor of STING, SN-011, blocks inflammation and autoimmune disease manifestations in TREX1-deficient mice ([84]). A peptide inhibitor of STING has also recently been described that acts in a stromal interaction molecule 1 (STIM1)–dependent manner to block STING trafficking from the ER to the Golgi. This peptide, ISD017, inhibits known STING downstream activities and has no overt toxic effects on cells. Interestingly, ISD017 blocks STING activation in mice and has efficacy in a mouse model of lupus. Lastly, ISD017 also reduced IFN and cytokine responses in PBMCs from lupus patients ([85]). Beyond STING, studies are also underway to identify and study cGAS inhibitors in both monogenic diseases and more complex diseases ([86]). Collectively, these observations highlight the therapeutic potential of targeting the cGAS/STING pathway for the treatment of several diseases and the need for further study to investigate methods to specifically harness these therapeutic approaches.

Conclusion

Studies of autoinflammatory diseases have improved our understanding of the complexities of the innate immune system and have demonstrated how alterations in innate immune pathways can drive human disease. In particular, these diseases highlight that intracellular DNA both serves as a potent activator of the immune system in response to pathogens and has the power to elicit autoinflammation. Detection of intracellular DNA is a core mechanism leading to activation of the innate immune system. Yet, alterations in DNA sensing pathways can yield unique disease manifestations in terms of organ involvement. This diversity is highlighted by the heterogeneity of tissue involvement in the family of diseases caused by alterations in TREX1. Moreover, site-specific mutations yield unique pathologies, as demonstrated

by the SAVI-activating mutations. It follows that a network of mechanisms must exist to regulate pathogen- and tissue-specific responses. Pharmaceutical agents targeting activation or inhibition of STING are early examples of utilizing this powerful pathway for the clinical management of disease. It is likely that future drug design will leverage other members of intracellular DNA–sensing pathways to generate more selective therapies (e.g., cGAS). Several mechanistic questions warrant exploration in this fascinating and growing field that will further refine these therapies. Future research will likely lead to an improved understanding of the regulatory mechanisms that refine the immune response to intracellular DNA and address whether the intracellular DNA–sensing pathways are foundational in other rheumatic diseases.

AUTHOR CONTRIBUTIONS

All authors were involved in drafting the article or revising it critically for important intellectual content, and all authors approved the final version to be published.

REFERENCES

1. Nigrovic PA, Lee PY, Hoffman HM. Monogenic autoinflammatory disorders: conceptual overview, phenotype, and clinical approach. J Allergy Clin Immunol 2020;146:925–37.

2. Cetin Gedik K, Lamot L, Romano M, Demirkaya E, Piskin D, Torreggiani S, et al. The 2021 EULAR and ACR points to consider for diagnosis and management of autoinflammatory type I interferonopathies: CANDLE/PRAAS, SAVI and AGS. Ann Rheum Dis 2022;81:601–13.

3. Tan X, Sun L, Chen J, Chen ZJ. Detection of microbial infections through innate immune sensing of nucleic acids. Annu Rev Microbiol 2018;72:447–8.

4. Mankan AK, Schmidt T, Chauhan D, Goldeck M, Höning K, Gaidt M, et al. Cytosolic RNA: DNA hybrids activate the cGAS-STING axis. EMBO J 2014;33:2937–46.

5. Kawai T, Akira S. The role of pattern-recognition receptors in innate immunity: update on Toll-like receptors. Nat Immunol 2010;11:373–84.

6. Ishii KJ, Coban C, Kato H, Takahashi K, Torii Y, Takeshita F, et al. A Toll-like receptor-independent antiviral response induced by double-stranded B-form DNA. Nat Immunol 2006;7:40–8.

7. Stetson DB, Medzhitov R. Recognition of cytosolic DNA activates an IRF3-dependent innate immune response. Immunity 2006;24:93–103.

8. Zhu H, Zhao M, Chang C, Chan V, Lu Q, Wu H. The complex role of AIM2 in autoimmune diseases and cancers. Immun Inflamm Dis 2021;9:649–65.

9. Xiao TS, Fitzgerald KA. The cGAS-STING pathway for DNA sensing [review]. Mol Cell 2013;51:135–9.

10. Wu J, Sun L, Chen X, Du F, Shi H, Chen C, et al. Cyclic GMP-AMP is an endogenous second messenger in innate immune signaling by cytosolic DNA. Science 2013;339:826–30.

11. Ishikawa H, Ma Z, Barber GN. STING regulates intracellular DNA-mediated, type I interferon-dependent innate immunity. Nature 2009;461:788–92.

12. Hornung V, Latz E. Intracellular DNA recognition [review]. Nat Rev Immunol 2010;10:123–130.

13. Liu S, Cai X, Wu J, Cong Q, Chen X, Li T, et al. Phosphorylation of innate immune adaptor proteins MAVS, STING, and TRIF induces IRF3 activation. Science 2015;347:aaa2630.

14. Agalioti T, Lomvardas S, Parekh B, Yie J, Maniatis T, Thanos D. Ordered recruitment of chromatin modifying and general transcription factors to the IFN-β promoter. Cell 2000;103:667–78.

15. Motwani M, Pesiridis S, Fitzgerald KA. DNA sensing by the cGAS-STING pathway in health and disease [review]. Nat Rev Genet 2019;20:657–74.

16. Wu J, Yan N. No longer a one-trick pony: STING signaling activity beyond interferon. J Mol Biol 2021;434:167257.

17. Wu J, Dobbs N, Yang K, Yan N. Interferon-independent activities of mammalian STING mediate antiviral response and tumor immune evasion. Immunity 2020;53:115–126.

18. Volkman HE, Cambier S, Gray EE, Stetson DB. Tight nuclear tethering of cGAS is essential for preventing autoreactivity. Elife 2019;8:e47491.

19. Gentili M, Lahaye X, Nadalin F, Nader GP, Lombardi EP, Herve S, et al. The N-terminal domain of cGAS determines preferential association with centromeric DNA and innate immune activation in the nucleus. Cell Rep 2019;26:2377–93.

20. De Oliveira Mann CC, Hopfner KP. Nuclear cGAS: guard or prisoner? EMBO J 2021;40:e108293.

21. Crow YJ, Hayward BE, Parmar R, Robins P, Leitch A, Ali M, et al. Mutations in the gene encoding the 3′-5′ DNA exonuclease TREX1 cause Aicardi-Goutieres syndrome at the AGS1 locus. Nat Genet 2006;38:917–20.

22. Rice G, Newman WG, Dean J, Patrick T, Parmar R, Flintoff K, et al. Heterozygous mutations in TREX1 cause familial chilblain lupus and dominant Aicardi-Goutieres syndrome. Am J Hum Genet 2007;80:811–5.

23. Richards A, van den Maagdenberg AM, Jen JC, Kavanagh D, Bertram P, Spitzer D, et al. C-terminal truncations in human 3′-5′ DNA exonuclease TREX1 cause autosomal dominant retinal vasculopathy with cerebral leukodystrophy. Nat Genet 2007;39:1068–70.

24. Stam AH, Kothari PH, Shaikh A, Gschwendter A, Jen JC, Hodgkinson S, et al. Retinal vasculopathy with cerebral leukoencephalopathy and systemic manifestations. Brain 2016;139:2909–22.

25. Lee-Kirsch MA, Gong M, Chowdhury D, Senenko L, Engel K, Lee YA, et al. Mutations in the gene encoding the 3′–5′ DNA exonuclease TREX1 are associated with systemic lupus erythematosus. Nat Genet 2007;39:1065–7.

26. Grieves JL, Fye JM, Harvey S, Grayson JM, Hollis T, Perrino FW. Exonuclease TREX1 degrades double-stranded DNA to prevent spontaneous lupus-like inflammatory disease. Proc Natl Acad Sci U S A 2015;112:5117–22.

27. Crow YJ, Leitch A, Hayward BE, Garner A, Parmar R, Griffith E, et al. Mutations in genes encoding ribonuclease H2 subunits cause Aicardi-Goutières syndrome and mimic congenital viral brain infection. Nat Genet 2006;38:910–6.

28. Uggenti C, Lepelley A, Depp M, Badrock AP, Rodero MP, El-Daher MT, et al. cGAS-mediated induction of type I interferon due to inborn errors of histone pre-mRNA processing. Nat Genet 2020;52:1364–72.

29. Yi C, Li Q, Xiao J. Familial chilblain lupus due to a novel mutation in TREX1 associated with Aicardi-Goutie'res syndrome. Pediatr Rheumatol Online J 2020;18:32.

30. De Boer I, Pelzer N, Terwindt G. Retinal vasculopathy with cerebral leukoencephalopathy and systemic manifestations. In: Adam MP, Ardinger HH, Pagon RA, Wallace SE, Bean LJ, Gripp KW, et al, editors. GeneReviews. Seattle: University of Washington; 1993.

31. Morita M, Stamp G, Robins P, Dulic A, Rosewell I, Hrivnak G, et al. Gene-targeted mice lacking the Trex1 (DNase III) 3′→5′ DNA

exonuclease develop inflammatory myocarditis. Mol Cell Biol 2004; 24:6719–27.

32. Gall A, Treuting P, Elkon KB, Loo YM, Gale M Jr, Barber GN, et al. Autoimmunity initiates in nonhematopoietic cells and progresses via lymphocytes in an interferon-dependent autoimmune disease. Immunity 2012;36:120–31.

33. Stetson DB, Ko JS, Heidmann T, Medzhitov R. Trex1 prevents cell-intrinsic initiation of autoimmunity. Cell 2008;134:587–98.

34. Yang YG, Lindahl T, Barnes DE. Trex1 exonuclease degrades ssDNA to prevent chronic checkpoint activation and autoimmune disease. Cell 2007;131:873–86.

35. Gray EE, Treuting PM, Woodward JJ, Stetson DB. Cutting edge: cGAS is required for lethal autoimmune disease in the Trex1-deficient mouse model of Aicardi-Goutières syndrome. J Immunol 2015;195:1939–43.

36. Sakai T, Miyazaki T, Shin DM, Kim YS, Qi CF, Fariss R, et al. DNase-active TREX1 frame-shift mutants induce serologic autoimmunity in mice. J Autoimmun 2017;81:13–23.

37. Xiao N, Wei J, Xu S, Du H, Huang M, Zhang S, et al. cGAS activation causes lupus-like autoimmune disorders in a TREX1 mutant mouse model. J Autoimmun 2019;100:84–94.

38. Rodero MP, Tesser A, Bartok E, Rice GI, Mina ED, Depp M, et al. Type I interferon-mediated autoinflammation due to DNase II deficiency. Nat Commun 2017;8:2176.

39. Kawane K, Tanaka H, Kitahara Y, Shimaoka S, Nagata S. Cytokine-dependent but acquired immunity-independent arthritis caused by DNA escaped from degradation. Proc Natl Acad Sci U S A 2010; 107:19432–7.

40. Kawane K, Ohtani M, Miwa K, Kizawa T, Kanbara Y, Yoshioka Y, et al. Chronic polyarthritis caused by mammalian DNA that escapes from degradation in macrophages. Nature 2006;443:998–1002.

41. Baum R, Sharma S, Carpenter S, Li QZ, Busto P, Fitzgerald KA, et al. Cutting edge: AIM2 and endosomal TLRs differentially regulate arthritis and autoantibody production in DNase II-deficient mice. J Immunol 2015;194:873–7.

42. Yoshida H, Okabe Y, Kawane K, Fukuyama H, Nagata S. Lethal anemia caused by interferon-β produced in mouse embryos carrying undigested DNA. Nat Immunol 2005;6:49–56.

43. Jakobs C, Perner S, Hornung V. AIM2 drives joint inflammation in a self-DNA triggered model of chronic polyarthritis. PloS One 2015;10: e0131702.

44. Baum R, Sharma S, Organ JM, Jakobs C, Hornung V, Burr DB, et al. STING contributes to abnormal bone formation induced by deficiency of DNase II in mice. Arthritis Rheumatol 2017;69:460–71.

45. Ahn J, Gutman D, Saijo S, Barber GN. STING manifests self DNA-dependent inflammatory disease. Proc Natl Acad Sci U S A 2012; 109:19386–91.

46. Liu Y, Jesus AA, Marrero B, Yang D, Ramsey SE, Sanchez GA, et al. Activated STING in a vascular and pulmonary syndrome. N Engl J Med 2014;371:507–18.

47. Fremond ML, Hadchouel A, Berteloot L, Melki I, Bresson V, Barnabei L, et al. Overview of STING-associated vasculopathy with onset in infancy (SAVI) among 21 patients. J Allergy Clin Immunol Pract 2021;9:803–18.

48. Lin B, Torreggiani S, Kahle D, Rumsey DG, Wright BL, Montes-Cano MA, et al. Case report: novel SAVI-causing variants in STING1 expand the clinical disease spectrum and suggest a refined model of STING activation. Front Immunol 2021;12:636225.

49. Melki I, Rose Y, Uggenti C, Van Eyck L, Frémond ML, Kitabayashi N, et al. Disease-associated mutations identify a novel region in human STING necessary for the control of type I interferon signaling. J Allergy Clin Immunol 2017;140:543–52.

50. Staels F, Betrains A, Doubel P, Willemsen M, Cleemput V, Vanderschueren S, et al. Adult-onset ANCA-associated vasculitis in SAVI: extension of the phenotypic spectrum, case report and review of the literature. Front Immunol 2020;11:575219.

51. Volpi S, Insalaco A, Caorsi R, Santori E, Messia V, Sacco O, et al. Efficacy and adverse events during janus kinase inhibitor treatment of SAVI syndrome. J Clin Immunol 2019;39:476–85.

52. Banday AZ, Jindal AK, Singh S. Correspondence on 'Points to consider for the treatment of immune-mediated inflammatory diseases with Janus kinase inhibitors: a consensus statement.' Ann Rheum Dis doi:10.1136/annrheumdis-2021-219890 2021. E-pub ahead of print.

53. Keskitalo S, Haapaniemi E, Einarsdottir E, Rajamäki K, Heikkilä H, Ilander M, et al. Novel TMEM173 mutation and the role of disease modifying alleles. Front Immunol 2019;10:2770.

54. Motwani M, Pawaria S, Bernier J, Moses S, Henry K, Fang T, et al. Hierarchy of clinical manifestations in SAVI N153S and V154M mouse models. Proc Natl Acad Sci U S A 2019;116:7941–50.

55. Bouis D, Kirstetter P, Arbogast F, Lamon D, Delgado V, Jung S, et al. Severe combined immunodeficiency in stimulator of interferon genes (STING) V154M/wild-type mice. J Allergy Clin Immunol 2019;143: 712–25.

56. Warner JD, Irizarry-Caro RA, Bennion BG, Ai TL, Smith AM, Miner CA, et al. STING-associated vasculopathy develops independently of IRF3 in mice. J Exp Med 2017;214:3279–92.

57. Shmuel-Galia L, Humphries F, Lei X, Ceglia S, Wilson R, Jiang Z, et al. Dysbiosis exacerbates colitis by promoting ubiquitination and accumulation of the innate immune adaptor STING in myeloid cells. Immunity 2021;54:1137–53.

58. Siedel H, Roers A, Rösen-Wolff A, Luksch H. Type I interferon-independent T cell impairment in a Tmem173 N153S/WT mouse model of STING associated vasculopathy with onset in infancy (SAVI). Clin Immunol 2020;216:108466.

59. Volpi S, Tsui J, Mariani M, Pastorino C, Caorsi R, Sacco O, et al. Type I interferon pathway activation in COPA syndrome. Clin Immunol 2018; 187:33–6.

60. Deng Z, Chong Z, Law CS, Mukai K, Ho FO, Marintu T, et al. A defect in COPI-mediated transport of STING causes immune dysregulation in COPA syndrome. J Exp Med 2020;217:e20201045.

61. Lepelley A, Martin-Niclós MJ, Le Bihan M, Marsh JA, Uggenti C, Rice GI, et al. Mutations in COPA lead to abnormal trafficking of STING to the Golgi and interferon signaling. J Exp Med 2020;217: e20200600.

62. Kato T, Yamamoto M, Honda Y, Orimo T, Sasaki I, Murakami K, et al. Augmentation of STING-induced type I interferon production in COPA syndrome. Arthritis Rheumatol 2021;73:2105–15.

63. Steiner A, Schaale HK, Prigione I, De Nardo D, Dagley LF, Yu CH, et al. Activation of STING due to COPI-deficiency [preprint]. bioRxiv 2021.

64. Crow MK. Type I interferon in the pathogenesis of lupus. J Immunol 2014;192:5459–68.

65. Rönnblom L, Leonard D. Interferon pathway in SLE: one key to unlocking the mystery of the disease. Lupus Sci Med 2019;6: e000270.

66. An J, Durcan L, Karr RM, Briggs TA, Rice GI, Teal TH, et al. Expression of cyclic GMP-AMP synthase in patients with systemic lupus erythematosus. Arthritis Rheumatol 2017;69:800–7.

67. Kato Y, Park J, Takamatsu H, Konaka H, Aoki W, Aburaya S, et al. Apoptosis-derived membrane vesicles drive the cGAS-STING pathway and enhance type I IFN production in systemic lupus erythematosus. Ann Rheum Dis 2018;77:1507–15.

68. Yasutomo K, Horiuchi T, Kagami S, Tsukamoto H, Hashimora C, Urushihara M, et al. Mutation of DNASE1 in people with systemic lupus erythematosus. Nat Genet 2001;28:313–4.

69. Bodaño A, Amarelo J, González A, Gómez-Reino JJ, Conde C. Novel DNASE I mutations related to systemic lupus erythematosus. Arthritis Rheum 2004;50:4070–1.

70. Zervou MI, Andreou A, Matalliotakis M, Spandidos DA, Goulielmos GN, Eliopoulos EE. Association of the DNASE1L3 rs35677470 polymorphism with systemic lupus erythematosus, rheumatoid arthritis and systemic sclerosis: structural biological insights. Mol Med Rep 2020;22:4492–8.

71. Carbonella A, Mancano G, Gremese E, Alkuraya FS, Patel N, Gurrieri F, et al. An autosomal recessive DNASE1L3-related autoimmune disease with unusual clinical presentation mimicking systemic lupus erythematosus. Lupus 2017;26:768–72.

72. Napirei M, Gultekin A, Kloeckl T, Moroy T, Frostegard J, Mannherz HG. Systemic lupus-erythematosus: deoxyribonuclease 1 in necrotic chromatin disposal. Int J Biochem Cell Biol 2006;38:297–306.

73. Napirei M, Karsunky H, Zevnik B, Stephan H, Mannherz HG, Möröy T. Features of systemic lupus erythematosus in Dnase1-deficient mice. Nat Genet 2000;25:177–81.

74. Kenny EF, Raupach B, Abu Abed U, Brinkmann V, Zychlinsky A. Dnase1-deficient mice spontaneously develop a systemic lupus erythematosus-like disease. Eur J Immunol 2019;49:590–9.

75. Caielli S, Cardenas J, de Jesus AA, Baisch J, Walters L, Blanck JP, et al. Erythroid mitochondrial retention triggers myeloid-dependent type I interferon in human SLE. Cell 2021;184:4464–79.

76. Johnson BM, Uchimura T, Gallovic MD, Thamilarasan M, Chou WC, Gibson SA, et al. STING agonist mitigates experimental autoimmune encephalomyelitis by stimulating Type I IFN-dependent and -independent immune-regulatory pathways. J Immunol 2021;206:2015–28.

77. Lemos H, Mohamed E, Huang L, Chandler PR, Ou R, Pacholczyk R, et al. Stimulator of interferon genes agonists attenuate type I diabetes progression in NOD mice. Immunology 2019;158:353–61.

78. An J, Woodward JJ, Lai W, Minie M, Sun X, Tanaka L, et al. Inhibition of cyclic GMP-AMP synthase using a novel antimalarial drug derivative in Trex1-deficient mice. Arthritis Rheumatol 2018;70:1807–19.

79. Ding C, Song Z, Shen A, Chen T, Zhang A. Small molecules targeting the innate immune cGAS–STING–TBK1 signaling pathway. Acta Pharm Sin B 2020;10:2272–98.

80. Li M, Ferretti M, Ying B, Descamps H, Lee E, Dittmar M, et al. Pharmacological activation of STING blocks SARS-CoV-2 infection. Sci Immunol 2021;6:eabi9007.

81. Humphries F, Shmuel-Galia L, Jiang Z, Wilson R, Landis P, Ng SL, et al. A diamidobenzimidazole STING agonist protects against SARS-CoV-2 infection. Sci Immunol 2021;6:eabi9002.

82. Su T, Zhang Y, Valerie K, Wang XY, Lin S, Zhu G. STING activation in cancer immunotherapy. Theranostics 2019;9:7759–71.

83. Haag SM, Gulen MF, Reymond L, Gibelin A, Abrami L, Decout A, et al. Targeting STING with covalent small-molecule inhibitors. Nature 2018;559:269–73.

84. Hong Z, Mei J, Li C, Bai G, Maimaiti M, Hu H, et al. STING inhibitors target the cyclic dinucleotide binding pocket. Proc Natl Acad Sci U S A 2021;118:e2105465118.

85. Prabakaran T, Troldborg A, Kumpunya S, Alee I, Marinković, Windross SJ, et al. A STING antagonist modulating the interaction with STIM1 blocks ER-to-Golgi trafficking and inhibits lupus pathology. EBioMedicine 2021;66:103314.

86. Decout A, Katz JD, Venkatraman S, Ablasser A. The cGAS-STING pathway as a therapeutic target in inflammatory diseases. Nat Rev Immunol 2021;21:548–69.

87. König N, Fiehn C, Wolf C, Schuster M, Costa EC, Tüngler V, et al. Familial chilblain lupus due to a gain-of-function mutation in STING. Ann Rheum Dis 2017;76:468–72.

88. Deng Z, Law CS, Ho FO, Wang KM, Jones KD, Shin JS, et al. A defect in thymic tolerance causes T cell-mediated autoimmunity in a murine model of COPA syndrome. J Immunol 2020;204:2360–73.

AMERICAN COLLEGE
of **RHEUMATOLOGY**
Empowering Rheumatology Professionals

NOTES FROM THE FIELD

The Transition From Residency to Fellowship: Enhancing Training by Increasing Transparency

Eli M. Miloslavsky[1] and Anisha B. Dua[2] iD

INTRODUCTION

The events of the last several years have highlighted the challenges of bias and systemic racism and the importance of trainee wellness and support within graduate medical education. Coupled with the rapid shift to virtual interviews, these events spotlight a critical point in training at which residents transition into fellowship programs. Each trainee enters a fellowship program with a unique background and skillset, which can make it challenging for a program to meet the needs of its fellows. In order to provide an ideal training environment, the residency-to-fellowship transition process should ensure an optimal match between the program and the candidate and mitigate bias inherent to the application process (pre–match phase). Additionally, the transition process should facilitate rapid and accurate learner assessment and enable programs to provide an appropriate level of support for their accepted candidates (post–match phase). However, the current process is not optimized to accomplish these goals.

There has been a robust national conversation regarding the transition from medical school to residency, culminating with a recent report by the Coalition for Physician Accountability (CoPA) (1). This initiative outlined important goals such as increasing transparency in the application process, better defining competencies and assessment metrics, addressing inequities, and improving the post–match transition process. The residency-to-fellowship transition faces many of the same challenges. Herein, we review the major barriers to an optimal transition process and propose potential solutions.

PRE–MATCH PHASE: FELLOWSHIP PREPARATION AND THE APPLICATION PROCESS

Student/resident performance assessment. An optimal application process would ensure the best match between the applicant and the program while minimizing bias, inequity, stress, and financial expenditure. However, emerging evidence suggests that the core assessments program directors use in fellow selection have significant limitations, including bias and structural racism.

The residency training program of an applicant is one of the most important factors in a fellowship application. The clinical training and opportunities for research, mentorship, and leadership are highly dependent on where the candidate trained in residency (2). However, the key determinants of the residency match, such as clerkship grades, United States Medical Licensing Examination (USMLE) scores, and Alpha Omega Alpha (AΩA) membership, have all been shown to have significant biases and limitations. Moreover, these metrics are also used in the fellowship application process, amplifying their impact. USMLE scores have been associated with performance on in-training and certification exams; however, USMLE scores have not been shown to predict achievement of competencies during residency training (3). A study of more than 45,000 medical students found that USMLE Step scores were lower among underrepresented in medicine (URiM) students and female students as compared to White male students, suggesting possible bias (4). Clerkship grades are subject to shortcomings in assessment instruments, differing criteria for grading across schools, and variability in faculty evaluation skills. Evidence suggests that there is also systemic racial bias in clerkship grading and selection of candidates for AΩA membership, with a study reporting that Black and Asian medical students were less likely to be awarded AΩA membership than White medical students after controlling for USMLE Step 1 scores and extracurricular activities (adjusted odds ratio for Black students 0.16 [95% confidence interval (95% CI) 0.07–0.37]; adjusted odds ratio for Asian students 0.52 [95% CI 0.42–0.65]) (5).

Letters of recommendation are challenging to interpret because they are highly subjective and can lack substantiating objective criteria. These letters of recommendation may not be comparable across residents because of variations in the source of the letters, whether written by an individual, who may write only 1 letter or a few letters each year, or by a program director, who may be accustomed to writing multiple letters each year. Even letters written by program directors that adhere to the guidelines for standardized letters of recommendation have demonstrated the presence of race and sex bias, with more use of doubt-raising

[1]Eli M. Miloslavsky, MD: Massachusetts General Hospital, Boston; [2]Anisha B. Dua, MD, MPH: Northwestern University Hospital, Chicago, Illinois.

Author disclosures are available at https://onlinelibrary.wiley.com/action/downloadSupplement?doi=10.1002%2Fart.42158&file=art42158-sup-0001-Disclosureform.pdf.

Address correspondence to Anisha Dua, MD, MPH, Northwestern University, Department of Medicine, Galter Pavilion, 675 North St Clair Street, Suite 14-100, Chicago, IL 60611. Email: Anisha.dua@northwestern.edu.

language and terms describing behaviors of empathy and inter-personal skills in letters for URiM applicants, which are 2 types of language that have been negatively associated with hiring in academia (6). Program directors in particular may have a conflict of interest between accurately describing the skills of their trainees and enhancing the reputation of the residency program. However, we would argue that increased transparency would garner trust in the residency program and minimize the likelihood of applicants matching in programs where they may struggle.

Away rotations also introduce inequity into the residency-to-fellowship transition process, as financial constraints and flexibility may disproportionately affect residents who are from underprivileged backgrounds or groups who are URiM. These inequities may particularly impact residents in smaller programs that do not have structured rheumatology rotations. In sum, the metrics in the current application process for both residency and fellowship programs have drawbacks and may disadvantage students who are URiM, as well as students whose relative performance improves later in medical school, thereby limiting the potential for an optimal match between the applicant and the program. Awareness of these limitations and working to reduce bias in assessment are important steps in optimizing the fellowship program application process.

Fellowship applications and interviews. Fellowship programs often receive more applications than can be meaningfully reviewed, and applications may lack discrete details that would help to meaningfully differentiate between similar candidates, making holistic review challenging. With a consistently increasing volume of applicants per fellowship spot (7), filters (such as AΩA and exam scores) may be more frequently used to identify candidates who meet selection criteria. The use of these filters in the application review process can perpetuate bias (5). Utilizing best practices during application screening and during the interview process may ameliorate these challenges (Table 1).

From a national perspective, and mirroring recommendations set forth by CoPA, specialty-specific best practices for recruitment should be considered in order to increase diversity across the educational continuum, and this information should be disseminated to program directors, residency programs, and institutions. Further, the development of a database of fellowship program applicants that is widely accessible, reliable, and searchable for the characteristics (demographics, geography, scores, degree, visa status, and other areas of interest) of individuals who applied, were interviewed, were ranked, and matched for each subspecialty fellowship program would enhance transparency and enable applicants to focus more on the nature of programs to which they should apply. This should be available at no cost to applicants and their advisors. Career advising is nuanced and can also introduce conflicts of interest. Reflective and honest discussion between applicants and their advisors, combined with accurate, transparent portrayal of information by programs, can enhance the value and outcomes of the application process.

The fellowship program application process is further confounded by the ways in which interviews are offered to candidates.

Table 1. Suggested best practices for fellowship program application screening and interviews

Best practice	How to implement best practice
Application screening	
Determine program values and priorities	Defining these attributes with input from faculty participating in recruitment can help create a shared value model and enable the program to focus on applicant attributes that best match the mission of the program.
Maximize the utility of data in the application	Understanding the meaning of "code words" and tiered rankings in the program director's letter across years may allow for direct comparison of applicants. Triangulating performance data from medical school, residency, and letters of recommendation can shift focus away from outlier data.
Limit bias	Strategies such as implicit bias training, screening without applicant photos, and utilizing multiple screeners may help to reduce bias inherent in the screening process.
Interviews*	
Increase standardization and limit bias	Utilizing standard interview questions or multiple mini interviews as well as blinding interviewers to parts of the application that may introduce bias (USMLE scores, AΩA) are strategies that can limit interviewer bias.
Limit the impact of technology and the applicant's living situation	Provide training and support for both applicants and faculty around the use of technology and increased cognitive load present during virtual interviews. Allow make-up opportunities for interviews disrupted by technology failure.

* For more details, see refs. 14 and 15. USMLE = United States Medical Licensing Examination; AΩA = Alpha Omega Alpha.

The process by which interviews are offered varies from program to program and can be unnecessarily complex, with little regulation or structure. This can lead to increased applicant anxiety, "hoarding" of interview invitations, and hindering of the mutual interests of applicants and fellowship programs. Equity and fairness for candidates and fellowship programs could be improved by the implementation of standards for the interview offer and acceptance, including standards for the timing and methods of communication. In residency programs, there has been discussion of implementing an "early match" process for applicants and potentially limiting the number of interviews each applicant may attend. While this could significantly level the playing field by redistributing interview slots to other interested candidates, it could also have negative

consequences, such as potentially increasing unmatched programs or applicants, or limiting opportunities for some candidates to fully explore potential programs, mentors, and training resources. A coordinated, informed, and concerted effort from all stakeholders in the residency-to-fellowship transition process will be needed to minimize biases, enhance opportunities, and optimize the match process for fellowship applicants and programs.

POST–MATCH PHASE: TRANSITION TO FELLOWSHIP

In addition to ensuring the best match between the fellowship program and the applicant, residency assessment metrics should help fellowship programs train fellows effectively. Further complicating the frequent lack in fellowship applications of detailed, objective, and actionable data on resident performance is the fact that resident evaluation over the final year is not disclosed to fellowship programs. Studies suggest that milestone ratings in residency correlate with milestone ratings in fellowship (8), but that milestone ratings may go down from the end of residency to the beginning of fellowship (9). Therefore, a mechanism that allows residency programs to provide fellowship programs with data on resident performance over the final year would help facilitate the assessment of fellows and address the differences in ratings with trainees, thus furthering mutual understanding and buy-in.

Individualized learning plans (ILPs) developed by residency programs and shared with the fellowship program would further enhance the residency-to-fellowship handover (10). The amount of time new fellows must devote to becoming familiar with a new institution, relocating to a new geographic area, and preparing for the Internal Medicine board exam makes the rapid and accurate assessment of new fellows challenging. Further, the ability of new fellows to be effective partners in developing a learning plan may be limited. Studies have demonstrated that learners, particularly those who are struggling, can lack the ability to effectively assess their skills (11). Fellows may also be hesitant to share their learning needs and perceived weaknesses with their new training program. An ILP is a learner-directed tool with which trainees identify their personal educational goals, perform self-evaluation in competencies and/or milestones, and create actionable objectives in consultation with faculty that are reviewed periodically in order to enhance the trainee's professional development (12). An ILP, agreed on by both the trainee and the residency training program, that is provided transparently to the fellowship program would facilitate early assessment and partnering with the trainee to develop and carry out a learning plan. While there is a theoretical concern that such a process would influence fellow assessment, a recent study using simulated encounters suggested that an educational handover does not influence subsequent assessment (13).

CONCLUSION

Limitations in assessment instruments, in the application process, and in the communication of residents' strengths and areas of development hinder the ability of fellowship programs to provide optimal training. More objective and transparent assessment of residents, optimization of the application process, and the sharing of resident evaluations and ILPs between the residency and fellowship programs after the match may enhance the residency-to-fellowship transition, help limit the perpetuation of health disparities and lack of diversity in the rheumatology workforce, and positively impact trainees, faculty, and most importantly our patients.

REFERENCES

1. Coalition for Physician Accountability. Initial summary report and preliminary recommendations of the undergraduate medical education to graduate medical education review committee (UGRC), 2021. URL: https://physicianaccountability.org/wp-content/uploads/2021/04/UGRC-Initial-Summary-Report-and-Preliminary-Recommendations-1.pdf.

2. Krueger CA, Helms JR, Bell AJ, Israel H, Cannada LK. How the reputation of orthopaedic residency programs is associated with orthopaedic fellowship match results. J Bone Joint Surg Am 2020;102:e28.

3. Prober CG, Kolars JC, First LR, Melnick DE. A plea to reassess the role of United States medical licensing examination step 1 scores in residency selection. Acad Med 2016;91:12–5.

4. Rubright JD, Jodoin M, Barone MA. Examining demographics, prior academic performance, and United States medical licensing examination scores. Acad Med 2019;94:364–70.

5. Boatright D, Ross D, O'Connor P, Moore E, Nunez-Smith M. Racial disparities in medical student membership in the AΩA honor society. JAMA Intern Med 2017;177:659–65.

6. Zhang N, Blissett S, Anderson D, O'Sullivan P, Qasim A. Race and gender bias in internal medicine program director letters of recommendation. J Grad Med Educ 2021;13:335–44.

7. The National Resident Matching Program. Fellowship Match Data & Reports, 2021. URL: https://www.nrmp.org/fellowship-match-data/.

8. Heath JK, Wang T, Santhosh L, Denson JL, Holmboe E, Yamazaki K, et al. Longitudinal milestone assessment extending through subspecialty training: the relationship between ACGME internal medicine residency milestones and subsequent pulmonary and critical care fellowship milestones. Acad Med 2021;96:1603–8.

9. Sawyer T, Gray M, Chabra S, Johnston LC, Carbajal MM, Gilliam-Krakauer M, et al. Milestone level changes from residency to fellowship: a multicenter cohort study. J Grad Med Educ 2021;13:377–84.

10. Morgan HK, Mejicano GC, Skochelak S, Lomis K, Hawkins R, Tunkel AR, et al. A responsible educational handover: improving communication to improve learning. Acad Med 2020;95:194–9.

11. Kruger J, Dunning D. Unskilled and unaware of it: how difficulties in recognizing one's own incompetence lead to inflated self-assessments. J Pers Soc Psychol 1999;77:1121–34.

12. Li ST, Burke AE. Individualized learning plans: basics and beyond. Acad Pediatr 2010;10:289–92.

13. Dory V, Danoff D, Plotnick LH, Cummings BA, Gomez-Garibello C, Pal NE, et al. Does educational handover influence subsequent assessment? Acad Med 2021;96:118–25.

14. Marbin J, Hutchinson YV, Schaeffer S. Avoiding the virtual pitfall: identifying and mitigating biases in graduate medical education videoconference interviews. Acad Med 2021. doi: 10.1097/ACM.0000000000003914. E-pub ahead of print.

15. Huppert LA, Hsiao EC, Cho KC, Marquez C, Chaudhry RI, Frank J, et al. Virtual interviews at graduate medical education training programs: determining evidence-based best practices. Acad Med 2020. doi: 10.1097/ACM.0000000000003868. E-pub ahead of print.

The Efficacy of Short-Term Bridging Strategies With High- and Low-Dose Prednisolone on Radiographic and Clinical Outcomes in Active Early Rheumatoid Arthritis: A Double-Blind, Randomized, Placebo-Controlled Trial

Dietmar Krause,[1] Anna Mai,[2] Renate Klaassen-Mielke,[2] Nina Timmesfeld,[2] Ulrike Trampisch,[2] Henrik Rudolf,[2] Xenofon Baraliakos,[3] Elmar Schmitz,[4] Claas Fendler,[5] Claudia Klink,[6] Stephanie Boeddeker,[7] Ertan Saracbasi-Zender,[8] Hans-Joachim Christoph,[9] Manfred Igelmann,[10] Hans-Juergen Menne,[11] Albert Schmid,[12] Rolf Rau,[13] Siegfried Wassenberg,[14] Nilüfer Sonuc,[15] Claudia Ose,[16] Carmen Schade-Brittinger,[17] Hans J. Trampisch,[2] and Juergen Braun[3]

Objective. In active early rheumatoid arthritis (RA), glucocorticoids are often used for bridging, due to the delayed action of methotrexate. This study was undertaken to compare the effect of 3 bridging strategies, including high-dose and low-dose prednisolone, on radiographic and clinical outcomes.

Methods. Adult RA patients from 1 rheumatology hospital and 23 rheumatology practices who presented with moderate/high disease activity were randomized (1:1:1) to receive 60 mg prednisolone (high-dose prednisolone [HDP]) or 10 mg prednisolone (low-dose prednisolone [LDP]) daily (tapered to 0 mg within 12 weeks) or placebo. The 12-week intervention period was followed by 40 weeks of therapy at the physicians' discretion. The primary outcome measure was radiographic change at 1 year measured using the total modified Sharp/van der Heijde score (SHS). Disease activity was assessed with the Disease Activity Score in 28 joints using the erythrocyte sedimentation rate (DAS28-ESR).

Results. Of 395 randomized patients (HDP, n = 132; LDP, n = 131; placebo, n = 132), 375 (95%) remained in the modified intention-to-treat analysis. Mean ± SD changes in SHS scores in the 3 groups after 1 year were comparable: mean ± SD 1.0 ± 2.0 units in the HDP group, 1.1 ± 2.2 units in the LDP group, and 1.1 ± 1.5 units in the placebo group. The primary analysis showed no superiority of HDP compared to placebo (estimated difference of the mean change −0.04 [95% confidence interval (95% CI) −0.5, 0.4]). At week 12, the mean DAS28-ESR differed: −0.6 (95% CI −1.0, −0.2) for HDP versus placebo; −0.8 (95% CI −1.2, −0.5) for LDP versus placebo. At week 52, there was no significant difference in DAS28-ESR between the 3 groups (range 2.6–2.8). Serious adverse events occurred similarly often.

Conclusion. Short-term glucocorticoid bridging therapy at a high dose showed no benefit with regard to progression of radiographic damage at 1 year.

[1]Dietmar Krause, MD: Department of Medical Informatics, Biometry and Epidemiology, Ruhr University Bochum, Bochum, Germany, and Rheumatology Practice Gladbeck, Gladbeck, Germany; [2]Anna Mai, PhD, Renate Klaassen-Mielke, Dipl. Stat., Nina Timmesfeld, PhD, Ulrike Trampisch, PhD, Henrik Rudolf, PhD, Hans J. Trampisch, PhD: Department of Medical Informatics, Biometry and Epidemiology, Ruhr University Bochum, Bochum, Germany; [3]Xenofon Baraliakos, MD, Juergen Braun, MD: Ruhr Area Rheumatism Centre, Ruhr University Bochum, Bochum, Germany; [4]Elmar Schmitz, MD: Rheumatology Practice Hattingen, Hattingen, Germany; [5]Claas Fendler, MD: Rheumatology Practice Duisburg, Duisburg, Germany; [6]Claudia Klink, MD: Rheumatology Practice Gladbeck, Gladbeck, Germany; [7]Stephanie Boeddeker, MD: Rheumatology Practice Marl, Marl, Germany; [8]Ertan Saracbasi-Zender, MD: Rheumatology Practice Oberhausen, Oberhausen, Germany; [9]Hans-Joachim Christoph, MD: Rheumatology Practice Minden, Minden, Germany; [10]Manfred Igelmann, MD: Rheumatology Practice Bochum, Bochum, Germany; [11]Hans-Juergen Menne, MD: Rheumatology Practice Dortmund, Dortmund, Germany; [12]Albert Schmid, MD: Rheumatology Practice Bielefeld, Bielefeld, Germany; [13]Rolf Rau, MD: Department of Rheumatology, Evangelisches Fachkrankenhaus und Altenhilfe Ratingen gGmbH, Ratingen, Germany; [14]Siegfried Wassenberg, MD: Rheumatology Practice Ratingen, Ratingen, Germany; [15]Nilüfer Sonuc, PhD: Centre for Clinical Studies, Institute of Medical Informatics, Biometry and Epidemiology, University of Duisburg-Essen, Duisburg, Germany; [16]Claudia Ose, PhD: University of Applied Sciences Düsseldorf, Düsseldorf, Germany; [17]Carmen Schade-Brittinger, med. Dok.: Centre for Clinical Studies, Philipps University of Marburg, Marburg, Germany.

INTRODUCTION

The most important rheumatoid arthritis (RA) management strategy is the treat-to-target approach that includes the (early) use of conventional synthetic disease-modifying antirheumatic drugs (csDMARDs) and, if necessary, targeted synthetic or biologic DMARDs (1). According to the 2019 recommendations of the European Alliance of Associations for Rheumatology (EULAR), the concept of disease modification "most characteristically [includes] the inhibition of occurrence or progression of structural damage to cartilage and bone" (2). Structural joint damage may occur early after disease onset. One important clinical problem is that csDMARDS such as methotrexate (MTX) have a delayed onset of action. This is the main reason for the development of bridging strategies using glucocorticoids (GCs) (3). GCs are fast-acting antiinflammatory drugs, also considered as disease-modifying because of their ability to decelerate structural damage (4).

There is strong evidence of structural efficacy for 5–10 mg oral prednisolone per day over 2 years (5,6) and for 60 mg oral prednisolone initially, tapered to low-dose prednisolone or 0 mg over 6–8 months administered in addition to csDMARDs (7,8). An initial prednisolone dosage of 30 mg was shown to be nearly as efficacious as 60 mg prednisolone, both tapered down to 5 mg over a 26-week period (9).

According to the 2015 American College of Rheumatology (ACR) Guideline for the Treatment of RA, the risk/benefit ratio of GCs is favorable as long as the dose is low (≤10 mg prednisolone per day) and the duration of therapy short (<3 months of treatment) (10). However, there is no solid evidence for this recommendation (11). Therefore, the 2021 ACR Guideline for the Treatment of RA emphasizes that neither high- nor low-dose GCs should be used (12). In 2019, EULAR recommended short-term GC use when initiating or changing csDMARDs such as MTX, and short-term GC use means "aiming at discontinuation within about 3 months" (13).

The aim of our study was to test the paradigm of a disease-modifying effect of high and low GC doses in short-term administration combined with a now well established tight-control treat-to-target approach (14) in patients with early RA. In addition to radiographic outcomes, clinical efficacy and safety of the strategies were assessed.

PATIENTS AND METHODS

Study design. CORRA (Corticoid bridging in Rheumatoid Arthritis) is an investigator-initiated, randomized, multicenter, double-blind, placebo-controlled trial designed to compare 2 short-term GC bridging schedules and placebo in addition to MTX following a tight-control treat-to-target regimen in early RA (ClinicalTrials.gov identifier: NCT02000336). It was approved by the ethics committees at the universities of Muenster (leading

ethics committee: 2013-250-f-A), Duesseldorf, and Hanover, Germany. The study was conducted at 23 rheumatology private practices and 1 tertiary hospital in North Rhine-Westphalia, Germany. The study protocol had already been published at study initiation (15). The principles of good clinical practice were an essential component of the trial. It was conducted in accordance with the Declaration of Helsinki. A supervision of the trial was carried out by an independent data and safety monitoring board.

Patients. Adult patients with diagnosed active RA who fulfilled the 2010 ACR/EULAR RA classification criteria (16) and had a symptom duration of less than 3 years were eligible. Patients had to be naive to MTX treatment (MTX pretreatment was allowed within 4 weeks before baseline) and without GC treatment 2 weeks before study entry. Disease activity had to be upper moderate or high as measured by the Disease Activity Score in 28 joints using the erythrocyte sedimentation rate (DAS28-ESR) (17) of >4 with ≥3 swollen joints. Exclusion criteria included severe liver disease, active hepatitis B or C viral infection, advanced renal disease, clinically relevant hematologic diseases, relevant immunodeficiency including HIV infection, clinically relevant pulmonary fibrosis, complicated gastric or duodenal ulcer, a history of malignant melanoma, severe infections within the previous 6 weeks before baseline, uncontrolled diabetes mellitus, uncontrolled arterial hypertension, and high intraocular pressure. All patients provided written informed consent.

Randomization and masking. Patients were randomly assigned (1:1:1) to initially receive 60 mg prednisolone (high-dose prednisolone [HDP]) or 10 mg prednisolone (low-dose prednisolone [LDP]) orally once a day (both tapered down to 0 mg prednisolone within 12 weeks) or placebo. The sealed study medication boxes had a sequential mark but otherwise the same appearance. In each box there were 12 blisters (marked 1 to 12 for each week) with 7 capsules containing the actual drug. All capsules looked identical and had the same smell and taste. A central pharmacy provided a computer-generated randomization list with a randomly permuted block design. Patients, physicians, and readers of radiographs were blinded with regard to treatment group assignment until the reading of radiographs was finished and the study database was locked.

Procedures. The intervention period lasted 12 weeks, followed by an extension period of 40 weeks with therapy at the physicians' discretion. Patients were advised to take 1 capsule of the study medication per day in chronological order during the intervention period. In the LDP group, the study schedule began with 10 mg prednisolone daily for 4 weeks, followed by 7.5 mg during weeks 5–8, and 5 mg during weeks 9–12. In the HDP group, the schedule was 60 mg, 40 mg, 25 mg, 20 mg, 15 mg, 10 mg during weeks 1–6, respectively, 7.5 mg during weeks

7–8, and 5 mg during weeks 9–12. Patients were asked to return their study medication boxes after 12 weeks to assess compliance (see Supplementary Appendix S1, available on the *Arthritis & Rheumatology* website at https://onlinelibrary.wiley.com/doi/10.1002/art.42245).

All patients started MTX treatment, the usual dosage being 15 mg/week (modifications could be made by the rheumatologist, e.g., in case of minor renal failure, MTX intolerance, or older age), followed by 5 mg folic acid the next day. Patients were seen every 4 weeks within the first 3 months. In case of lack of efficacy, the MTX dose was planned to be increased to 20 mg/week and further up to 25 mg/week after 4 or 8 weeks, respectively (18). In the further course of the study, a change of the DMARD medication according to the EULAR recommendations (19) was allowed in the case of lack of efficacy and/or intolerability. These decisions were made by the treating rheumatologist and the patient, based on the treat-to-target paradigm for RA (14). Intraarticular GC injections of up to 40 mg triamcinolone acetonide were allowed every 4 weeks during the intervention period and were then left to the physicians' discretion.

Study visits took place at baseline and at weeks 4, 8, 12, 24, and 52. Radiographs of hands and feet were taken at baseline and after 1 year. A physical examination including the determination of the DAS28-ESR, safety measures with laboratory examinations, and patient-reported outcomes were performed at every visit. The treating rheumatologist recorded all adverse events (AEs), including serious AEs (SAEs), and made treatment adjustments in accordance with the protocol. Dual x-ray absorptiometry (DXA) of the lumbar spine and hip was performed at baseline and after 24 weeks in patients at an increased risk of osteoporosis (age >60 years in men, age >50 years in women, current smoking, history of nontraumatic fracture, parent history of hip fracture).

Outcome measures. The primary end point was the change in radiographic joint damage after 1 year compared to baseline, as determined by the modified Sharp/van der Heijde score (SHS) (20). Two independent readers (JB and DK) evaluated radiographs of hands and feet with regard to joint space narrowing and erosions. They were unaware of the treatment assignments and performed the reading in a paired manner and in chronological order (21). In case of a difference between the 2 readings of >4 total SHS points, a third reading took place for the respective radiographs with 2 readers for adjudication (RR and SW). In case of smaller differences, the mean of these 2 readings was used for analysis.

Major secondary end points were concomitant medication (e.g., intraarticular GC, MTX), disease activity (assessed by the DAS28-ESR, with values of <2.6 labeled as "minimal disease activity"), Boolean remission (as defined by the ACR/EULAR provisional definition of remission in RA for clinical trials [22]), and physical functioning (assessed by the Hannover questionnaire of

physical functioning [23]), as well as patient global assessment of disease activity and pain (numerical rating scale).

Safety end points included serious reportable AEs (SRAEs), treatment-emergent AEs of special interest (HbA1c >7.5% or an increase of >1.0% compared to baseline; intraocular pressure >21.0 mm Hg), and other AEs, coded by the Medical Dictionary for Regulatory Activities (MedDRA), German versions 17.1 to 21.0. SRAEs had to be reported to an independent SAE manager for safety evaluation, in case they either occurred in the period from patient consent to 30 days after the last intake of the study medication or if the treating rheumatologist assumed a causal relationship of the SAE with the study medication. Bone mineral density (DXA lumbar spine and hip) at 24 weeks was compared to baseline.

Statistical analysis. In the prespecified statistical analysis plan, primary analysis was planned with 3 hierarchical steps comparing the 3 treatment groups using analysis of covariance. The first hierarchical step was a superiority test for the HDP schedule versus placebo, and the possible second step was a superiority test of the LDP schedule versus placebo, both conducted in a modified intention-to-treat population (details on all analysis populations are provided in Supplementary Appendix S2, https://onlinelibrary.wiley.com/doi/10.1002/art.42245). The last hierarchical step should show noninferiority of the LDP versus the HDP schedule using the data of the per-protocol population (the SHS erosion score as a secondary outcome measure should be analyzed accordingly). Six sensitivity analyses of the primary analysis were performed (Supplementary Appendices S2 and S3).

For sample size calculation, data from the Behandel Strategieen (BeSt) study (effect ± SD 3.7 ± 7.5) was used (8). Accounting for a dropout rate of 5%, a sample size of 150 patients per group was estimated to have a power of >95% for a 2-sided *t*-test of superiority ($\alpha = 0.05$) of HDP versus placebo in the first step and for LDP versus placebo in the second hierarchical step. Accepting a noninferiority margin of 1.3 SHS units (one-third of the assumed placebo/verum difference) for the difference of change in radiographic joint damage between the prednisolone groups results in a power of >85% for 150 patients per group in the third step. In the course of the study, the number of participants had to be reduced due to recruitment problems. With 125 patients per group, the power for the first 2 steps in the hierarchical design was >90%, whereas the power in the third step decreased from >85% to >80%. Depending on the proportion of missing values, these were substituted by randomly chosen items pertaining to the individual or by multiple imputation according to predictive mean matching (n = 20) (Supplementary Appendix S4).

Secondary outcome measures were examined in suitable regression models (modified intention-to-treat population), linear models for quantitative outcomes and logistic models for dichotomous outcomes, with adjustment for baseline values (if possible), age, sex, and symptom duration. A random patient effect was included for target values repeatedly measured over time. An

overall 3-group test per outcome and time point was conducted. Additionally, 95% confidence intervals (95% CIs) for pairwise comparisons were calculated. Statistical analyses were performed using R, version 3.6.1, and SAS software, version 9.4.

Exploratory post hoc analyses of the primary end point and the erosion score were subsequently added and included a pairwise comparison of the treatment groups in the per-protocol population. For this purpose, family-wise 95% CIs adjusted according to Tukey's method were calculated.

Data availability. Requests for sharing the trial data can be addressed to the corresponding author and will be considered on an individual basis by the authors.

RESULTS

Between February 5, 2014, and March 1, 2017, 395 of the 450 patients screened participated in the baseline visit and were randomized to receive treatment. According to the International Council for Harmonisation of Technical Requirements for Pharmaceuticals for Human Use E9 guideline (24), 20 patients were excluded from the intention-to-treat population (Figure 1). Of the remaining 375 patients, 345 (92%) completed the 52-week study visit.

Baseline characteristics. At baseline, patients had high disease activity (mean DAS28-ESR of ~6.0) with a mean of

13 swollen joints and SHS score of 5 units (mean erosion subscore 2 SHS units). Baseline characteristics were fairly similar between the 3 treatment groups within the modified intention-to-treat population except for the proportion of women, C-reactive protein (CRP) level, ESR level, and total SHS score (Table 1).

Primary end point analysis. Intraclass correlation coefficient (ICC) estimates for the SHS score at baseline and week 52 were 0.97, and the ICC estimate for changes in the total SHS score during weeks 0–52 was 0.85 (indicating good reader reliability). The smallest detectable change in the total SHS score was 1.9 for weeks 0–52 (25). The observed mean ± SD increase in SHS score (primary end point) was 1.0 ± 2.0 in the HDP group, 1.1 ± 2.2 in the LDP group, and 1.1 ± 1.5 in the placebo group (Table 2). The probability plots for total SHS score and erosion score are shown in Supplementary Appendix S5 (https://onlinelibrary.wiley.com/doi/10.1002/art.42245). After adjustment for the baseline total SHS score, the estimated difference of the mean change between HDP versus placebo was –0.04 (95% CI –0.5, 0.4). Thus, no significant difference was seen in the first step, and the hierarchical testing was stopped. All sensitivity and subgroup analyses yielded similar results (Supplementary Appendix S5).

Secondary end point analysis. The observed mean ± SD increase in SHS erosion score at 1 year was 0.6 ± 1.7, 0.7 ± 1.3, and 0.7 ± 1.2 for the HDP, LDP, and placebo groups,

	Placebo	Low dose	High dose
Patients screened	450		
Ineligible	55		
Did not meet eligibility criteria	29		
Withdrew consent	26		
Randomized	395	132	131	132
Did not start taking study medication *	2	4	2
Included in safety analysis	130	127	130
Excluded *#	5	3	4
Symptom duration > 3 years	1	-	-
Pre-treated with methotrexate	1	2	-
Unconfirmed diagnosis	-	1	1
Without any radiograph	3	-	3
Included in modified intention-to-treat analysis	125	124	126
Dropouts in 12-week intervention period	7	8	0
Lost to follow-up	4	6	-
Withdrew consent	3	2	-
Dropouts in 40-week observation period	3	6	6
Lost to follow-up	2	5	6
Withdrew consent	-	1	-
Death	1	-	-
Intake of less than 80% of study medication	27	13	11
Missing SHS score at baseline or study end	6	8	6
Included in per protocol analysis	82	89	103

Low-dose therapy started at 10 mg prednisolone, and high-dose therapy started at 60 mg prednisolone. SHS modified Sharp van der Heijde;
* Exclusion according to the International Council for Harmonisation of Technical Requirements for Pharmaceuticals for Human Use E9 guideline (ICH E9) guideline (24). # Eligibility violations or no information on the primary endpoint.

Figure 1. Trial profile.

Table 1. Baseline characteristics of the study participants with active early rheumatoid arthritis (modified intention-to-treat population)*

	Missing values	Placebo group (n = 125)	Low-dose group (n = 124)	High-dose group (n = 126)
Age, years	0	58 ± 11	59 ± 12	57 ± 13
Female, no. (%)	0	64 (51)	75 (61)	79 (63)
Symptom duration, weeks	0	25 ± 29	23 ± 25	26 ± 27
MTX pretreatment within 4 weeks before baseline, no. (%)†	1	3 (2.4)	7 (5.6)	9 (7.1)
Rheumatoid factor positivity, no. (%)	4	63 (51)	70 (57)	72 (58)
ACPA positive, no. (%)	22	65 (53)	56 (50)	64 (54)
No. swollen joints (range 0–28)	0	13 ± 6.7	13 ± 6.7	13 ± 6.8
No. tender joints (range 0–28)	0	14 ± 7.3	15 ± 7.6	14 ± 7.9
ESR, mm/hour	3	29 ± 23	34 ± 24	37 ± 27
CRP, mg/liter	0	1.5 ± 2.0	2.2 ± 3.7	3.0 ± 3.5
DAS28-ESR score	1	6.0 ± 1.1	6.1 ± 1.1	6.0 ± 1.2
CDAI score	0	40 ± 14	40 ± 15	39 ± 16
Total SHS score	20	5.5 ± 8.4	4.7 ± 8.0	4.5 ± 5.2
SHS erosion score	20	2.1 ± 3.5	2.1 ± 5.2	2.1 ± 3.4
Physician assessment of disease activity score (NRS range 0–10)	0	6.4 ± 1.5	6.5 ± 1.7	6.6 ± 1.8
Patient assessment of disease activity score (NRS range 0–10)	0	6.0 ± 1.8	5.7 ± 2.1	5.9 ± 2.2
Patient assessment of pain score (NRS range 0–10)	3	6.4 ± 1.9	6.2 ± 2.1	6.5 ± 2.0
Patient global assessment score (NRS range 0–10)	6	5.9 ± 1.9	5.8 ± 2.1	6.2 ± 1.9
Patient assessment of fatigue score (NRS range 0–10)	5	4.6 ± 3.2	4.8 ± 2.8	5.4 ± 2.8
Patient assessment of sleep disorder score (NRS range 0–10)	4	4.9 ± 3.4	5.2 ± 3.4	5.3 ± 3.4
Hannover score of physical functioning (range 0–100)‡	4	73 ± 18	69 ± 20	70 ± 21

* Except where indicated otherwise, values are the mean ± SD. Low-dose therapy started at 10 mg prednisolone, and high-dose therapy started at 60 mg prednisolone. Higher values on the numerical rating scale (NRS) indicate worse status. ACPA = anti–citrullinated peptide antibody; CRP = C-reactive protein; DAS28-ESR = Disease Activity Score in 28 joints using the erythrocyte sedimentation rate; CDAI = Clinical Disease Activity Index; SHS = modified Sharp/van der Heijde score.
† Pretreatment with disease-modifying antirheumatic drugs (DMARDs) within the 4 weeks before baseline: 25 patients overall, 19 with methotrexate (MTX), 5 with hydroxychloroquine, and 7 with sulfasalazine (combination of DMARDs in 4 patients).
‡ Higher values indicate better functioning.

respectively (Table 2). The corresponding estimated difference of HDP versus placebo was –0.2 (95% CI –0.5, 0.2). Further details on the radiographic change are presented in Supplementary Appendix S5.

Results on other secondary end points are shown in Table 3 and Figure 2. In summary, the course of disease activity (according to the DAS28-ESR and patient assessment) and pain revealed benefits of both prednisolone schedules over placebo until week

Table 2. Modified SHS scores of radiographic damage at week 0 and week 52 in patients with active early rheumatoid arthritis*

	Baseline (week 0)			Week 52		
	Placebo group	Low-dose group	High-dose group	Placebo group	Low-dose group	High-dose group
Total SHS score	5.4 ± 8.3	4.7 ± 7.9	4.5 ± 5.2	6.6 ± 8.9	5.8 ± 9.7	5.4 ± 6.5
SHS erosion score	2.0 ± 3.4	2.2 ± 5.1	2.0 ± 3.3	2.8 ± 3.8	2.8 ± 6.0	2.6 ± 4.3
SHS JSN score	3.4 ± 5.6	2.5 ± 3.7	2.4 ± 2.9	3.8 ± 5.9	3.0 ± 4.6	2.8 ± 3.4
Change in total SHS score	–	–	–	1.1 ± 1.5	1.1 ± 2.2	1.0 ± 2.0
Change in SHS erosion score	–	–	–	0.7 ± 1.2	0.7 ± 1.3	0.6 ± 1.7
Change in SHS JSN score	–	–	–	0.4 ± 0.8	0.4 ± 1.3	0.4 ± 0.9
Total SHS score >0, no. (%)	100 (80)	99 (80)	95 (75)	115 (92)	103 (83)	102 (81)
Change in total SHS score >0.5, no. (%)	–	–	–	67 (54)	57 (46)	53 (42)
Change in total SHS score, SDD >1.9, no. (%)	–	–	–	31 (25)	22 (18)	18 (14)

* Descriptive analysis of imputed data. Except where indicated otherwise, values are the mean ± SD. Low-dose therapy started at 10 mg prednisolone, and high-dose therapy started at 60 mg prednisolone. SHS = Sharp/van der Heijde score; JSN = joint space narrowing; SDD = smallest detectable difference.

Table 3. Secondary clinical end points at week 12 in patients with active early rheumatoid arthritis*

	Observed score at week 12, mean ± SD				Estimated difference in score (95% CI)		
	Placebo group	Low-dose group	High-dose group	P†	Low-dose vs. placebo	High-dose vs. placebo	High-dose vs. low-dose
DAS28-ESR	3.6 ± 1.4	2.8 ± 1.2	3.1 ± 1.3	<0.01	−0.8 (−1.2, −0.5)	−0.6 (−1.0, −0.2)	0.2 (−0.1, 0.6)
Physician assessment of disease activity score (NRS range 0–10)	2.9 ± 2.0	1.7 ± 1.6	2.0 ± 1.7	<0.01	−1.2 (−1.7, −0.7)	−0.9 (−1.5, −0.4)	0.3 (−0.3, 0.8)
Patient assessment of disease activity score (NRS range 0–10)	3.8 ± 2.2	2.9 ± 2.5	3.2 ± 2.4	<0.01	−1.0 (−1.7, −0.2)	−0.6 (−1.3, 0.1)	0.3 (−0.4, 1.1)
Patient assessment of pain score (NRS range 0–10)	3.6 ± 2.2	2.5 ± 2.2	2.8 ± 2.3	<0.01	−1.1 (−1.8, −0.4)	−0.8 (−1.5, −0.2)	0.3 (−0.4, 1.0)
Patient global assessment score (NRS range 0–10)	3.8 ± 2.0	2.9 ± 2.1	3.4 ± 2.4	<0.01	−1.0 (−1.7, −0.3)	−0.5 (−1.2, 0.1)	0.5 (−0.2, 1.1)
Patient assessment of fatigue score (NRS range 0–10)	3.5 ± 2.7	2.7 ± 2.6	3.0 ± 2.6	0.012	−0.8 (−1.6, −0.1)	−0.8 (−1.6, −0.04)	0.04 (−0.7, 0.8)
Patient assessment of sleep disorders score (NRS range 0–10)	3.4 ± 3.1	2.6 ± 2.7	2.5 ± 2.7	0.01	−0.9 (−1.8, −0.1)	−1.0 (−1.9, −0.2)	−0.1 (−1.0, 0.7)
Hannover score of physical functioning (range 0–100)‡	81.7 ± 15.3	85.9 ± 16.0	85.1 ± 17.0	0.01	5.5 (1.1, 9.8)	4.9 (0.6, 9.1)	−0.6 (−4.9, 3.7)

* Low-dose therapy started at 10 mg prednisolone, and high-dose therapy started at 60 mg prednisolone. Higher values on the NRS indicate worse status. See Table 1 for definitions.
† Based on a 3-group comparison of mean change from baseline to week 12.
‡ Higher values indicate better functioning.

12, but not at week 24 or 52. Physical functioning was better, and the proportion of patients in Boolean remission was higher for both prednisolone schedules compared to placebo at week 12, but not thereafter. The same was true for physician assessment of disease activity, patient global assessment, patient assessment of fatigue, and patient assessment of sleep disorders. Detailed tables for all visits and the course of additional secondary end points (tender/swollen joints, ESR, CRP) are presented in Supplementary Appendix S6 (https://onlinelibrary.wiley.com/doi/10.1002/art.42245).

Concomitant medication. The number of patients with GC joint injections during the first 12 weeks was 11 (8.7%) in the HDP group, 10 (8.5%) in the LDP group, and 27 (23%) in the placebo group (odds ratio [OR] 0.3 [95% CI 0.1, 0.8] for HDP versus placebo; OR 0.3 [95% CI 0.1, 0.8] for LDP versus placebo). The mean cumulative triamcinolone dose was 10 mg in the placebo group compared to 2.5 mg in the LDP group (mean cumulative oral prednisolone dose 606 mg) and 3.4 mg in the HDP group (mean cumulative oral prednisolone dose 1,387 mg).

The oral prednisolone dose in the 40-week follow-up period, which was left to the discretion of the physicians and the patients, did not differ between the groups. For cumulative GC doses see Supplementary Appendix S6.2. Concerning the 12-week intervention period, there was no significant difference in MTX dose either. During the study, 15% of the patients switched to or added another csDMARD. Eleven patients (3%) started treatment with a biologic drug during the observation period, 3 patients from the HDP group, 3 from the LDP group,

and 5 from the placebo group (for details on medication, see Supplementary Appendix S6.3).

Safety. In the safety analysis population, 239 patients (62%) had 758 AEs during the whole study period. There were no significant group differences for the predefined AE "high intraocular pressure," the MedDRA system organ class "infections or infestations," or SRAE. There were significant differences with regard to the AE "increased HbA1c" (n = 9 [6.9%] in the HDP group, n = 2 [1.6%] in the LDP group, n = 3 [2.3%] in the placebo group) in the HDP group (P = 0.04), with 1 patient newly diagnosed as having diabetes mellitus. For details on AEs see Supplementary Appendix S7.1 (https://onlinelibrary.wiley.com/doi/10.1002/art.42245). Results of the DXA measurements showed no significant differences between the treatment groups (Supplementary Appendix S7.2). One participant, assigned to the placebo group, died more than 30 days after the intervention period (the cause of death could not be elucidated).

Exploratory post hoc analyses of radiographic change. An additional analysis of the total modified SHS score was carried out in the per-protocol population for the differences in the adjusted mean change in total modified SHS score in the HDP group versus placebo group, LDP group versus placebo group, and HDP group versus LDP group at 1 year. All 95% CIs fell between −0.7 and 0.6 for total SHS score. The results were comparable in the exploratory post hoc analysis of the differences in adjusted mean change in erosion score. Results are presented in Figure 3 and Supplementary Appendix S5.
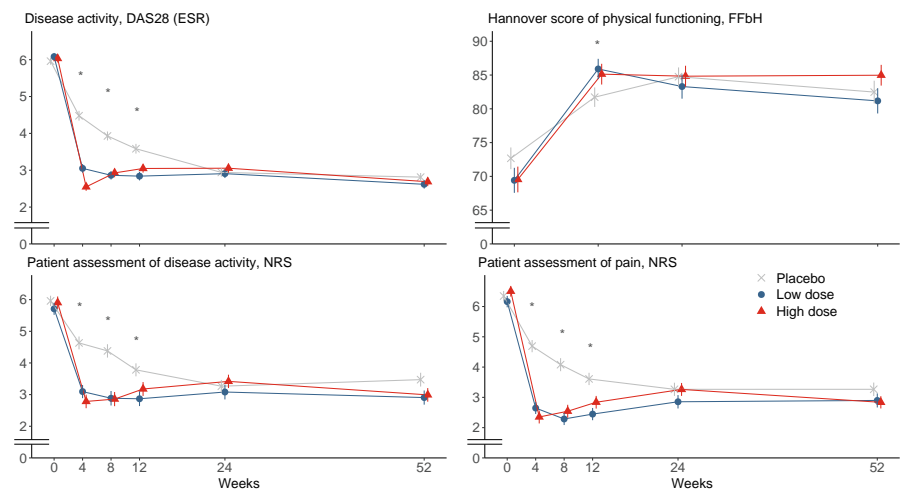
Figure 2. Course of the 4 major secondary end points: Disease Activity Score in 28 joints using the erythrocyte sedimentation rate (DAS28-ESR), Hannover score of physical functioning (FFbH; range 0–100), patient assessment of disease activity (numerical rating scale [NRS] range 0–10), and patient assessment of pain (NRS range 0–10). Vertical lines show the mean ± SD. * = $P < 0.05$ for 3-group comparisons.

DISCUSSION

This study was designed to test the paradigm of a disease-modifying effect of high- and low-dose short-term GC bridging in patients with early RA who were treated with MTX, according to a tight-control treat-to-target approach. The first analysis of the hierarchical 3-step design did not show superiority of the high-dose prednisolone schedule over placebo in terms of structural joint damage. An exploratory post hoc comparison of the 3 treatment groups suggests that the 1-year radiographic change in the placebo group was not different from the prednisolone bridging groups.

This result is in some contrast to the paradigm of a disease-modifying efficacy of GCs in the treatment of RA, first shown in 1995 for long-term use of low-dose GCs (4) and confirmed 2 years later for a high-dose prednisolone schedule tapered and stopped after 28 weeks in early RA (as observed in the Combinatietherapie Bij Reumatoïde Artritis [COBRA] study) (7).

However, there are important differences in the design of the COBRA trial and our study. The initial dosage of MTX was higher and the intervention period was shorter in our study. In the COBRA study, the cumulative prednisolone dose administered over 28 weeks was 2,345 mg compared to 1,435 mg in the HDP group in our study and 630 mg in the LDP group given over 12 weeks.

The tight-control treat-to-target strategy (14) has substantially changed the course of RA, including the burden of structural joint damage which has decreased considerably over the last 20 years. In 2 UK inception cohorts (1986–2001 and 2002–2013) the mean annual increase in SHS score fell from 6.9 to 2.5 units (26). The annual radiographic change reported in 1997 for COBRA (7) was 5.6 SHS units in the high-dose prednisolone group, compared to 0.49 units in the COBRA-light trial reported in 2015 (9). In other studies, even lower prednisolone dosages in bridging schedules have resulted in only small SHS score changes (27). Similar results have been reported for low-risk
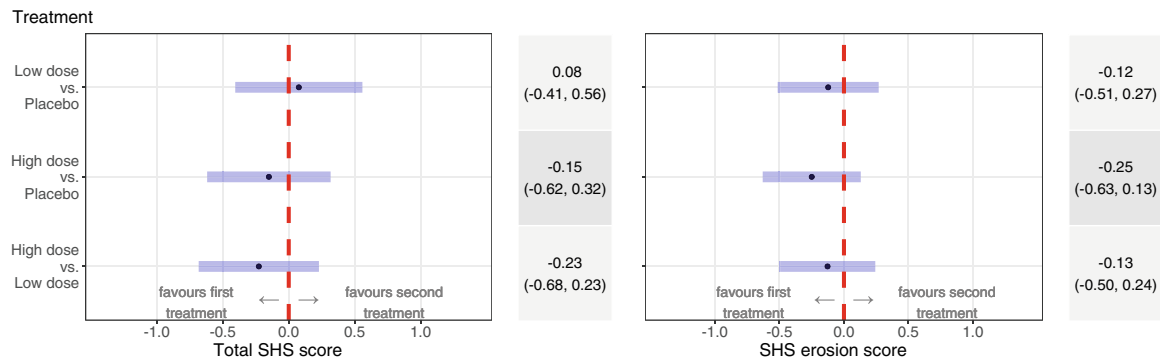
Figure 3. Exploratory post hoc analysis of differences in the adjusted mean change in total modified Sharp/van der Heijde (SHS) radiographic damage scores and erosion scores between treatment groups, with Tukey's adjusted confidence intervals, in the per-protocol population at 1 year. Dashed red lines indicate "no difference" in the total score between groups.

patients receiving MTX in a tight-control step-up schedule without prednisolone bridging (28). This general decrease in structural joint damage may be explained in part by modern treatment strategies and earlier intervention (29), but this hypothesis has not been formally proven and may not explain all differences.

In our study, rescue therapy with intraarticular injections of triamcinolone were allowed at the physicians' discretion, similar to other RA trials (30). During the intervention period, these were used in 9% of patients in the GC groups but in 23% of patients in the placebo group. Intraarticular GC injections may effectively control disease activity, as shown in the Optimized Treatment Algorithm for Patients With Early RA (OPERA) trial (31). Thus, the 2.5-fold proportion of patients with intraarticular injections in the placebo group might have reduced the difference of the GC effect between the groups. However, this effect reduction is likely to be very small, as the mean cumulative GC dose attributable to intraarticular triamcinolone in the placebo group during the intervention period was as low as 2% of the mean cumulative GC dose of study medication in the LDP group and 1% in the HDP group.

In contrast to the comparability in structural joint damage, the differences in disease activity outcomes between the GC groups and the placebo group at the end of the 12-week intervention period were significant, comparable to the results from the Steroid Elimination in RA (SEMIRA) trial (32). This was also true for the proportions of Boolean remission and DAS28-ESR–defined minimal disease activity for both prednisolone schedules over placebo until week 12 (Supplementary Appendix S6.1, https://onlinelibrary.wiley.com/doi/10.1002/art.42245). However, the noticeable difference in disease activity at the end of the intervention period did not result in differences in radiographic change at 12 months, nor in differences in disease activity at weeks 26 and 52. The course of the patient-reported secondary outcome measures like physical functioning, disease activity, pain, fatigue, and sleep disorders was similar, with better improvements in the GC groups within the first few weeks of treatment.

Regarding safety issues, there was a numerically increased amount of AEs and SRAEs in patients receiving HDP. However, only the number of patients with increased HbA1c values was significantly higher in the HDP group (with 1 newly diagnosed as having diabetes mellitus) compared to the other groups. Other important short-term or long-term safety issues (e.g., the number of vascular disorders, infections, or the course of the DXA findings) did not show significant differences between the GC groups and the placebo group. This was similar in other studies (28). The rapid reduction of signs and symptoms of the disease as suggested by the secondary outcome measures and the long-term safety profile are important aspects to consider during shared decision-making when discussing with the patient whether GC bridging should be initiated.

A strength of this study is the inclusion of a placebo group that enabled evaluation of the efficacy of the 2 prednisolone bridging schedules, although it may have been somewhat mitigated by the use of intraarticular GC injections. The short-term administration of prednisolone allowed for evaluation of the EULAR recommendations.

A limitation of our study is the number of missing values in the modified intention-to-treat population that caused imputations. We addressed this weakness by performing sensitivity analyses that yielded comparable results. The handover of the study medication was actually performed in a double-blind manner. Of course, a rapid clinical effect or side effects might have triggered reasonable guesses of the patient concerning the group assignment. The patients of the placebo group were more often male, had lower ESR and lower CRP levels at baseline than those in the GC groups, and had a slightly higher weekly MTX dose in the course of the study. This might introduce some bias, as all these parameters are known to be associated with a less aggressive disease course and a smaller radiographic progression. However, an additional sensitivity analysis with adjustment for sex, ESR, CRP level, and MTX showed comparable results. The different use of intraarticular injections in the GC groups and the placebo group may have biased the results. A sensitivity analysis excluding patients with intraarticular GC-injections did not show different results.

In summary, if one decides to use short-term GC bridging, no benefits to the structural outcome can be expected. The shared decision of patient and physician on the use of GCs in the treatment of early RA should take this into account.

ACKNOWLEDGMENTS

AUTHOR CONTRIBUTIONS

All authors were involved in drafting the article or revising it critically for important intellectual content, and all authors approved the final version to be published. Dr. Krause had full access to all of the data in the study and takes responsibility for the integrity of the data and the accuracy of the data analysis.

Study conception and design. Krause, U. Trampisch, Sonuc, Ose, Schade-Brittinger, H. Trampisch, Braun.

Acquisition of data. Krause, Baraliakos, Schmitz, Fendler, Klink, Boeddeker, Saracbasi-Zender, Christoph, Igelmann, Menne, Schmid, Rau, Wassenberg.

Analysis and interpretation of data. Krause, Mai, Klaassen-Mielke, Timmesfeld, Rudolf, H. Trampisch, Braun.

REFERENCES

1. Smolen JS, van der Heijde D, Machold KP, Aletaha D, Landewé R. Proposal for a new nomenclature of disease-modifying antirheumatic drugs. Ann Rheum Dis 2014;73:3–5.

2. Smolen JS, Landewé RB, Bijlsma JW, Burmester GR, Dougados M, Kerschbaumer A, et al. EULAR recommendations for the management of rheumatoid arthritis with synthetic and biological disease-modifying antirheumatic drugs: 2019 update. Ann Rheum Dis 2020; 79:685–99.

3. Van der Veen MJ, Bijlsma JW. The effect of methylprednisolone pulse therapy on methotrexate treatment of rheumatoid arthritis. Clin Rheumatol 1993;12:500–5.

4. Kirwan JR. The effect of glucocorticoids on joint destruction in rheumatoid arthritis. The Arthritis and Rheumatism Council Low-Dose Glucocorticoid Study Group. N Engl J Med 1995;333:142–6.

5. Bakker MF, Jacobs JW, Welsing PM, Verstappen SM, Tekstra J, Ton E, et al. Low-dose prednisone inclusion in a methotrexate-based, tight control strategy for early rheumatoid arthritis: a randomized trial. Ann Intern Med 2012;156:329–39.

6. Wassenberg S, Rau R, Steinfeld P, Zeidler H. Very low-dose prednisolone in early rheumatoid arthritis retards radiographic progression over two years: a multicenter, double-blind, placebo-controlled trial. Arthritis Rheum 2005;52:3371–80.

7. Boers M, Verhoeven AC, Markusse HM, van de Laar MA, Westhovens R, van Denderen JC, et al. Randomised comparison of combined step-down prednisolone, methotrexate and sulphasalazine with sulphasalazine alone in early rheumatoid arthritis. Lancet 1997; 350:309–18.

8. Goekoop-Ruiterman YP, de Vries-Bouwstra JK, Allaart CF, van Zeben D, Kerstens PJ, Hazes JM, et al. Clinical and radiographic outcomes of four different treatment strategies in patients with early rheumatoid arthritis (the BeSt study): a randomized, controlled trial. Arthritis Rheum 2005;52:3381–90.

9. Ter Wee MM, den Uyl D, Boers M, Kerstens P, Nurmohamed M, van Schaardenburg D, et al. Intensive combination treatment regimens, including prednisolone, are effective in treating patients with early rheumatoid arthritis regardless of additional etanercept: 1-year results of the COBRA-light open-label, randomised, non-inferiority trial. Ann Rheum Dis 2015;74:1233–40.

10. Singh JA, Saag KG, Bridges SL, Akl EA, Bannuru RR, Sullivan MC, et al. 2015 American College of Rheumatology guideline for the treatment of rheumatoid arthritis. Arthritis Care Res (Hoboken) 2016;68:1–25.

11. Hua C, Buttgereit F, Combe B. Glucocorticoids in rheumatoid arthritis: current status and future studies [review]. RMD Open 2020;6:e000536.

12. Fraenkel L, Bathon JM, England BR, St Clair EW, Arayssi T, Carandang K, et al. 2021 American College of Rheumatology guideline for the treatment of rheumatoid arthritis. Arthritis Care Res (Hoboken) 2021;73:924–39.

13. Smolen JS, Landewé R, Bijlsma J, Burmester G, Chatzidionysiou K, Dougados M, et al. EULAR recommendations for the management of rheumatoid arthritis with synthetic and biological disease-modifying antirheumatic drugs: 2016 update. Ann Rheum Dis 2017;76:960–77.

14. Smolen JS, Aletaha D, Bijlsma JW, Breedveld FC, Boumpas D, Burmester G, et al. Treating rheumatoid arthritis to target: recommendations of an international task force. Ann Rheum Dis 2010;69:631–7.

15. Trampisch US, Krause D, Trampisch HJ, Klaassen-Mielke R, Baraliakos X, Braun J. Comparison of the efficacy and safety of two starting dosages of prednisolone in early active rheumatoid arthritis (CORRA): study protocol for a randomized controlled trial. Trials 2014;15:344.

16. Aletaha D, Neogi T, Silman AJ, Funovits J, Felson DT, Bingham CO III, et al. 2010 Rheumatoid arthritis classification criteria: an American College of Rheumatology/European League Against Rheumatism collaborative initiative. Arthritis Rheum 2010;62:2569–81.

17. Prevoo ML, van't Hof MA, Kuper HH, van Leeuwen MA, van de Putte LB, van Riel PL. Modified disease activity scores that include twenty-eight–joint counts: development and validation in a prospective longitudinal study of patients with rheumatoid arthritis. Arthritis Rheum 1995;38:44–8.

18. Braun J, Kästner P, Flaxenberg P, Währisch J, Hanke P, Demary W, et al. Comparison of the clinical efficacy and safety of subcutaneous versus oral administration of methotrexate in patients with active rheumatoid arthritis: results of a six-month, multicenter, randomized, double-blind, controlled, phase IV trial. Arthritis Rheum 2008;58: 73–81.

19. Smolen JS, Landewé R, Breedveld FC, Buch M, Burmester G, Dougados M, et al. EULAR recommendations for the management of rheumatoid arthritis with synthetic and biological disease-modifying antirheumatic drugs: 2013 update. Ann Rheum Dis 2014;73:492–509.

20. Van der Heijde D, Dankert T, Nieman F, Rau R, Boers M. Reliability and sensitivity to change of a simplification of the Sharp/van der Heijde radiological assessment in rheumatoid arthritis. Rheumatology (Oxford) 1999;38:941–7.

21. Van Tuyl LH, van der Heijde D, Knol DL, Boers M. Chronological reading of radiographs in rheumatoid arthritis increases efficiency and does not lead to bias. Ann Rheum Dis 2014;73:391–5

22. Felson DT, Smolen JS, Wells G, Zhang B, van Tuyl LH, Funovits J, et al. American College of Rheumatology/European League Against Rheumatism provisional definition of remission in rheumatoid arthritis for clinical trials. Arthritis Rheum 2011;63:573–86.

23. Zochling J, Stucki G, Grill E, Braun J. A comparative study of patient-reported functional outcomes in acute rheumatoid arthritis. J Rheumatol 2007;34:64–9.

24. International Conference On Harmonisation Of Technical Requirements For Registration Of Pharmaceuticals For Human Use. ICH harmonized tripartite guideline. Statistical principles for clinical trials: E9. 1998. URL: https://database.ich.org/sites/default/files/E9_Guideline.pdf.

25. Van der Heijde D, Simon L, Smolen J, Strand V, Sharp J, Boers M, et al. How to report radiographic data in randomized clinical trials in rheumatoid arthritis: guidelines from a roundtable discussion. ArthritisRheum 2002;47:215–8.

26. Carpenter L, Norton S, Nikiphorou E, Jayakumar K, McWilliams DF, Rennie KL, et al. Reductions in radiographic progression in early rheumatoid arthritis over twenty-five years: changing contribution from rheumatoid factor in two multicenter UK inception cohorts. Arthritis Care Res (Hoboken) 2017;69:1809–17.

27. De Jong PH, Hazes JM, Han HK, Huisman M, van Zeben D, van der Lubbe PA, et al. Randomised comparison of initial triple DMARD therapy with methotrexate monotherapy in combination with low-dose glucocorticoid bridging therapy; 1-year data of the tREACH trial. Annals Rheum Dis 2014;73:1331–9.

28. Verschueren P, de Cock D, Corluy L, Joos R, Langenaken C, Taelman V, et al. Effectiveness of methotrexate with step-down glucocorticoid remission induction (COBRA Slim) versus other intensive treatment strategies for early rheumatoid arthritis in a treat-to-target approach: 1-year results of CareRA, a randomised pragmatic open-label superiority trial. Ann Rheum Dis 2017;76: 511–20.

29. Landewé R, Strand V, van der Heijde D. From inhibition of radiographic progression to maintaining structural integrity: a methodological framework for radiographic progression in rheumatoid arthritis and psoriatic arthritis clinical trials. Ann Rheum Dis 2013; 72:1113–7.

30. Gvozdenović E, Dirven L, van den Broek M, Han KH, Molenaar ET, Landewé RB, et al. Intra articular injection with corticosteroids in patients with recent onset rheumatoid arthritis: subanalyses from the BeSt study. Clinical Rheumatol 2014;33:263–7.

31. Hørslev-Petersen K, Hetland ML, Ørnbjerg LM, Junker P, Pødenphant J, Ellingsen T, et al. Clinical and radiographic outcome of a treat-to-target strategy using methotrexate and intra-articular glucocorticoids with or without adalimumab induction: a 2-year investigator-initiated, double-blinded, randomised, controlled trial (OPERA). Ann Rheum Dis 2016;75:1645–53.

32. Burmester GR, Buttgereit F, Bernasconi C, Álvaro-Gracia JM, Castro N, Dougados M, et al. Continuing versus tapering glucocorticoids after achievement of low disease activity or remission in rheumatoid arthritis (SEMIRA): a double-blind, multicentre, randomised controlled trial. Lancet 2020;396: 267–76.

Clinical images: Granulomatosis with polyangiitis and transthyretin-related amyloidosis
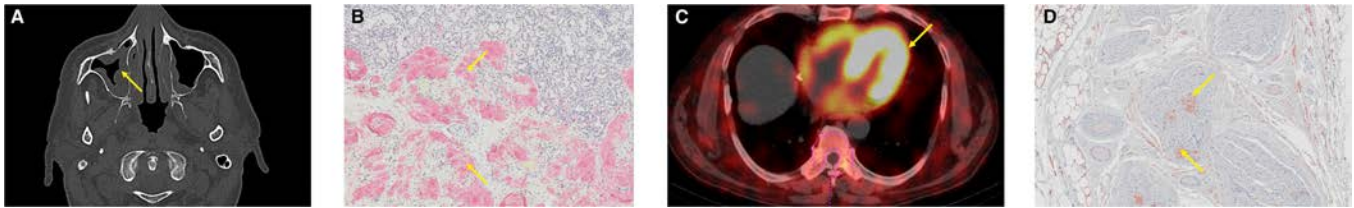
The patient, a 62-year-old man, was admitted with acute inflammation, arthralgia, and fever. Laboratory tests indicated elevated C-reactive protein, leukocytosis with left shift, slight elevation of transaminase, and serum negativity for rheumatoid factor, anti–cyclic citrullinated peptide, and antineutrophil cytoplasmic antibodies. Computed tomography (CT) of the abdomen showed bilateral pyelonephritis. The patient was started on antibiotics, but after lack of response, this was changed to prednisolone, leading to rapid improvement and treatment phase out. Four weeks after first admission, the patient presented with new-onset sinusitis, cephalgia, and pharyngitis, clearly indicating another humoral inflammatory reaction. CT of the paranasal sinuses revealed polypoid chronic inflammatory mucosal swelling of both maxillary sinuses (**A**, **arrow**). Histologic analysis revealed necrotizing vasculitis, partly containing giant cells and granulocytes, which confirmed a diagnosis of granulomatosis with polyangiitis (GPA). The patient was started on systemic immunosuppressive therapy with prednisolone and methotrexate, which quickly led to remission. Further histologic analysis revealed pronounced amyloid deposits immunohistochemically positive for the transthyretin (TTR) subtype (**B**, **arrows**). A mutation in the gene encoding TTR (p.-Arg54Gly) was confirmed. Subsequent ^{99m}Tc-3,3-diphosphono-1,2-propanodicarboxylic acid scintigraphy showed cardiac involvement by nuclide enhancement of the entire myocardium (**C**, **arrow**). The patient had pronounced muscle weakness and gait ataxia. Electroneurography confirmed mild sensorimotor mixed axonal–demyelinating polyneuropathy of the lower extremities. Congo red staining of the sural nerve indicated TTR deposits in the *endoneurium* (**D**, **arrows**). The patient was started on siRNA-based therapy with patisiran. This case is a rare coincidence of both TTR-related amyloidosis and GPA involving the upper respiratory tract, heart, and peripheral nerves.

Justas Grimalauskas-Suchina, MD
justas.grimalauskas@gmail.com
Frank Behrendt, PhD
Corina Schuster-Amft, PhD
Research Department
Reha Rheinfelden
Rheinfelden, Switzerland
Katrin Parmar, MD, PhD
Leo Bonati, MD
Research Department
Reha Rheinfelden
Rheinfelden, Switzerland

and Department of Neurology
University Hospital Basel
Basel, Switzerland
Hans U. Gerth, MD, PhD
Research Department
Reha Rheinfelden
Rheinfelden, Switzerland
and Department of Medicine
University Hospital Münster
Münster, Germany

AMERICAN COLLEGE
of RHEUMATOLOGY
Empowering Rheumatology Professionals

Genetic Liability to Rheumatoid Arthritis in Relation to Coronary Artery Disease and Stroke Risk

Shuai Yuan,[1] Paul Carter,[2] Amy M. Mason,[2] Fangkun Yang,[3] Stephen Burgess,[2] and Susanna C. Larsson[4]

Objective. To assess the causality of the associations of rheumatoid arthritis (RA) with coronary artery disease (CAD) and stroke using the Mendelian randomization approach.

Methods. Independent single-nucleotide polymorphisms strongly associated with RA (n = 70) were selected as instrumental variables from a genome-wide association meta-analysis including 14,361 RA patients and 43,923 controls of European ancestry. Summary-level data for CAD, all stroke, any ischemic stroke and its subtypes, intracerebral hemorrhage (ICH), and subarachnoid hemorrhage were obtained from meta-analyses of genetic studies, international genetic consortia, the UK Biobank, and the FinnGen consortium. We obtained summary-level data for common cardiovascular risk factors and related inflammatory biomarkers to assess possible mechanisms.

Results. Genetic liability to RA was associated with an increased risk of CAD and ICH. For a 1-unit increase in log odds of RA, the combined odds ratios were 1.02 (95% confidence interval [1.01, 1.03]; P = 0.003) for CAD and 1.05 (95% confidence interval [1.02, 1.08]; P = 0.001) for ICH. Genetic liability to RA was associated with increased levels of tumor necrosis factor and C-reactive protein (CRP). The association with CAD was attenuated after adjustment for genetically predicted CRP levels. There were no associations of genetic liability to RA with the other studied outcomes.

Conclusion. This study found that genetic liability to RA was associated with an increased risk of CAD and ICH and that the association with CAD might be mediated by CRP. The heightened cardiovascular risk should be actively monitored and managed in RA patients, and this may include dampening systemic inflammation.

INTRODUCTION

Rheumatoid arthritis (RA) is the most common autoimmune arthritis, with a prevalence of 1%, and cardiovascular disease (CVD) is the leading cause of mortality worldwide (1,2). Interestingly, CVD risk is substantially increased in RA and to a similar extent as other established risk factors such as diabetes mellitus (3). In meta-analyses, both cardiovascular morbidity and mortality have been found to be 1.5-fold elevated in RA compared to the general population (4,5). The reasons for this remain poorly understood but may relate to shared risk factors (e.g., obesity and smoking) or an influence of RA on traditional cardiovascular risk factors (e.g., side effects of antirheumatic therapies or

reduced physical activity due to pain). Importantly though, traditional risk factors do not fully explain the augmented CVD risk in RA, and observational studies suggest that RA may be a novel and independent risk factor for coronary disease (6–9). CVD and RA have overlapping pathophysiologic mechanisms which may contribute, such as systemic inflammation, with cytokines raised in RA known to be important in driving atherosclerotic diseases (10). Consistent with this, systemic markers of inflammation are associated with cardiovascular risk in RA (11,12). However, previous observational studies may have been limited by residual confounding or reverse causality. As such, whether RA is an independent and causal risk factor for CVDs and cardiometabolic risk factors remains equivocal.

[1]Shuai Yuan, B.Med, MMedSc: Karolinska Institutet, Stockholm, Sweden; [2]Paul Carter, MBChB, Amy M. Mason, PhD, Stephen Burgess, PhD: University of Cambridge, Cambridge, UK; [3]Fangkun Yang, MD: Ningbo First Hospital and Zhejiang University, Ningbo, China; [4]Susanna C. Larsson, PhD: Karolinska Institutet, Stockholm, Sweden, and Uppsala University, Uppsala, Sweden.

Author disclosures are available at https://onlinelibrary.wiley.com/action/downloadSupplement?doi=10.1002%2Fart.42239&file=art42239-sup-0001-Disclosureform.pdf.

Address correspondence to Susanna C. Larsson, PhD, Institute of Environmental Medicine, Karolinska Institutet, Nobelsväg 13, Stockholm, 17 177, Sweden. Email: susanna.larsson@ki.se.

Submitted for publication December 9, 2021; accepted in revised form May 12, 2022.

Mendelian randomization (MR) analysis is an epidemiologic approach that can strengthen causal inference by using genetic variants as instrumental variables for the exposure (13). The method can minimize the influence of residual confounding, since genetic variants are randomly distributed at conception and are therefore unrelated to self-adopted lifestyle and environmental confounders (13). In addition, the method can diminish reverse causality because the germline genotype cannot be modified by the onset and progression of the disease (13). Here, we conducted a 2-sample MR study to examine the associations of genetic predisposition to RA with coronary artery disease (CAD), stroke, and its subtypes and cardiometabolic risk factors. We aimed to provide important evidence regarding the causal role of RA in causing a range of CVD and whether this could be through influencing traditional risk factors or systemic inflammation.

MATERIALS AND METHODS

Study design. We first examined the genetic correlations and MR associations of genetic predisposition to RA with CAD and stroke and its subtypes. To assess potential mechanisms, we investigated the associations of genetic predisposition to RA with common cardiovascular risk factors and related inflammatory biomarkers. We then conducted multivariable MR analysis to examine the mediation effects of RA-associated factors in the associations between genetic predisposition to RA and the cardiovascular end points. This study was based on summary-level data from international consortia, the UK Biobank, and the FinnGen consortium. All included studies had obtained ethical permits from corresponding ethics committees. The UK Biobank received ethical permits from the North West Multi-centre Research Ethics Committee, the National Information Governance Board for Health and Social Care in England and Wales, and the Community Health Index Advisory Group in Scotland. All participants provided written informed consent. The present MR analyses were approved by the Swedish Ethical Review Authority (no. 2019-02793). This study was conducted in accordance with the MR guideline (14).

Instrumental variable selection. Single-nucleotide polymorphisms (SNPs) strongly associated with RA ($P < 5 \times 10^{-8}$) were obtained from a genome-wide association meta-analysis that included 14,361 RA patients and 43,923 controls of European ancestry (15). All RA cases were defined by the 1987 criteria of the American College of Rheumatology for RA diagnosis (16) or by a rheumatologist (15). Linkage disequilibrium in selected SNPs was estimated using the 1000 Genomes European reference panel. SNPs in high linkage disequilibrium ($r^2 > 0.01$ or clump windows <10,000 kb) were excluded, and the SNP with the lowest P value for the genome-wide association with RA was retained. A total of 70 independent SNPs with beta and SE coefficients scaled to log-transformed odds of RA were used as instrumental variables (Supplementary Table 1, on the *Arthritis & Rheumatology* website

at https://onlinelibrary.wiley.com/doi/10.1002/art.42239). To provide estimates with a more intuitive interpretation, we estimated absolute genetic associations with RA using linear regression and used these summary-level data for SNP–RA associations in a supplementary analysis (Supplementary Table 1). This enables the calculation of MR estimates that represent odds ratios (ORs) for the studied CVDs per 1% increase in the absolute probability of RA. Genetic associations were estimated in participants of genetic European descent in the UK Biobank. The outcome was defined using electronic health records and International Classification of Diseases codes (ICD-9 714.0, ICD-10: M05 or M06). Linear regression was performed with adjustment for age, sex, and 10 genomic principal components.

Data sources for outcomes. Summary-level data for the associations of RA-associated SNPs with CAD, all stroke, any ischemic stroke and its subtypes, ICH, and subarachnoid hemorrhage were obtained from meta-analyses of genetic studies, international genetic consortia (17–20), the UK Biobank, and the FinnGen consortium (21). There was minimal sample overlap between the exposure and outcome data sets. Detailed information, including case and control number and covariates adjusted for in the genome-wide association analysis, is shown in Table 1. The associations of RA-associated SNPs with the above outcomes are presented in Supplementary Table 2 (https://onlinelibrary.wiley.com/doi/10.1002/art.42239).

Data sources for cardiovascular risk factors, inflammatory biomarkers, and inflammatory bowel disease (IBD). We obtained summary-level data for cardiovascular risk factors (including body mass index [22], blood pressure [23], fasting glucose and insulin [24], high-density and low-density lipoprotein cholesterol and triglyceride [25], smoking initiation [26], and moderate-to-vigorous physical activity [the Neale Lab data, http://www.nealelab.is/uk-biobank] and inflammatory biomarkers such as interleukin-6 [IL-6] [27], tumor necrosis factor [TNF] [27], and C-reactive protein [CRP] [28]) from international consortia and the UK Biobank (the Neale Lab data). Summary-level data on IBD were obtained from a genome-wide association meta-analysis study including 59,957 individuals of European descent (29). Detailed information on the studies used are shown in Supplementary Table 3 (https://onlinelibrary.wiley.com/doi/10.1002/art.42239).

Genetic correlation analysis. Genome-wide pairwise correlations between RA and studied CVD outcomes based on consortia data were estimated using linkage disequilibrium score regression (LDSC) that leverages genome-wide association analysis summary-level data and linkage disequilibrium to estimate genetic correlation (30). This method estimates universal genetic correlation by measuring correlation of effect size between SNP exposure and SNP outcome associations across all genetic variants in the genome. A genetic correlation (*rg*) of >0.7 was deemed

Table 1. Included studies and consortia*

Data source/outcome	Outcome	Ancestry	No. of patients	No. of controls	Adjustments in the GWAS
CARDIoGRAMplusC4D and UKBB					
CAD		Mixed	122,733	424,528	Not reported
MEGASTROKE consortium					
All stroke		European	40,585	406,111	Age and sex
Any ischemic stroke		European	34,217	406,111	Age and sex
Large artery stroke		European	3,373	406,111	Age and sex
Small vessel stroke		European	5,386	406,111	Age and sex
Cardioembolic stroke		European	7,193	406,111	Age and sex
ISGC Intracerebral hemorrhage		European	3,223	3,725	Age, sex, and principal components
GWAS by Bakker et al Subarachnoid hemorrhage		European	5,140	71,952	Not reported
UKBB					
All stroke		European	12,036	355,525	Age, sex, and 10 genetic principal components
Any ischemic stroke		European	6,566	360,995	Age, sex, and 10 genetic principal components
Intracerebral hemorrhage		European	1,504	366,057	Age, sex, and 10 genetic principal components
Subarachnoid hemorrhage		European	1,292	366,269	Age, sex, and 10 genetic principal components
FinnGen consortium					
CAD		European	30,952	187,840	Age, sex, first 10 genetic principal components, and genotyping batch
All stroke		European	18,661	166,201	Age, sex, first 10 genetic principal components, and genotyping batch
Any ischemic stroke		European	10,551	202,223	Age, sex, first 10 genetic principal components, and genotyping batch
Intracerebral hemorrhage		European	1,687	201,146	Age, sex, first 10 genetic principal components, and genotyping batch
Subarachnoid hemorrhage		European	1,338	201,230	Age, sex, first 10 genetic principal components, and genotyping batch

* GWAS = genome-wide association study; CARDIoGRAMplusC4D = Coronary Artery Disease Genome-wide Replication and Meta-analysis plus The Coronary Artery Disease Genetics consortium; UKBB = UK Biobank; CAD = coronary artery disease; ISGC = International Stroke Genetic Consortium.

a strong correlation. P values less than 0.006 (0.05 for 8 outcomes) was treated as significant in LDSC analysis.

Statistical analysis. We aligned the SNPs based on allele letter and allele frequency. SNPs that were missing in the outcome data sets were replaced by proxy SNPs, which were searched in https://ldlink.nci.nih.gov/ by implementing a setting of $r^2 > 0.8$ and using European populations as reference groups. Missing SNPs without proxies were excluded from the analysis. We searched phenotypes associated with RA-associated SNPs at the genome-wide significance level in PhenoScanner V2, a database of human genotype–phenotype associations (31).

The inverse variance–weighted method under the multiplicative random effects model was used as the main method to calculate the associations of genetic liability to RA with cardiovascular outcomes, cardiovascular risk factors, and inflammatory biomarkers. This method can provide the most precise estimate; however, it is sensitive to horizontal pleiotropy and outliers. Several

sensitivity analyses, including the weighted median (32), MR-Egger (33), MR-PRESSO (34), and contamination mixture (35) methods, were used to examine the consistency of results and detect and correct for horizontal pleiotropy. The weighted median analysis can provide consistent causal estimates, given that more than half of weight derives from valid SNPs (32). The MR-Egger regression can detect the horizontal pleiotropy by its intercept test and provide estimates after correcting for pleiotropic effects; however, the analysis is less powerful for most scenarios (33). In a comparative study, power to detect causal effect is usually greater for the inverse variance–weighted method compared to the MR-Egger method in scenarios of different status of pleiotropy and satisfaction of the Instrument Strength Independent of Direct Effect assumption (33). The MR-PRESSO method can also correct for horizontal pleiotropy by identifying and removing outlying SNPs (34). The contamination mixture method is good at analysis based on multiple genetic instruments and can generate causal estimates even when instruments contain invalid SNPs (35).

In addition, we used scatter plots to visualize the heterogeneity in estimates of the SNPs used and to determine whether the association was driven by certain SNPs. Estimates from different data sets, but for the same CVD, were combined using the fixed-effects meta-analysis method in which study-specific estimates were weighted based on the amount of information captured by that study (i.e., more weight was given to a large study with many patients than a small study with few patients). Given that the HLA gene regions are shared by RA and other autoimmune disorders (36), we performed a sensitivity analysis after removal of SNPs in these gene regions (including HLA–A, HLA–B, HLA–C, HLA–DPA1, HLA–DPB1, HLA–DQA1, HLA–DQB1, HLA–DRA, HLA–DRB1, and HLA–DRB3). We used the multivariable MR analysis to estimate the mediation effects of RA-associated factors in the associations between RA and cardiovascular outcomes. The multivariable MR analysis was based on the same set of genetic instruments (SNPs for RA), and the model was based on summary-level beta coefficients and the corresponding standard error for RA, the outcome, and the mediator. In addition, we conducted a multivariable MR analysis to adjust for genetic liability to IBD (a common autoimmune disease) to minimize its influence. Likewise, this analysis used the same genetic variants as the main analysis, and MR estimates were obtained from a multivariable inverse variance–weighted analysis on the association between genetic liability to RA with a CVD outcome with adjustment for genetic liability to IBD.

Cochran's Q statistic and P value for MR-Egger intercept were used to assess the heterogeneity and horizontal pleiotropy, respectively. The Bonferroni correction was used to account for multiple testing in examining the association between RA and CVDs. Associations with a P value less than 0.006 (0.05 for 8 outcomes) were deemed significant in order to correct for multiple testing. All tests were 2-sided and were conducted using the TwoSampleMR and MendelianRandomization package (37,38).

RESULTS

Results of the search in PhenoScanner V2 are presented in Supplementary Table 4 (https://onlinelibrary.wiley.com/doi/10.1002/art.42239). Several RA-associated SNPs were found to be associated with other autoimmune diseases, including IBD, systemic lupus erythematosus, and type 1 diabetes, at the genome-wide significance levels. A few other traits, such as immune cells, were identified to be associated with the SNPs that were used. There were few strong genetic correlations between RA and the studied cardiovascular outcomes (Supplementary Table 5, https://onlinelibrary.wiley.com/doi/10.1002/art.42239).

Outcome	Cases	Controls		OR (95% CI)	P-value
Coronary artery disease					
CARDIoGRAMplusC4D+UKBB	122 733	424 528		1.02 (1.00, 1.03)	0.009
FinnGen	30 952	187 840		1.01 (0.99, 1.03)	0.164
Combined				**1.02 (1.01, 1.03)**	**0.003**
All stroke					
MEGASTROKE	40 585	406 111		1.00 (0.98, 1.02)	0.983
UKBB	12 036	355 525		1.00 (0.99, 1.02)	0.743
FinnGen	18 661	162 201		1.01 (0.99, 1.03)	0.351
Combined				**1.00 (0.99, 1.01)**	**0.498**
Any ischemic stroke					
MEGASTROKE	34 217	406 111		1.00 (0.98, 1.02)	0.950
UKBB	6566	360 995		0.99 (0.97, 1.02)	0.650
FinnGen	10 551	202 223		0.99 (0.97, 1.01)	0.382
Combined				**1.00 (0.99, 1.01)**	**0.507**
Cardioembolic stroke					
MEGASTROKE	7193	406 111		1.00 (0.97, 1.02)	0.922
Small vessel stroke					
MEGASTROKE	5386	406 111		1.03 (0.99, 1.07)	0.102
Large artery stroke					
MEGASTROKE	3373	406 111		1.02 (0.97, 1.07)	0.468
Intracerebral hemorrhage					
ISGC	3223	3725		1.07 (0.93, 1.22)	0.335
UKBB	1504	366 057		1.04 (1.00, 1.08)	0.030
FinnGen	1687	201 146		1.05 (1.01, 1.09)	0.019
Combined				**1.05 (1.02, 1.08)**	**0.001**
Subarachnoid hemorrhage					
Bakker et al GWAS	5140	71 934		1.01 (0.95, 1.06)	0.816
UKBB	1292	366 269		0.98 (0.94, 1.02)	0.365
FinnGen	1338	201 230		1.01 (0.97, 1.06)	0.542
Combined				**1.00 (0.97, 1.03)**	**0.903**

OR (95% CI): 0.90   1.0   1.1   1.2

Figure 1. Associations of genetic liability to rheumatoid arthritis with coronary artery disease and stroke. OR = odds ratio; 95% CI = 95% confidence interval; CARDIoGRAMplusC4D = Coronary Artery Disease Genome-wide Replication and Meta-analysis plus The Coronary Artery Disease Genetics consortium; UKBB = UK Biobank; ISGC = International Stroke Genetic Consortium; GWAS = genome-wide association study.

A. Scatter plot of associations for coronary artery disease

CARDIoGRAMplusC4D+UKBB   FinnGen

B. Scatter plot of associations for intracerebral hemorrhage

International Stroke Genetic Consortium   UK Biobank   FinnGen
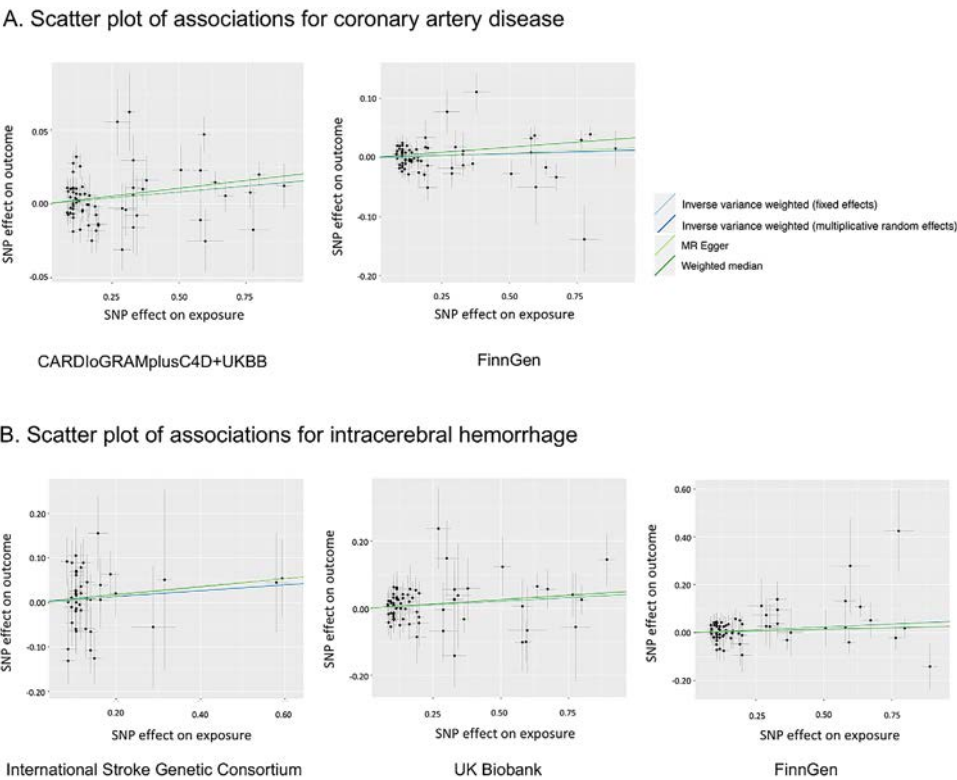
Figure 2. Scatter plots of associations with coronary artery disease and intracerebral hemorrhage. SNP = single-nucleotide polymorphism; CARDIoGRAMplusC4D = Coronary Artery Disease Genome-wide Replication and Meta-analysis plus The Coronary Artery Disease Genetics consortium; MR = Mendelian randomization.

RA showed a weak significant association with overall stroke ($rg = 0.20$; $P = 0.003$).

Genetic liability to RA was associated with an increased risk of CAD and ICH (Figure 1) consistently across sources. For a 1-unit increase in log odds of RA, the combined odds ratios (ORs) were 1.02 (95% confidence interval [95% CI] 1.01, 1.03; $P = 0.003$) for CAD and 1.05 (95% CI 1.02, 1.08; $P = 0.001$) for ICH. The results were stable in all sensitivity analyses

Factor	N	Beta (95% CI)	P-value
Cardiovascular risk factor			
Body mass index	681 275	-0.001 (-0.006, 0.004)	0.573
Systolic blood pressure	757 601	0.042 (-0.027, 0.111)	0.235
Diastolic blood pressure	757 602	0.034 (-0.007, 0.075)	0.104
Fasting glucose	46 186	-0.004 (-0.013, 0.006)	0.442
Fasting insulin	38 238	0.004 (-0.005, 0.013)	0.379
High-density lipoprotein cholesterol	187 167	0.019 (0.006, 0.032)	0.005
Low-density lipoprotein cholesterol	173 082	-0.006 (-0.018, 0.006)	0.351
Triglyceride	177 861	-0.009 (-0.019, 0.001)	0.089
Smoking initiation	1 232 091	-0.010 (-0.018, -0.001)	0.021
Moderate to vigorous physical activity	377 234	0.001 (-0.003, 0.004)	0.782
Inflammatory factor			
Interleukin-6	8293	0.029 (-0.002, 0.060)	0.070
Tumor necrosis factor	8293	0.052 (0.000, 0.104)	0.048
C-reactive protein	343 524	0.065 (0.041, 0.089)	<0.001

Figure 3. Associations of genetic liability to rheumatoid arthritis with cardiometabolic risk factors and inflammatory cytokines. 95% CI = 95% confidence interval.

Outcome		OR (95% CI)	P-value
Coronary artery disease			
Without adjustment			
CARDIoGRAMplusC4D+UKBB		1.02 (1.00, 1.03)	0.009
FinnGen		1.01 (0.99, 1.03)	0.164
Combined		**1.02 (1.01, 1.03)**	**0.003**
Adjusted for TNF			
CARDIoGRAMplusC4D+UKBB		1.03 (1.01, 1.05)	0.012
FinnGen		1.02 (0.99, 1.05)	0.151
Combined		**1.03 (1.01, 1.05)**	**0.004**
Adjusted for CRP			
CARDIoGRAMplusC4D+UKBB		1.01 (1.00, 1.02)	0.178
FinnGen		1.00 (0.98, 1.02)	0.852
Combined		**1.01 (0.99, 1.02)**	**0.268**
Intracerebral hemorrhage			
Without adjustment			
ISGC		1.07 (0.93, 1.22)	0.335
UKBB		1.04 (1.00, 1.08)	0.030
FinnGen		1.05 (1.01, 1.09)	0.019
Combined		**1.05 (1.02, 1.08)**	**0.001**
Adjusted for TNF			
ISGC		1.13 (0.98, 1.31)	0.085
UKBB		1.04 (0.96, 1.13)	0.291
FinnGen		1.03 (0.96, 1.11)	0.379
Combined		**1.05 (1.00, 1.10)**	**0.059**
Adjusted for CRP			
ISGC		1.07 (0.93, 1.22)	0.370
UKBB		1.03 (0.97, 1.08)	0.344
FinnGen		1.06 (1.01, 1.12)	0.029
Combined		**1.04 (1.01, 1.08)**	**0.018**

OR (95% CI) — 0.90   1.0   1.1   1.2   1.3

Figure 4. Associations of genetic liability to rheumatoid arthritis with coronary artery disease and intracerebral hemorrhage after adjustment for tumor necrosis factor (TNF) and C-reactive protein (CRP). See Figure 1 for other definitions.

(Supplementary Table 6, https://onlinelibrary.wiley.com/doi/10.1002/art.42239). In a supplementary analysis in which estimates for the CVD outcomes were scaled per 1% increase 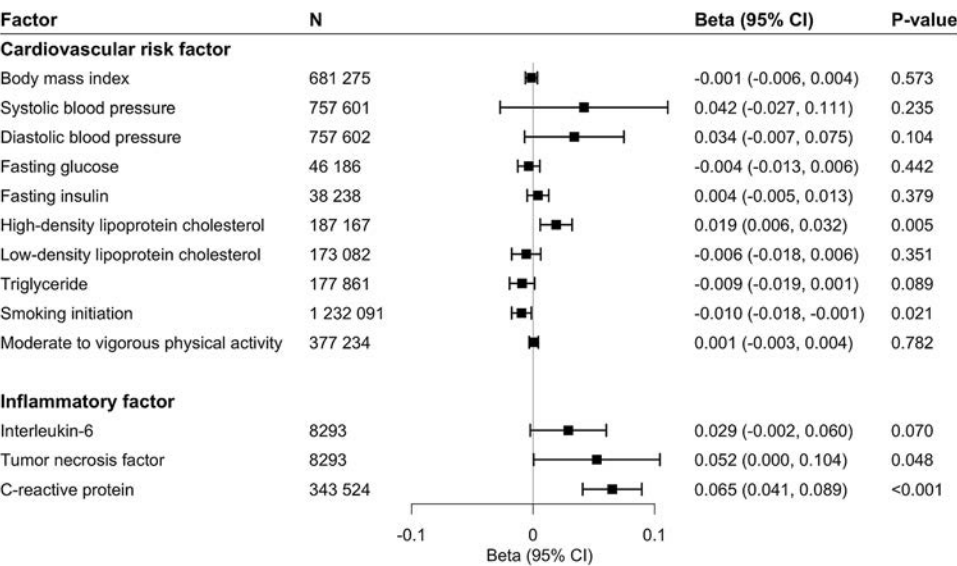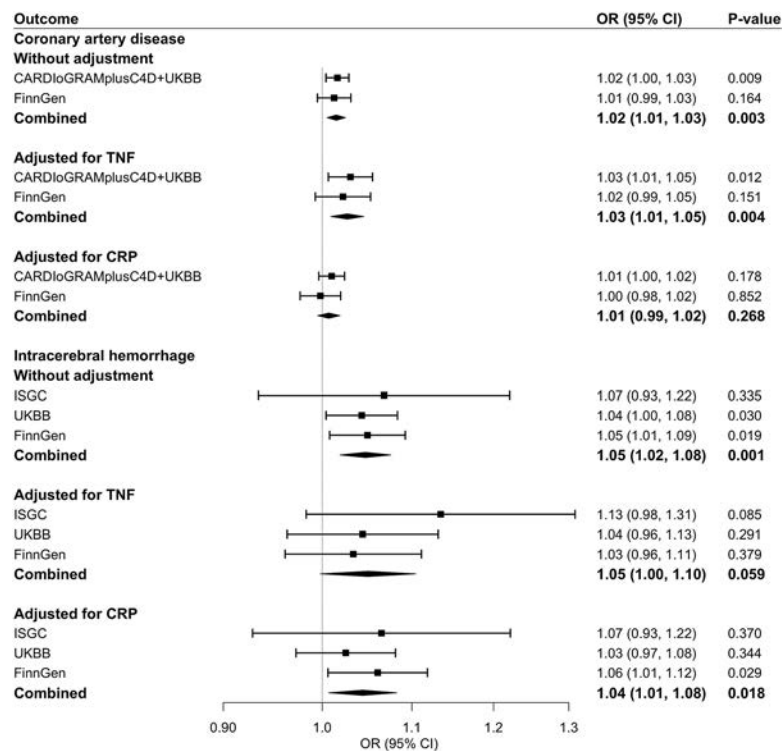in genetic liability to RA on the risk difference scale, the OR was 1.03 (95% CI 1.01, 1.05) for CAD and 1.06 (95% CI, 1.01, 1.11) for ICH (Supplementary Table 7, https://onlinelibrary.wiley.com/doi/10.1002/art.42239).

We detected moderate heterogeneity in the analyses for CAD and no horizontal pleiotropy (P for MR-Egger intercept test > 0.4) (Supplementary Table 6). Even though a few outliers were detected in the MR-PRESSO analyses for CAD, the associations remained consistent after removal of these outliers (Supplementary Table 6). As for associations with ICH in the 3 data sets, we observed no or modest heterogeneity, no indication of horizontal pleiotropy in the MR-Egger intercept tests, and no outliers were detected by the MR-PRESSO analyses (Supplementary Table 6). In scatter plots of associations with CAD and ICH, we did not observe any SNPs that drove the overall positive associations (Figure 2). Otherwise, there were no associations of genetic liability to RA with all stroke, any ischemic stroke and its subtypes, or subarachnoid hemorrhage (Figure 1 and Supplementary Table 6).

The observed associations with CAD and ICH remained stable in the sensitivity analysis after removal of SNPs in HLA gene regions (Supplementary Table 8, https://onlinelibrary.wiley.com/doi/10.1002/art.42239). The associations were also stable in the multivariable MR analysis with adjustment for genetic liability to IBD (Supplementary Table 9, https://onlinelibrary.wiley.com/doi/10.1002/art.42239).

With respect to cardiometabolic risk factors, genetic liability to RA was associated with reduced log odds ratio of smoking initiation and increased levels of high-density lipoprotein cholesterol, TNF, and CRP (Figure 3). The associations remained directionally consistent in sensitivity analyses (Supplementary Table 10, https://onlinelibrary.wiley.com/doi/10.1002/art.42239). There were no associations of genetic liability to RA with the other cardiovascular risk factors and inflammatory biomarkers studied (Figure 3).

Multivariate MR analyses were conducted to adjust for genetically predicted levels of TNF and CRP levels. The association between RA and CAD attenuated in the analysis with adjustment for genetically predicted CRP levels but not in the analysis with adjustment for genetically predicted TNF. The association between RA and ICH changed only slightly in the multivariable MR analyses (Figure 4).

DISCUSSION

We conducted a 2-sample MR study to investigate the causal associations of RA with CAD and stroke using data from large consortia and genetic studies. Few strong genetic correlations were

observed between RA and studied cardiovascular outcomes. We found that genetic liability to RA was associated with elevated risk of CAD and ICH but not ischemic stroke or subarachnoid hemorrhage. These associations were consistent across different data sources, after removal of SNPs in HLA gene regions, and in the multivariable MR analysis with adjustment for genetic liability to IBD. Genetic liability to RA was associated with elevated levels of TNF and CRP. The increased levels of CRP appeared to mediate the association with CAD. We thus provide important genetic evidence supporting the link between RA and some CVDs and underscore the role of inflammation in driving CAD specifically.

RA has widely been reported as an important risk factor for CAD and impaired vascular function (33). A higher prevalence, extent, and severity of coronary plaque measured by coronary calcification (6) is found in RA patients, and this is related to disease duration, being increased in established compared to early RA (31). Similarly, invasive angiographic studies have also demonstrated RA to be associated with an increased extent of coronary atherosclerosis, with a higher prevalence of multivessel CAD, even after adjustment for some traditional risk factors (9). Importantly, this accelerated coronary atherosclerosis also appears to confer a substantially elevated risk of cardiovascular events, with incident myocardial infarction and CAD-related mortality increased by 68% and 59% in RA, respectively, according to large meta-analyses (3,4).

Our findings support a causal role for RA in driving CAD, although we report a more modest effect size of 2% in the main analysis. This likely relates to differences in outcome definition (myocardial infarction versus the softer end point of CAD), more healthy populations included, and the calculation of risk according to log odds of RA. Overall, though, the totality of evidence suggests CAD to be increased in RA, and our study strongly suggests a causal role in this. There are ~14 million people globally with RA (39). As lifetime risk of CAD for people in general is already high (40), even a small increase in odds of CVD raises the expected number of CAD events in this population by tens of thousands compared to that expected for a similar sized group without RA. This potentially impacts public health policy around targeting of education, screening, and treatment at RA patients. Second, it provides insight into potential mechanisms of CAD. Even though we identified that chronic inflammation might mediate the association between RA and CAD, future research may be able to pinpoint exactly which metabolic or inflammatory changes occur in people with RA that lead to this increase in CAD, potentially identifying treatment or screening options for the whole population.

Stroke risk, of both ischemic and hemorrhagic types, has also widely been reported in observational studies to be increased in RA patients (41). Our study did not detect an association between genetic liability to RA and risk of stroke overall or ischemic stroke. This discrepancy may be related to confounding in observational studies, or increased stroke risk may not be caused by RA per se but by certain features of RA patients. Consistent with this, incident adverse events, including serious infections and insufficient treatment of CVDs, have been found to be drivers of the increased risk of stroke in RA patients (42). These null MR findings might be caused by inadequate power. Our study did, however, suggest a causal role for RA in causing ICH and supports the 68% increased risk reported in meta-analysis of observational studies (41). Our consistent findings across 3 data sets highly suggest the validity of this association, and the underlying mechanisms warrant further investigation.

Several mechanisms have been proposed to explain the increased risk of CVD in RA patients. First, it has been suggested that RA may influence the development of traditional cardiovascular risk factors. We did not find genetic liability to RA to be associated with the majority of cardiometabolic risk factors, and only high-density lipoprotein cholesterol, a protective factor, was significantly increased. We therefore provide some mechanistic evidence against the role of traditional risk factors, although it is possible that RA may indirectly influence traditional risk factors, such as due to side effects of antirheumatic or antiinflammatory medications. In addition, our null MR findings for the associations of genetic liability to RA with cardiometabolic risk factors could not completely rule out the effects of shared nongenetic factors on these associations. Furthermore, although far from significant, relatively large effect sizes were found for blood pressure in our study. In a recent published MR analysis including 461,880 hypertension patients and 337,653 controls, RA was associated with a high risk of hypertension (43), which is an important risk factor for CAD and the main cause of hemorrhagic stroke. However, a key hypothesis is that elevated systemic inflammation and remarkably overlapping inflammatory processes between the 2 conditions lead to progression of CVD (11,44). In agreement with this, circulating levels of inflammatory markers such as CRP, erythrocyte sedimentation rate, and IL-6 in RA patients are associated with a risk of cardiovascular events (11,45) and with radiologic measures of coronary atherosclerosis (46).

Our study supports the notion that chronic inflammation drives CAD risk in RA, as CRP mediates the association between RA and CAD risk. However, our multivariable MR analysis did not suggest an important role of TNF for CAD or for RA-associated inflammation on ICH. Other RA-related abnormalities that may predispose one to CAD or ICH may include endothelial dysfunction, oxidative stress, lipid alterations, and posttranslational modifications of peptides (45). Further investigation is required into the mechanisms underlying the association between RA and ICH.

Elevated CVD in RA has long been recognized, and in recent years this has been incorporated into European clinical guidelines written for use by both rheumatology (European Alliance of Associations for Rheumatology) (47) and cardiology (European Society of Cardiology) (48) clinicians. In particular, the importance of regular cardiovascular risk assessment every 5 years is emphasized,

as is the use of a 1.5-fold multiplication factor to account for RA in risk scores based solely on traditional risk factors. However, evidence exists that cardiovascular risk factors remain undiagnosed in RA patients, and, even when detected, they may be undermanaged compared to patients with other risk factors like diabetes (49). Our study provides the first MR evidence supporting a causal role of RA in driving heightened cardiovascular risk. This not only emphasizes the importance of monitoring this high-risk population, but also supports the notion in clinical guidelines that combating rheumatic disease activity is also integral to reducing cardiovascular risk. Current strategies to do this remain controversial, as some therapies have been associated with adverse cardiovascular effects (47,50).

We provide the causal genetic evidence that inflammation drives CAD risk in RA and implicate this as an effective therapeutic target. TNF inhibitors are commonly used in clinical practice, and although some evidence exists for reduced cardiovascular risk in patients on such treatments (51), our results do not support this. CRP is a broad inflammatory marker raised by many pathways, including the IL-1/IL-6 axis. IL-1 inhibition reduced cardiovascular events in the Canakinumab Antiinflammatory Thrombosis Outcome Study trial, and IL-6 inhibition has been found to have beneficial effects on markers of atherosclerosis such as carotid intima-media thickness (47) and to reduce cardiovascular events in RA (52). Although antiinflammatory treatments may prove useful in cardiovascular prevention in RA, studies to date have had inadequate follow-up times and have been confounded by therapies being allocated to those with the most severe disease. Well-designed clinical trials studying the impact of antiinflammatory therapies on cardiovascular risk in RA are required.

Given that autoimmune diseases have some overlapping genetic architecture, whether the observed associations between RA and CAD and between RA and ICH in our MR analysis were exclusive to RA remained undetermined, even though we employed several approaches to examine this. First, the results from the search of phenotypes associated with RA-associated SNPs in PhenoScanner V2 showed no clear pattern that these used RA-associated SNPs could systematically mimic the effects of other immune-mediated disorders, although several RA-associated SNPs were associated with several other immune-mediated diseases at the genome-wide significance level. Second, the observed associations with CAD and ICH remained stable in the sensitivity analysis after removal of SNPs in the HLA gene regions shared by autoimmune disorders (36), which indicated that the effects of most shared genes among autoimmune diseases did not drive the associations. Third, the associations remained in the multivariable MR analysis with adjustment for IBD. However, we could not perform this analysis to adjust for genetic liability to other common autoimmune diseases due to lack of data or too many missing SNPs in corresponding analysis. Even though our exploration implies the

observed associations with CAD and ICH are likely to be specific to RA, further studies are needed to confirm our hypothesis.

The present study has several strengths, including MR design, the use of multiple genetic instruments, the use of different outcome data sources, the use of the multivariable MR analysis to explore possible mechanisms, and the population confinement to individuals of European descent (reducing population structure bias). In addition, lack of strong genetic correlations between RA and studied outcomes suggest that the observed associations with CAD and ICH may not be driven by shared genetic risk.

Several limitations should be considered when interpreting our findings. We observed moderate heterogeneity in the analyses for CAD in the CARDIoGRAMplusC4D (Coronary Artery Disease Genome-wide Replication and Meta-analysis plus The Coronary Artery Disease Genetics) consortium, UK Biobank, and FinnGen data sets. However, the corresponding MR-Egger regression analysis did not detect any indication of horizontal pleiotropy, which suggests possible balanced horizontal pleiotropy that is unlikely to bias the MR estimate (53). In addition, the associations with CAD in 2 data sets were consistent across different sensitivity analyses with different assumptions. Even though there were a few outliers detected by MR-PRESSO analyses, the associations remained after removal of these outliers. We did not take anti-RA treatments into consideration in the current analysis. Nonetheless, whether corresponding treatments, such as anti-TNF drugs and nonsteroidal antiinflammatory drugs, are associated with cardiovascular risk is unclear (44,54). In addition, these treatments should not bias our causal estimation, as their use follows the diagnosis of RA and would therefore be classified as vertical pleiotropy (53).

The population confinement to European populations might limit the generalizability of our findings to other populations. In addition, whether the null findings for stroke and its subtypes (except for ICH) could be robustly held are uncertain, as the lack of significant associations might be caused by inadequate power despite the large sample size, at least for ischemic stroke. A power calculation for the current analysis was not possible due to the lack of information on phenotypic variance in RA explained by the SNPs used in the analysis, as this information cannot be calculated for a binary phenotype. Thus, future studies are needed to confirm these null findings. Whether the observed associations could be applied to subgroups defined by sex and status of anti–citrullinated protein autoantibodies could not be assessed due to lack of data.

In conclusion, this MR study found positive associations of genetic liability to RA with CAD and ICH, and the association with CAD appeared to be mediated by high levels of CRP. These findings highlight the importance of active monitoring and prevention of cardiovascular risk to combat CAD and ICH in RA patients. We further suggest that dampening inflammation might be a preventive strategy for CAD in RA patients, and well-designed clinical trials are required to assess this.

AUTHOR CONTRIBUTIONS

All authors were involved in drafting the article or revising it critically for important intellectual content, and all authors approved the final version to be published. Dr. Yuan had full access to all of the data in the study and takes responsibility for the integrity of the data and the accuracy of the data analysis.
Study conception and design. Yuan, Carter, Larsson.
Acquisition of data. Yuan, Carter, Mason, Burgess, Larsson.
Analysis and interpretation of data. Yuan, Carter, Mason, Yang, Burgess, Larsson.

REFERENCES

1. Safiri S, Kolahi AA, Hoy D, Smith E, Bettampadi D, Mansournia MA, et al. Global, regional and national burden of rheumatoid arthritis 1990-2017: a systematic analysis of the Global Burden of Disease study 2017. Ann Rheum Dis 2019;78:1463–71.

2. Joseph P, Leong D, McKee M, Anand SS, Schwalm JD, Teo K, et al. Reducing the global burden of cardiovascular disease, part 1: the epidemiology and risk factors. Circ Res 2017;121:677–94.

3. Van Halm VP, Peters MJ, Voskuyl AE, Boers M, Lems WF, Visser M, et al. Rheumatoid arthritis versus diabetes as a risk factor for cardiovascular disease: a cross-sectional study, the CARRE Investigation. Ann Rheum Dis 2009;68:1395–400.

4. Avina-Zubieta JA, Thomas J, Sadatsafavi M, Lehman AJ, Lacaille D. Risk of incident cardiovascular events in patients with rheumatoid arthritis: a meta-analysis of observational studies. Ann Rheum Dis 2012;71:1524–9.

5. Aviña-Zubieta JA, Choi HK, Sadatsafavi M, Etminan M, Esdaile JM, Lacaille D. Risk of cardiovascular mortality in patients with rheumatoid arthritis: a meta-analysis of observational studies. Arthritis Rheum 2008;59:1690–7.

6. Karpouzas GA, Malpeso J, Choi TY, Li D, Munoz S, Budoff MJ. Prevalence, extent and composition of coronary plaque in patients with rheumatoid arthritis without symptoms or prior diagnosis of coronary artery disease. Ann Rheum Dis 2014;73:1797–804.

7. Løgstrup BB, Olesen KK, Masic D, Gyldenkerne C, Thrane PG, Ellingsen T, et al. Impact of rheumatoid arthritis on major cardiovascular events in patients with and without coronary artery disease. Ann Rheum Dis 2020;79:1182–8.

8. Del Rincón ID, Williams K, Stern MP, Freeman GL, Escalante A. High incidence of cardiovascular events in a rheumatoid arthritis cohort not explained by traditional cardiac risk factors. Arthritis Rheum 2001;44:2737–45.

9. Warrington KJ, Kent PD, Frye RL, Lymp JF, Kopecky SL, Goronzy JJ, et al. Rheumatoid arthritis is an independent risk factor for multi-vessel coronary artery disease: a case control study. Arthritis Res Ther 2005;7:R984–91.

10. Yuan S, Lin A, He QQ, Burgess S, Larsson SC. Circulating interleukins in relation to coronary artery disease, atrial fibrillation and ischemic stroke and its subtypes: a two-sample Mendelian randomization study. Int J Cardiol 2020;313:99–104.

11. Zhang J, Chen L, Delzell E, Muntner P, Hillegass WB, Safford MM, et al. The association between inflammatory markers, serum lipids and the risk of cardiovascular events in patients with rheumatoid arthritis. Ann Rheum Dis 2014;73:1301–8.

12. Navarro-Millán I, Yang S, DuVall SL, Chen L, Baddley J, Cannon GW, et al. Association of hyperlipidaemia, inflammation and serological status and coronary heart disease among patients with rheumatoid arthritis: data from the National Veterans Health Administration. Ann Rheum Dis 2016;75:341–7.

13. Burgess S, Thompson SG. Mendelian randomization: methods for using genetic variants in causal estimation. London: Chapman and Hall/CRC; 2015.

14. Burgess S, Davey Smith G, Davies NM, Dudbridge F, Gill D, Glymour MM, et al. Guidelines for performing Mendelian randomization investigations. Wellcome Open Res 2019;4:186.

15. Okada Y, Wu D, Trynka G, Raj T, Terao C, Ikari K, et al. Genetics of rheumatoid arthritis contributes to biology and drug discovery. Nature 2014;506:376–81.

16. Arnett FC, Edworthy SM, Bloch DA, McShane DJ, Fries JF, Cooper NS, et al. The American Rheumatism Association 1987 revised criteria for the classification of rheumatoid arthritis. Arthritis Rheum 1988;31:315–24.

17. Van der Harst P, Verweij N. Identification of 64 novel genetic loci provides an expanded view on the genetic architecture of coronary artery disease. Circ Res 2018;122:433–43.

18. Malik R, Chauhan G, Traylor M, Sargurupremraj M, Okada Y, Mishra A, et al. Multiancestry genome-wide association study of 520,000 subjects identifies 32 loci associated with stroke and stroke subtypes. Nat Genet 2018;50:524–37.

19. Woo D, Falcone GJ, Devan WJ, Brown WM, Biffi A, Howard TD, et al. Meta-analysis of genome-wide association studies identifies 1q22 as a susceptibility locus for intracerebral hemorrhage. Am J Hum Genet 2014;94:511–21.

20. Bakker MK, van der Spek RA, van Rheenen W, Morel S, Bourcier R, Hostettler IC, et al. Genome-wide association study of intracranial aneurysms identifies 17 risk loci and genetic overlap with clinical risk factors. Nat Genet 2020;52:1303–13.

21. consortium TF. R5 release of FinnGen consortium genome-wide association analysis data. 2021. URL: https://finngen.gitbook.io/documentation/.

22. Yengo L, Sidorenko J, Kemper KE, Zheng Z, Wood AR, Weedon MN, et al. Meta-analysis of genome-wide association studies for height and body mass index in ∼700000 individuals of European ancestry. Hum Mol Genet 2018;27:3641–9.

23. Evangelou E, Warren HR, Mosen-Ansorena D, Mifsud B, Pazoki R, Gao H, et al. Genetic analysis of over 1 million people identifies 535 new loci associated with blood pressure traits. Nat Genet 2018;50:1412–25.

24. Dupuis J, Langenberg C, Prokopenko I, Saxena R, Soranzo N, Jackson AU, et al. New genetic loci implicated in fasting glucose homeostasis and their impact on type 2 diabetes risk. Nat Genet 2010;42:105–16.

25. Willer CJ, Schmidt EM, Sengupta S, Peloso GM, Gustafsson S, Kanoni S, et al. Discovery and refinement of loci associated with lipid levels. Nat Genet 2013;45:1274–83.

26. Liu M, Jiang Y, Wedow R, Li Y, Brazel DM, Chen F, et al. Association studies of up to 1.2 million individuals yield new insights into the genetic etiology of tobacco and alcohol use. Nat Genet 2019;51: 237–44.

27. Ahola-Olli AV, Wurtz P, Havulinna AS, Aalto K, Pitkanen N, Lehtimaki T, et al. Genome-wide association study identifies 27 loci influencing concentrations of circulating cytokines and growth factors. Am J Hum Genet 2017;100:40–50.

28. Folkersen L, Gustafsson S, Wang Q, Hansen DH, Hedman ÅK, Schork A, et al. Genomic and drug target evaluation of 90 cardiovascular proteins in 30,931 individuals. Nat Metab 2020;2:1135–48.

29. De Lange KM, Moutsianas L, Lee JC, Lamb CA, Luo Y, Kennedy NA, et al. Genome-wide association study implicates immune activation of multiple integrin genes in inflammatory bowel disease. Nat Genet 2017;49:256–61.

30. Bulik-Sullivan B, Finucane HK, Anttila V, Gusev A, Day FR, Loh PR, et al. An atlas of genetic correlations across human diseases and traits. Nat Genet 2015;47:1236–41.

31. Kamat MA, Blackshaw JA, Young R, Surendran P, Burgess S, Danesh J, et al. PhenoScanner V2: an expanded tool for searching human genotype-phenotype associations. Bioinformatics 2019;35: 4851–3.

32. Bowden J, Davey Smith G, Haycock PC, Burgess S. Consistent estimation in mendelian randomization with some invalid instruments using a weighted median estimator. Genet Epidemiol 2016;40: 304–14.

33. Bowden J, Smith GD, Burgess S. Mendelian randomization with invalid instruments: effect estimation and bias detection through Egger regression. Int J Epidemiol 2015;44:512–25.

34. Verbanck M, Chen CY, Neale B, Do R. Detection of widespread horizontal pleiotropy in causal relationships inferred from Mendelian randomization between complex traits and diseases. Nat Genet 2018; 50:693–8.

35. Burgess S, Foley CN, Allara E, Staley JR, Howson JM. A robust and efficient method for Mendelian randomization with hundreds of genetic variants. Nat Commun 2020;11:376.

36. Shiina T, Hosomichi K, Inoko H, Kulski JK. The HLA genomic loci map: expression, interaction, diversity and disease. J Hum Genet 2009;54:15–39.

37. Hemani G, Zheng J, Elsworth B, Wade KH, Haberland V, Baird D, et al. The MR-Base platform supports systematic causal inference across the human phenome. Elife 2018;7:e34408.

38. Yavorska OO, Burgess S. MendelianRandomization: an R package for performing Mendelian randomization analyses using summarized data. Int J Epidemiol 2017;46:1734–9.

39. Almutairi K, Nossent J, Preen D, Keen H, Inderjeeth C. The global prevalence of rheumatoid arthritis: a meta-analysis based on a systematic review. Rheumatol Int 2021;41:863–77.

40. Lloyd-Jones DM, Larson MG, Beiser A, Levy D. Lifetime risk of developing coronary heart disease. Lancet. 1999;353:89–92.

41. Wiseman SJ, Ralston SH, Wardlaw JM. Cerebrovascular disease in rheumatic diseases: a systematic review and meta-analysis. Stroke 2016;47:943–50.

42. Meissner Y, Richter A, Manger B, Tony HP, Wilden E, Listing J, et al. Serious adverse events and the risk of stroke in patients with rheumatoid arthritis: results from the German RABBIT cohort. Ann Rheum Dis 2017;76:1583–90.

43. Qiu S, Li M, Jin S, Lu H, Hu Y. Rheumatoid arthritis and cardiocerebrovascular disease: a mendelian randomization study. Front Genet 2021;12:745224.

44. Yuan S, Carter P, Bruzelius M, Vithayathil M, Kar S, Mason AM, et al. Effects of tumour necrosis factor on cardiovascular disease and cancer: a two-sample Mendelian randomization study. EBioMedicine 2020;59:102956.

45. England BR, Thiele GM, Anderson DR, Mikuls TR. Increased cardiovascular risk in rheumatoid arthritis: mechanisms and implications. BMJ 2018;361:k1036.

46. Chung CP, Oeser A, Raggi P, Gebretsadik T, Shintani AK, Sokka T, et al. Increased coronary-artery atherosclerosis in rheumatoid arthritis: relationship to disease duration and cardiovascular risk factors. Arthritis Rheum 2005;52:3045–53.

47. Agca R, Heslinga SC, Rollefstad S, Heslinga M, McInnes IB, Peters MJ, et al. EULAR recommendations for cardiovascular disease risk management in patients with rheumatoid arthritis and other forms of inflammatory joint disorders: 2015/2016 update. Ann Rheum Dis 2017;76:17–28.

48. Piepoli MF, Hoes AW, Agewall S, Albus C, Brotons C, Catapano AL, et al. 2016 European Guidelines on cardiovascular disease prevention in clinical practice: the Sixth Joint Task Force of the European Society of Cardiology and Other Societies on Cardiovascular Disease Prevention in Clinical Practice (constituted by representatives of 10 societies and by invited experts) developed with the special contribution of the European Association for Cardiovascular Prevention & Rehabilitation (EACPR). Eur Heart J 2016;37:2315–81.

49. Desai SS, Myles JD, Kaplan MJ. Suboptimal cardiovascular risk factor identification and management in patients with rheumatoid arthritis: a cohort analysis. Arthritis Res Ther 2012;14:R270.

50. Semb AG, Ikdahl E, Wibetoe G, Crowson C, Rollefstad S. Atherosclerotic cardiovascular disease prevention in rheumatoid arthritis. Nat Rev Rheumatol 2020;16:361–79.

51. Westlake SL, Colebatch AN, Baird J, Curzen N, Kiely P, Quinn M, et al. Tumour necrosis factor antagonists and the risk of cardiovascular disease in patients with rheumatoid arthritis: a systematic literature review. Rheumatology (Oxford) 2011;50:518–31.

52. Singh S, Fumery M, Singh AG, Singh N, Prokop LJ, Dulai PS, et al. Comparative risk of cardiovascular events with biologic and synthetic disease-modifying antirheumatic drugs in patients with rheumatoid arthritis: a systematic review and meta-analysis. Arthritis Care Res (Hoboken) 2020;72:561–76.

53. Holmes MV, Ala-Korpela M, Smith GD. Mendelian randomization in cardiometabolic disease: challenges in evaluating causality. Nat Rev Cardiol 2017;14:577–90.

54. Antman EM. Evaluating the cardiovascular safety of nonsteroidal antiinflammatory drugs. Circulation 2017;135:2062–72.

Tofacitinib and Risk of Malignancy: Results From the Safety of Tofacitinib in Routine Care Patients With Rheumatoid Arthritis (STAR-RA) Study

Farzin Khosrow-Khavar,[1] Rishi J. Desai,[1] Hemin Lee,[1] Su Been Lee,[1] and Seoyoung C. Kim[2]

Objectives. Results of the ORAL Surveillance safety trial have indicated that there is an increased risk for the development of malignancies with tofacitinib therapy when compared to treatment with tumor necrosis factor inhibitors (TNFi). This study was undertaken to further examine this safety concern in rheumatoid arthritis (RA) patients in a real-world setting.

Methods. Using US insurance claims data from Optum Clinformatics (2012–2020), IBM MarketScan Research Databases (2012–2018), and Medicare (parts A, B, and D, 2012–2017), we created 2 cohorts of RA patients who had initiated treatment with tofacitinib or TNFi. The first cohort, designated the real-world evidence (RWE) cohort, included RA patients from routine care. For the second cohort, designated the randomized controlled trial (RCT)–duplicate cohort, we emulated the inclusion and exclusion criteria that were applied in the ORAL Surveillance trial of tofacitinib, which allowed us to assess the comparability of our results with the results of that trial. Cox proportional hazards models with propensity score fine-stratification weighting were used to estimate hazard ratios (HRs) and 95% confidence intervals (95% CIs) for the risk of any malignancy (excluding nonmelanoma skin cancer). Database-specific estimates were meta-analyzed using fixed-effects models with inverse-variance weighting.

Results. The RWE cohort consisted of 83,295 patients, including 10,504 patients (12.6%) who received treatment with tofacitinib. The pooled weighted HR for the primary outcome of any malignancy associated with tofacitinib treatment compared to any malignancy associated with TNFi therapy was 1.01 (95% CI 0.83, 1.22) in the RWE cohort and 1.17 (95% CI 0.85, 1.62) in the RCT-duplicate cohort (compared to the ORAL Surveillance trial HR of 1.48 [95% CI 1.04, 2.09]).

Conclusion. We did not find evidence of an increased risk of malignancy development with tofacitinib therapy, in comparison with TNFi therapy, in RA patients treated in a real-world setting. However, our results cannot rule out the possibility of an increase in risk that may accrue with a longer duration of treatment with tofacitinib.

INTRODUCTION

Rheumatoid arthritis (RA) is a chronic systemic inflammatory disease that affects ~0.2% of the adult population globally (1). Tofacitinib is the first JAK inhibitor approved by the US Food and Drug Administration (FDA) in 2012 for the treatment of RA. Since then, the FDA has approved the use of tofacitinib for the treatment of other autoimmune conditions, including active psoriatic arthritis

(2017), moderate-to-severe ulcerative colitis (2018), and most recently for active polyarticular juvenile idiopathic arthritis (2020).

The utilization of tofacitinib has markedly increased for the management of moderate-to-severe RA since 2012 (2–4). However, recent results from the ORAL Surveillance post-marketing safety trial indicated that tofacitinib, in comparison with tumor necrosis factor inhibitors (TNFi), may be associated with an increased risk of malignancies in patients with RA who are

≥50 years of age and have cardiovascular risk factors (hazard ratio [HR] 1.48 [95% confidence interval (95% CI) 1.04, 2.09]) (5–8). As a result, the FDA has issued a warning regarding a risk of malignancy associated with tofacitinib (9). Given these findings and the increasing use of tofacitinib in the treatment of patients with RA, our aim was to conduct a large, population-based observational study to further examine the risk of malignancies with tofacitinib in representative RA patients treated in a real-world clinical setting.

PATIENTS AND METHODS

Data sources and study design. We conducted an active-comparator, new-user cohort study (see Supplementary Figure 1, available on the *Arthritis & Rheumatology* website at http://onlinelibrary.wiley.com/doi/10.1002/art.42250) using claims data from Optum Clinformatics (November 2012–June 2020), IBM MarketScan Research Databases (November 2012–December 2018), and fee-for-service Medicare (parts A, B, and D, November 2012–December 2017) in the US (10). Optum and MarketScan provide de-identified longitudinal patient-level health data from over 78 million and 200 million commercially insured patients, respectively, across the US. Medicare is a federal health insurance program which provides health care coverage for US residents who are age 65 years or older and for some younger patients with disabilities. All of these data sources capture information on patient demographics, health plan enrollment status, and patient-level longitudinal data on medical diagnoses in inpatient and outpatient settings, diagnostic tests, procedures, and pharmacy prescription dispensation records (including medication start and refill dates, strength, quantity, and days' supply).

The protocol for this study received ethics approval (project number 2011P002580, 207) from the Institutional Review Board of Brigham and Women's Hospital, and the full protocol was registered on ClinicalTrials.gov (NCT04798287) (11). The Strengthening the Reporting of Observational Studies in Epidemiology (STROBE) guidelines were followed (12). Informed consent requirements for the participating patients were waived as in the data sets from Optum, MarketScan, and Medicare, all personal identifiers had been removed and patient confidentiality was protected in each of the 3 data sources. Signed data license agreements were obtained for all data sources.

Study population. We first identified RA patients who had initiated treatment with tofacitinib or with a TNFi (infliximab, adalimumab, certolizumab pegol, etanercept, and golimumab) in each of the 3 data sources. The cohort entry date was defined as the first record of pharmacy dispensation of tofacitinib or TNFi. For inclusion in a cohort, patients were required to have had a minimum of 365 days of continuous enrollment in a health care plan prior to and inclusive of the cohort entry date. We

selected patients with at least 2 visits occurring 7–365 days apart that were coded for RA in the year prior to the cohort entry date (Supplementary Figure 1, http://onlinelibrary.wiley.com/doi/10.1002/art.42250). In a previous study, a positive predictive value of 86% was demonstrated for this claims-based algorithm (13). Further, the study population was restricted to patients who were new to treatment with tofacitinib and with TNFi. Thus, patients who received a prescription for tofacitinib within the 365 days prior to the cohort entry date were excluded from the study. We also excluded patients treated with tofacitinib who had also received prescriptions for baricitinib or upadacitinib on or at any time prior to the cohort entry date. Similarly, patients treated with TNFi who had received a prescription for an index TNFi agent within the 365 days prior to the cohort entry date, patients treated with TNFi who had previously received treatment with any JAK inhibitor (i.e., tofacitinib, baricitinib, upadacitinib), and patients treated with TNFi who had received prescriptions for other agents from the TNFi class on the cohort entry date were excluded from the study. We also excluded patients who had a concurrent prescription for tofacitinib and TNFi on the cohort entry date. Additionally, patients who were missing data on age or sex and patients admitted to a nursing facility or to hospice care at any point prior to the cohort entry date were excluded from the study. Finally, to identify incident cases of cancer, we excluded patients who had been diagnosed as having any type of malignancy (including nonmelanoma skin cancer [NMSC]) prior to the cohort entry date.

From this source population, we created 2 study cohorts: 1) the real-world evidence (RWE) cohort, which included all RA patients from routine care, and 2) the randomized controlled trial (RCT)–duplicate cohort, which emulated the ORAL Surveillance trial by applying the same inclusion and exclusion criteria. The RCT-duplicate cohort was used to assess the comparability of our findings with the results of the ORAL Surveillance trial of tofacitinib (5,6,8).

The RWE cohort included all RA patients who were at least 18 years of age in the Optum and MarketScan data sets (≥65 years of age in the Medicare data set) at the cohort entry date. In contrast, the RCT-duplicate cohort was restricted to patients who were 50 years of age or older (65 years of age in the Medicare data set), and who had received at least 1 methotrexate dispensation within 6 months prior to the cohort entry date, and who had at least 1 cardiovascular risk factor (including a history of smoking, hypertension, dyslipidemia, diabetes mellitus, ischemic heart disease, or a family history of ischemic heart disease) in the year prior to the cohort entry date. Patients who had been hospitalized with infections in the 30-day period prior to the cohort entry date and patients who were pregnant were excluded from the RCT-duplicate cohort. The complete list of the International Classification of Diseases, Ninth Revision (ICD-9) and ICD-10 diagnosis and procedure codes used for

exclusion criteria can be found in the full protocol published on ClinicalTrials.gov (11).

Outcomes. In the primary as-treated analysis, we followed up patients from the day after the date treatment with tofacitinib or with TNFi was initiated, until treatment discontinuation (defined as 60 days without prescription refills for the index exposure after the end of the days' supply for the most recent dispensation) or switch, insurance disenrollment, death, or the end of the study period, whichever occurred first (Supplementary Figure 1, http://onlinelibrary.wiley.com/doi/10.1002/art.42250). The primary outcome was defined as a composite end point of any new malignancies (based on 2 inpatient or outpatient ICD-9 or ICD-10 diagnosis codes of the same type of malignancy occurring within 60 days), excluding NMSC (14,15). This outcome definition demonstrated a high specificity (≥98%) for the majority of cancer outcomes. However, the sensitivity of this outcome definition was somewhat lower for the identification of common solid tumors, including lung cancer (76.2%), colorectal cancer (80.4%), breast cancer (78.9%), and lymphoma (79.8%). All cases of carcinoma in situ were excluded from the composite outcome definition. Secondary outcomes were individual types of malignancy, including lung cancer, breast cancer, colorectal cancer, prostate cancer, lymphatic/hematopoietic tissue cancers, and NMSC. Finally, we examined the association between tofacitinib and the risk of herpes zoster as a positive control outcome, a known association established in previous studies (16,17).

Covariate assessment. We assessed 75 predefined suspected confounders or risk factors for malignancy in the Optum and Medicare data sets (74 confounders in the MarketScan data set) during the 365 days prior to and including the cohort entry date (i.e., the baseline period). These potential confounders included demographic variables such as age, sex, and race (available in the Optum and Medicare data sets), and lifestyle-related variables including obesity and smoking status, which were assessed on the cohort entry date (18,19). We also assessed RA-related history of treatment with conventional disease-modifying antirheumatic drugs (DMARDs), including the use of individual agents and the total number of distinct agents used during the baseline period. Recent treatment with glucocorticoids (treatment occurring in the 60 days prior to and including the cohort entry date) was also assessed as a potential confounder. Prior treatment with glucocorticoids, cumulative prednisone equivalent dose of glucocorticoids, and the number of distinct biologic DMARDs (bDMARDs) (including index drugs) that each patient had been treated with were assessed during the baseline period (20,21).

Comorbidities that have been shown to be associated with or that share risk factors with malignancies were assessed as potential confounders, including hypertension, hyperlipidemia, type 2 diabetes mellitus, cardiovascular disease (atrial fibrillation, coronary artery disease, heart failure, stroke or transient ischemic attack, peripheral vascular disease), venous thromboembolism, chronic liver disease, chronic kidney disease (stage 3 and higher), chronic obstructive pulmonary disease, inflammatory bowel disease, psoriasis, combined comorbidity index score, and claims-based frailty index score (22–27). We also assessed treatment with the following medications: anticoagulants, antiplatelets, antidepressant drugs, antihypertensive drugs, antiarrhythmic drugs, lipid-lowering drugs, chronic obstructive pulmonary disease maintenance drugs, insulin and noninsulin antidiabetic drugs, nonsteroidal antiinflammatory drugs, selective cyclooxygenase 2 inhibitors, opioids, and hormonal agents (18,25,28–31). Additionally, we assessed 25 markers of health care utilization in order to account for potential differences in participants' use and access to health care systems and to account for potential differential surveillance during the baseline period. Finally, we assessed the calendar year of cohort entry as a marker of temporal changes in the treatment of patients with RA and of temporal changes in malignancy diagnoses during the study period.

Statistical analysis. Using descriptive statistics, we summarized the baseline characteristics of patients who had initiated treatment with tofacitinib or with TNFi drugs. We provided Poisson distribution–based estimates of incidence rates, as well as incidence rate differences (comparing patients receiving tofacitinib and patients receiving TNFi therapy) and corresponding 95% CIs for each study outcome.

We used propensity score fine-stratification to account for 75 measured potential confounders (74 potential confounders in the MarketScan data set) independently in each data set (32). In studies with a low prevalence of exposure in the cohort, which is common in studies on newer treatments compared to studies on more established treatments, this method has been shown to increase precision without compromising bias adjustment, in comparison with propensity score–matching methods (32). To generate propensity score fine-stratification weights, multivariable logistic regression was first used to calculate the propensity score as the predicted probability of initiating treatment with tofacitinib, conditional on baseline covariates in each of the data sets (33). We restricted the study population to the overlapping region of the propensity score distribution in order to include patients treated with tofacitinib and patients treated with TNFi agents along the entire distribution of the propensity score and to exclude patients with extreme propensity scores (33). Subsequently, we created 50 strata based on the distribution of propensity scores for patients who had initiated treatment with tofacitinib (32). Patients treated with tofacitinib received a weight of 1.

To calculate the weights for patients who had received TNFi therapy, first the proportion of patients treated with tofacitinib in each propensity score stratum was calculated by dividing the number of patients treated with tofacitinib in a given stratum by the total number of patients treated with tofacitinib in the study

population. Similarly, the proportion of patients treated with TNFi agents was calculated by dividing the number of patients treated with TNFi agents in a given propensity score stratum by the total number of patients treated with TNFi agents. The ratio of these proportions (i.e., the proportion of patients treated with tofacitinib in a given strata divided by the proportion of patients treated with TNFi agents in a given strata) defined the weight for patients treated with TNFi agents. This method estimates the average treatment effect on the treated population ([32]).

To assess covariate balances between patients treated with tofacitinib and patients treated with TNFi agents, we calculated standardized differences (expressed as a percentage) before and after propensity score fine-stratification weighting. Standardized differences of <10% indicated sufficient covariate balance when comparing patients treated with tofacitinib and patients treated with TNFi agents ([33–35]). We used Cox proportional hazards models to estimate crude and weighted hazard ratios and corresponding 95% CIs with propensity score fine-stratification weights used to account for potential confounders. Robust variance estimation was used to generate 95% CIs in the weighted population. We also examined the cumulative incidence of composite malignancies and 95% CIs for each treatment group in the propensity score–weighted populations. All analyses were conducted independently in each data set. We used a fixed-effects model with inverse variance weighting to meta-analyze database-specific effect estimates ([36]).

The Aetion Evidence Platform was used for cohort construction ([37]). All analyses were conducted using version 9.4 of the SAS Institute software and R software from the R Foundation for Statistical Computing.

Secondary and sensitivity analyses. We conducted prespecified subgroup analyses in the RWE cohort by stratifying patients by age (≤65 and >65 years) and sex. Further, we examined the risk of malignancies by stratifying patients based on the number of unique bDMARDs they had received in the year prior to cohort entry date (0 versus ≥1). For sensitivity analysis, we conducted 1:1 propensity score matching using a greedy nearest neighbor matching algorithm without replacement, using a caliper of 0.025 on the natural scale of the propensity score ([33,38]). We also restricted the TNFi comparator group to patients treated with adalimumab and etanercept in both the RWE cohort and the RCT-duplicate cohort, which was similar to the comparator group in the ORAL Surveillance trial ([5–8]).

We further assessed different follow-up methods in the RWE cohort and the RCT-duplicate cohort (Supplementary Figure 2, http://onlinelibrary.wiley.com/doi/10.1002/art.42250). First, we implemented an intent-to-treat (ITT) exposure definition whereby patients were followed up until the end of the study period after initiation of treatment, in order to minimize the impact informative censoring based on discontinuation of treatment could have had on the results. Second, we implemented an ITT exposure

definition but truncated follow-up until a maximum of 365 days after initiation of treatment with tofacitinib or TNFi agents. Third, we conducted sensitivity analysis by lagging exposure by 3 months after treatment initiation to account for potential latency of the treatment effect, to exclude prevalent cases of cancer, and to minimize surveillance bias. Finally, we extended the grace period to 6 months after treatment discontinuation to account for the potential carryover effect of the treatments on cancer outcomes. We also conducted a sensitivity analysis whereby we required at least 2 years of continuous enrollment in a health care plan prior to the cohort entry date, excluded patients who received dispensations of the index drug at any point prior to the cohort entry date, and assessed comorbidities over a 2-year baseline period prior to and including the cohort entry date.

RESULTS

RWE cohort. The RWE cohort consisted of 83,295 RA patients identified in the following data sets: 25,410 patients from the Optum data set, 29,511 patients from the MarketScan data set, and 28,374 patients from the Medicare data set (Supplementary Table 1, http://onlinelibrary.wiley.com/doi/10.1002/art.42250). Within these data sets, the following proportions of RA patients initiated treatment with tofacitinib: 3,304 patients (13.0%) in the Optum data set, 4,508 patients (15.3%) in the MarketScan data set, and 2,692 patients (9.5%) in the Medicare data set (Supplementary Table 2, http://onlinelibrary.wiley.com/doi/10.1002/art.42250). The mean age of patients treated with tofacitinib compared to patients treated with TNFi agents was 55.9 years versus 53.6 years in the Optum data set, 53.8 years versus 51.6 years in the MarketScan data set, and 71.3 years versus 71.4 years in the Medicare data set (Supplementary Table 2). The majority of patients in each data set were female (77–80%), were White (66–83%), and had received treatment with conventional DMARDs (75–82%) and glucocorticoids (69–72%) prior to the initiation of treatment with tofacitinib or TNFi agents (Supplementary Table 2). In patients treated with tofacitinib compared to patients treated with TNFi, the number of unique bDMARDs received prior to and including the cohort entry date was a mean ± SD of 1.6 ± 0.7 versus 1.3 ± 0.5 bDMARDs in the Optum data set, 1.8 ± 0.8 versus 1.4 ± 0.6 bDMARDs in the MarketScan data set, and 1.6 ± 0.7 versus 1.3 ± 0.5 bDMARDs in the Medicare data set (Supplementary Table 2). There were no discernable differences between patients who initiated treatment with tofacitinib and patients who initiated treatment with TNFi agents across most comorbidities, prior prescriptions, and markers of health care utilization (Supplementary Table 2). We obtained covariate balance after propensity score fine-stratification weighting, with standardized differences of <5% for all covariates in all 3 data sets (Table 1 and Supplementary Table 3, http://onlinelibrary.wiley.com/doi/10.1002/art.42250).

Primary outcome. The mean ± SD number of months of follow-up time in the as-treated analysis in patients treated with

Table 1. Select baseline characteristics of rheumatoid arthritis patients included in the real-world evidence (RWE) cohort who initiated treatment with tofacitinib and patients who initiated treatment with tumor necrosis factor inhibitors (TNFi) after propensity score fine-stratification weighting

Variables	Optum data set			MarketScan data set			Medicare data set		
	Tofacitinib (n = 3,301)	TNFi (n = 21,934)	Standardized difference, %	Tofacitinib (n = 4,499)	TNFi (n = 24,960)	Standardized difference, %	Tofacitinib (n = 2,689)	TNFi (n = 25,673)	Standardized difference, %
Demographic variables									
Age, mean ± SD years	55.8 ± 12.4	56.1 ± 13.1	-2.3	53.8 ± 11.4	54.0 ± 11.7	-1.8	71.3 ± 5.4	71.4 ± 5.3	-1.3
Female	2,690 (81.5)	17,963 (81.9)	-1.0	3,699 (82.2)	20,562 (82.4)	-1.8	2,300 (85.5)	22,082 (86.0)	-1.4
White	2,069 (62.7)	13,683 (62.4)	0.6	-	-	-	2,064 (76.8)	19,537 (76.1)	1.5
Black	368 (11.1)	2,473 (11.3)	-0.4	-	-	-	344 (12.8)	3,397 (13.2)	-1.3
Asian	98 (3.0)	613 (2.8)	1.1	-	-	-	73 (2.7)	710 (2.8)	-0.3
Hispanic	426 (12.9)	2,903 (13.2)	-1.0	-	-	-	100 (3.7)	980 (3.8)	-0.5
Unique bDMARDs, mean ± SD number†	1.6 ± 0.7	1.6 ± 0.7	2.1	1.8 ± 0.8	1.8 ± 0.8	1.5	1.6 ± 0.7	1.6 ± 0.7	2.9
Nonbiologic DMARDs									
Distinct csDMARDs, mean ± SD number	1.0 ± 0.8	1.0 ± 0.8	0.1	1.0 ± 0.8	1.0 ± 0.8	2.0	1.1 ± 0.8	1.1 ± 0.8	0.7
Any csDMARD use	2,402 (72.8)	15,971 (72.8)	-0.1	3,374 (75.0)	18,576 (74.4)	1.3	2,075 (77.2)	19,725 (76.8)	0.8
Methotrexate	1,523 (46.1)	10,037 (45.8)	0.8	2,303 (51.2)	12,618 (50.6)	1.3	1,403 (52.2)	13,214 (51.5)	1.4
Hydroxychloroquine	829 (25.1)	5,528 (25.2)	-0.2	1,053 (23.4)	5,711 (22.9)	1.2	679 (25.3)	6,425 (25.0)	0.5
Leflunomide	703 (21.3)	4,702 (21.4)	-0.3	893 (19.8)	4,917 (19.7)	0.4	605 (22.5)	5,845 (22.8)	-0.6
Sulfasalazine	343 (10.4)	2,287 (10.4)	-0.1	424 (9.4)	2,287 (9.2)	0.9	314 (11.7)	3,025 (11.8)	-0.3
Prior use of oral glucocorticoids within 365 days	2,432 (73.7)	16,177 (73.8)	-0.2	3,284 (73.0)	18,275 (73.2)	-0.5	2,018 (75.0)	19,258 (75.0)	0.1
Recent use of oral glucocorticoids within 60 days	1,633 (49.5)	10,825 (49.4)	0.2	2,192 (48.7)	12,188 (48.8)	-0.2	1,505 (56.0)	14,329 (55.8)	0.3
Cumulative dose of oral steroids, mean ± SD mg	901.4 ± 1,277.6	911.5 ± 6,555.1	-0.2	1,754.5 ± 21,873.2	1,859.6 ± 20,903.4	-0.5	1,023.3 ± 1,202.8	1,015.8 ± 1,262.7	0.6
Comorbidities									
Obesity	767 (23.2)	5,139 (23.4)	-0.5	691 (15.4)	3,844 (15.4)	-0.1	430 (16.0)	4,118 (16.0)	-0.1
Smoking	654 (19.8)	4,292 (19.6)	0.6	382 (8.5)	2,146 (8.6)	-0.4	665 (24.7)	6,377 (24.8)	-0.2
Atrial fibrillation	116 (3.5)	783 (3.6)	-0.3	94 (2.1)	533 (2.1)	-0.3	246 (9.1)	2,324 (9.1)	0.3
Coronary artery disease	296 (9.0)	1,986 (9.1)	-0.3	326 (7.2)	1,899 (7.6)	-1.4	593 (22.1)	5,641 (22.0)	0.2
Type 2 diabetes mellitus	702 (21.3)	4,672 (21.3)	-0.1	683 (15.2)	3,835 (15.4)	-0.5	821 (30.5)	7,801 (30.4)	0.3
Heart failure	154 (4.7)	1,073 (4.9)	-1.1	131 (2.9)	733 (2.9)	-0.2	292 (10.9)	2,791 (10.9)	0.0
Hypertension	1,671 (50.6)	11,226 (51.2)	-1.1	1,928 (42.9)	10,842 (43.4)	-1.2	2,207 (82.1)	21,048 (82.0)	0.2
Hyperlipidemia	1,371 (41.5)	9,201 (42.0)	-0.8	1,643 (36.5)	9,215 (36.9)	-0.8	1,780 (66.2)	16,896 (65.8)	0.8

(Continued)

Table 1. (Cont'd)

Variables	Optum data set			MarketScan data set			Medicare data set		
	Tofacitinib (n = 3,301)	TNFi (n = 21,934)	Standardized difference, %	Tofacitinib (n = 4,499)	TNFi (n = 24,960)	Standardized difference, %	Tofacitinib (n = 2,689)	TNFi (n = 25,673)	Standardized difference, %
Stroke or transient ischemic attack	81 (2.5)	554 (2.5)	-0.5	81 (1.8)	473 (1.9)	-0.7	88 (3.3)	830 (3.2)	0.2
Peripheral vascular disease	137 (4.2)	936 (4.3)	-0.6	106 (2.4)	611 (2.4)	-0.6	268 (10.0)	2,542 (9.9)	0.2
Venous thromboembolism	76 (2.3)	518 (2.4)	-0.4	99 (2.2)	559 (2.2)	-0.3	72 (2.7)	694 (2.7)	-0.2
Chronic liver disease	238 (7.2)	1,582 (7.2)	0.0	246 (5.5)	1,341 (5.4)	0.4	209 (7.8)	1,987 (7.7)	0.1
Chronic kidney disease (Stage 3+)	164 (5.0)	1,090 (5.0)	0.0	135 (3.0)	753 (3.0)	-0.1	287 (10.7)	2,776 (10.8)	-0.4
COPD	490 (14.8)	3,302 (15.1)	-0.6	501 (11.1)	2,804 (11.2)	-0.3	693 (25.8)	6,674 (26.0)	-0.5
Inflammatory bowel disease	58 (1.8)	388 (1.8)	-0.1	48 (1.1)	258 (1.0)	0.3	34 (1.3)	324 (1.3)	0.0
Psoriasis	146 (4.4)	960 (4.4)	0.2	140 (3.1)	749 (3.0)	0.7	81 (3.0)	728 (2.8)	1.0
Combined Comorbidity Index, mean ± SD score	1.0 ± 1.8	1.0 ± 1.8	-0.1	0.6 ± 1.4	0.6 ± 1.4	-0.8	1.6 ± 2.2	1.6 ± 2.3	-0.4
Frailty index, mean ± SD score	0.2 ± 0.0	0.2 ± 0.0	-0.4	0.1 ± 0.0	0.1 ± 0.0	-1.6	0.2 ± 0.0	0.2 ± 0.0	0.3

* Except where indicated otherwise, values are the number (%) of patients. bDMARDs = biologic disease-modifying antirheumatic drugs; csDMARDs = conventional synthetic disease-modifying antirheumatic drugs; COPD = chronic obstructive pulmonary disease. Full tables describing all patient characteristics before and after propensity score weighting are provided in the Supplementary Material.
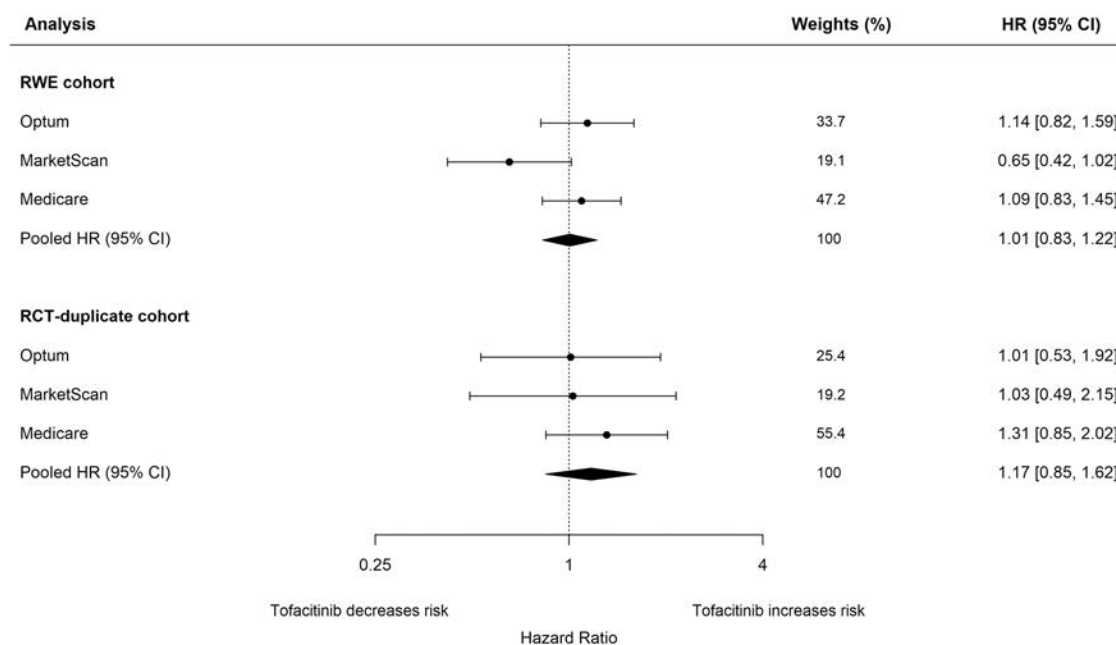† Includes index drug.

Figure 1. Forest plots of propensity score fine-stratification weighted hazard ratios (HRs) with 95% confidence intervals (95% CIs) for each data set as well as the pooled HRs with 95% CIs for the composite outcome of all new malignancies (excluding nonmelanoma skin cancer) when comparing treatment with tofacitinib to treatment with tumor necrosis factor inhibitors in patients with rheumatoid arthritis in the real-world evidence (RWE) cohort (top panel) and randomized controlled trial (RCT)–duplicate cohort (bottom panel).

tofacitinib compared to patients treated with TNFi agents was 10.3 ± 11.2 months versus 11.3 ± 12.2 months in the Optum data set, 10.6 ± 11.0 months versus 11.4 ± 11.5 months in the MarketScan data set, and 10.3 ± 10.6 months versus 10.2 ± 10.4 months in the Medicare data set. Nevertheless, 9,237 patients (11.1%) had a follow-up time of at least 2 years. Overall, 13,893 patients (54.7%) in the Optum data set, 15,445 patients (52.3%) in the MarketScan data set, and 19,124 patients (67.4%) in the Medicare data set discontinued treatment.

The crude incidence rates of composite malignancy outcomes per 100 person-years in patients treated with tofacitinib compared to patients treated with TNFi agents were 1.68 (95% CI 1.24, 2.23) versus 1.36 (95% CI 1.21, 1.53) in the Optum data set, 0.60 (95% CI 0.39, 0.90) versus 0.86 (95% CI 0.74, 0.98) in the MarketScan data set, and 2.70 (95% CI 2.07, 3.46) versus 2.49 (95% CI 2.29, 2.71) in the Medicare data set (Supplementary Table 4, http://onlinelibrary.wiley.com/doi/10.1002/art.42250). Between-group differences in the crude incidence rates of composite malignancy outcomes per 100 person-years in patients treated with tofacitinib compared to patients treated with TNFi agents were 0.32 (95% CI –0.18, 0.83) in the Optum data set, –0.25 (95% CI –0.52, 0.01) in the MarketScan data set, and 0.21 (95% CI –0.50, 0.91) in the Medicare data set (Supplementary Table 4). Overall, the pooled weighted HR (95% CI) for composite malignancy outcome when comparing treatment with tofacitinib to treatment with TNFi agents was 1.01 (95% CI 0.83, 1.22), corresponding to a weighted incidence rate difference per 100 person-years of –0.16 (95% CI –0.40, 0.09)

(Figure 1 and Supplementary Table 4). The 95% CI for cumulative incidence of malignancies from time since initiation of treatment overlapped when patients treated with tofacitinib were compared to patients treated with TNFi agents in each of the 3 data sets (Supplementary Figure 3, http://onlinelibrary.wiley.com/doi/10.1002/art.42250).

In subgroup analysis, the pooled weighted HR (95% CI) for composite malignancy outcome was 0.93 (95% CI 0.73, 1.18) among female patients, 1.21 (95% CI 0.86, 1.71) among male patients, 0.89 (95% CI 0.63, 1.24) among patients ≤65 years of age, and 1.08 (95% CI 0.85, 1.37) among patients >65 years of age in the RWE cohort. Among patients treated with tofacitinib, 1,650 patients (49.9%) in the Optum data set, 2,797 patients (62.0%) in the MarketScan data set, and 1,298 patients (48.2%) in the Medicare data set had a history of treatment with bDMARDs prior to the cohort entry date (Supplementary Table 4). Among patients treated with TNFi agents, 5,165 patients (23.4%) in the Optum data set, 7,775 patients (31.1%) in the MarketScan data set, and 7,624 patients (29.7%) in the Medicare data set had a history of treatment with bDMARDs (Supplementary Table 4). The pooled weighted HR for composite malignancy outcome was 0.81 (95% CI 0.60, 1.10) among patients with a history of treatment with bDMARDs and 1.22 (95% CI 0.96, 1.57) among patients with no history of treatment with bDMARDs (Figure 2 and Supplementary Table 4).

In other analyses, the pooled weighted HR (95% CI) for composite malignancy outcome was 1.12 (95% CI 0.90, 1.39) when we implemented a 3-month exposure lag, 0.97 (95% CI 0.82, 1.15)
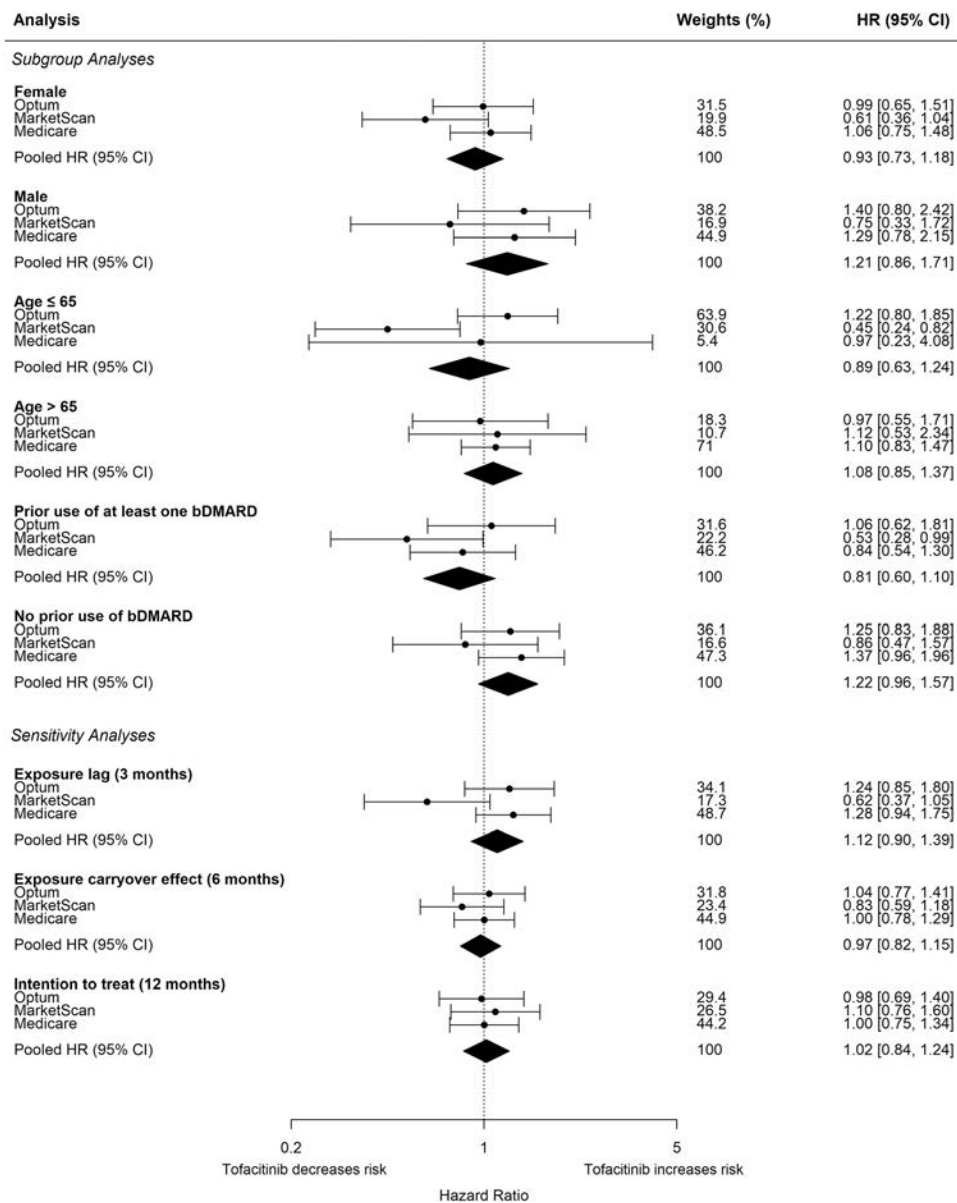
Figure 2. Forest plots of propensity score fine-stratification weighted HRs with 95% CIs for each data set as well as the pooled HRs with 95% CIs for the composite malignancy outcome when comparing tofacitinib and tumor necrosis factor inhibitor treatment groups in subgroup and sensitivity analyses in the RWE study cohort. bDMARD = biologic disease-modifying antirheumatic drug (see Figure 1 for other definitions).

with a 6-month carryover effect after discontinuation of treatment, and 1.00 (95% CI 0.88, 1.14) when an ITT definition of exposure was used (Figure 2 and Supplementary Table 4). The pooled weighted HR for composite malignancy outcome was 1.02 (95% CI 0.84, 1.24) when we used an ITT definition of exposure but truncated follow-up time at 365 days after the initiation of treatment (Figure 2 and Supplementary Table 4). Using the 6-month carryover effect and the ITT definition of exposure led to a longer follow-up time. When the 6-month carryover exposure definition was used, the mean ± SD number of months of follow-up time in patients treated with tofacitinib compared to patients treated with TNFi agents was 13.7 ± 13.2 months versus 16.1 ± 14.9 months in the Optum data set, 14.0 ± 12.8 months versus 16.1 ±

14.1 months in the MarketScan data set, and 13.4 ± 11.6 months versus 17.3 ± 13.7 months in the Medicare data set. When the ITT definition of exposure was used, the mean ± SD number of months of follow-up in patients treated with tofacitinib compared to patients treated with TNFi agents was 22.6 ± 20.2 months versus 25.2 ± 12.8 months in the Optum data set, 22.1 ± 17.9 months versus 23.1 ± 18.5 months in the MarketScan data set, and 23.3 ± 16.4 months versus 26.0 ± 17.1 months in the Medicare data set.

The pooled HR (95% CI) for composite malignancy outcome was 0.95 (95% CI 0.75, 1.21) in analyses using 1:1 propensity score matching. The pooled weighted HR (95% CI) was 0.93 (95% CI 0.75, 1.16) when the comparator was restricted to
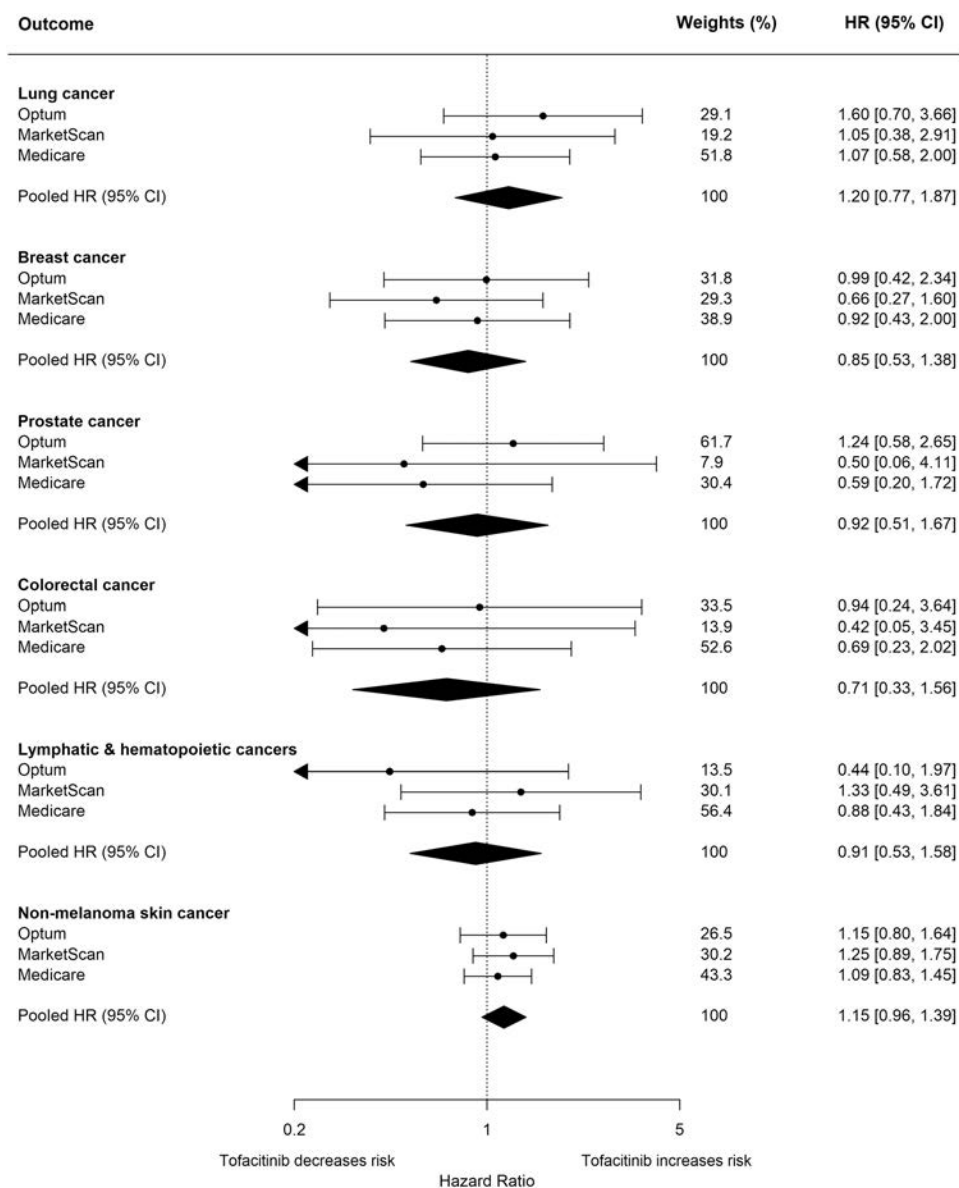
Figure 3. Forest plots of propensity score fine-stratification weighted HRs with 95% CIs for each data set as well as the pooled HRs with 95% CIs for individual malignancy outcomes when comparing tofacitinib and tumor necrosis factor inhibitor treatment groups in the RWE study cohort. See Figure 1 for definitions.

patients treated with adalimumab and etanercept, and 0.94 (95% CI 0.74, 1.19) among patients with at least 2 years of continuous enrollment in a health plan prior to the cohort entry date, with a minimum of 2 years of washout for the index drug and a 2-year window for assessment of comorbidities (Supplementary Table 4, http://onlinelibrary.wiley.com/doi/10.1002/art.42250).

Secondary outcomes. The pooled weighted HR for the risk of malignancy in patients treated with tofacitinib compared to patients treated with TNFi agents was 1.20 (95% CI 0.77, 1.87) for lung cancer, 0.85 (95% CI 0.53, 1.38) for breast cancer, 0.92 (95% CI 0.51, 1.67) for prostate cancer, 0.71 (95% CI 0.33, 1.56) for colorectal cancer, 0.91 (95% CI 0.53, 1.58) for lymphatic and hematopoietic cancers, and 1.15 (95% CI 0.96, 1.39) for

NMSC in the RWE cohort (Figure 3 and Supplementary Table 5, http://onlinelibrary.wiley.com/doi/10.1002/art.42250). The pooled weighted HR was 2.02 (95% CI 1.80, 2.27) for herpes zoster as the positive control outcome, which is consistent with the findings of previous studies (Supplementary Table 5) (16,17).

RCT-duplicate cohort. The RCT-duplicate cohort consisted of 27,035 RA patients who met the inclusion and exclusion criteria: 5,899 patients in the Optum data set, 6,588 patients in the MarketScan data set, and 14,548 patients in the Medicare data set (Supplementary Table 1). Among these patients, 668 patients (11.3%) in the Optum data set, 938 patients (14.2%) in the MarketScan data set, and 1,100 patients (7.6%)

in the Medicare data set had initiated treatment with tofacitinib (Supplementary Table 6, http://onlinelibrary.wiley.com/doi/10.1002/art.42250). After propensity score fine-stratification, standardized differences close to 0 were achieved for most covariates (Supplementary Table 7, http://onlinelibrary.wiley.com/doi/10.1002/art.42250).

The crude incidence rate of malignancy per 100 person-years in patients treated with tofacitinib compared to patients treated with TNFi agents was 2.41 (95% CI 1.35, 3.98) versus 2.01 (95% CI 1.63, 2.43) in the Optum data set, 1.13 (95% CI 0.54, 2.08) versus 0.96 (95% CI 0.72, 1.25) in the MarketScan data set, and 2.76 (95% CI 1.80, 4.04) versus 2.31 (95% CI 2.05, 2.61) in the Medicare data set (Supplementary Table 8, http://onlinelibrary.wiley.com/doi/10.1002/art.42250). In the primary analysis, the pooled weighted HR (95% CI) for malignancy was 1.17 (95% CI 0.85, 1.62) in patients treated with tofacitinib compared to patients treated with TNFi agents (compared to HR 1.48 [95% CI 1.04, 2.09] in the ORAL Surveillance trial) corresponding to a pooled weighted rate difference of 0.20 (95% CI –0.42, 0.82) per 100 person-years (Figure 1 and Supplementary Table 8).

In sensitivity analyses, the pooled weighted HR for malignancy was 1.33 (95% CI 0.94, 1.89) when exposure was lagged by 3 months, 1.04 (95% CI 0.78, 1.38) when a carryover of 6 months was used, 1.03 (95% CI 0.83, 1.29) when the ITT definition of exposure was used, and 1.07 (95% CI 0.77, 1.50) when the ITT definition of exposure was used with follow-up limited to a maximum of 365 days after initiation of treatment (Supplementary Table 8). We observed consistent results when restricting the comparator to patients treated with adalimumab and etanercept (pooled weighted HR 1.18 [95% CI 0.83, 1.67]) (Supplementary Table 8). Overall, the results for cumulative incidence of malignancy outcomes from time since treatment initiation was inconclusive due to overlapping 95% CIs when comparing patients treated with tofacitinib to patients treated with TNFi (Supplementary Figure 4, http://onlinelibrary.wiley.com/doi/10.1002/art.42250).

DISCUSSION

In this large multi-database cohort study, we did not observe an increased risk of malignancies when comparing tofacitinib with TNFi agents in RA patients treated in real-world settings (pooled weighted HR 1.01 [95% CI 0.83, 1.22]). However, our results do not rule out the possibility of a small increase in risk that may accrue with longer periods of treatment. Tofacitinib was associated with a numerically increased risk of malignancies in the RCT-duplicate population, which consisted of patients 50 years of age and older who had at least 1 risk factor for cardiovascular disease (pooled weighted HR 1.17 [95% CI 0.85, 1.62]).

The ORAL Surveillance trial, a large, phase IIIb and IV (n = 4,362 patients) post-marketing trial required by the US Food and Drug Administration, assessed the safety of treatment with tofacitinib (5 mg and 10 mg) compared to the safety of treatment with adalimumab/etanercept in patients 50 years of age and older who had at least 1 risk factor for cardiovascular disease, and who also had a history of treatment with methotrexate (5,6,8). Reports from this trial indicated that twice daily dosages of tofacitinib at both 5 mg and 10 mg were associated with increased risk of malignancies excluding NMSC (HR 1.47 [95% CI 1.00, 2.18] and HR 1.48 [95% CI 1.00, 2.19], respectively) (6–8). A higher risk of malignancies was observed in North America where the comparator was adalimumab (HR 1.92 [95% CI 1.10, 3.34]), compared to the rest of the world where the comparator was etanercept (HR 1.25 [95% CI 0.79, 1.97]) (8). There were also imbalances in the risks of lung cancer (HR 2.17 [95% CI 0.95, 4.93]) and lymphoma (HR 5.09 [95% CI 0.65, 39.78]) among patients receiving tofacitinib, although precision was low (7,8,39).

A significant difference between the RWE cohort of the present study and the ORAL Surveillance trial population is that the RWE cohort included all RA patients treated in routine care. Our results suggest a potential heterogeneity of treatment effect. We did not observe an increased risk of malignancies among all RA patients treated in a real-world setting when comparing treatment with tofacitinib to treatment with TNFi agents. However, we observed a numerically increased risk of malignancies in the RCT-duplicate cohort, which included patients who were ≥50 years of age with cardiovascular risk factors (pooled weighted HR 1.17 [95% CI 0.85, 1.62]). We also observed this numerically increased risk in the RCT-duplicate cohort when we restricted the comparator to patients treated with adalimumab and etanercept (pooled weighted HR 1.18 [95% CI 0.83, 1.67]). Nevertheless, there are other differences between our study and the ORAL Surveillance trial, including a longer follow-up period in the ORAL Surveillance trial (median of 4 years) and potential differential adherence to treatment (8).

Three other studies have also examined the association between tofacitinib and the risk of malignancies (40–42). In a meta-analysis of 6 phase II, 6 phase III, and 2 long-term extension studies, the incidence rate of malignancies (excluding NMSC) among patients treated with tofacitinib was reported to be 0.85 events (95% CI 0.70, 1.02) per 100 person-years (40), an incidence rate consistent with the expected range of patients with moderate-to-severe RA, although lower than the pooled crude incidence rate observed across the 3 data sets in this study (pooled crude incidence 1.74 [95% CI 1.47, 2.06] per 100 person-years). Similarly, a study conducted using the Corrona RA registry which includes more than 50,605 RA patients across private and academic practices in the US, did not find an association between tofacitinib and malignancies excluding NMSC (adjusted HR 1.04 [95% CI 0.68, 1.61]) or between tofacitinib and NMSC (adjusted HR 1.02 [95% CI 0.69, 1.50]) (41). Last, a recent observational study which included 69,308 RA patients identified using the Swedish Rheumatology Quality Register demonstrated that TNFi agents and other biologic/targeted synthetic DMARDs were not associated with an increased risk of noncutaneous malignancies when compared to no treatment with these drugs

(42). However, this study did not assess the risk associated with JAK inhibitors due to the low number of events (<5). Multiple factors may account for the differences between the results of these studies, including the definition of study population, the exposure and outcome definition, and follow-up time.

The potential mechanistic effects of tofacitinib on the risk of malignancies is complex. Tofacitinib is an inhibitor of JAK1 and JAK3, which are enzymes involved in the activation of the JAK/STAT signaling pathway. The effect of the JAK/STAT pathway on tumor initiation and progression is complex and multifaceted, particularly given the possible indirect effects of crosstalk with other intracellular signaling pathways that may occur (43,44). While some members of the STAT family (such as STAT3 and STAT5) may play a detrimental role in tumor initiation and progression, others (such as STAT1 and STAT2) may have a protective effect through the mediation of long-term antitumor immune response (43,44). Further mechanistic studies are required to understand the potential direct effect of tofacitinib and the role of the JAK/STAT pathway in tumor initiation and progression.

This study had several strengths. First, we conducted analyses across 3 US insurance claims databases (both commercial and public health plans) encompassing RA patients treated in a real-world setting, and thus, the results are generalizable to the setting of routine clinical care. Second, we calibrated our results with the ORAL Surveillance trial through the use of the RCT-duplicate cohort in order to ensure that the results of our study were valid and comparable with the findings of the ORAL Surveillance trial. Third, we used an active-comparator, new-user design to control for confounding by indication and prevent immortal time bias (10). Fourth, we observed consistent results in sensitivity analyses that accounted for potential latency and for a carryover effect of treatment after discontinuation. Finally, we registered the protocol for this study prior to conducting the analyses (11).

This study had some limitations. First, the follow-up time was relatively short (mean follow-up <1 year) due to the imposed as-treated definition in which patients were censored at treatment discontinuation or switch. Nevertheless, 9,237 patients (11.1% of the study population) had a follow-up time of at least 2 years, a sample size greater than the ORAL Surveillance trial (n = 4,362 patients). Second, we did not assess the risk of malignancies for other JAK inhibitors including baricitinib and upadacitinib. Additional studies will be needed to examine the class effect of JAK inhibitors. Third, we did not have an adequate sample size to examine the risk of some individual malignancies such as leukemia and lymphoma. In addition, some subgroups indicated treatment heterogeneity, although no conclusions can be made due to low precision for the estimates. Fourth, outcome misclassification is possible, although we used a validated claims-based algorithm with a high specificity (≥98%) for most cancer types (15). Fifth, we also relied on diagnosis and procedure codes to select the study cohort. While we assessed obesity and smoking status, it is likely that the sensitivity of our claims definitions is low (45,46). Finally, residual confounding due to some unmeasured RA-related variables is possible, although a recent study that used the Corrona RA registry demonstrated that RA patients in the US initiating treatment with tofacitinib are similar to bDMARD users with regard to RA-related factors such as disease activity index scores (41).

In conclusion, in this large, population-based, real-world cohort of 83,295 RA patients, tofacitinib was not associated with an increased risk of malignancies in comparison to TNFi agents. However, tofacitinib was associated with a numerically increased risk of malignancies in older patients who had risk factors for cardiovascular disease, a finding that was similarly observed in participants in the ORAL Surveillance trial. Future studies with large sample sizes and long-term follow-up periods are required to confirm these findings.

AUTHOR CONTRIBUTIONS

All authors were involved in drafting the article or revising it critically for important intellectual content, and all authors approved the final version to be published. Dr. Kim had full access to all the data in the study and takes responsibility for the integrity of the data and the accuracy of the data analysis.

Study conception and design. Khosrow-Khavar, Desai, H. Lee, S. Lee, Kim.

Acquisition of data. Khosrow-Khavar, Desai, Kim.

Analysis and interpretation of data. Khosrow-Khavar, Desai, H. Lee, S. Lee, Kim.

REFERENCES

1. Safiri S, Kolahi AA, Hoy D, Smith E, Bettampadi D, Mansournia MA, et al. Global, regional and national burden of rheumatoid arthritis 1990-2017: a systematic analysis of the Global Burden of Disease study 2017. Ann Rheum Dis 2019;78:1463–71.

2. Brigham and Women's Hospital, sponsor. Safety of TofAcitinib in Routine Care Patients with Rheumatoid Arthritis (STAR-RA)-cardiovascular endpoints. ClinicalTrials.gov identifier: NCT04772248; 2021.

3. Fraenkel L, Bathon JM, England BR, St Clair EW, Arayssi T, Carandang K, et al. 2021 American College of Rheumatology guideline for the treatment of rheumatoid arthritis. Arthritis Rheumatol 2021;73:1108–23.

4. Park SH, Jeon HL, Kim SC, Hillen J, Gadzhanova S, Shin JY, et al. Utilization of targeted disease-modifying anti-rheumatic drugs (DMARDs) for managing rheumatoid arthritis in the last decade: a two-country comparison. Int J Clin Pharmacol Ther 2021;59:639–44.

5. Pfizer, Inc, sponsor. Safety study of tofacitinib versus tumor necrosis factor (TNF) inhibitor in subjects with rheumatoid arthritis. ClinicalTrials.gov identifier: NCT02092467; 2014.

6. Pfizer, Inc. Pfizer shares co-primary endpoint results from post-marketing required safety study of XELJANZ® (tofacitinib) in subjects with rheumatoid arthritis (RA). 2021. URL: https://www.pfizer.com/news/press-release/press-release-detail/pfizer-shares-co-primary-endpoint-results-post-marketing.

7. Curtis J, Yamaoka K, Chen Y, Gunay L, Sugiyama N, Cornnell C, et al. Malignancies in patients aged ≥ 50 years with RA and ≥1 additional cardiovascular risk factor: results from a phase 3b/4 randomized safety study of tofacitinib vs TNF inhibitors [abstract]. Arthritis Rheumatol 2021;73 Suppl 10. URL: https://acrabstracts.org/abstract/malignancies-in-patients-aged-%e2%89%a5-50-years-with-ra-and-%e2%89%a5-1-additional-cardiovascular-risk-factor-results-from-a-phase-3b-4-randomized-safety-study-of-tofacitinib-vs-tnf-inhibitors/.

8. Ytterberg SR, Bhatt DL, Mikuls TR, Koch GG, Fleischmann R, Rivas JL, et al. Cardiovascular and cancer risk with tofacitinib in rheumatoid arthritis. N Engl J Med 2022;386:316–26.

9. US Food and Drug Administration. Initial safety trial results find increased risk of serious heart-related problems and cancer with arthritis and ulcerative colitis medicine Xeljanz, Xeljanz XR (tofacitinib). 2021 URL: https://www.fda.gov/drugs/drug-safety-and-availability/initial-safety-trial-results-find-increased-risk-serious-heart-related-problems-and-cancer-arthritis.

10. Lund JL, Richardson DB, Sturmer T. The active comparator, new user study design in pharmacoepidemiology: historical foundations and contemporary application. Curr Epidemiol Rep 2015;2:221–8.

11. Brigham and Woman's Hospital, sponsor. Safety of TofAcitinib in Routine Care Patients With Rheumatoid Arthritis (STAR-RA)-Cancer Endpoints. ClinicalTrials.gov identifier: NCT04798287; 2021.

12. Von Elm E, Altman DG, Egger M, Pocock SJ, Gotzsche PC, Vandenbroucke JP, et al. The Strengthening the Reporting of Observational Studies in Epidemiology (STROBE) statement: guidelines for reporting observational studies. Lancet 2007;370:1453–7.

13. Kim SY, Servi A, Polinski JM, Mogun H, Weinblatt ME, Katz JN, et al. Validation of rheumatoid arthritis diagnoses in health care utilization data. Arthritis Res Ther 2011;13:R32.

14. Kim SC, Pawar A, Desai RJ, Solomon DH, Gale S, Bao M, et al. Risk of malignancy associated with use of tocilizumab versus other biologics in patients with rheumatoid arthritis: a multi-database cohort study. Semin Arthritis Rheum 2019;49:222–8.

15. Setoguchi S, Solomon DH, Glynn RJ, Cook EF, Levin R, Schneeweiss S. Agreement of diagnosis and its date for hematologic malignancies and solid tumors between medicare claims and cancer registry data. Cancer Causes Control 2007;18:561–9.

16. Lee EB, Fleischmann R, Hall S, Wilkinson B, Bradley JD, Gruben D, et al. Tofacitinib versus methotrexate in rheumatoid arthritis. N Engl J Med 2014;370:2377–86.

17. Pawar A, Desai RJ, Gautam N, Kim SC. Risk of admission to hospital for serious infection after initiating tofacitinib versus biologic DMARDs in patients with rheumatoid arthritis: a multidatabase cohort study. Lancet Rheumatol 2020;2:e84–98.

18. Cogliano VJ, Baan R, Straif K, Grosse Y, Lauby-Secretan B, El Ghissassi F, et al. Preventable exposures associated with human cancers. J Natl Cancer Inst 2011;103:1827–39.

19. Siegel RL, Miller KD, Fuchs HE, Jemal A. Cancer Statistics, 2021. CA Cancer J Clin 2021;71:7–33.

20. De Cock D, Hyrich K. Malignancy and rheumatoid arthritis: epidemiology, risk factors and management. Best Pract Res Clin Rheumatol 2018;32:869–86.

21. Simon TA, Thompson A, Gandhi KK, Hochberg MC, Suissa S. Incidence of malignancy in adult patients with rheumatoid arthritis: a meta-analysis. Arthritis Res Ther 2015;17:212.

22. Gagne JJ, Glynn RJ, Avorn J, Levin R, Schneeweiss S. A combined comorbidity score predicted mortality in elderly patients better than existing scores. J Clin Epidemiol 2011;64:749–59.

23. Kim DH, Patorno E, Pawar A, Lee H, Schneeweiss S, Glynn RJ. Measuring frailty in administrative claims data: comparative performance of four claims-based frailty measures in the U.S. medicare data. J Gerontol A Biol Sci Med Sci 2020;75:1120–5.

24. Lau ES, Paniagua SM, Liu E, Jovani M, Li SX, Takvorian K, et al. Cardiovascular risk factors are associated with future cancer. JACC CardioOncol 2021;3:48–58.

25. Tu H, Wen CP, Tsai SP, Chow WH, Wen C, Ye Y, et al. Cancer risk associated with chronic diseases and disease markers: prospective cohort study. BMJ 2018;360:k134.

26. He MM, Lo CH, Wang K, Polychronidis G, Wang L, Zhong R, et al. Immune-mediated diseases associated with cancer risks. JAMA Oncol 2021;8:209–19.

27. Llovet JM, Kelley RK, Villanueva A, Singal AG, Pikarsky E, Roayaie S, et al. Hepatocellular carcinoma. Nat Rev Dis Primers 2021;7:6.

28. Tokajuk A, Krzyzanowska-Grycel E, Tokajuk A, Grycel S, Sadowska A, Car H. Antidiabetic drugs and risk of cancer. Pharmacol Rep 2015;67:1240–50.

29. Wong RSY. Role of nonsteroidal anti-inflammatory drugs (NSAIDs) in cancer prevention and cancer promotion. Adv Pharmacol Sci 2019;2019:3418975.

30. Lavergne F, Jay TM. Antidepressants promote and prevent cancers. Cancer Invest 2020;38:572–98.

31. Wigmore T, Farquhar-Smith P. Opioids and cancer: friend or foe? Curr Opin Support Palliat Care 2016;10:109–18.

32. Desai RJ, Franklin JM. Alternative approaches for confounding adjustment in observational studies using weighting based on the propensity score: a primer for practitioners. BMJ 2019;367:l5657.

33. Austin PC. An introduction to propensity score methods for reducing the effects of confounding in observational studies. Multivariate Behav Res 2011;46:399–424.

34. Austin PC. Using the standardized difference to compare the prevalence of a binary variable between two groups in observational research. Commun Stat Simul Comput 2008;38:1228–34.

35. Franklin JM, Rassen JA, Ackermann D, Bartels DB, Schneeweiss S. Metrics for covariate balance in cohort studies of causal effects. Stat Med 2014;33:1685–99.

36. Borenstein M, Hedges LV, Higgins JP, Rothstein HR. A basic introduction to fixed-effect and random-effects models for meta-analysis. Res Synth Methods 2010;1:97–111.

37. Aetion, Inc. Aetion Evidence Platform (2020). Software for real-world data analysis. URL: http://www.aetion.com.

38. Austin PC. A comparison of 12 algorithms for matching on the propensity score. Stat Med 2014;33:1057–69.

39. The Health Products Regulatory Authority. Xeljanz (tofacitinib) - Important safety information from Pfizer Healthcare Ireland as approved by the HPRA (July 2021). 2021. URL: https://www.hpra.ie/homepage/medicines/safety-notices/item?t=/xeljanz-(tofacitinib)—important-safety-information-from-pfizer-healthcare-ireland-as-approved-by-the-hpra-(july-2021)&id=99e90f26-9782-6eee-9b55-ff00008c97d0.

40. Curtis JR, Lee EB, Kaplan IV, Kwok K, Geier J, Benda B, et al. Tofacitinib, an oral Janus kinase inhibitor: analysis of malignancies across the rheumatoid arthritis clinical development programme. Ann Rheum Dis 2016;75:831–41.

41. Kremer JM, Bingham CO III, Cappelli LC, Greenberg JD, Madsen AM, Geier J, et al. Postapproval comparative safety study of Tofacitinib and biological disease-modifying antirheumatic drugs: 5-year results from a United States-based rheumatoid arthritis registry. ACR Open Rheumatol 2021;3:173–84.

42. Huss V, Bower H, Wadstrom H, Frisell T, Askling J. Short- and longer-term cancer risks with biologic and targeted synthetic disease modifying antirheumatic drugs as used against rheumatoid arthritis in clinical practice. Rheumatology (Oxford) 2022;61:1810–8.

43. Brooks AJ, Putoczki T. JAK-STAT signalling pathway in cancer [editorial]. Cancers (Basel) 2020;12:1971.

44. Owen KL, Brockwell NK, Parker BS. JAK-STAT signaling: a double-edged sword of immune regulation and cancer progression [review]. Cancers (Basel) 2019;11:2002.

45. Desai RJ, Solomon DH, Shadick N, Iannaccone C, Kim SC. Identification of smoking using Medicare data–a validation study of claims-based algorithms. Pharmacoepidemiol Drug Saf 2016;25:472–5.

46. Suissa K, Kim SC, Patorno E. Misclassification of obesity in claims data. Clin Transl Gastroenterol 2021;12:e00423.

Association Between Walking for Exercise and Symptomatic and Structural Progression in Individuals With Knee Osteoarthritis: Data From the Osteoarthritis Initiative Cohort

Grace H. Lo,[1] Surabhi Vinod,[2] Michael J. Richard,[3] Matthew S. Harkey,[4] Timothy E. McAlindon,[3] Andrea M. Kriska,[5] Bonny Rockette-Wagner,[5] Charles B. Eaton,[6] Marc C. Hochberg,[7] Rebecca D. Jackson,[8] C. Kent Kwoh,[9] Michael C. Nevitt,[10] and Jeffrey B. Driban[3]

Objective. To assess the relationship between walking for exercise and symptomatic and structural disease progression in individuals with knee osteoarthritis (OA).

Methods. We assessed a nested cohort of participants age 50 years or older within the Osteoarthritis Initiative, a community-based observational study in which subjects were enrolled between 2004 and 2006. We focused on 4 dichotomous outcomes from baseline to the 48-month visit, involving determination of the frequency of knee pain and radiographic severity of knee OA on posteroanterior semiflexed knee radiographs. The outcomes assessed included 1) new frequent knee pain, 2) worsening of radiographic severity of knee OA based on the Kellgren/Lawrence grade, 3) progression of medial joint space narrowing, and 4) improved frequent knee pain. We used a modified version of the Historical Physical Activity Survey Instrument to ascertain those subjects who reported walking for exercise after age 50 years. The survey was administered at the 96-month visit (2012–2014).

Results. Of 1,212 participants with knee OA, 45% were male and 73% reported walking for exercise. The mean ± SD age was 63.2 ± 7.9 years, and the mean ± SD body mass index was 29.4 ± 4.6 kg/m². The likelihood of new frequent knee pain was reduced in participants with knee OA who walked for exercise as compared to those who were non-walkers (odds ratio [OR] 0.6, 95% confidence interval [95% CI] 0.4–0.8), and progression of medial joint space narrowing was less common in walkers compared to non-walkers (OR 0.8, 95% CI 0.6–1.0).

Conclusion. In individuals with knee OA who were age 50 years or older, walking for exercise was associated with less frequent development of knee pain. These findings support the notion that walking for exercise should be encouraged for people with knee OA. Furthermore, we offer a proof of concept that walking for exercise could be disease modifying, which warrants further study.

INTRODUCTION

Osteoarthritis (OA) is the most common type of arthritis in the US and is a leading cause of pain for those affected (1). Current pharmacologic therapies are limited to topical and oral nonsteroidal antiinflammatory drugs, intraarticular glucocorticoids, and analgesics such as tramadol, which only treat pain and do not modify structure (2). Professional societies, including the

American College of Rheumatology (ACR) and the Osteoarthritis Research Society International (OARSI), have endorsed treatment recommendations under a comprehensive care strategy incorporating educational, behavioral, and physical interventions (2,3).

Exercise is a physical intervention often touted as a treatment for OA (2–4). The ACR guidelines specifically mention walking as a reasonable means of obtaining such exercise (2). Two clinical trials of land-based exercises that included walking as a treatment for knee OA (5,6) and 1 trial of walking alone as an intervention (n = 92) (7) support these recommendations. However, these trials were relatively short in duration. To address whether walking for exercise over time is beneficial in terms of alleviating long-term symptoms and structural progression, ascertainment of the effectiveness of walking for exercise over many years and longer follow-up periods is required.

To our knowledge, the Osteoarthritis Initiative is the only cohort study in which walking for exercise over several years has been assessed, and in which outcomes of knee OA, including symptoms and structural changes, have been carefully characterized. Thus, we used data from the Osteoarthritis Initiative cohort to address whether this exposure to walking is beneficial or detrimental in terms of modifying the course of symptoms or radiographic disease severity in individuals who have knee OA.

PATIENTS AND METHODS

Study design. The study was designed as a nested cohort study within the Osteoarthritis Initiative, a multicenter, prospective, longitudinal observational study involving individuals with or without symptomatic knee OA enrolled between 2004 and 2006. Staff at the following 4 clinic sites recruited participants: Memorial Hospital of Rhode Island, Ohio State University, the University of Pittsburgh, and the University of Maryland/Johns Hopkins. Participants attended annual evaluations from baseline to month 48, and thereafter every 2 years to month 96. Institutional review board approval was obtained at each clinic site, coordinating center, and the Baylor College of Medicine. Each participant provided written informed consent.

All publicly available data can be accessed through the Osteoarthritis Initiative website at https://nda.nih.gov/oai/.

Study timeline. The Historical Physical Activity Survey Instrument was administered to the included participants from the Osteoarthritis Initiative cohort at the 96-month visit, as part of an ancillary study to the parent Osteoarthritis Initiative. The radiographs and knee pain questions were planned as part of the parent study and ascertained at the Osteoarthritis Initiative baseline and 48-month visits, representing the 2 time points with the largest number of outcomes available in this cohort. The timing of the exposure was not optimal, since it was ascertained after the outcomes of interest; however, this was an unprecedented opportunity to capture information on physical activity over a lifetime in a cohort with highly characterized knee OA outcomes, not available in any other cohort.

Inclusion criteria. To be eligible, participants had to be age ≥50 years at baseline, to have complete data on knee-specific pain and knee radiographs at the 36-month or 48-month visits, and to have completed a modified version of the Historical Physical Activity Survey Instrument (8) at the 96-month visit. Participants were required to have radiographic evidence of knee OA (see below for further details) in at least one native knee at the time of enrollment.

Knee radiographs. The largest number of funded radiographic readings within the Osteoarthritis Initiative occurred at the baseline and 48-month visits, and therefore we chose these as the time points of interest for our study. If radiographs from the 48-month visit were missing, we used films from the 36-month visit instead. Bilateral, fixed-flexion, weight-bearing posteroanterior radiographs of the knees were obtained at these visits.

Kellgren/Lawrence (K/L) grades of radiographic knee OA severity (scale 0–4) (9) and the extent of medial joint space narrowing (JSN) were scored centrally based on the OARSI atlas of individual radiographic features (10). The reliability of these readings (read–reread) was good (weighted kappa for intrarater reliability 0.71, 95% confidence interval [95% CI] 0.55–0.87) (11). Radiographic OA was defined as a K/L grade ≥2.

Pain assessment. Participants were assessed for symptoms using a general screening assessment of frequent knee pain. Participants were asked the following question: "During the last 12 months, have you had pain, aching, or stiffness in or around your right/left knee on most days for at least one month? By most days, we mean more than half the days of a month" (12).

Knee arthroplasty. Knee replacement (partial or total) was reported or observed on radiographs at or before the 4-year visit of the Osteoarthritis Initiative study (>96% of participants adjudicated). A knee replacement was recorded if 1 of 3 criteria for a partial or total knee replacement were met, as follows: 1) the knee

School of Brown University and Department of Epidemiology, School of Public Health of Brown University, Providence, Rhode Island; [7]Marc C. Hochberg, MD: Department of Medicine and Epidemiology and Public Health, University of Maryland School of Medicine, Baltimore; [8]Rebecca D. Jackson, MD: Division of Endocrinology, Diabetes and Metabolism, The Ohio State University, Columbus; [9]C. Kent Kwoh, MD: University of Arizona Arthritis Center, University of Arizona College of Medicine, Tucson; [10]Michael C. Nevitt, PhD: Department of Epidemiology and Biostatistics, University of California, San Francisco.

replacement was centrally adjudicated (medical records reviewed by 2 adjudicators and also by a physician adjudicator if there was disagreement between the first 2 adjudicators), 2) the knee replacement was observed on a study radiograph, or 3) the knee replacement was self-reported (even if the self-reported replacement had not gone through the adjudication process).

Static alignment. We defined static alignment using hip–knee–ankle angles measured on long-limb films. Long-limb films were acquired between months 12 and 48, based on participant availability. Staff obtained bilateral films with participants standing with the tibial tubercle forward. Hip–knee–ankle angles were calculated at the intersection of 2 lines: 1) from the ankle talar surface center to the tibial interspinous sulcus base, and 2) from the femoral head and intercondylar notch centers (13,14). Alignment was classified as varus if the angle was less than or equal to $-2°$, valgus if the angle was greater than or equal to $2°$, and neutral if the angle was any value in between (15). These radiographs were obtained as part of a separate ancillary grant to the Osteoarthritis Initiative. As a result, these radiographs were not obtained at the baseline visit; they were collected at month 12 (40%), month 24 (41%), month 36 (18%), and month 48 (2%). In total, 985 (81%) of the 1,212 participants had long-limb films available, and 1,484 (82%) of the 1,808 knees assessed by radiography were included.

Historical Physical Activity Survey Instrument. To ascertain the exposure of walking for exercise, we administered a modified version of the Historical Physical Activity Survey Instrument (8). This survey questionnaire was mailed to participants. We altered the survey so that a participant could complete it as a take-home survey, similar to the self-administered questionnaire previously described by Chasan-Taber et al (16). If the survey was incomplete at the time of the closest in-person follow-up clinic visit (the 96-month visit), clinic staff asked participants to complete it at the clinic visit; clinic staff assistance was available if requested. These data were acquired between September 12, 2012 and October 31, 2014.

The walking for exercise exposure was assessed using the following question: "When you were 50 and older, did you walk for exercise at least 10 times? Please include walking outdoors and walking on a treadmill or track." Those who answered "yes" were considered walkers. Those who answered "no" or "don't know" (n = 25) were considered non-walkers. For those who responded to the questionnaire overall but had missing data on walking (n = 17), we coded them as non-walkers as well.

Those who answered "yes" were then asked further questions about the amount they walked for exercise. First, they were asked the question: "While you were 50 and older, did you walk for exercise at least 20 minutes within a given day (these do not have to be consecutive minutes)." If the answer was affirmative, then they were asked the question: "How many years did you

walk for exercise? These do not have to be consecutive years." The response choices they were given were 1–5 years, 6–10 years, 11–20 years, >20 years, or "don't know." Thereafter, they were asked: "How many months per year did you walk for exercise? Again, these do not have to be consecutive months." The response choices they were given were 1–4 months per year, 5–8 months per year, 9–12 months per year, or "don't know." Finally, they were asked: "How many times per month did you walk for exercise?" The response choices they were given were 1–3 times per month, 4–8 times per month, 9 or more times per month, or "don't know." Using the median value for the answers given to each of these questions, an estimate was made regarding the number of times that the participant had walked for exercise since turning age 50 years.

Covariates. Date of birth and date of the baseline visit were used to calculate each participant's age. Body mass index was calculated as weight divided by height squared (kg/m^2), measured at the baseline visit.

Outcome measures. *New frequent knee pain.* Using the frequent knee pain question as defined under the "Pain Assessment" section of the questionnaire, the outcome of new frequent knee pain was defined as a knee without frequent knee pain at baseline but with frequent knee pain at the 48-month visit. To be explicit, the question focused on frequent knee pain, not any knee pain.

Improved frequent knee pain. The outcome of improved frequent knee pain was similarly defined using the frequent knee pain question. Specifically, improvement was defined as a knee having frequent knee pain at baseline but not at the 48-month visit.

Medial JSN worsening. The outcome of medial JSN worsening was defined as an increase in medial JSN score from baseline to the 48-month visit, including within-grade worsening (17). We chose to evaluate JSN worsening in the medial compartment, as most of the loading within a knee passes through the medial tibiofemoral compartment.

K/L grade worsening. The outcome of K/L grade worsening was defined as an increase in the K/L radiographic severity grade over the same time period. For all outcomes, if data from the 48-month visit were not available, data from the 36-month visit were carried forward, which occurred for 8% of the participants.

Statistical analysis. We performed unadjusted and adjusted knee-based logistic regression analyses, using generalized estimating equations to account for correlation within person (18), in which the predictor was walking for exercise. Walking for exercise was defined dichotomously (walkers versus non-walkers).

For the 4 outcome measures (new frequent knee pain, improved frequent knee pain, medial JSN worsening, and K/L grade worsening), adjusted analyses included age, sex, and baseline K/L grade as covariates. For the pain analyses, we excluded knees that already had the outcomes of interest from those respective analyses (e.g., those with baseline frequent knee pain were excluded from new frequent knee pain analyses). We included knees with K/L grade 4 and medial JSN grade 3 in the structural analyses, since, for these knees, they still had the potential of requiring an interval knee replacement, which would have allowed for the outcomes of K/L grade worsening and medial JSN worsening, respectively. We also performed analyses stratified by baseline age (age 50–59 years, age 60–69 years, and age 70–79 years) to address the possibility of reverse causation. Finally, we examined the frequency of each outcome among walkers and non-walkers stratified by knee static alignment (varus, neutral, or valgus). No statistical analyses stratified by alignment were performed, because of a limited sample size in some strata. The prospective protocol describing the statistical analysis plan for this study is provided in the Supplementary Statistical Analysis (available on the *Arthritis & Rheumatology* website at https://onlinelibrary.wiley.com/doi/10.1002/art.42241).

Because data on walking were missing for some participants, we performed a simplistic nonresponder imputation sensitivity analysis. We used a best case imputation and worst case imputation to provide a manual "extreme case," in which all those who had missing data on walking status were assumed to be walkers in one imputation and assumed to be non-walkers in another imputation.

RESULTS

Of the original 4,796 participants enrolled in the Osteoarthritis Initiative, 549 were younger than age 50 years at the time of the baseline visit, leaving 4,247 participants. Of these, 267 had missing baseline radiographs, leaving 3,980 participants who were evaluated for evidence of radiographic knee OA at the baseline visit. Of these, 1,624 did not have evidence of radiographic knee OA, leaving 2,356 participants considered eligible to have been surveyed at the 96-month visit, which we refer to as the "intent-to-survey" group. Of the 2,356 in the "intent-to-survey" group, 417 participants attended the 96-month visit prior to the date at which the Historical Physical Activity Survey Instrument was first administered within the Osteoarthritis Initiative, leaving 1,939 participants; 346 participants did not attend the 96-month visit at all, leaving 1,593 participants. Of these, 337 people attended the 96-month visit when the survey was being administered but chose not to complete the questionnaire, leaving 1,256 participants for whom we had exposure data and who were considered eligible to participate in this study. Of these, 44 did not have follow-up radiographs, leaving a total of 1,212
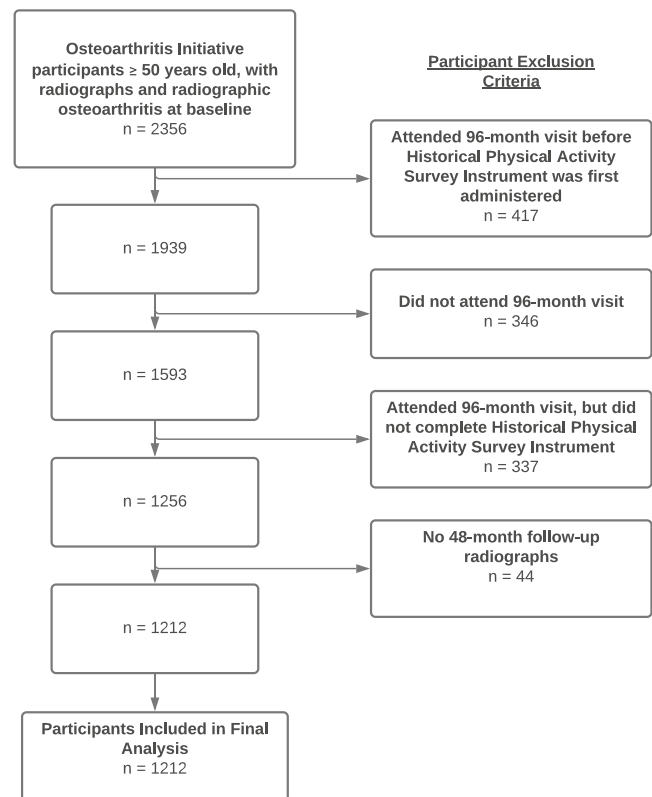
Figure 1. Flow diagram showing the eligibility criteria applied to the cohort and the sample size identified for final analysis of the effects of walking for exercise among a subset of individuals with knee osteoarthritis from the Osteoarthritis Initiative cohort.

participants. Figure 1 illustrates how we arrived at the sample that was included in our study.

Among the 1,212 participants (who contributed 1,808 knees for assessment), 887 (73%) reported walking for exercise. In total, 45% of participants were male, the mean ± SD age was 63.2 ± 7.9 years, and the mean ± SD body mass index was 29.5 ± 4.6 kg/m^2 (Table 1).

Knee-based descriptors at baseline were assessed in this Osteoarthritis Initiative sample. We observed that 64%, 29%, and 7% of participants had K/L radiographic knee OA severity grades of 2, 3, and 4, respectively, 65% of participants had some medial JSN, and 37% of participants reported having frequent knee symptoms. Rates of total knee replacement over the 48-month follow-up period were similar between those who walked for exercise and those who did not walk for exercise (Table 1). For 151 participants (12.6%), 36-month follow-up data instead of 48-month data were used. The characteristics of the participants who were not included in the study were similar to those who were included (see Supplementary Table 1, available on the *Arthritis & Rheumatology* website at https://onlinelibrary.wiley.com/doi/10.1002/art.42241).

Participants with knee OA who walked for exercise had a 40% decreased odds of new frequent knee pain compared to

Table 1. Characteristics of the included participants with knee OA from the Osteoarthritis Initiative cohort at baseline and 48 months, among non-walkers, walkers, and in total*

Time point, characteristic	Non-walkers	Walkers	All participants
Baseline			
Person-based characteristics			
No. of participants	325	887	1,212
Age, mean ± SD years	64.5 ± 8.3	62.7 ± 7.7	63.2 ± 7.9
Male sex	167/325 (51)	381/887 (43)	548/1,212 (45)
Body mass index, mean ± SD kg/m^2	30.2 ± 4.6	29.2 ± 4.6	29.4 ± 4.6
Estimated total no. of days of walking for exercise after age 50 years			
Minimum	0	13	–
25th percentile	0	337	–
Median	0	845	–
75th percentile	0	1,417	–
Maximum	0	2,100	–
Knee-based characteristics			
No. of participants	503	1,305	1,808
OA severity by K/L grade			
Grade 2	284/503 (56)	869/1,305 (67)	1,153/1,808 (64)
Grade 3	175/503 (35)	354/1,305 (27)	529/1,808 (29)
Grade 4	44/503 (9)	82/1,305 (6)	126/1,808 (7)
Medial JSN grade			
Grade 0	151/503 (30)	487/1,305 (37)	638/1,808 (35)
Grade 1	173/503 (34)	475/1,305 (36)	648/1,808 (36)
Grade 2	144/503 (29)	293/1,305 (22)	437/1,808 (24)
Grade 3	35/503 (7)	50/1,305 (4)	85/1,808 (5)
Frequent knee symptoms	223/503 (44)	453/1,305 (35)	676/1,808 (37)
Static alignment			
No. of participants	418	1,066	1,484
Varus	227/418 (54)	480/1,066 (45)	707/1,484 (48)
Neutral	129/418 (31)	407/1,066 (38)	536/1,484 (36)
Valgus	62/418 (15)	179/1,066 (17)	241/1,484 (16)
48 months, knee-based characteristics			
Frequent knee symptoms	233/503 (46)	496/1,305 (38)	729/1,808 (40)
Knee replacement	27/503 (5)	50/1,305 (4)	77/1,808 (4)

* Except where indicated otherwise, values are the number/total number (%) of participants. OA = osteoarthritis; K/L = Kellgren/Lawrence; JSN = joint space narrowing.

Table 2. Prevalence and odds of outcomes according to worsened or improved status among walkers versus non-walkers with knee OA*

	Prevalence of outcome, no./total (%)	Unadjusted odds ratio (95% CI)	Adjusted odds ratio (95% CI)†
Worsened outcome			
New frequent knee pain			
Non-walkers	103/280 (37)	Referent	Referent
Walkers	223/852 (26)	0.6 (0.4–0.8)‡	0.6 (0.4–0.8)‡
Worsening of K/L OA severity grade			
Non-walkers	105/503 (21)	Referent	Referent
Walkers	234/1,305 (18)	0.8 (0.6–1.1)	0.8 (0.6–1.1)
Worsening of medial JSN grade			
Non-walkers	137/503 (27)	Referent	Referent
Walkers	281/1,305 (22)	0.7 (0.6–1.0)‡	0.8 (0.6–1.0)‡
Improved outcome			
Improved frequent knee pain			
Non-walkers	93/223 (42)	Referent	Referent
Walkers	180/453 (40)	0.9 (0.7–1.3)	0.8 (0.6–1.2)

* Each outcome was assessed for its presence versus absence (yes/no) in walkers relative to non-walkers. OA = osteoarthritis; 95% CI = 95% confidence interval; JSN = joint space narrowing.
† Adjusted for age, sex, and baseline Kellgren/Lawrence (K/L) grade.
‡ Statistically significant at *P* < 0.05.

Table 3. Frequency of outcomes among walkers versus non-walkers with knee OA stratified by static alignment*

	Varus knees	Neutral knees	Valgus knees
New frequent knee pain			
Non-walkers	47/120 (39)	28/77 (36)	9/31 (29)
Walkers	82/290 (28)	60/266 (23)	40/122 (33)
Worsening of K/L OA severity grade			
Non-walkers	59/227 (26)	13/129 (10)	9/62 (15)
Walkers	97/480 (20)	58/407 (14)	35/179 (20)
Worsening of medial JSN grade			
Non-walkers	88/227 (39)	14/129 (11)	3/62 (5)
Walkers	149/480 (31)	69/407 (17)	16/179 (9)
Improved frequent knee pain			
Non-walkers	43/107 (40)	20/52 (38)	15/31 (48)
Walkers	74/190 (39)	66/141 (47)	20/57 (35)

* Values are the number/total number (%) of participants. Each outcome was assessed for its presence versus absence (yes/no) in walkers relative to non-walkers. OA = osteoarthritis; K/L = Kellgren/Lawrence; JSN = joint space narrowing.

non-walkers, with an adjusted odds ratio (OR) of 0.6 (95% CI 0.4–0.8) (Table 2). The adjusted OR for the outcome of medial JSN progression in walkers compared to non-walkers was 0.8 (95% CI 0.6–1.0) (Table 2). The other 2 outcomes, worsening of K/L grade and improved frequent knee pain, did not show statistically significant increased odds of occurring in walkers compared to non-walkers.

Results of stratified analyses based on age groups were similar to those observed in the whole group for all ages, and did not provide any suggestion of reverse causation (data not shown). In sensitivity analyses based on the assumption that all participants who had missing data on walking were non-walkers, the results were similar to those in the primary analysis (see Supplementary Table 2, available on the *Arthritis & Rheumatology* website at https://onlinelibrary.wiley.com/doi/10.1002/art.42241). In analyses based on the assumption that all participants who had missing data on walking were walkers, the results were also similar, though the point estimates for medial JSN grade worsening were closer to 1 and no longer statistically significant (see Supplementary Table 3, available on the *Arthritis & Rheumatology* website at https://onlinelibrary.wiley.com/doi/10.1002/art.42241). Importantly for the outcome of new frequent knee pain, the finding was robust in both imputation models.

In stratified analyses based on static knee alignment (Table 3), walkers with varus alignment less frequently developed new frequent knee pain compared to non-walkers in this group (28% versus 39%), and fewer walkers with varus alignment experienced K/L grade worsening (20% versus 26%) and medial JSN grade worsening (31% versus 39%) compared to non-walkers with varus alignment. In the group of participants with neutral static alignment, walkers less frequently developed new frequent knee pain (23% versus 36%) and more frequently experienced improved frequent knee pain (47% versus 38%) compared to non-walkers. However, among those with neutral alignment, walkers more frequently experienced medial JSN worsening (17% versus 11% of non-walkers). Interestingly, walkers with

valgus alignment more frequently had K/L grade worsening (20% versus 15%) and less frequently had improved frequent knee pain (35% versus 48%) than non-walkers with valgus alignment. Thus, there did appear to be a potentially differential effect of walking for exercise based on knee static alignment.

DISCUSSION

Findings from our study support the idea that walking is beneficial in patients with knee OA, in terms of both structural modifications and symptom improvements. Specifically, we found that those who walked for exercise were less likely to develop new frequent knee pain; however, we found no relationship between walking and improvement in frequent knee pain. Hence, it may be especially beneficial to advise people to walk for exercise to help prevent the onset of frequent knee pain. These findings also offer the first reported evidence that walking may be an effective treatment to slow the structural progression of knee OA. Our findings highlight the possibility that biomechanical interventions may hold the key to the elusive treatments in this disease and might provide benefit in alleviating the structural progression and symptoms of OA. This is potentially an important paradigm shift in the field of OA research.

To our knowledge, this is the first study to explore the effects of walking stratified by knee static alignment. Specifically, we observed that walking might be related to less symptomatic and structural progression among knees with varus alignment (48% of cohort), less symptomatic progression among knees with neutral alignment (36% of cohort), and possibly little benefit among knees with valgus alignment (16% of cohort). Previous studies have yielded a wealth of data indicating that knee OA is largely biomechanically driven (15,19–27), and therefore it is not surprising that we found that static alignment could be an important effect measure modifier in evaluating the association between walking and knee OA progression. It will be important to replicate these analyses in other epidemiologic studies with larger groups

of subjects with knee OA stratified according to neutral alignment versus valgus alignment to confirm these findings.

As supported by our study, the current guidelines advocate that walking is beneficial for knee OA. Investigators who conducted a systematic review to inform the 2018 Physical Activity Guidelines for Americans (28) reported that, while there is moderate evidence of the safety of walking for exercise involving up to 10,000 steps/day, there is limited evidence to indicate that walking more than 10,000 steps/day may adversely affect knee OA progression (29). It is unclear if our findings address those concerns, since we focused on walking for exercise, and fewer than 14% of participants in a US-based cohort, similar to the Osteoarthritis Initiative, exceeded 10,000 steps/day (30). There are 2 moderate to large-sized epidemiologic studies, including those with and those without knee OA, suggesting harmful outcomes related to walking (31,32). These studies used step counts from activity monitors over 7 days to quantify daily step counts. This is the standard method of using physical activity monitoring data; however, this is potentially problematic as the exposure ascertainment time frame is very short and not specific to walking for exercise, and people are known to modify their activity when they know they are being monitored. Thus, these measures may not be a true reflection of the amount people walk for exercise over an extended time. In our study, we used a retrospective, self-reported measure of walking. While our measurement method has limitations due to recall bias, a benefit to our method of ascertaining walking is that it provides an average amount of data on walking for exercise over a much longer time period.

There are some limitations to our study. This is an observational study wherein the walkers were self-selected. There is the possibility that the association observed may result from reverse causation; people might walk more because they have less severe knee OA, as opposed to the possibility that walking is protective against progression of OA. We performed age-stratified analyses in which the findings were similar to those obtained in the whole group, making this possibility of reverse causation less likely, based on the idea that people self-selected walking for exercise; if the situation of reverse causation existed, then those who had knee pain at a younger age when they did walk would presumably stop over time because they had pain, which was not observed in our study.

Another limitation is that, as mentioned previously, the walking exposure was ascertained retrospectively, which raises concerns about recall bias. Beyond the idea that people had to think back over their life to estimate their walking exposure, the addition of the Historical Physical Activity Survey Instrument was part of an ancillary study to the main Osteoarthritis Initiative study, and therefore the ascertainment of the exposure of physical activity was performed after the outcomes of interest. Admittedly, this is not ideal; however, since the participants were reviewing their lifetime of physical activity, which was already a retrospective activity, it is less likely that the timing of the administration of the instrument detracts from the observed findings. Of important note, participants were unaware of our specific study questions when they completed the surveys, making the retrospective aspects of the ascertainment less likely to impact our results.

Another limitation of our study is that it used participants who had radiographic knee OA and who were ages 50 years and older. Therefore, it is not clear if these results would apply to those without OA and those in younger age groups.

Finally, because of the nature of the cohort, static knee alignment was not ascertained at the same time for all participants. However, static alignment is unlikely to change rapidly over time. Future studies should make a particular effort to assess static alignment at the baseline evaluations.

This study only addresses walking for exercise. It does not address the situation of compulsory walking, such as occupational walking (e.g., mail carriers) or walking for transportation. Although the study assesses walking for exercise over several years, it was based on self-report, not step counts from an activity monitor; thus, specific statements about extremely high exposures to walking cannot be made.

In conclusion, the findings from our study provide a glimmer of hope that there may be an inexpensive intervention that modifies the structure and symptoms related to knee OA, the most common type of arthritis and a source of substantial disability. Clinicians should encourage patients to walk and consider in-person or web-based walking programs, such as "Walk with Ease," which has demonstrated durable benefits over 1 year (33,34). Our findings support recommendations by professional societies that walking for exercise should be encouraged. Beyond a benefit in terms of alleviating the symptoms of knee OA, the findings from our study also suggest that walking may also provide a structural benefit for a large portion of the community with OA. A randomized controlled trial of walking in those with knee OA stratified by alignment is warranted.

AUTHOR CONTRIBUTIONS

REFERENCES

1. Zhang Y, Jordan JM. Epidemiology of osteoarthritis [Review]. Clin Geriatr Med 2010;26:355–69.

2. Kolasinski SL, Neogi T, Hochberg MC, Oatis C, Guyatt G, Block J, et al. 2019 American College of Rheumatology/Arthritis Foundation guideline for the management of osteoarthritis of the hand, hip, and knee. Arthritis Rheumatol 2020;72:220–33.

3. Bannuru RR, Osani MC, Vaysbrot EE, Arden NK, Bennell K, Bierma-Zeinstra SM, et al. OARSI guidelines for the non-surgical management of knee, hip, and polyarticular osteoarthritis [Review]. Osteoarthritis Cartilage 2019;27:1578–89.

4. Nelson AE, Allen KD, Golightly YM, Goode AP, Jordan JM. A systematic review of recommendations and guidelines for the management of osteoarthritis: the chronic osteoarthritis management initiative of the U.S. bone and joint initiative. Semin Arthritis Rheum 2014;43:701–12.

5. Ettinger WH Jr, Burns R, Messier SP, Applegate W, Rejeski WJ, Morgan T, et al. A randomized trial comparing aerobic exercise and resistance exercise with a health education program in older adults with knee osteoarthritis. The Fitness Arthritis and Seniors Trial (FAST). JAMA 1997;277:25–31.

6. Bautch JC, Malone DG, Vailas AC. Effects of exercise on knee joints with osteoarthritis: a pilot study of biologic markers. Arthritis Care Res (Hoboken) 1997;10:48–55.

7. Kovar PA, Allegrante JP, MacKenzie CR, Peterson MG, Gutin B, Charlson ME. Supervised fitness walking in patients with osteoarthritis of the knee: a randomized, controlled trial. Ann Intern Med 1992;116:529–34.

8. Friedenreich CM, Courneya KS, Bryant HE. The lifetime total physical activity questionnaire: development and reliability. Med Sci Sports Exerc 1998;30:266–74.

9. Kellgren JH, Lawrence JS. Radiological assessment of osteo-arthrosis. Ann Rheum Dis 1957;16:494–502.

10. Altman RD, Gold GE. Atlas of individual radiographic features in osteoarthritis, revised. Osteoarthritis Cartilage 2007;15:A1–56.

11. National Institute of Mental Health Data Archive. Osteoarthritis I. Project 15 test-retest reliability of semi-quantitative readings from knee radiographs, 2016. URL: https://nda.nih.gov/oai/study_documentation.html.

12. O'Reilly SC, Muir KR, Doherty M. Screening for pain in knee osteoarthritis: which question? Ann Rheum Dis 1996;55:931–3.

13. Sled EA, Sheehy LM, Felson DT, Costigan PA, Lam M, Cooke TD. Reliability of lower limb alignment measures using an established landmark-based method with a customized computer software program. Rheumatol Int 2011;31:71–7.

14. Cooke TD, Sled EA, Scudamore RA. Frontal plane knee alignment: a call for standardized measurement [editorial]. J Rheumatol 2007;34:1796–801.

15. Sharma L, Song J, Dunlop D, Felson D, Lewis CE, Segal N, et al. Varus and valgus alignment and incident and progressive knee osteoarthritis. Ann Rheum Dis 2010;69:1940–5.

16. Chasan-Taber L, Erickson JB, McBride JW, Nasca PC, Chasan-Taber S, Freedson PS. Reproducibility of a self-administered lifetime physical activity questionnaire among female college alumnae. Am J Epidemiol 2002;155:282–9.

17. Felson DT, Nevitt MC, Yang M, Clancy M, Niu J, Torner JC, et al. A new approach yields high rates of radiographic progression in knee osteoarthritis. J Rheumatol 2008;35:2047–54.

18. Zhang Y, Glynn RJ, Felson DT. Musculoskeletal disease research: should we analyze the joint or the person? J Rheumatol 1996;23:1130–4.

19. Sharma L, Song J, Felson DT, Cahue S, Shamiyeh E, Dunlop DD. The role of knee alignment in disease progression and functional decline in knee osteoarthritis. JAMA 2001;286:188–95.

20. Felson DT, McLaughlin S, Goggins J, LaValley MP, Gale ME, Totterman S, et al. Bone marrow edema and its relation to progression of knee osteoarthritis. Ann Intern Med 2003;139:330–6.

21. Hunter DJ, Zhang Y, Niu J, Goggins J, Amin S, Lavalley MP, et al. Increase in bone marrow lesions associated with cartilage loss: a longitudinal magnetic resonance imaging study of knee osteoarthritis. Arthritis Rheum 2006;54:1529–35.

22. Chang A, Hayes K, Dunlop D, Hurwitz D, Song J, Cahue S, et al. Thrust during ambulation and the progression of knee osteoarthritis. Arthritis Rheum 2004;50:3897–903.

23. Shakoor N, Block JA, Shott S, Case JP. Nonrandom evolution of end-stage osteoarthritis of the lower limbs. Arthritis Rheum 2002;46:3185–9.

24. Lo GH, Harvey WF, McAlindon TE. Associations of varus thrust and alignment with pain in knee osteoarthritis. Arthritis Rheum 2012;64:2252–9.

25. Lo GH, Hunter DJ, Nevitt M, Lynch J, McAlindon TE. Strong association of MRI meniscal derangement and bone marrow lesions in knee osteoarthritis: data from the osteoarthritis initiative. Osteoarthritis Cartilage 2009;17:743–7.

26. Lo GH, Hunter DJ, Zhang Y, McLennan CE, Lavalley MP, Kiel DP, et al. Bone marrow lesions in the knee are associated with increased local bone density. Arthritis Rheum 2005;52:2814–21.

27. Lo GH, Niu J, McLennan CE, Kiel DP, McLean RR, Guermazi A, et al. Meniscal damage associated with increased local subchondral bone mineral density: a Framingham study. Osteoarthritis Cartilage 2008;16:261–7.

28. Physical Activity Guidelines for Americans. In: U.S. Department of Health and Human Services PHS. 2nd edition. Washington DC; 2018.

29. Kraus VB, Sprow K, Powell KE, Buchner D, Bloodgood B, Piercy K, et al. Effects of physical activity in knee and hip osteoarthritis: a systematic umbrella review. Med Sci Sports Exerc 2019;51:1324–39.

30. White DK, Tudor-Locke C, Zhang Y, Fielding R, LaValley M, Felson DT, et al. Daily walking and the risk of incident functional limitation in knee osteoarthritis: an observational study. Arthritis Care Res (Hoboken) 2014;66:1328–36.

31. Voinier D, Neogi T, Stefanik JJ, Guermazi A, Roemer FW, Thoma LM, et al. Using cumulative load to explain how body mass index and daily walking relate to worsening knee cartilage damage over two years: the MOST study. Arthritis Rheumatol 2020;72:957–65.

32. Dore DA, Winzenberg TM, Ding C, Otahal P, Pelletier JP, Martel-Pelletier J, et al. The association between objectively measured physical activity and knee structural change using MRI. Ann Rheum Dis 2013;72:1170–5.

33. Callahan LF, Shreffler JH, Altpeter M, Schoster B, Hootman J, Houenou LO, et al. Evaluation of group and self-directed formats of the Arthritis Foundation's Walk With Ease Program. Arthritis Care Res (Hoboken) 2011;63:1098–107.

34. Talbot LA, Gaines JM, Huynh TN, Metter EJ. A home-based pedometer-driven walking program to increase physical activity in older adults with osteoarthritis of the knee: a preliminary study. J Am Geriatr Soc 2003;51:387–92.

AMERICAN COLLEGE
of RHEUMATOLOGY
Empowering Rheumatology Professionals

The Relationship of Pain Reduction With Prevention of Knee Replacement Under Dynamic Intervention Strategies

S. Reza Jafarzadeh,[1] (iD) Tuhina Neogi,[1] (iD) Daniel K. White,[2] (iD) and David T. Felson[1] (iD)

Objective. Knee replacement (KR) rates are increasing exponentially in the US and straining insurance budgets. This study was undertaken to investigate how many KRs would be prevented at different levels of pain improvement, a major target of osteoarthritis (OA) trials.

Methods. We used data from the Osteoarthritis Initiative (OAI) to emulate a trial of knee pain interventions on KR risk changes. We modeled hypothetical 1-, 2- or 3-unit reductions of the Western Ontario and McMaster Universities Osteoarthritis Index (WOMAC) pain subscale whenever a person reported a pain score of ≥5 (of 20) in an affected knee at any clinic visit. We used causal inference–based targeted learning to estimate treatment effects for hypothesized pain intervention strategies adjusted for time-dependent confounding. Sensitivity analyses assessed interventions at WOMAC pain scores of ≥4 and ≥7.

Results. Of the 9,592 knees studied (n = 4,796 participants; 58.5% female; baseline age 61.2 years), 40.7% experienced WOMAC pain scores of ≥5. The estimated knee-level (reference) risk of a KR, adjusted for loss to follow-up and death, was 6.3% (95% confidence interval 5.0, 7.7%) in the OAI. Reductions of WOMAC pain scores by 1, 2, or 3 units decreased the KR risk from 6.3% to 5.8%, 5.3%, and 4.9%, respectively. Larger reductions in KR risk were achieved when interventions were applied at a WOMAC pain score of ≥4.

Conclusion. Modest pain reductions from OA interventions would substantially reduce the number of KRs, with greater reductions achieved when pain decreased more and when interventions were introduced at lower pain levels.

INTRODUCTION

Rates of knee replacement (KR), which are primarily performed for osteoarthritis (OA) when medical and rehabilitative remedies fail, are rising in the US and worldwide (1,2). The Global Burden of Disease (GBD) reports OA as a leading cause of disability and the most common form of arthritis that affects ~91.2 million adults in the US (3). The rising rates of obesity and aging in the population will only exacerbate the need for a KR, which is expected to overwhelm the US health care system in the coming decades. Painful knee OA affects ~4.9% of the American population ages 26 and over and 16.7% of those ages 45 and above (4,5). Randomized trials testing the efficacy of OA treatments often consider pain improvement as the primary efficacy target

(6–10). It is uncertain, however, what amount of pain improvement would be needed to ultimately reduce the risk of a KR.

Studying the amount of pain reduction needed to affect KR rates through trials is problematic for a variety of reasons beyond the prohibitive sample size and costs of using KR as an outcome in trials. Trials often assess short-term interventions, and treatment assignment in trials is often based on a one-time randomization that does not allow treatment modification or switching in response to the observed course of a disease. This is especially problematic for the assessment of long-term interventions for conditions such as chronic knee pain in OA. Patient characteristics may change over time, violating the balance of confounders among intervention groups achieved with the initial randomization. Further, a substantial proportion of trial participants may

[1]S. Reza Jafarzadeh, DVM, MPVM, PhD, Tuhina Neogi, MD, PhD, David T. Felson, MD, MPH: Section of Rheumatology, Department of Medicine, Boston University School of Medicine, Boston, Massachusetts; [2]Daniel K. White, PT, ScD: Department of Physical Therapy, University of Delaware, Newark.

switch to another intervention strategy given a change in health status or disease progression.

One approach to addressing these challenges is through the use of a multistep sequential study that allows participants to be reassigned to a different treatment level or strategy as their health status changes over time (11). Observational studies are uniquely positioned to address the long-term assessment of dynamic intervention strategies for chronic or progressive conditions (12).

In this study, we used data from an observational cohort to examine whether a strategy that reduced pain when the knee pain of participants reached a certain threshold could reduce the risk of a KR and, if so, by how much. We did not examine one specific treatment but rather assessed intervention strategies that led to a prespecified reduction in pain. We used causal inference–based methods to provide an assessment of several long-term pain intervention strategies, in which hypothetical intervention decisions were tailored to a patient's evolving characteristics.

MATERIALS AND METHODS

Setting. We included data from the Osteoarthritis Initiative (OAI), a National Institutes of Health–sponsored multicenter longitudinal cohort of persons with or at risk of knee OA. The included OAI study visit data were from baseline, 12 months, 24 months, 36 months, 48 months, 72 months, and 96 months, which consisted of clinical, radiographic, and medication data.

Measurements. Our study outcome measure was defined as an incident KR (either total or partial) recorded in the OAI by medical reports or radiographic adjudication. Our study exposure that was used to define "hypothetical interventions" was based on knee pain quantified by the Western Ontario and McMaster Universities Osteoarthritis Index (WOMAC) pain subscale (13) at each visit. The term "intervention" in the context of our analytical method refers to any hypothetical treatment that reduces WOMAC pain (e.g., medication, physical activity, weight loss, etc.).

Covariates consisted of the following: demographic characteristics; body mass index; Kellgren/Lawrence grade (14); WOMAC stiffness and function scores; objective functional performance measures of chair stand time; 20- and 400-meter walk tests; malalignment; Charlson comorbidity index; Center for Epidemiologic Studies Depression scale (15); Physical Activity Scale for the Elderly score (16); knee injury, hip pain, or stiffness in the past 12 months; family history of a knee or a hip replacement; regular use of prescription nonsteroidal antiinflammatory drugs (NSAIDs) or cyclooxygenase 2 inhibitors in the past 12 months; and regular use of prescription opioids in the past 12 months. The regular use of a prescription pain medication for a given OAI study visit was determined based on the Medical Inventory Form, in which duration of use (up to 12 months prior to a given OAI study visit) and use frequency (i.e., regular versus as needed) were recorded.

Analytical approach. We summarized the study sample's baseline characteristics by frequencies for binary and categorical variables and by distribution summaries of continuous variables. We used the causal inference–based method of targeted learning (17,18) to estimate the effect of "following an intervention strategy" (19). Interventions were dynamic based on time-evolving patient characteristics (20). Specifically, at an examination in which an OAI participant's knee attained a pain score that triggered the intervention, the patient hypothetically received it. All knees in the OAI were included in the analyses. The intervention protocol was specified as hypothetical pain intervention strategies consisting of knee pain reduction by 1, 2, or 3 units on a 0–20 WOMAC pain subscale for an individual with a painful knee at a given OAI study visit (i.e., an intervention decision point). We chose these hypothetical levels of pain reduction for several reasons. The minimal clinically important difference or improvement for pain varies by the circumstances (e.g., KR versus medical treatment) and by study. For example, Angst et al (21) suggested values ~8–10% of the scale that corresponds to a reduction in pain of ≥2 in our study, which uses the 0–20 scale. Further, a KR would be unlikely to be carried out in those with low pain levels; thus, we implemented interventions whenever knee pain reached or exceeded a score of 5 (of 20).

Our initial goal was to estimate the risk of a KR based on observed WOMAC pain data without any hypothetical intervention, which we shall label the "reference risk." We then aimed to quantify how much this reference risk would have changed if we could hypothetically intervene and reduce WOMAC pain. Therefore, at each intervention decision point, an intervention could change according to a patient's knee pain level (Figure 1). Let us assume that an OAI participant presented with knee pain at ≥1 clinic visit. Our goal was to compare the participant's observed real-world outcome (i.e., KR risk) with the outcome if we had intervened to reduce knee pain (by any means such as pain medication, physical activity, weight loss, etc.) whenever
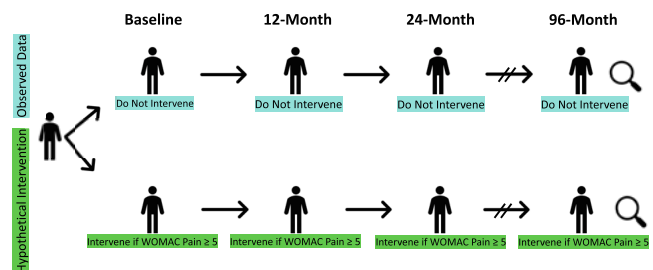
Figure 1. Schematic of the study design. The top row depicts observed data in which no (hypothetical) intervention was applied. The bottom row depicts the same knees, but hypothetical interventions were applied if knees experienced pain scores of ≥5 on the Western Ontario and McMaster Universities Osteoarthritis Index (WOMAC) subscale. The risk of knee replacement was compared between the hypothesized intervention strategy and observed data.

Table 1. Baseline patient characteristics of the OAI knee-level study data (n = 9,592 knees)*

Baseline characteristic	Mean
Age, years	61.2 ± 9.2
Female sex, no. (%)	5,608 (58.5)
Race, no. (%)	
White (Ref.)	7,580 (79.1)
African American	1,748 (18.2)
Asian	90 (0.9)
Other	164 (1.7)
Education level, no. (%)	
Less than high school graduate (Ref.)	336 (3.5)
High school graduate	1,214 (12.8)
Some college	2,292 (24.1)
College graduate	2,002 (21.1)
Some graduate school	794 (8.3)
Graduate degree	2,872 (30.2)
Income level, no. (%)	
<$10K (Ref.)	320 (3.6)
$10K to <$25K	908 (10.2)
$25K to <$50K	2,270 (25.6)
$50K to <$100K	3,220 (36.3)
≥$100K	2,150 (24.2)
Marital status, no. (%)	
Married (Ref.)	6,356 (66.8)
Widowed	768 (8.1)
Divorced	1,358 (14.3)
Separated	172 (1.8)
Never married	856 (9.0)
BMI, kg/m^2	28.62 ± 4.84
K/L grade, no. (%)	
0 (Ref.)	3,448 (38.5)
1	1,597 (17.8)
2	2,374 (26.5)
3	1,239 (13.8)
4	295 (3.3)
Alignment, no. (%)	
Neither (Ref.)	2,770 (29.7)
Varus	2,522 (27.1)
Valgus	4,026 (43.2)
Charlson comorbidity index	0.39 ± 0.84
WOMAC pain score	2.4 ± 3.3
WOMAC stiffness score	1.5 ± 1.7
WOMAC disability score	8.1 ± 11.0
Chair stand time, seconds†	11.55 ± 3.98
20-meter walk test, meter/second†	29.40 ± 4.05
400-meter walk time, seconds	307.06 ± 57.38
Total walked distance in 400-meter walk test, meters	397.79 ± 22.62
CES-D score	6.6 ± 7.0
PASE score	160.8 ± 82.5
History of a knee injury with walking difficulty for ≥2 days, no. (%)	2,584 (27.2)
Hip pain, aching, or stiffness in past 12 months, no. (%)	3,951 (41.3)
Family history of knee replacement, no. (%)	1,326 (14.0)
Family history of hip replacement, no. (%)	858 (9.1)
Regular user of prescription NSAIDs or COX-2 inhibitors in past 12 months, no. (%)	392 (4.1)
Regular prescription opioids use in past 12 months, no. (%)	22 (0.2)

* Except where indicated otherwise, values are the mean ± SD. OAI = Osteoarthritis Initiative; BMI = body mass index; K/L = Kellgren/Lawrence scale; WOMAC = Western Ontario and McMaster Universities Osteoarthritis Index; CES-D = Center for Epidemiologic Studies Depression scale; PASE = Physical Activity Scale for the Elderly; NSAIDs = nonsteroidal antiinflammatory drugs; COX-2 = cyclooxygenase 2.
† Average across 2 trials.

the knee pain level was ≥5 on the WOMAC subscale. In sensitivity analyses, we further tested intervention strategies in which a hypothetical pain intervention was triggered at WOMAC pain cutoff points of ≥4 and ≥7 to allow us to compare KR risk if we were to initiate or maintain knee pain interventions at lower or higher levels of pain.

Table 2. Knee-level distributions of time-varying exposure and frequencies of loss to follow-up and death across visits in the OAI cohort*

OAI visit	Knee pain WOMAC score, mean ± SD (median)		Loss to follow-up, no. participants	Death, no. participants
	All knees	Knees with WOMAC pain scores ≥5		
Baseline	2.4 ± 3.3 (1.0)	7.9 ± 2.9 (7.0)	N/A	N/A
12 months	2.1 ± 3.2 (1.0)	7.8 ± 2.8 (7.0)	0	16
24 months	2.1 ± 3.1 (1.0)	7.7 ± 2.8 (7.0)	125	24
36 months	2.1 ± 3.1 (1.0)	7.9 ± 2.9 (7.0)	104	30
48 months	2.1 ± 3.1 (1.0)	7.9 ± 2.9 (7.0)	116	21
72 months	2.2 ± 3.2 (1.0)	7.8 ± 2.9 (7.0)	420	65
96 months	N/A	N/A	176	76

* N/A = not applicable in this study due to time precedence of time-dependent confounders, time-varying exposure, and outcome (see Table 1 for other definitions).

Estimating the effect. Targeted learning (22,23) is a semi-parametric statistical method in which a potential misspecification of either the outcome model or the exposure-based model can still yield a consistent estimate of the treatment effect. In this regard, targeted learning (24) has advantages over traditional parametric regression–based models (25). Other strengths of targeted learning have been noted (26). We followed the method proposed by Díaz (27), in which we computed a statistical estimand, referred to as a longitudinal modified treatment policy, which relies on the observed value of an exposure (i.e., in the absence of an intervention) to measure treatment effect for an intervention strategy.

Targeted learning–based estimation of the treatment effect to reduce the risk of KR allowed us to adjust for both time-dependent confounding and selection bias due to informative censoring because of loss to follow-up or death in the OAI cohort. We considered the time sequence of exposure, outcome, and confounders across all OAI visits such that any intervention decision point was adjusted for the preceding confounders. Time-dependent confounding adjustment avoided the bias of adjusting for intermediate factors (28). Missing data were imputed using R's mice library (29), which implemented the multiple imputation by chained equations approach using a random forest algorithm (30).

Our analytical approach included several specific steps. We first calculated the risk of KR for a knee in the OAI cohort under a "no-intervention" strategy (i.e., the reference risk) in all knees regardless of pain score. If there was no loss to follow-up or death in the OAI cohort, the reference risk would have equaled the observed proportion of KR among all knees. By accounting for loss to follow-up and death, the reference risk for a KR in the OAI cohort was estimated using observed data without pain modification (i.e., no-intervention strategy).

In the second step of our analysis, we compared this reference risk of a KR with those under hypothetical intervention strategies of reducing pain to estimate the treatment effect. We adjusted for the following fixed confounders: sex, race, education, family history of knee or hip replacements, and income variables from baseline visit. For time-dependent confounding, adjustment at each study visit used the lagged-variables approach (31–33), in which measurements from the preceding visit (or from the current visit if the variable was defined based on an event before the current visit) were included. For example, at the 36-month visit, time-dependent confounding factors included NSAIDs and an opioid use variable from the 36-month visit, because it was ascertained by a questionnaire on pain medication use in the 12 months preceding the 36-month visit. This ensured that confounding measurements preceded the WOMAC pain assessment during

Table 3. Estimated knee-level risk of a KR in the OAI cohort under dynamic intervention strategies of pain reduction*

Pain intervention strategy†	Risk ratio (95% CI)	Absolute risk by following a strategy, % (95% CI)	Risk difference, % (95% CI)‡	No. KRs prevented by following a strategy§
1	0.91 (0.88, 0.95)	5.8 (4.5, 7.1)	0.6 (−0.8, −0.4)	55
2	0.84 (0.76, 0.92)	5.3 (3.8, 6.8)	1.0 (−1.6, −0.5)	101
3	0.77 (0.64, 0.92)	4.9 (2.7, 7.0)	1.5 (−2.4, −0.6)	142

* 95% CI = 95% confidence interval (see Table 1 for other definitions).
† Pain reduction by 1, 2, or 3 units on the WOMAC subscale whenever a knee pain score was ≥5.
‡ Reference risk = 6.3%.
§ Total number of knees = 9,592; total number of knee replacements (KRs) = 528.

the 36-month visit. We created 3 different models, one in which the strategy assumed a reduction of 1 WOMAC point when pain reached a score of ≥5, a second in which it assumed a reduction of 2, and a third in which it assumed a reduction of 3.

Finally, we calculated an E-value to quantify the potential effect of unmeasured or residual confounding on our estimated effect sizes ([34]). A large E-value suggests that it would be unlikely that an unknown or unmeasured factor could exist at a magnitude necessary to totally explain away (i.e., nullify) our estimated effect size.

RESULTS

The baseline characteristics of our study sample that included 9,592 knees from 4,796 OAI participants are summarized in Table [1]. The outcome of KR was observed in 5.5% of knees (528 of 9,592) after the baseline visit (i.e., no OAI participant had a KR at baseline). The reference risk of KR in the OAI (i.e., estimated mean population of KR outcome under a no-intervention strategy), after adjustment for loss to follow-up and death, was estimated to be 6.3% (95% confidence interval [95% CI] 5.0, 7.7%).

In the OAI, 40.8% of knees (3,911 of 9,592) experienced pain that reached or exceeded 5 on the WOMAC pain scale at ≥1 study visit (with a median of 2 study visits, mean 2.4 [range 1–6 visits]) during follow-up; thus, these knees were subject to hypothetical pain interventions. In total, there were 57,552 instances (i.e., intervention decision points), in which a knee in the OAI study sample was assessed for pain to see if it reached or exceeded the threshold (i.e., 5 of 20 on WOMAC pain subscale) that we set for the hypothetical intervention (i.e., 9,592 knees × 6 follow-up visits = 57,552). Of these, the knee pain level reached or exceeded 5 on the WOMAC scale in 9,509 instances (16.5%) across all visits; therefore, knee pain level was hypothetically reduced by 1, 2, or 3 WOMAC units in these instances. Table [2] presents distributions of WOMAC pain across our study sample's OAI visits for all knees and those with WOMAC pain scores of ≥5.

The risk of KR in the OAI using our strategies to reduce pain by 1, 2, or 3 WOMAC pain units in knees with a WOMAC pain score of ≥5 was reduced from 6.3% to 5.8%, 5.3%, and 4.9%, respectively. Estimated treatment effects corresponding to our estimands for pain reduction strategies of 1, 2, and 3 units on the WOMAC scale suggest a risk ratio of 0.91, 0.84, and 0.77, respectively. Table [3] presents the number of KRs that could have been prevented if OAI participants followed the corresponding intervention strategies, compared to observed data representing no modification in pain.

In sensitivity analyses, we investigated interventions triggered at WOMAC pain scores of ≥4 and ≥7. Findings were consistent with the primary analyses, except that larger reductions in KR risks were observed in strategies that triggered an intervention at a lower WOMAC pain level (i.e., WOMAC pain score ≥4)

(see Supplementary Table 1, on the *Arthritis & Rheumatology* website at https://onlinelibrary.wiley.com/doi/10.1002/art.42272).

Sensitivity analyses to estimate the strength of a potential unmeasured confounder needed to nullify our estimated risk ratios for the intervention strategies showed E-values of 1.42, 1.67, and 1.92 for pain reduction of 1, 2, and 3 units on the WOMAC scale, respectively. This means that, for example, using the strategy of reducing WOMAC pain by 1 unit, an unmeasured factor must have a minimum risk ratio of 1.42 beyond those already adjusted for in the analysis to nullify our estimated effect size of 0.91. This suggests that as pain reduction increases, substantial unmeasured confounding above and beyond confounders already adjusted for in our analyses would be needed for our estimated effect measure confidence intervals to include the null.

DISCUSSION

By testing hypothetical pain intervention strategies, we found that the absolute long-term risk of a KR decreased from 6.3% to ≥5.8% when pain interventions that actually reduced pain were applied as knee pain reached ≥5 on the WOMAC pain subscale (translating into 6 KRs avoided per 1,000 painful knees). As knee pain affects millions of Americans, and given the rising burden of KR in the US that is accompanied by growing obesity rates and an aging population, these findings suggest that developing long-term intervention strategies to successfully address chronic knee pain will have significant but modest public health and economic benefits.

Our study is the first to quantify the long-term expected risk of KR for a time-varying (i.e., dynamic) intervention trajectory. Approaches such as ours have been used for many conditions ([35–38]), especially in study settings that are impractical to implement through randomized trials, such as quantifying the multidecade-long risk of chronic conditions by modifiable lifestyle factors ([39]).

Our tested intervention strategies assumed a fixed reduction in pain severity. Our approach has parallels with the treat-to-target approach in rheumatoid arthritis. However, treatments are inconsistent in their effectiveness. While our analysis mandated a specific level of pain reduction, a similar average pain reduction would yield comparable results. Few studies have used WOMAC pain scores to quantify the effects of various interventions and have focused on similar levels of pain reduction. For example, a meta-analysis of high- versus low-intensity exercise on OA pain found that, compared to low-intensity exercise, there was a ~1-unit (point) reduction in WOMAC pain score in the high-intensity exercise group, but that effect diminished after 40 weeks ([40]). In a placebo-controlled tanezumab trial evaluating low doses of tanezumab, participants receiving the active treatment had an advantage over those receiving placebo and showed a reduction of 1 WOMAC pain unit ([41]). In another large trial of exercise versus education, the difference between groups

in WOMAC pain scores was 2.5 units (42). If treatments do not reduce pain by as much as our models assumed, there will be less reduction in KR risk.

Additionally, we studied reductions in the WOMAC score as a target of OA interventions, and our results suggest, as noted in Tubach et al (43), that absolute levels of knee pain at which interventions are triggered is as important as the extent of pain reduction to decrease KR risk. Specifically, our findings suggest that the same extent of pain reduction would diminish KR risk more effectively when triggered at a lower knee pain level, likely due to patients attaining lower absolute levels of pain.

Our study assessed the relation of long-term pain reduction to KR risk and tested a hypothetical intervention that reduced pain. Other studies have addressed specific interventions that target pain but have not demonstrated a decrease in KRs. For example, a study on long-term prescription analgesics such as NSAIDs, cyclooxygenase 2 inhibitors, acetaminophen, salicylates, and narcotics in the OAI cohort showed that analgesic use was associated with an increased risk of KR (44). The aforementioned study, however, did not adjust for time-dependent confounding and only compared those receiving analgesics at all time points to those who never received them (which included both nonpainful knees and painful knees). In contrast, in another study assessing the effects of prescription NSAIDs on OA progression in the OAI cohort, pain interventions resulted in a decreased rate of OA progression defined by joint space width reduction (45).

Our study cannot rule out the existence of residual confounding that may have biased our estimated effect measures. For example, there may be factors that affect both the receipt of a pain intervention and the decision to undergo KR. We implemented an analytical approach that enables time-dependent confounding adjustment by a comprehensive set of factors and also quantified the magnitude of extra potential confounding needed to nullify our estimated effect sizes. One advantage of our analytical approach is that it includes more participants and visits and evaluates real-world patterns of exposure to treatments, in contrast to models that only compare outcomes of patients who are assumed to be treated at all time points to those who are untreated during the entire study period. Few real-world patients would exist in these extreme levels of interventions across strata of evolving comorbidities. Our study did not focus on a specific pain remedy, and the findings are assumed to be broadly applicable to any intervention that reduces pain, which could be helpful in future randomized trials design that target OA pain by medications, exercise, weight loss (e.g., through bariatric surgery in extremely obese patients), or future treatments. Our results may be limited by the modest reduction in pain experienced by those with knee pain in the OAI cohort. If widely used intervention strategies produced larger reductions in pain, they would likely have reduced KR risks to a greater degree.

Approximately 20% of OAI participants were persons of Black, Asian, or other racial/ethnic backgrounds. There may be differences in perception, tolerance, or reporting of pain among different groups, or there may be disparities in KR therapy. The number of non-White participants in OAI was not large enough to allow us to generate race-specific estimates of pain intervention effects on KR risk; therefore, the findings may not be generalizable to other groups.

We note that pain improvement is not the only factor that can affect KR risk; for example, improvements in function may likely also impact KR risk. Further, the effect of pain improvement on KR risk may be mediated by function or other factors. We focused here on pain improvements as a proof-of-concept illustration of this type of study design and approach to address clinically relevant questions that are infeasible to address in traditional randomized trials.

In conclusion, KR rates are increasing, straining the capacity of the health care system as well as health care budgets. While trials of potential treatments for OA do not generally have a long enough follow-up period or sufficient size to evaluate the effect of pain reduction on KRs, our findings suggest that treatments with even modest reductions in pain commensurate with current treatments would substantially decrease KR rates. These data provide additional strong evidence that effective treatments for OA are critically needed.

AUTHOR CONTRIBUTIONS

REFERENCES

1. Losina E, Thornhill TS, Rome BN, Wright J, Katz JN. The dramatic increase in total knee replacement utilization rates in the United States cannot be fully explained by growth in population size and the obesity epidemic. J Bone Joint Surg Am 2012;94:201–7.

2. Ackerman IN, Bohensky MA, de Steiger R, Brand CA, Eskelinen A, Fenstad AM, et al. Substantial rise in the lifetime risk of primary total knee replacement surgery for osteoarthritis from 2003 to 2013: an international, population-level analysis. Osteoarthritis Cartilage 2017; 25:455–61.

3. Jafarzadeh SR, Felson DT. Updated estimates suggest a much higher prevalence of arthritis in United States adults than previous ones. Arthritis Rheumatol 2018;70:185–192.

4. Lawrence RC, Felson DT, Helmick CG, Arnold LM, Choi H, Deyo RA, et al. Estimates of the prevalence of arthritis and other rheumatic conditions in the United States: part II. Arthritis Rheum 2008;58:26–35.

5. Zhang Y, Jordan JM. Epidemiology of osteoarthritis. Clin Geriatr Med 2010;26:355–69.

6. Juhl C, Christensen R, Roos EM, Zhang W, Lund H. Impact of exercise type and dose on pain and disability in knee osteoarthritis: a systematic review and meta-regression analysis of randomized controlled trials. Arthritis Rheumatol 2014;66:622–36.

7. Fransen M, McConnell S, Harmer AR, Van der Esch M, Simic M, Bennell KL. Exercise for osteoarthritis of the knee: a Cochrane systematic review. Br J Sports Med 2015;49:1554–7.

8. Machado GC, Maher CG, Ferreira PH, Pinheiro MB, Lin C-WC, Day RO, et al. Efficacy and safety of paracetamol for spinal pain and osteoarthritis: systematic review and meta-analysis of randomised placebo controlled trials. BMJ 2015;350:h1225.

9. Liu X, Machado GC, Eyles JP, Ravi V, Hunter DJ. Dietary supplements for treating osteoarthritis: a systematic review and meta-analysis. Br J Sports Med 2018;52:167–75.

10. Megale RZ, Deveza LA, Blyth FM, Naganathan V, Ferreira PH, McLachlan AJ, et al. Efficacy and safety of oral and transdermal opioid analgesics for musculoskeletal pain in older adults: a systematic review of randomized, placebo-controlled trials. J Pain 2018;19:475.

11. Bembom O, van der Laan MJ. Statistical methods for analyzing sequentially randomized trials. J Natl Cancer Inst 2007;99:1577–82.

12. Bembom O, van der Laan MJ. Analyzing sequentially randomized trials based on causal effect models for realistic individualized treatment rules. Stat Med 2008;27:3689–716.

13. Bellamy N, Buchanan WW, Goldsmith CH, Campbell J, Stitt LW. Validation study of WOMAC: a health status instrument for measuring clinically important patient relevant outcomes to antirheumatic drug therapy in patients with osteoarthritis of the hip or knee. J Rheumatol 1988;15:1833–40.

14. Kellgren JH, Lawrence JS. Radiological assessment of osteo-arthrosis. Ann Rheum Dis 1957;16:494–502.

15. Radloff L. The CES-D Scale: a self-report depression scale for research in the general population. Appl Psychol Meas 1977;1: 385–401.

16. Washburn RA, Smith KW, Jette AM, Janney CA. The Physical Activity Scale for the Elderly (PASE): development and evaluation. J Clin Epidemiol 1993;46:153–62.

17. Van der Laan MJ, Rose S. Targeted learning: causal inference for observational and experimental data. New York: Springer New York; 2011. URL: http://link.springer.com/10.1007/978-1-4419-9782-1.

18. Van der Laan MJ, Rose S. Targeted learning in data science: causal inference for complex longitudinal studies. New York: Springer International Publishing; 2018. URL: www.springer.com/us/book/9783319653037.

19. Hernán MA, Robins JM. Per-protocol analyses of pragmatic trials. N Engl J Med 2017;377:1391–8.

20. Zhang Y, Young JG, Thamer M, Hernán MA. Comparing the effectiveness of dynamic treatment strategies using electronic health records: an application of the parametric g-formula to anemia management strategies. Health Serv Res 2018;53:1900–18.

21. Angst F, Benz T, Lehmann S, Aeschlimann A, Angst J. Multidimensional minimal clinically important differences in knee osteoarthritis after comprehensive rehabilitation: a prospective evaluation from the Bad Zurzach Osteoarthritis Study. RMD Open 2018;4:e000685.

22. Van der Laan MJ. Targeted maximum likelihood based causal inference: part I. Int J Biostat 2010;6:Article 2.

23. Van der Laan MJ. Targeted maximum likelihood based causal inference: part II. Int J Biostat 2010;6:Article 3.

24. Van der Laan MJ, Luedtke AR. Targeted learning of the mean outcome under an optimal dynamic treatment rule. J Causal Inference 2015;3:61–95.

25. Neugebauer R, Schmittdiel JA, van der Laan MJ. Targeted learning in real-world comparative effectiveness research with time-varying interventions. Stat Med 2014;33:2480–520.

26. Petersen ML, Porter KE, Gruber S, Wang Y, van der Laan MJ. Diagnosing and responding to violations in the positivity assumption. Stat Methods Med Res 2012;21:31–54.

27. Díaz I, Williams N, Hoffman KL, Schenck EJ. Nonparametric causal effects based on longitudinal modified treatment policies. J Am Stat Assoc 2021;0:1–16.

28. Cole SR, Platt RW, Schisterman EF, Chu H, Westreich D, Richardson D, et al. Illustrating bias due to conditioning on a collider. Int J Epidemiol 2010;39:417–20.

29. Buuren S. Flexible Imputation of Missing Data. London: Chapman and Hall/CRC; 2012. URL: http://www.crcnetbase.com/isbn/9781439868256#/doi/book/10.1201/b11826.

30. Shah AD, Bartlett JW, Carpenter J, Nicholas O, Hemingway H. Comparison of random forest and parametric imputation models for imputing missing data using MICE: a CALIBER study. Am J Epidemiol 2014;179:764–74.

31. Daniel RM, Cousens SN, De Stavola BL, Kenward MG, Sterne JA. Methods for dealing with time-dependent confounding. Stat Med 2013;32:1584–618.

32. Robins JM, Hernán MA. Estimation of the causal effects of time-varying exposures. In: Longitudinal Data Analysis. Chapman & Hall/CRC Handbooks of Modern Statistical Methods. London: Chapman and Hall/CRC; 2008:553–99. URL: http://www.crcnetbase.com/doi/abs/10.1201/9781420011579.ch23.

33. Mansournia MA, Naimi AI, Greenland S. The implications of using lagged and baseline exposure terms in longitudinal causal and regression models. Am J Epidemiol 2019;188:753–9.

34. Ding P, VanderWeele TJ. Sensitivity analysis without assumptions. Epidemiol Camb Mass 2016;27:368–77.

35. Danaei G, Rodríguez LA, Cantero OF, Logan R, Hernán MA. Observational data for comparative effectiveness research: an emulation of randomised trials of statins and primary prevention of coronary heart disease. Stat Methods Med Res 2013;22:70–96.

36. Danaei G, Rodríguez LA, Cantero OF, Hernán MA. Statins and risk of diabetes: an analysis of electronic medical records to evaluate possible bias due to differential survival. Diabetes Care 2013;36:1236–40.

37. Picciotto S, Chevrier J, Balmes J, Eisen EA. Hypothetical Interventions to limit metalworking fluid exposures and their effects on COPD mortality: g-estimation within a public health framework. Epidemiol Camb Mass 2014;25:436–43.

38. Mokhayeri Y, Hashemi-Nazari SS, Khodakarim S, Safiri S, Mansournia N, Mansournia MA, et al. Effects of hypothetical interventions on ischemic stroke using parametric g-formula. Stroke 2019;50: 3286–8.

39. Danaei G, Pan A, Hu FB, Hernan MA. Hypothetical midlife interventions in women and risk of type 2 diabetes. Epidemiol January 2013 2013;24:122–8.

40. Regnaux JP, Lefevre-Colau MM, Trinquart L, Nguyen C, Boutron I, Brosseau L, et al. High-intensity versus low-intensity physical activity or exercise in people with hip or knee osteoarthritis. Cochrane Database Syst Rev 2015:CD010203.

41. Schnitzer TJ, Easton R, Pang S, Levinson DJ, Pixton G, Viktrup L, et al. Effect of tanezumab on joint pain, physical function, and patient global assessment of osteoarthritis among patients with osteoarthritis of the hip or knee: a randomized clinical trial. JAMA 2019;322:37–48.

42. Bennell KL, Nelligan R, Dobson F, Rini C, Keefe F, Kasza J, et al. Effectiveness of an internet-delivered exercise and pain-coping skills training intervention for persons with chronic knee pain: a randomized trial. Ann Intern Med 2017;166:453–62.

43. Tubach F, Ravaud P, Baron G, Falissard B, Logeart I, Bellamy N, et al. Evaluation of clinically relevant states in patient reported outcomes in knee and hip osteoarthritis: the patient acceptable symptom state. Ann Rheum Dis 2005;64:34–37.

44. Hafezi-Nejad N, Guermazi A, Roemer FW, Eng J, Zikria B, Demehri S. Long term use of analgesics and risk of osteoarthritis progressions and knee replacement: propensity score matched cohort analysis of data from the Osteoarthritis Initiative. Osteoarthritis Cartilage 2016; 24:597–604.

45. Lapane KL, Yang S, Driban JB, Liu SH, Dubé CE, McAlindon TE, et al. Effects of prescription nonsteroidal antiinflammatory drugs on symptoms and disease progression among patients with knee osteoarthritis. Arthritis Rheumatol 2015;67: 724–32.

Clinical images: Huriez syndrome, a rare scleroderma mimic

The patient, a 34-year-old woman, presented with symptoms of tightness in the fingers and the bilateral upper and lower limbs, which she had experienced since childhood. The patient stated that redness occurred first, followed by puffiness in her fingers and then progressive tightening of the skin over the hands and feet. She noticed progressive discoloration of her palm and sole and skin thickening and then desquamation with fissuring over the palmoplantar surface. The patient had a strong family history of similar illness, including 1 brother, 4 of 6 sisters, and her mother, who died in early adulthood. She had no history suggestive of Raynaud's phenomenon, oral ulcers, photosensitivity, arthritis, or myositis. Skin tightening or darkening was not evident elsewhere on her body. On clinical examination, she was noted to have scleroatrophy with fissuring of palms (**A**), shortened digits with multiple contractures in the fingers (**B**), bilateral symmetric clubbing (**C**), and depigmented thickened skin over the palms and soles (**D**) with surrounding hyperpigmented areas without any nail changes. Sweating was preserved in the palms and soles. Results of systemic examination were unremarkable. Radiograph of the hands showed acro-osteolysis with osteopenia. Autoimmune profile and hormone studies were normal. Genetic analysis was not easily available; however, based on the predominance of these symptoms in the patient's family and the patient's clinical profile, a diagnosis of Huriez syndrome was made. She was started on topical keratolytic agents and counseled regarding prognosis. Huriez syndrome is an autosomal-dominant genodermatosis characterized by scleroatrophy of the palms and soles, palmoplantar keratoderma, and hypoplastic nails. It can mimic scleroderma, as both sclerodactyly and acro-osteolysis are evident, but absence of Raynaud's phenomenon is the key feature. Early-onset squamous cell carcinoma in the scleroatrophic area is the most dreaded complication (1) but was not observed in the patient. Recent studies on families with Huriez syndrome showed heterozygous mutation in the *SMARCAD1* gene with a phenotype overlapping with that of Basan syndrome and isolated adermatoglyphia (2).

Author disclosures are available at https://onlinelibrary.wiley.com/action/downloadSupplement?doi=10.1002%2Fart.42242&file=art42242-sup-0001-Disclosureform.pdf.

1. Hamm H, Traupe H, Bröcker EB, Schubert H, Kolde G. The scleroatrophic syndrome of Huriez: a cancer-prone genodermatosis. Br J Dermatol 1996;134:512–8.

2. Loh AY, Špoljar S, Neo GY, Escande-Beillard N, Leushacke M, Luijten MN, et al. Huriez syndrome: additional pathogenic variants supporting allelism to SMARCAD syndrome. Am J Med Genet A 2022;188: 1752–60.

Sayan Mukherjee, MD [ID]
drsayanmukherjee90@gmail.com
Mukesh K. Maurya, MD
Puneet Kumar, MD
Department of Clinical Immunology and Rheumatology
King George Medical University
Lucknow, India

AMERICAN COLLEGE
of RHEUMATOLOGY
Empowering Rheumatology Professionals

Dynamics of Methylation of CpG Sites Associated With Systemic Lupus Erythematosus Subtypes in a Longitudinal Cohort

Cristina M. Lanata,[1] Joanne Nititham,[1] Kimberly E. Taylor,[2] Olivia Solomon,[3] Sharon A. Chung,[2] Ashira Blazer,[4] Laura Trupin,[2] Patricia Katz,[2] Maria Dall'Era,[2] Jinoos Yazdany,[2] Marina Sirota,[2] Lisa F. Barcellos,[3] and Lindsey A. Criswell[1]

Objective. Findings from cross-sectional studies have revealed associations between DNA methylation and systemic lupus erythematosus (SLE) outcomes. This study was undertaken to investigate the dynamics of DNA methylation by examining participants from an SLE longitudinal cohort using samples collected at 2 time points.

Methods. A total of 101 participants from the California Lupus Epidemiology Study were included in our analysis. DNA was extracted from blood samples collected at the time of enrolment in the cohort and samples collected after 2 years and was analyzed using Illumina EPIC BeadChip kit. Paired *t*-tests were used to identify genome-wide changes which included 256 CpG sites previously found to be associated with SLE subtypes. Linear mixed models were developed to understand the relationship between DNA methylation and disease activity, medication use, and sample cell-type proportions, adjusted for age, sex, and genetic principal components.

Results. The majority of CpGs that were previously determined to be associated with SLE subtypes remained stable over 2 years (185 CpGs [72.3%]; *t*-test false discovery rate >0.05). Compared to background genome-wide methylation, there was an enrichment of SLE subtype–associated CpGs that changed over time (27.7% versus 0.34%). Changes in cell-type proportions were associated with changes at 67 CpGs ($P < 2.70 \times 10^{-5}$), and 15 CpGs had at least 1 significant association with immunosuppressant use.

Conclusion. In this longitudinal SLE cohort, we identified a subset of SLE subtype–associated CpGs that remained stable over time and may be useful as biomarkers of disease subtypes. Another subset of SLE subtype–associated CpGs changed at a higher proportion compared to the genome-wide methylome. Additional studies are needed to understand the etiology and impact of these changes on methylation of SLE-associated CpGs.

INTRODUCTION

Systemic lupus erythematosus (SLE) is a heterogeneous autoimmune disease that affects 1 in 600 women in the US, and it is among the leading causes of death in young women, despite modern treatments (1,2). Prior studies suggest that epigenetics informs SLE disease heterogeneity and pathophysiology. Epigenetics is the study of chromatin modifications,

including DNA methylation, that regulate gene expression and cell differentiation (3). Changes in methylation of CpG sites within interferon-responsive genes and regulatory regions of the genome and in different immune cell types are associated with SLE risk, disease activity, and specific organ manifestations such as lupus nephritis (4–9). However, causality of these associations cannot be determined given the cross-sectional nature of previous studies. Furthermore, the stability of CpG

methylation changes and the prognostic implications for long-term outcomes remain unclear.

There are many challenges in treating SLE, and there is a lack of available biomarkers that can be used to accurately predict clinical outcomes and response to treatment. DNA methylation in whole blood samples is an attractive biomarker, as samples can be easily obtained and do not require the isolation of peripheral blood mononuclear cells (PBMCs) or cell sorting. Thus, whole blood DNA methylation has potential to be easily applied in clinical practice as a tool for precision medicine. Therefore, understanding the longitudinal stability and variability of the methylome in SLE patients is fundamental to its utility as a biomarker.

In this study, we investigated the longitudinal trajectory of DNA methylation in whole blood samples from a diverse multiethnic cohort of SLE patients followed up for over 2 years. We had previously performed an epigenome-wide association study (EWAS) of all participants from the California Lupus Epidemiology Study (CLUES) at cohort enrolment (10). We identified 3 patient subtypes at enrolment in the cohort according to American College of Rheumatology (ACR) classification criteria and subcriteria (11,12). We classified the patients as mild (M), severe 1 (S1), and severe 2 (S2) according to autoantibody pattern and internal organ involvement and identified 256 CpGs that were significantly associated with these subtypes, many of which mapped to the interferon pathway.

Here, we examined the dynamics of this previously described DNA methylation signature as well as the genome-wide longitudinal trajectory of the methylome in participants from the CLUES cohort (n = 101). We studied the impact of disease activity, medication use, cell-type proportions, genetic variation, and self-reported ethnicity and race on changes in methylation at CpG sites.

PATIENTS AND METHODS

Subjects. CLUES is a multiracial and multiethnic cohort of individuals with physician-confirmed SLE. This study was approved by the Institutional Review Board of the University of California, San Francisco. Written informed consent was obtained from all patients prior to participation in the study. Participants were recruited from the California Lupus Surveillance Project, a population-based cohort of individuals with SLE living in the County of San Francisco from 2007 to 2009 (13). Additional participants residing in the geographic region were recruited through local academic and community rheumatology clinics and through existing local research cohorts. This study included a subset of 101 CLUES participants from the following self-reported races and ethnicities: White (n = 29), Black (n = 13), Asian (n = 34), Hispanic (n = 22), and other or unspecified (n = 3). Clinical and demographic characteristics are shown in Supplementary Table 1 (available on the *Arthritis & Rheumatology* website at http://onlinelibrary.wiley.com/doi/10.1002/art.42237).

Study procedures involved an in-person research clinic visit every 2 years including the collection and review of medical records prior to each visit, a history of SLE and physical examination conducted by a physician specializing in lupus, collection of biologic specimens including peripheral blood samples for clinical and research purposes, and completion of a structured interview administered by an experienced research assistant. For the 101 participants, the mean ± SD time between visits was 2.3 ± 0.3 years. All SLE diagnoses were confirmed by study physicians (CML, MD, and JY) according to 1 of the following definitions: 1) meeting ≥4 of 11 ACR revised criteria for the classification of SLE as defined in 1982 (11) and updated in 1997 (12), 2) meeting 3 of 11 ACR criteria and having a documented rheumatologist's diagnosis of SLE, or 3) a rheumatologist-confirmed diagnosis of lupus nephritis, defined as having evidence of lupus nephritis on kidney biopsy. Medication use at the time of blood collection was recorded. For data analyses, we grouped immunosuppressive medications into the following categories: biologic treatments (belimumab, abatacept, rituximab), low-dose prednisone (<10 mg), moderate or high-dose prednisone (>10 mg), antimalarials, calcineurin inhibitors, methotrexate and leflunomide, azathioprine, mycophenolate mofetil, and cyclophosphamide. Self-reported race and ethnicity data was collected from each study participant.

DNA methylation and quality control. Methylation of genomic DNA from whole blood samples was profiled using an Illumina Methylation EPIC BeadChip kit. This chip kit assesses the methylation level of ~850,000 CpGs in enhancer regions, gene bodies, promoters, and CpG islands. All subsequent processing was conducted using the R minfi package. Signal intensities were background subtracted using the minfi noob function and were then quantile normalized (14,15). We removed sites with a poor detection rate ($P > 0.05$) in more than 5% of the samples (1,746 CpG sites). We removed sites where probes were predicted to hybridize to multiple loci (44,097) and sites on nonautosomal chromosomes (19,627 CpG sites). We also excluded 91,799 CpGs that have been shown to poorly perform due to single-nucleotide polymorphisms (SNPs) near probes in diverse populations (16). Additionally, we removed 3,413 CpGs where the assay control sample had a variance >0.01 across the 9 plates. After implementing these quality control measures, 720,682 CpGs were included in the analysis.

DNA genotyping. Genotyping of genomic DNA from blood samples was performed using Affymetrix Axiom Genome-Wide LAT 1 Array. This genotyping array is composed of 817,810 SNP markers across the genome and was specifically designed to provide maximal coverage of diverse racial and ethnic populations, including West Africans, Europeans, and American Indians (17). Samples were retained with Dish QC ≥0.82. SNP genotypes were first filtered for high-quality cluster differentiation and 95% call rate within batches using SNPolisher. Additional quality

control was performed using Plink. SNPs with an overall call rate <95% or discordant calls in duplicate samples were removed. Samples were excluded if there were unexpected duplicates in identity by descent analysis or if the sex was mismatched between genetic data and self report; 1 sample was retained for first-degree relatives. All samples had at least 95% genotyping and no evidence of excess heterozygosity (maximum <2.5*SD). We tested for Hardy-Weinberg equilibrium and cross-batch association for batch effects using a subset of subjects that were of European ancestry and were negative for double-stranded DNA (dsDNA) antibodies and renal disease to minimize genetic heterogeneity. SNPs were excluded if Hardy-Weinberg equilibrium $P < 1 \times 10^{-5}$ or any cross-batch association $P < 5 \times 10^{-8}$. Genetic principal components were calculated to account for population structure using PCAmixdata R package.

Genetic ancestry. We performed ADMIXTURE ([18]) analysis using genome-wide SNP data to estimate the percent contribution of each ancestral population for each participant in the study. We first combined our sample data with 1000 Genomes genotype data and removed SNPs for linkage disequilibrium

according to software recommendations, excluding each SNP with an $R^2 > 0.1$ in a 50-SNP sliding window advanced by 10 SNPs each time. After exclusion, 162,159 SNPs were used to estimate global ancestry. We then ran ADMIXTURE unsupervised assuming 5 subpopulations (European, African, East Asian, South Asian, and American Indian). We then used labels from 1000 Genomes to determine the ancestry of the estimated proportions of each of our subjects for downstream analysis.

Differential methylation analysis. Our analysis pipeline is shown in Figure 1. Samples from different time points were quantile normalized together. Principal components analysis plots between different time points, plates, and race and ethnicities are shown (Supplementary Figures 1–3, http://onlinelibrary.wiley.com/doi/10.1002/art.42237). Significance testing was performed using M values, with effect sizes converted to beta values for reporting. To adjust for differences between plates, we used ComBat ([19]). We adjusted the beta values with residual values for estimated cell-type proportions using the reference-based Houseman algorithm to account for cell-type proportion heterogeneity ([20,21]). We initially performed a genome-wide paired

The California Lupus Epidemiology Study (CLUES)
Racially and ethnically diverse longitudinal cohort of over 332 deeply phenotyped SLE patients with DNA methylation at cohort enrollment

101 patients were selected from the CLUES cohort

DNA methylation on whole blood at cohort enrollment and at a 2 year follow up

Quality Control: Total CpGs retained for analysis =720,682

Adjusted matrix with residuals for cell proportions

Unadjusted matrix

Paired t-test between DNA methylation at each time point
Significant CpGs selected: FDR<0.05 and |β|>0.03

Examined significant CpGs from paired t-test

Significant CpGs that changed over time were examined in repeated measures mixed linear models adjusting for age, genetic PCs and sex to explore the effects of:
a) SLEDAI score, dsDNA positivity and lupus nephritis
b) medications

glm models with change in methylation as a function of change in cell proportions, adjusting for age, sex and genetic PCs

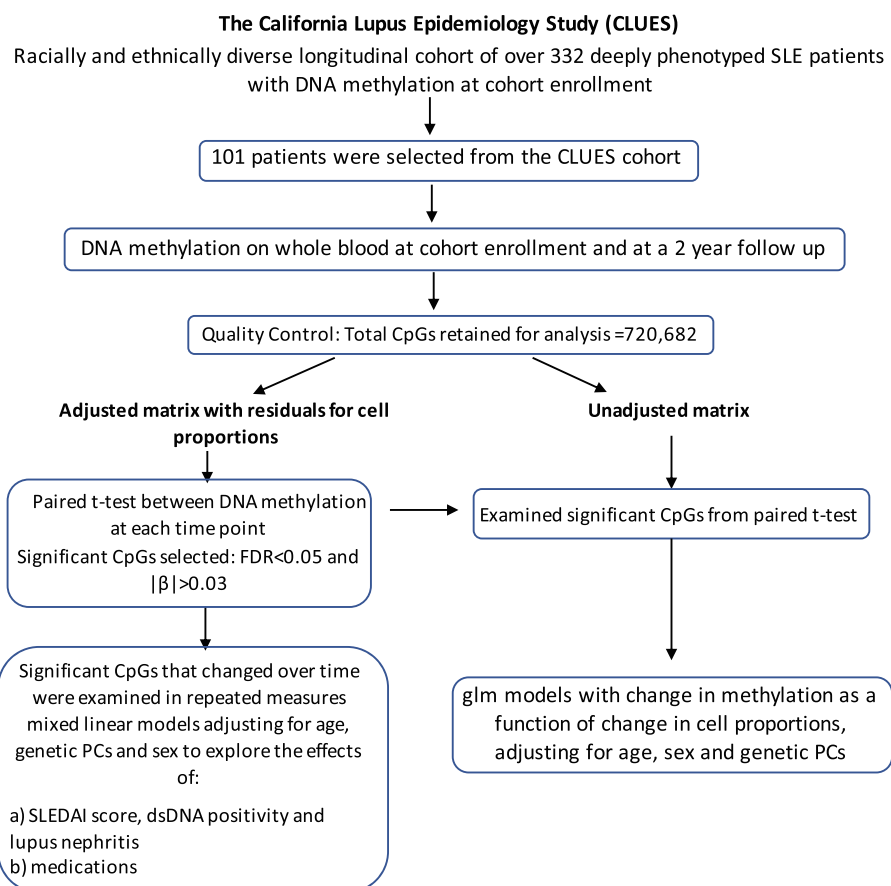**Figure 1.** Analysis pipeline of our study of 101 participants from the CLUES study. SLE = systemic lupus erythematosus; FDR = false discovery rate; PCs = principal components; SLEDAI = Systemic Lupus Erythematosus Disease Activity Index; dsDNA = double-stranded DNA; glm = generalized linear model. Color figure can be viewed in the online issue, which is available at http://onlinelibrary.wiley.com/doi/10.1002/art.42237/abstract.

t-test of the 2 time points and retained CpG sites that had a false discovery rate (FDR) $P < 0.05$ and an absolute beta value difference of >0.03, as a threshold for an effect size to be biologically meaningful (22).

We then took a closer look at the previously described SLE subtype–associated CpGs within the genome-wide results. We constructed linear mixed models to analyze repeated measurements with DNA methylation as the outcome to investigate the effect of disease activity, dsDNA titer at the time of blood was drawn, lupus nephritis status, and medication use adjusted for sex, age, and genetic principal components (principal components 1–3). To examine the role of cell-type proportion heterogeneity, significant CpGs from the paired *t*-tests were reanalyzed without adjusting for cell-type proportions. Changes in DNA methylation was modeled with the change in each cell-type proportion as a predictor, adjusting for sex, age, and genetic principal components (principal components 1–3). All association analyses were performed using R version 3.6 and Stata 13.1. Pathway analysis was performed using ToppFun (23).

SLE subtype–associated CpGs enrichment analysis. Enrichment of SLE subtype–associated CpGs in CpGs with a significant change over time was determined via the following methods. Briefly, we determined the methylation variance of the 256 CpGs that were associated with SLE subtypes at cohort enrolment. Then, randomly selected 256 CpG sites with similar methylation variance distribution compared to SLE subtype–associated CpGs throughout the genome were tested to see if there was any difference in methylation at the 2 time points (paired *t*-test). We tested this for a total of 100 random samples. Results were compared to CpGs associated with SLE subtypes.

Statistical methylation quantitative trait loci (QTLs) analysis. We previously reported methylation QTL analysis findings on SLE subtype–associated CpGs at the time of enrolment in the cohort (10). Briefly, this was performed by fitting a linear model adjusted for sex, age, cell-type proportions, alcohol use, smoking status, the top 3 genetic principal components, and the top 3 medication principal components using the Matrix eQTL R package (24). There are also larger established data sets of CpGs in healthy individuals that provide evidence of genetic control (25). Combining our own findings and available resources, we identified a total of 39,899 CpGs with evidence of methylation QTL within the Illumina Methylation EPIC BeadChip kit that passed our quality control. We used a 2-sample test to see if the proportion of methylation QTLs in CpGs that had a significant change over time was higher than the proportion of methylation QTLs in stable CpGs.

Table 1. Selected candidate CpGs that were stable over time and had the greatest difference in methylation between SLE clinical subtypes at the time of enrollment in the CLUES cohort*

| CpG | Gene | CpG position | Mean methylation beta values at enrollment, by cluster | | | Variance‡ | IFNα-responsive gene | IFNγ-responsive gene |
			Mild†	Severe 1†	Severe 2†			
cg16987437	SP100	Body	0.623	0.536	0.481	0.0178	No	No
cg15065340	TNK2	5′-UTR	0.623	0.555	0.499	0.0152	No	No
cg19188021	ODF3B	5′-UTR	0.264	0.174	0.142	0.0142	No	No
cg17114584	IRF7	Body	0.513	0.451	0.399	0.0137	Yes	Yes
cg22012079	IFI44L	5′-UTR	0.586	0.501	0.462	0.0126	Yes	Yes
cg12461141	TRIM22	TSS1500	0.493	0.423	0.380	0.0115	No	No
cg14333162	RSAD2	TSS1500	0.698	0.647	0.602	0.0092	Yes	Yes
cg26531432	RABGAP1L	5′-UTR	0.698	0.634	0.605	0.0087	No	No
cg20343278	PTPRM	Body	0.323	0.361	0.304	0.0087	No	No
cg03540917	SPINK2	Body	0.599	0.627	0.669	0.0086	No	No
cg15378061	NA	NA	0.186	0.231	0.257	0.0084	No	No
cg15331332	HLA-F	Body	0.599	0.568	0.538	0.0081	No	No
cg00272009	PARP14	TSS1500	0.631	0.581	0.552	0.0080	Yes	Yes
cg25178683	LGALS3BP	TSS1500	0.554	0.509	0.470	0.0077	Yes	Yes
cg13045500	NA	NA	0.659	0.604	0.569	0.0072	No	No
cg06168856	OAS1	Body	0.630	0.598	0.575	0.0067	Yes	No
cg05167074	SHKBP1	Body	0.555	0.511	0.489	0.0067	No	No
cg06708931	NA	NA	0.906	0.867	0.828	0.0064	No	No
cg06650861	DDX60	5′-UTR	0.868	0.830	0.792	0.0064	Yes	Yes
cg06376949	IFIT5	TSS1500	0.255	0.210	0.177	0.0063	No	No

* Mean methylation beta values at the time of enrollment were compared by paired *t*-test, with a false discovery rate of >0.05. Cohort participants were clustered according to American College of Rheumatology systemic lupus erythematosus (SLE) classification criteria and subcriteria (11,12) using an unsupervised clustering approach (10). CLUES = California Lupus Epidemiology Study; IFN = interferon; UTR = untranslated region; TSS = transcription start site; NA = not applicable.
† Patients were classified as mild, severe 1, and severe 2 according to autoantibody pattern and internal organ involvement.
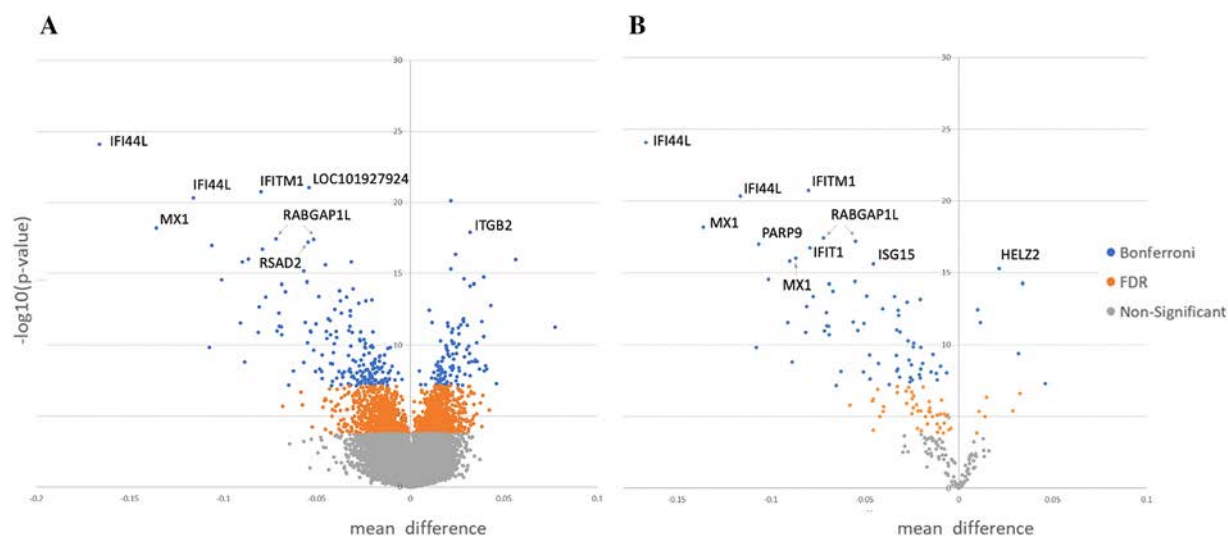‡ By analysis of variance F test.

Figure 2. **A**, Systemic lupus erythematosus (SLE) subtype–associated CpGs with a significant change in methylation over the 2 time points. **B**, Methylation levels of 2,423 CpGs across the genome that significantly changed over a period of 2 years (0.34% of the represented methylome). Symbols represent individual samples. FDR = false discovery rate.
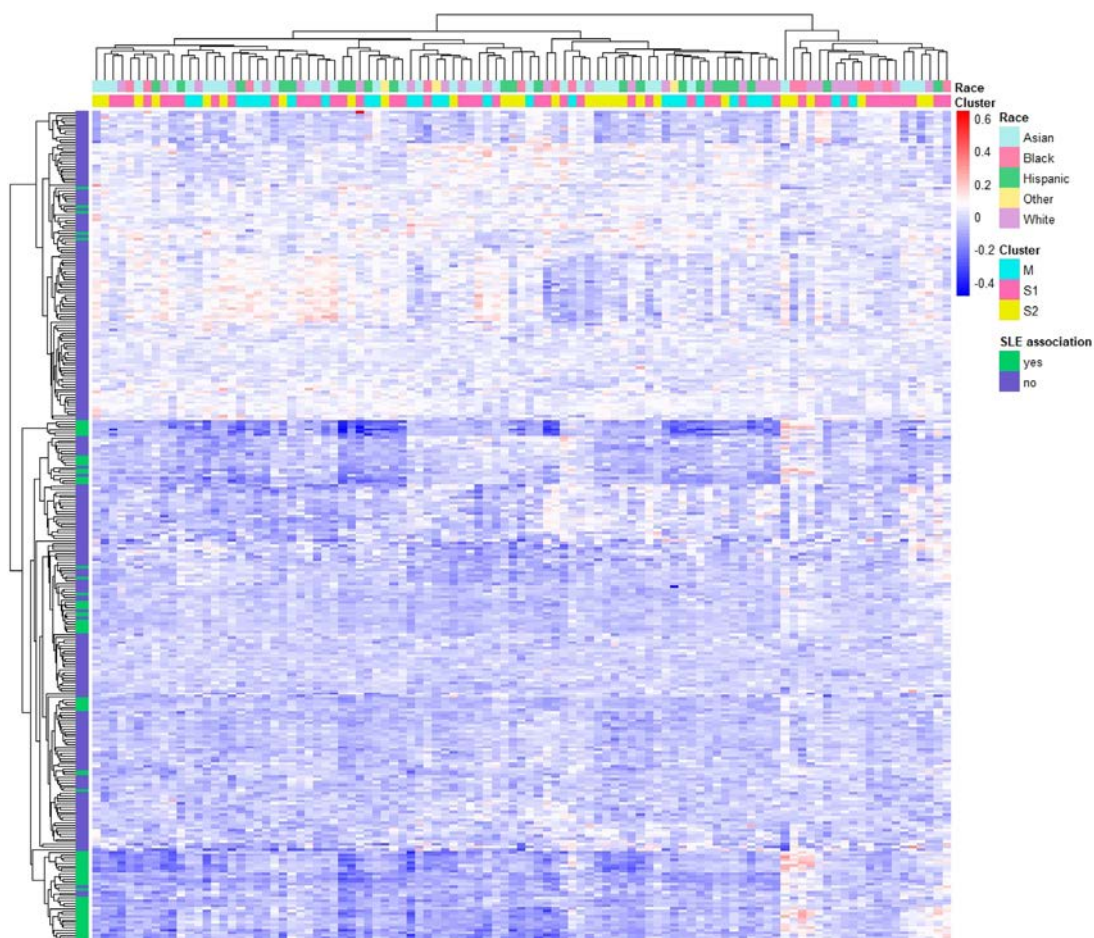

Figure 3. Heat map of CpG sites with a significant methylation change in a 2 year period. We observed 309 CpGs with a DNA methylation difference (absolute beta value difference >0.03, false disovery rate <0.05) in a 2-year time period. Each row represents a CpG and each column represents a participant with systemic lupus erythematosus (SLE).

Table 2. Top 20 CpGs whose methylation significantly changed over a 2-year time period among SLE patients in the CLUES cohort*

CpG	Gene	Mean methylation beta values, time point 1 to time point 2				Paired t-test	
		Time point 1	Time point 2	Delta	Fold change	P	FDR
cg13452062	IFI44L†	0.31	0.14	0.17	–1.17	8×10^{-25}	5.97×10^{-19}
cg07929412	LOC101927924	0.75	0.70	0.05	–0.08	9×10^{-22}	3.33×10^{-16}
cg23570810	IFITM1†	0.49	0.41	0.08	–0.20	2×10^{-21}	4.32×10^{-16}
cg05696877	IFI44L†	0.31	0.19	0.12	–0.60	5×10^{-21}	8.45×10^{-16}
cg21549285	MX1†	0.40	0.26	0.14	–0.52	7×10^{-19}	7.94×10^{-14}
cg14628347	ITGB2	0.63	0.67	0.03	0.05	1×10^{-18}	1.33×10^{-13}
cg25984164	RABGAP1L†	0.71	0.63	0.07	–0.11	4×10^{-18}	3.29×10^{-13}
cg10549986	RSAD2	0.15	0.10	0.05	–0.51	4×10^{-18}	3.29×10^{-13}
cg09948374	RABGAP1L†	0.60	0.55	0.05	–0.10	6×10^{-18}	4.65×10^{-13}
cg07815522	PARP9†	0.45	0.34	0.11	–0.31	1×10^{-17}	6.88×10^{-13}
cg05552874	IFIT1†	0.40	0.32	0.08	–0.25	2×10^{-17}	1.14×10^{-12}
cg22862003	MX1†	0.41	0.33	0.09	–0.27	1×10^{-16}	5.06×10^{-12}
cg18467790	RADIL	0.52	0.58	0.06	0.10	1×10^{-16}	5.06×10^{-12}
cg16526047	ISG15	0.49	0.46	0.03	–0.07	2×10^{-16}	6.43×10^{-12}
cg24678928	DDX60†	0.70	0.61	0.09	–0.15	2×10^{-16}	6.43×10^{-12}
cg20062691	ISG15†	0.66	0.62	0.05	–0.07	3×10^{-16}	1.01×10^{-11}
cg07469075	PAMR1	0.58	0.52	0.06	–0.11	7×10^{-16}	2.44×10^{-11}
cg11317199	TRIM14	0.59	0.63	0.04	0.06	2×10^{-15}	5.99×10^{-11}
cg08565796	HKR1	0.32	0.35	0.03	0.08	2×10^{-15}	8.09×10^{-11}
cg12439472	EPSTI1†	0.31	0.21	0.10	–0.48	3×10^{-15}	8.94×10^{-11}
cg05883128	DDX60†	0.33	0.27	0.06	–0.20	4×10^{-15}	1.19×10^{-10}
cg13100600	AGRN†	0.51	0.54	0.03	0.06	5×10^{-15}	1.52×10^{-10}
cg07839457	NLRC5†	0.24	0.17	0.07	–0.40	6×10^{-15}	1.56×10^{-10}
cg25267487	NA	0.67	0.71	0.03	0.05	7×10^{-15}	1.86×10^{-10}
cg13207212	APBB2	0.56	0.52	0.03	–0.06	1×10^{-14}	2.81×10^{-10}

* For the full list of 309 CpGs, see Supplementary Table 3, available on the *Arthritis & Rheumatology* website at http://onlinelibrary.wiley.com/doi/10.1002/art.42237. CLUES = California Lupus Epidemiology Study; FDR = false discovery rate; NA = not applicable.
† CpGs were associated with systemic lupus erythematosus (SLE) subtypes at the time of enrollment in the cohort.

RESULTS

Stability of the majority of SLE subtype–associated CpGs over time. In previous studies, CLUES cohort participants were clustered into 3 subtypes according to ACR classification criteria at the time of enrolment in the cohort. We identified 256 CpGs that were differentially methylated according to subtype (10).

In the current study, we observed the dynamics of DNA methylation in our previous findings by comparing data collected at 2 time points. Of the 256 CpGs that were associated with disease subtypes, 184 CpGs (71.9%) were stable between the 2 time points. Since we observed an enrichment of CpGs in interferon (IFN)–responsive genes in 256 CpGs, we investigated whether there was a difference in terms of dynamics between CpGs in IFN-responsive genes compared to non–IFN-responsive genes. We found that 53% of CpGs in IFN-responsive genes were stable compared to 87% of CpGs in non–IFN-responsive genes ($P = 1.4 \times 10^{-9}$ by chi-square test), indicating that CpGs in IFN-responsive genes are more susceptible to change in methylation. Regarding CpG position relative to genes, 74 were in gene bodies (40.2%), 50 were in transcription start sites (27.2%), and 30 were in untranslated regions (16.3%). Twenty CpGs with the most variance across clinical clusters (10) that did not change over time are shown in Table 1, and the full list of stable CpGs is shown in Supplementary Table 2 (http://onlinelibrary.wiley.com/doi/10.1002/art.42237).

These include CpGs in *TNK2, RABGAP1L, IRF7, IFI44L, TRIM22*, and many IFN-responsive genes. DNA methylation within/near these genes has been implicated in SLE in previous studies; for example *TNK2* has been implicated in renal disease in CD4+ naive cells (4) and *RABGAP1L* has been implicated with anti-dsDNA antibody production. Volcano plots of representative stable CpGs are shown in Supplementary Figure 4 (http://onlinelibrary.wiley.com/doi/10.1002/art.42237).

SLE subtype–associated CpGs compared to the genome-wide methylome over time. Although the majority of SLE subtype–associated CpGs were stable, 71 CpGs (27.7%) had a significant change in methylation (>0.03) (FDR $P < 0.05$) (Figure 2A). We also examined the dynamics of the genome-wide methylome. Paired t-test analysis revealed that the methylation level of 2,423 CpGs across the genome significantly changed over a period of 2 years (FDR <0.05), which is 0.34% of the represented methylome (Figure 2B). We also

Table 3. Pathway analysis of 309 CpG sites that showed significant methylation changes (FDR <0.05) and an absolute methylation beta value difference of >0.03 over 2 years in the CLUES cohort*

CpG site identifier	Pathway name	P	FDR†	No. of genes from input	No. of genes in annotation
M39748	Human immune response to tuberculosis	2.82×10^{-8}	1.70×10^{-5}	6	23
M39583	Novel intracellular components of RLR pathway	1.20×10^{-5}	3.60×10^{-3}	6	61
M1462	CTL-mediated immune response against target cells	1.59×10^{-4}	0.023	3	13
M39909	Host–pathogen interaction of human coronaviruses–IFN induction	1.64×10^{-4}	0.023	4	33
M22023	Antigen processing and presentation	2.01×10^{-4}	0.023	3	14
M39363	Type II IFN signaling (*IFNG*)	2.58×10^{-4}	0.023	4	37
M40067	SARS–CoV-2 innate immunity evasion and cell-specific immune response	2.68×10^{-4}	0.023	5	68
M15913	RLR signaling pathway	3.28×10^{-4}	0.024	5	71
M39837	Cytosolic DNA-sensing pathway	3.98×10^{-4}	0.025	5	74
MAP00430‡	MAP00430 taurine and hypotaurine metabolism	4.22×10^{-4}	0.025	2	4
M19708	Type II diabetes mellitus	6.53×10^{-4}	0.036	4	47
M39543	Structural pathway of IL-1	8.27×10^{-4}	0.042	4	50

* Pathway analysis was performed using ToppFun (23). Unless otherwise indicated, the source of each CpG site was Molecular Signatures Database C2 BioCarta (version 7.3). CLUES = California Lupus Epidemiology Study; RLR = retinoic acid–inducible gene 1–like receptor; CTL = cytotoxic T lymphocyte; IFN = interferon; IL-1 = interleukin-1.
† Benjamini and Hochberg false discovery rate (FDR).
‡ GenMAPP was the source of this CpG site.

filtered results using a minimum difference in DNA methylation (absolute beta value difference >0.03) and observed that 309 CpG sites had the minimum difference and FDR (Figure 3 and Supplementary Table 3, http://onlinelibrary.wiley.com/doi/10.1002/art.42237).

These CpGs were distributed across the genome with the top results within or near *IFI44L, IFIT1, LOC101927924*, and *MX1*. The top 25 results according to smallest P value are shown in Table 2. Pathway analysis of the genes containing these 309 sites identified the human immune response to tuberculosis and retinoic acid–inducible gene 1–like receptor pathways as the most significant pathways; however, multiple immune pathways were represented, including antigen processing, virus response, type II IFN signaling, cytotoxic T lymphocyte–associated pathways, and taurine and hypotaurine metabolism (Table 3). Across S1, M1, and M2 clinical subtypes, we found no significant difference in terms of the change in methylation within changing CpGs was identified between the 3 subtypes (FDR >0.05 by analysis of variance).

In comparison to the genome-wide results, there was strong evidence of enrichment in SLE subtype–associated CpGs that changed over time (27% versus 0.34%, $P = 1.82 \times 10^{-175}$). These included CpGs in *IFI44L, MX1*, and *PRABCAP1L*. A total of 68 of these 71 CpGs had a decrease in methylation and only 3 had an increase in methylation at the second time point. An enrichment analysis was performed, with results supporting this finding. In 63 of 100 times, no CpG showed a significant difference in methylation (paired t-test FDR >0.05; methylation beta value difference < 0.03). In 2 samples, 3 CpGs had a significant change ($P < 7 \times 10^{-8}$; methylation beta value difference >0.03), 5 samples had 5 significant CpGs, and 30 samples 1 significant CpG. The distribution of CpGs with a significant change in the

enrichment analysis is shown (see Supplementary Figure 5, http://onlinelibrary.wiley.com/doi/10.1002/art.42237).

Association of CpG sites with clinical outcomes. Although the disease was stable or quiescent over time in most study participants, a small percentage of participants had significant changes in clinical manifestations, such as changing dsDNA titers or development of lupus nephritis. In these cases, we evaluated whether CpG sites that changed over time were associated with Systemic Lupus Erythematosus Disease Activity Index (SLEDAI) score (26), dsDNA antibody positivity, and/or lupus nephritis (Supplementary Table 4, http://onlinelibrary.wiley.com/doi/10.1002/art.42237). Overall, no CpGs met the threshold of significance ($P < 1.8 \times 10^{-5}$) but, according to SLEDAI scores, some evidence of an association was observed with cg09858955 in *VRK2* (β coefficient −1.2, $P = 0.001$), cg09128104 in *RARA* (β coefficient 0.69, $P = 0.00036$), and cg21524061 in *TLR6* (β coefficient 0.45, $P = 0.0005$). These genes are involved in granulopoiesis (*RARA*) (27), apoptosis (*VRK2*) (28), and immune activation (*TLR6*) (29), all of which are pathways relevant to lupus disease pathogenesis. The top associations with regard to dsDNA positivity were cg01971407 in *IFITM1* (β coefficient −0.30, $P = 0.0003$), cg05070493 in *TRAF3* (β coefficient −0.06, $P = 0.0003$), and cg00959259 and cg08122652 in *PARP9* (β coefficient −0.029, $P = 0.0003$ and β coefficient −0.11, $P = 0.0004$, respectively). Similarly, TNF receptor–associated factor 3 is known to be a powerful negative regulator of B cell survival and activation (30), *IFITM1* is an IFN-responsive gene, and *PARP9* is associated with macrophage activation (31,32).

Effect of medications on DNA methylation. Since medications such as prednisone and methotrexate can alter the

methylome in immune cells, we examined whether the changes in methylation at CpG sites were associated with the use of particular medications in a repeated measures model, adjusting for age, sex, and genetic principal components. A total of 15 of 309 CpGs (4.9%) had at least 1 significant association with use of an immunosuppressive medication (Supplementary Table 5, http://onlinelibrary.wiley.com/doi/10.1002/art.42237). Nine CpGs correlated with prednisone, 5 CpGs correlated with mycophenolate mofetil, and 2 CpGs correlated with azathioprine. There were no significant associations with changes in biologic treatments, inhibitors of purine and pyrimidine synthesis, calcineurin inhibitors, or antimalarials.

Effect of cell-type proportions on DNA methylation.
One of the limitations of using whole blood DNA methylation measures in population-based studies is that differences in methylation might be due to differences in cell-type proportions between individuals at the time blood was drawn or changes taking place in cell-type proportions between blood sample collections over time. As expected, paired comparisons between the 6 estimated cell types at the 2 time points revealed significant changes in terms of the proportions of monocytes, granulocytes, and CD8+ cells (paired t-test $P < 0.05$). In studies of SLE, overadjustment of cell-type proportion differences may lead to incorrect conclusions, since changes in cell-type proportions may be relevant to disease pathogenesis. To address these issues, we initially used the adjusted matrix of cell-type proportions to determine if there were any DNA methylation changes. Then, to examine the effects of changes in cell-type proportions on the change in methylation we used the unadjusted matrix and longitudinal models incorporating the difference in DNA methylation as the outcome and the difference in each cell type as a predictor, adjusting for age, sex, and genetic principal components. We observed that 67 CpGs of the initial 309 (21.7%) that changed over time had a significant correlation with changes in at least 1 cell type estimate ($P < 2.70 \times 10^{-5}$).

Changes in DNA methylation correlated with changes in cell-type proportions at 64 CpGs for granulocyte estimates, 39 CpGs for CD4+ T cell estimates, 24 CpGs for CD8+ T cell estimates, 5 CpGs for monocyte estimates, 12 CpGs for B cell estimates, and 6 CpGs for natural killer (NK) cell estimates. Supplementary Figure 6 shows the effect sizes of changes in DNA methylation in relation to changes in cell-type proportions (http://onlinelibrary.wiley.com/doi/10.1002/art.42237). Although the largest number of CpGs influenced by changes in cell-type proportions was in granulocytes, the largest effect sizes were observed for the NK cell estimates, for example, cg0571263 (β coefficient -20.25, $P = 5.9 \times 10^{-8}$), IFITM1 (cg09026253) (β coefficient -13.95, $P = 6.4 \times 10^{-7}$), and RAB6B (β coefficient 14.55, $P = 1.6 \times 10^{-5}$). Studies have shown RAB6B expression in NK cells as well as in mucosal-associated invariant T cells (33).

We found other interesting examples of correlations of changes in DNA methylation with the change in cell-type proportions in genes known to be enriched in a particular immune cell type. For example, methylation at RPS6KB1 correlated with B cell estimates (cg02095219) (β coefficient 10.01, $P = 4.839 \times 10^{-7}$), where RPS6KB1 expression is known to be enriched in treatment-naive B cells and memory B cells (34). Other examples include CD4+ T cell estimates with methylation in B2M (cg03425812) (β coefficient -7.45; $P = 2.489 \times 10^{-8}$) and IFIT1M (cg04582010) (β coefficient -6.40, $P = 4.540 \times 10^{-8}$), known to be widely expressed in multiple CD4+ T cell subsets (33,35). Methylation at B36NT3 (cg16744531) (β coefficient 5.50, $P = 0.00001$) was associated with CD8+ T cell estimates demonstrated to be expressed in CD8+ memory T cells. Methylation of TNFSF10 (cg10213935) (β coefficient -6.633, $P = 0.000012$) was associated with monocyte estimates, where tumor necrosis factor superfamily member 10 expression is known to be enriched in intermediate, classic, and nonclassic monocytes. Finally, methylation at IFITM1 (cg05552874) (β coefficient -2.93, $P = 2.136 \times 10^{-6}$) and HDAC4 (cg27074582) (β coefficient -1.52681, $P = 1.794 \times 10^{-9}$) was associated with granulocyte estimates.

Effect of self-reported ethnicity or race, genetic ancestry, and genetic variation on methylation changes over time.
There is substantial evidence that DNA methylation differs across ethnic groups. Some of these differences are due to genetic variation and some are not explained by genetics alone (36,37). To examine the effects of genetic ancestry as well as self-reported ethnicity and race, we constructed models with the methylation difference over time as the outcome and self-reported ethnicity and race or genetic ancestry estimates as predictors, adjusting for age and sex. Nine models were generated: 1 each for the self-reported ethnicities or races Hispanic, Black, White, or Asian and 1 each for the genetic ancestry estimates African, East Asian, American Indian, South Asian, European. Results are shown in Supplementary Table 6 (https://onlinelibrary.wiley.com/doi/10.1002/art.42237). No model was significant upon multiple hypothesis testing ($P < 3.2 \times 10^{-5}$); however, there are a few associations that are worth mentioning. The top methylation change association was at cg23876832 (no gene name is associated with this methylation site), with South Asian ancestry ($P = 3.75 \times 10^{-5}$). When looking at results with a nominal P value ($P < 0.05$), we found methylation change associations in 30 CpGs correlated with African ancestry, 5 CpGs correlated with European ancestry, 12 CpGs correlated with American Indian ancestry, 13 CpGs correlated with East Asian ancestry, and 12 correlated CpGs with South Asian ancestry. There were few overlaps, with 8 CpGs associated with 2 ancestries. When examining self-reported ethnicity or race, the top methylation change association was in cg00569896 (no gene name is associated with this site), associated with Black race ($P = 1.68 \times 10^{-4}$). Results

with a nominal P value ($P < 0.05$) indicated methylation change associations in 23 CpGs were associated with Black race, 19 CpGs were associated with Asian race, 8 CpGs were associated with Hispanic ethnicity, and 2 CpGs were associated with White race. Similarly, there were few overlaps, with 5 CpGs significantly associated with 2 ethnic or racial groups ($P < 0.05$). In terms of the significant overlap of CpGs between ancestry and self-reported ethnicity and race ($P < 0.05$), we found that 20 CpGs were associated with Black race and African ancestry, 2 CpGs were associated with Asian race and East Asian ancestry, there was no overlap between Asian race and South Asian ancestry, 2 CpGs were associated with Hispanic ethnicity and American Indian race, and there was no overlap between European ancestry and White race. These results suggest that both ancestry and self-reported ethnicity or race may be influencing methylation changes, primarily at different sites. The only exception was the high concordance between CpGs associated with Black race and African ancestry.

To test if genetic variation influenced methylation changes at specific sites, we investigated CpGs known to be under genetic control (methylation QTLs). Of the 309 CpGs that changed over time, there were 75 CpG with evidence of methylation QTL (24%). This is in comparison to 5.5% of methylation QTLs in stable CpGs genome wide (n = 39,824), suggesting an enrichment of methylation QTLs in CpGs with a significant change in methylation over time ($P = 4.8 \times 10^{-47}$ by 2-sample test). Of the 72 SLE subtype–associated CpGs that changed over time, 24 were methylation QTLs (33%). This was slightly higher than the proportion of methylation QTLs in SLEs subtype–associated CpGs that did not change over time, but the difference was not statistically significant (n = 46 of 184 [25%]) ($P = 0.179$ by 2-sample test).

DISCUSSION

In this study, we examined the dynamics of DNA methylation in CpGs previously associated with SLE subtypes in a longitudinal cohort of SLE patients. Overall, we observed that a large proportion of SLE subtype–associated CpGs did not show significant change over 2 years. However, a much higher proportion of SLE subtype–associated CpGs changed over time compared to the genome-wide methylome. Some of the methylation changes observed over 2 years in SLE subtype–associated CpGs were associated with changes in cell-type proportions (26%) and medication use (4.5%).

Since the epigenome is not static, an important question related to EWAS is if associations may change over time. These results are encouraging, providing evidence that, overall, the methylation status of the majority of CpGs that were previously found to be associated with specific SLE subtypes remained unchanged over a 2-year period. Therefore, the blood methylome has potential as a biomarker for disease subtypes. This is further supported by findings from a recent longitudinal study examining

DNA methylation in circulating granulocytes from SLE patients, where significant stability of the methylome was observed over a period of 4 years (38). With this in mind, we also refined our previous EWAS findings at the time of enrolment in the cohort by selecting CpGs that had the most robust difference in methylation between SLE subtypes and did not change over time. These candidate CpGs could be further prospectively studied at disease onset to determine their prognostic role in predicting SLE subtypes as well as their role as potential biomarkers for treatment response.

We observed a very small number of CpGs in which DNA methylation significantly changed over time. Interestingly, pathway analysis showed that most of these CpGs were involved in immune-related pathways such as intracellular viral sensing pathways, antigen processing, and IFN response as well as metabolic pathways (taurine metabolism, type II diabetes) (Table 3). We attempted to identify the underlying factors driving changes in DNA methylation. Overall, these changes were not correlated with disease activity, anti-dsDNA antibody titer, or lupus nephritis, although most individuals in our cohort had quiescent disease. Although most of the SLE subtype–associated CpGs were stable, there was a striking distinction between the increased proportion of SLE-associated CpGs that changed over time compared to genome-wide CpGs. One potential explanation for the progressive hypomethylation observed at SLE subtype–associated CpGs is that PBMCs in SLE patients have persistent exposure to cytokine milieu inherent in SLE, making immune-related CpGs in circulating PBMCs more susceptible to change. This is consistent with most EWAS that demonstrate hypomethylation of immune-related genes in SLE patients compared to healthy individuals, as well as severe SLE phenotypes compared to milder disease (5,8–10).

These findings have been attributed to defects in the enzymes responsible for the maintenance of DNA methylation (DNA methyltransferases) due to oxidative stress (39). Another potential hypothesis is that passive demethylation, the progressive loss of methylation over time, may be accelerated in SLE. The premise that passive demethylation can occur at different rates in individuals is the basis of epigenetic clocks or biomarkers of aging. These can drastically differ from chronological age (40). Whether accelerated passive demethylation, or epigenetic aging, occurs in SLE-relevant genes and pathways is unknown but should be examined in future longitudinal studies with longer periods of observation.

In studies with large sample sizes (>1,000), it is estimated that at least 10% and up to 45% of the methylome is influenced by nearby methylation QTLs (41). We investigated if genetic variation influenced methylation changes and found that a higher proportion of CpGs that changed over time were associated with methylation QTLs compared to stable CpGs. The leading hypothesis to explain cis-methylation QTL effects is that SNPs in protein binding sites alter or disrupt the activity of sequence-specific binding proteins such as transcription factors of methyl-binding

proteins which could lead to changes in methylation patterns of nearby CpGs (42–44). Since transcription factor binding is dynamic, one could hypothesize that this effect may influence the variability of methylation in addition to methylation itself. Other longitudinal methylation studies are needed to corroborate this observation.

As expected, when we examined our initial results in the unadjusted matrix for cell-type proportions, we found that a substantial proportion of changing CpGs (26%) were associated with at least 1 cell estimate. This is an important consideration for studies that use whole blood DNA methylation to study the epigenetic landscape in SLE. As cell-type proportions in peripheral blood samples are of biologic relevance to disease pathogenesis, we are faced with a conundrum: how to deal with a potential confounder that could itself be a disease outcome. In the current study, we addressed this by initially adjusting for cell-type proportions and then reexamining findings in an unadjusted matrix to assess the effects of cell-type proportions. Future studies of analytic approaches to whole blood DNA methylation data will be important given the low cost and feasibility of working with whole blood in comparison to sorted or single cells, particularly population-based studies that seek to provide a useful genomic clinical tool for precision medicine.

Limitations of this study include a relatively small sample size, which may have limited our ability to detect a larger number of CpG sites that varied over time or fully assess the association between self-reported ethnicity or race and genetic ancestry. In addition, the detection of methylation fluctuations associated with disease activity was not possible due to the fact that most participants had clinically inactive disease. Our study was underpowered to identify additional CpG sites associated with medication use. Finally, an extended interval of >2 years may have yielded different findings. However, there have been few studies that have reexamined cross-sectional DNA methylation associations in a longitudinal cohort. Our rigorous analysis pipeline addressed the potential limitations of studying whole blood DNA methylation in longitudinal studies, including effects of changes in cell-type proportions.

In summary, we characterized the DNA methylation dynamics of CpGs that were previously shown to be associated with SLE in this well-characterized CLUES longitudinal cohort. Among these SLE subtype–associated CpGs, we identified CpGs that remained stable over time. Given their association with SLE subtypes, these CpGs should be further evaluated to determine their potential role as biomarkers of disease outcomes. Additional longitudinal studies may also reveal whether SLE- and immune-related CpGs have accelerated passive demethylation in comparison to the genome-wide methylome. Future studies of methylome dynamics in SLE at the time of disease flare and remission may provide additional insight into epigenetic programs that may guide the development of precision medicine approaches for SLE.

REFERENCES

1. Jakes R, Bae SC, Louthrenoo W, Mok CC, Navarra S, Kwon N. Systematic review of the epidemiology of systemic lupus erythematosus in the Asia-Pacific region: prevalence, incidence, clinical features, and mortality. Arthritis Care Res (Hoboken) 2012;64:159–68.

2. Gianfrancesco MA, Dall'Era M, Murphy LB, Helmick CG, Li J, Rush S, et al. Mortality among minority populations with systemic lupus erythematosus, Including Asian and Hispanic/Latino Persons - California, 2007-2017. MMWR Morb Mortal Wkly Rep 2021;70:236–9.

3. Lanata CM, Chung SA, Criswell LA. DNA methylation 101: what is important to know about DNA methylation and its role in SLE risk and disease heterogeneity. Lupus Sci Med 2018;5:e000285.

4. Absher DM, Li X, Waite LL, Gibson A, Roberts K, Edberg J, et al. Genome–wide DNA methylation analysis of systemic lupus erythematosus reveals persistent hypomethylation of interferon genes and compositional changes to CD4+ T-cell populations. PLoS Genetics 2013;9:e1003678.

5. Coit P, Yalavarthi S, Ognenovski M, Zhao W, Hasni S, Wren JD, et al. Epigenome profiling reveals significant DNA demethylation of interferon signature genes in lupus neutrophils. J Autoimmun 2015;58:59–66.

6. Coit P, Renauer P, Jeffries MA, Merrill JT, McCune WJ, Maksimowicz-McKinnon K, et al. Renal involvement in lupus is characterized by unique DNA methylation changes in naive CD4+ T cells. J Autoimmun 2015;61:29–35.

7. Coit P, Dozmorov MG, Merrill JT, McCune WJ, Maksimowicz-McKinnon K, Wren JD, et al. Epigenetic reprogramming in naive CD4+ T cells favoring T cell activation and non-Th1 effector T cell immune response as an early event in lupus flares. Arthritis Rheumatol 2016;68:2200–9.

8. Imgenberg-Kreuz J, Almlöf JC, Leonard D, Alexsson A, Nordmark G, et al. DNA methylation mapping identifies gene regulatory effects in patients with systemic lupus erythematosus. Ann Rheum Dis 2018;77:736–43.

9. Chung SA, Nititham J, Elboudwarej E, Quach HL, Taylor KE, Barcellos LF, et al. Genome-wide assessment of differential DNA methylation associated with autoantibody production in systemic lupus erythematosus. Plos One 2015;10:e0129813.

10. Lanata CM, Paranjpe I, Nititham J, Taylor KE, Gianfrancesco M, Paranjpe M et al. A phenotypic and genomics approach in a multiethnic cohort to subtype systemic lupus erythematosus. Nat Commun 2019;10:3902.

11. Tan EM, Cohen AS, Fries JF, Masi AT, McShane DJ, Rothfield NF, et al. The 1982 revised criteria for the classification of systemic lupus erythematosus. Arthritis Rheum 1982;25:1271–7.

12. Hochberg MC, for the Diagnostic and Therapeutic Criteria Committee of the American College of Rheumatology. Updating the American College of Rheumatology revised criteria for the classification of systemic lupus erythematosus [letter]. Arthritis Rheum 1997;40:1725.

13. Dall'Era M, Cisternas MG, Snipes K, Herrinton LJ, Gordon C, Helmick CG. The incidence and prevalence of systemic lupus erythematosus in San Francisco County, California: the California Lupus Surveillance Project. Arthritis Rheumatol 2017;69:1996–2005.

14. Maksimovic J, Gordon L, Oshlack A. SWAN: subset-quantile within array normalization for illumina infinium HumanMethylation450 BeadChips. Genome Biol 2012;13:R44.

15. Aryee MJ, Jaffe AE, Corrada-Bravo H, Ladd-Acosta C, Feinberg AP, Hansen KD, et al. Minfi: a flexible and comprehensive Bioconductor package for the analysis of Infinium DNA methylation microarrays. Bioinformatics 2014;30:1363–9.

16. Zhou W, Laird PW, Shen H. Comprehensive characterization, annotation and innovative use of Infinium DNA methylation BeadChip probes. Nucleic Acids Res 2017;45:e22.

17. Hoffmann TJ, Zhan Y, Kvale MN, Hesselson SE, Gollub J, Iribarren C, et al. Design and coverage of high throughput genotyping arrays optimized for individuals of East Asian, African American, and Latino race/ethnicity using imputation and a novel hybrid SNP selection algorithm. Genomics 2011;98:422–30.

18. Alexander DH, Novembre J, Lange K. Fast model-based estimation of ancestry in unrelated individuals. Genome Res 2009;19:1655–64.

19. Muller C, Schillert A, Röthemeier C, Trégouët D, Proust C, Binder H, et al. Removing batch effects from longitudinal gene expression - quantile normalization plus ComBat as best approach for microarray transcriptome data. PLoS One 2016;11:e0156594.

20. Houseman EA, Accomando WP, Koestler DC, Christensen BC, Marsit CJ, Nelson HH, et al. DNA methylation arrays as surrogate measures of cell mixture distribution. BMC Bioinformatics 2012; 13:86.

21. Jones MJ, Islam SA, Edgar RD, Kobor MS. Adjusting for cell type composition in DNA methylation data using a regression-based approach. Methods Mol Biol 2017;1589:99–106.

22. Rhead B, Holingue C, Cole M, Shao X, Quacg HL, Quach D, et al. Rheumatoid arthritis naive T cells share hypermethylation sites with synoviocytes. Arthritis Rheumatol 2017;69:550–9.

23. Chen J, Bardes EE, Aronow BJ, Jegga AG. ToppGene Suite for gene list enrichment analysis and candidate gene prioritization. Nucleic Acids Res 2009;37:W305–11.

24. Shabalin AA. Matrix eQTL: ultra fast eQTL analysis via large matrix operations. Bioinformatics 2012;28:1353–8.

25. Hannon E, Gorrie-Stone TJ, Smart MC, Burrage J, Hughes A, Bao Y, et al. Leveraging DNA-methylation quantitative-trait loci to characterize the relationship between methylomic variation, gene expression, and complex traits. Am J Hum Genet 2018;103:654–65.

26. Bombardier C, Gladman DD, Urowitz MB, Caron D, Chang DH, and the Committee on Prognosis Studies in SLE. Derivation of the SLEDAI: a disease activity index for lupus patients. Arthritis Rheum 1992; 35:630–40.

27. Fujiki R, Chikanishi T, Hashiba W, Ito H, Takada I, Roeder RG, et al. GlcNAcylation of a histone methyltransferase in retinoic-acid-induced granulopoiesis [article retracted in Nature 2014;505:574]. Nature 2009;459:455–9.

28. Monsalve DM, Merced T, Fernandez IF, Blanco S, Vazquez-Cedeira M, Lazo PA. Human VRK2 modulates apoptosis by interaction with Bcl-xL and regulation of BAX gene expression. Cell Death Dis 2013;4:e513.

29. Patole PS, Pawar RD, Lech M, Zecher D, Schmidt H, Segerer S, et al. Expression and regulation of Toll-like receptors in lupus-like immune complex glomerulonephritis of MRL-Fas(lpr) mice. Nephrol Dial Transplant 2006;21:3062–73.

30. Whillock AL, Ybarra TK, Bishop GA. TNF receptor-associated factor 3 restrains B cell receptor signaling in normal and malignant B cells. J Biol Chem 2021:100465.

31. Hashimoto S, Imaizumi T, Watanabe S, et al. Expression of IFN-induced transmembrane protein 1 in glomerular endothelial cells. Pediatr Int 2021;63:1075–81.

32. Iwata H, Goettsch C, Sharma A, Ricchiuto P, Goh WW, Halu A, et al. PARP9 and PARP14 cross-regulate macrophage activation via STAT1 ADP-ribosylation. Nat Commun 2016;7:12849.

33. Monaco G, Lee B, Xu W, Mustafah S, Hwang YY, Carré C, et al. RNA-Seq signatures normalized by mRNA abundance allow absolute deconvolution of human immune cell types. Cell Rep 2019;26: 1627–40.

34. Schmiedel BJ, Singh D, Madrigal A, Valdovino-Gonzalez AG, White BM, Zapartiel-Gonzalo J, et al. Impact of genetic polymorphisms on human immune cell gene expression. Cell 2018;175:1701–15.

35. Thul PJ, Åkesson L, Wiking M, Mahdessian D, Geladaki A, Blal HA, et al. A subcellular map of the human proteome. Science 2017;356: eaal3321.

36. Kader F, Ghai M. DNA methylation-based variation between human populations. Mol Genet Genomics 2017;292:5–35.

37. McKennan C, Naughton K, Stanhope C, Kattan M, O'Connor GT, Sandel MT, et al. Longitudinal data reveal strong genetic and weak non-genetic components of ethnicity-dependent blood DNA methylation levels. Epigenetics 2021;16:662–76.

38. Coit P, Ortiz-Fernandez L, Lewis EE, McCune WJ, Maksimowicz-McKinnon K, Sawalha AH. A longitudinal and transancestral analysis of DNA methylation patterns and disease activity in lupus patients. JCI Insight 2020;5:e143654.

39. Li Y, Gorelik G, Strickland FM, Richardson BC. Oxidative stress, T cell DNA methylation, and lupus. Arthritis Rheumatol 2014;66:1574–82.

40. Tan Q, Heijmans BT, Hjelmborg JV, Soerensen M, Christensen K, Christiansen L. Epigenetic drift in the aging genome: a ten-year follow-up in an elderly twin cohort. Int J Epidemiol 2016;45:1146–58.

41. Villicana S, Bell JT. Genetic impacts on DNA methylation: research findings and future perspectives. Genome Biol 2021;22:127.

42. Gutierrez-Arcelus M, Lappalainen T, Montgomery SB, Buil A, Ongen H, Yurovsky A, et al. Passive and active DNA methylation and the interplay with genetic variation in gene regulation. Elife 2013;2: e00523.

43. Banovich NE, Lan X, McVicker G, van de Geijn, Degner JF, Blischak JD, et al. Methylation QTLs are associated with coordinated changes in transcription factor binding, histone modifications, and gene expression levels. PLoS Genet 2014;10:e1004663.

44. Benton MC, Lea RA, Macartney-Coxson D, Sutherland HG, White N, Kennedy D, et al. Genome-wide allele-specific methylation is enriched at gene regulatory regions in a multi-generation pedigree from the Norfolk Island isolate. Epigenetics Chromatin 2019;12:60.

AMERICAN COLLEGE
of RHEUMATOLOGY
Empowering Rheumatology Professionals

Multidimensional Immune Profiling of Cutaneous Lupus Erythematosus In Vivo Stratified by Patient Response to Antimalarials

Jay Patel,[1] ID Thomas Vazquez,[1] ID Felix Chin,[1] Emily Keyes,[1] ID Daisy Yan,[1] ID DeAnna Diaz,[1] Madison Grinnell,[1] ID Meena Sharma,[1] Yubin Li,[1] Rui Feng,[2] Grant Sprow,[1] Josh Dan,[1] and Victoria P. Werth[1] ID

Objective. The pathogenesis of cutaneous lupus erythematosus (CLE) is multifactorial, and CLE is difficult to treat due to the heterogeneity of inflammatory processes among patients. Antimalarials such as hydroxychloroquine (HCQ) and quinacrine (QC) have long been used as first-line systemic therapy; however, many patients do not respond to treatment with antimalarials and require systemic immunosuppressants that produce undesirable side effects. Given the complexity and the unpredictability of responses to antimalarial treatments in CLE patients, we sought to characterize the immunologic profile of patients with CLE stratified by subsequent treatment outcomes to identify potential biomarkers of inducible response.

Methods. We performed mass cytometry imaging of multiple immune cell types and inflammation markers in treatment-naive skin biopsy samples from 48 patients with CLE to identify baseline immunophenotypes that may predict the response to antimalarial therapy. Patients were stratified according to their response to treatment with antimalarials, as HCQ responders, QC responders, or nonresponders.

Results. HCQ responders demonstrated increased CD4+ T cells compared to the QC responder group. Patients in the nonresponder group were found to have decreased Treg cells compared to QC responders and increased central memory T cells compared to HCQ responders. QC responders expressed increased phosphorylated stimulator of interferon genes (pSTING) and interferon-κ (IFNκ) compared to HCQ responders. Phosphorylated STING and IFNκ were found to be localized to conventional dendritic cells (cDCs), and the intensity of pSTING and IFNκ staining was positively correlated with the number of cDCs on a tissue and cellular level. Neighborhood analysis revealed decreased regulatory cell interactions in nonresponder patients. Hierarchical clustering revealed that nonresponder patients could be further differentiated based on expression of pSTAT2, pSTAT3, pSTAT4, pSTAT5, phosphorylated interferon regulatory factor 3 (pIRF3), granzyme B, pJAK2, interleukin-4 (IL-4), IL-17, and IFNγ.

Conclusion. These findings indicate differential immune cell compositions between patients with CLE, offering guidance for future research on precision-based medicine and treatment response.

INTRODUCTION

Lupus erythematosus (LE) is a complex autoimmune disease with a variety of systemic and cutaneous manifestations.

Cutaneous lupus erythematosus (CLE) can occur with or without concomitant systemic lupus erythematosus (SLE) and occurs in 75–85% of patients with lupus. CLE significantly impacts quality of life through the psychological and physical distress it causes

(1–3). The pathogenesis of CLE is multifactorial, with a complex interaction between genetic and environmental factors leading to immune dysregulation. A multitude of mechanisms are thought to contribute to the pathogenesis of CLE, including ultraviolet radiation, smoking, NETosis, altered nucleic acid processing, cell death/apoptosis, type I interferon (IFN) production, JAK/STAT pathway activation, T cell dysregulation, myeloid and plasmacytoid dendritic cell stimulation, and autoantibody production, all of which contribute to dysregulation of immune tolerance (4).

Oral antimalarials such as hydroxychloroquine (HCQ) and quinacrine (QC) have been used to treat CLE since 1894 and have since become first-line systemic therapy for all types of CLE (5). While their exact mechanism of action is still incompletely understood, the therapeutic effects of HCQ and QC may be attributed to immunomodulatory properties including photoprotection, alteration of Toll-like receptor signaling, inhibition of dendritic cell antigen presentation, suppression of prostaglandins and cytokines, and lysosomal stabilization (6,7). In a previously published study, it was demonstrated that ~50% of CLE patients will respond to treatment with HCQ alone (3). Of those patients considered to be nonresponsive to HCQ, 66% will respond to the addition of QC. This leaves a sizeable number of nonresponding patients with CLE refractory to antimalarials, ultimately requiring immunosuppressive medications, which often carry an undesirable side-effect profile. These second- and third-line therapies encompass a broad range of medication classes and mechanisms of action that are incompletely understood, requiring lengthy periods of trial and error in which providers must determine the most effective therapy for their patients.

To our knowledge, there are few published studies in which the immune environment of CLE patients stratified by treatment response has been characterized. In a previous study by Zeidi et al, immunohistochemistry was used to identify increased CD11c+ dendritic cells and tumor necrosis factor (TNF) messenger RNA (mRNA) in QC-responding patients (8). The complexity of CLE pathogenesis requires immunologic analysis on a multiplexed scale to best identify differences between groups stratified by response to treatment. Given the diversity of responses to antimalarials and immunosuppressive drugs, we attempted to characterize the immunologic profile of treatment-naive CLE skin samples stratified by subsequent antimalarial response through the use of imaging mass cytometry (IMC). By understanding the differences in the immunologic profiles of CLE patients at baseline, we sought to identify potential biomarkers for the prediction of in vivo response to antimalarial treatment and to identify potential targets for precision-based medicine.

PATIENTS AND METHODS

Patients. Patients were retrospectively enrolled from a longitudinal, prospective CLE patient database at the University of Pennsylvania. All participants signed written informed consents and approval was obtained from the University of Pennsylvania and Philadelphia VA Medical Center Institutional Review Boards.

Patients were diagnosed as having CLE according to the Gilliam classification criteria (9) or investigator experience (VPW). SLE diagnosis was determined according to the 1997 American College of Rheumatology classification criteria (10). Archived treatment-naive, formalin-fixed paraffin-embedded lesioned biopsy samples were obtained. The CLE database and patient charts were reviewed to identify each patient's treatment course and response. Cutaneous Lupus Erythematosus Disease Area and Severity Index Activity (CLASI-A) scores (11) recorded at the time of biopsy were utilized.

Each patient was categorized according to their established response to antimalarials, which was ascertained by chart review and was verified by 3 investigators (DY, EK, and VPW). Patients whose symptoms improved with HCQ therapy and did not require the addition of any other drug were designated as HCQ responders. Patients who benefited from and required only HCQ and QC combination therapy were designated as QC responders. Patients who required the addition of other immunomodulatory agents (e.g., methotrexate, mycophenolate mofetil, lenalidomide, etc.) were designated as nonresponders. Treatment with topical medications and glucocorticoids was allowed in each group. Patients with other autoimmune connective tissue diseases were excluded from the study, with the exception of patients meeting criteria for Sjögren's syndrome. Patients whose responses to treatment with antimalarials were unclear were also excluded from the study. Patient demographics can be found in Table 1.

Data acquisition. A detailed description of IMC, in situ hybridization, and the statistical methods used in this study are included in the Supplementary Materials and Methods, available on the *Arthritis & Rheumatology* website at http://onlinelibrary.wiley.com/doi/10.1002/art.42235.

Data availability. Raw data are available on Mendeley Data at doi: 10.17632/b7vr75sbdz.1.

RESULTS

Study population. In total, 48 CLE patients met the criteria for inclusion. Thirteen patients were classified as HCQ responders, 13 as QC responders, and 22 as nonresponders. Patient demographics are detailed in Table 1. Notably, the 2 most prevalent clinical CLE subtypes represented in our patient population were discoid lupus erythematosus and subacute CLE, and their composition in each response group was relatively similar. Most patients were White, middle-aged women. African American patients were well-represented, making up 22.9% of the cohort.

Table 1. Demographic and baseline clinical characteristics of CLE patients included in the cohort*

	All CLE patients (n = 48)	Treatment response group		
		HCQ responders (n = 13)	QC responders (n = 13)	Nonresponders (n = 22)
Age, median (IQR) years	52.5 (32.25–64)	52 (26–63.5)	55 (34.5–66.5)	48 (31.5–60.25)
SLE	12 (25.0)	2 (15.4)	4 (30.8)	9 (40.9)
CLASI-A score, median (IQR)†	14 (5–25)	7 (3–28)	17 (6–29)	16 (13–21)
Sex				
Female	41 (85.4)	8 (61.5)	11 (84.6)	22 (100)
Male	7 (14.6)	5 (38.5)	2 (15.4)	0
Race				
African American	11 (22.9)	0	4 (30.8)	7 (31.8)
Asian	3 (6.3)	2 (15.4)	1 (7.7)	0
White	34 (70.8)	11 (84.6)	8 (61.5)	15 (68.2)
Smoking history, yes	20 (41.7)	6 (46.2)	4 (30.8)	10 (45.5)
CLE subtype				
Acute CLE	1 (2.1)	0	0	1 (4.5)
Subacute CLE	19 (39.6)	5 (38.5)	5 (38.5)	9 (40.9)
DLE	19 (39.6)	4 (30.8)	6 (46.2)	9 (40.9)
Lupus tumidus	2 (4.2)	1 (7.7)	0	1 (4.5)
HLE	3 (6.3)	1 (7.7)	2 (15.4)	0
Chilblain lupus	1 (2.1)	0	1 (7.7)	0
Lupus panniculitis	1 (2.1)	0	0	1 (4.5)

* Except where indicated otherwise, values are the number (%) of patients. CLE = cutaneous lupus erythematosus; HCQ = hydroxychloroquine; QC = quinacrine; IQR = interquartile range; SLE = systemic lupus erythematosus; CLASI-A = Cutaneous Lupus Erythematosus Disease Area and Severity Index Activity; DLE = discoid lupus erythematosus; HLE = hypertrophic lupus erythematosus.
† CLASI-A score ranges are as follows: mild (0–9), moderate (10–20), and severe (21–70).

Inflammatory cell makeup. Based on the data obtained from 2 IMC panels (panel 1 and panel 2), 12 unique cell phenotypes were identified through the use of PhenoGraph and were displayed using a heatmap of cell marker expression (Figures 1A and B). The most common cell types observed across all treatment response groups included conventional dendritic cells (cDCs), CD8+ T cells, CD4+ T cells, and Treg cells (Figure 1C). There was marked heterogeneity of cell composition in each treatment response group (Figure 1D). Proportions of CD4+ T cells and Treg cells differed significantly between the treatment response groups ($P < 0.05$) (Figure 1D). CD4+ T cells were significantly increased in HCQ responders compared to QC responders ($P < 0.05$) (Figure 1D). Treg cells were significantly increased in QC responders compared to nonresponders ($P < 0.05$) (Figure 1C). Similar to the findings of a previous study by Zeidi et al, there was a trend toward increased cDCs in QC responders (8).

We also observed a trend toward an increase in CD8+ T cells in HCQ responders (Figure 1D). The percentage of plasmacytoid dendritic cells (pDCs) was notably similar in each treatment response group. When CD4+ T cells (Figure 1E) and CD8+ T cells (Figure 1F) were gated into T cell subpopulations, a significant difference in the numbers of CD4+ central memory T (Tcm) cells and numbers of CD8+ Tcm cells was observed ($P < 0.05$) with a trend toward increased numbers of Tcm cells in nonresponders compared to HCQ responders (Figures 1E and F). Among all groups, effector memory T (Tem) cells were the largest constituent of the T cell compartment for both CD4+ T cells and CD8+ T cells (Figures 1E and F).

With regard to cellular composition, we determined that the CLASI-A score was negatively correlated with the numbers of CD14+CD16+ macrophages in HCQ responders (r = –0.0683), but not in QC responders or nonresponders (Supplementary Figure 1, available at http://onlinelibrary.wiley.com/doi/10.1002/art.42235). Similarly, a negative correlation (r = –0.759) between CLASI-A and γδ T cells was observed in nonresponders but not in HCQ responders or QC responders (Supplementary Figure 1).

Cytokines and signaling pathways. Multiple cell types are activated in CLE, and heatmaps of each intracellular cytokine or signaling pathway included in panel 1 (Figure 2A) and panel 2 (Figure 2B) were used to visualize activation. We found that the most activated cell types in skin biopsy samples from patients with CLE included cDCs, CD56+ natural killer (NK) cells, CD14+CD16+ macrophages, CD4+ T cells, neutrophils, and endothelial cells. The major producers of both antiviral IFNα and IFNβ were found to be cDCs and CD14+CD16+ macrophages, although type I IFNs are expressed in a multitude of immune cells. Neutrophils, though lacking in numbers, also showed significantly increased expression of proinflammatory cytokines, including type I IFNs, pSTAT3, and interleukin-18 (IL-18). Similarly, γδ T cells showed highly elevated expression of IFNα on a per-cell basis. Endothelial cells were found to be positive for numerous markers of CLE, especially IL-4, a Th2 cytokine.

We plotted the identified mean pixel intensity (MPI) per cell of each intracellular marker for each patient stratified according to
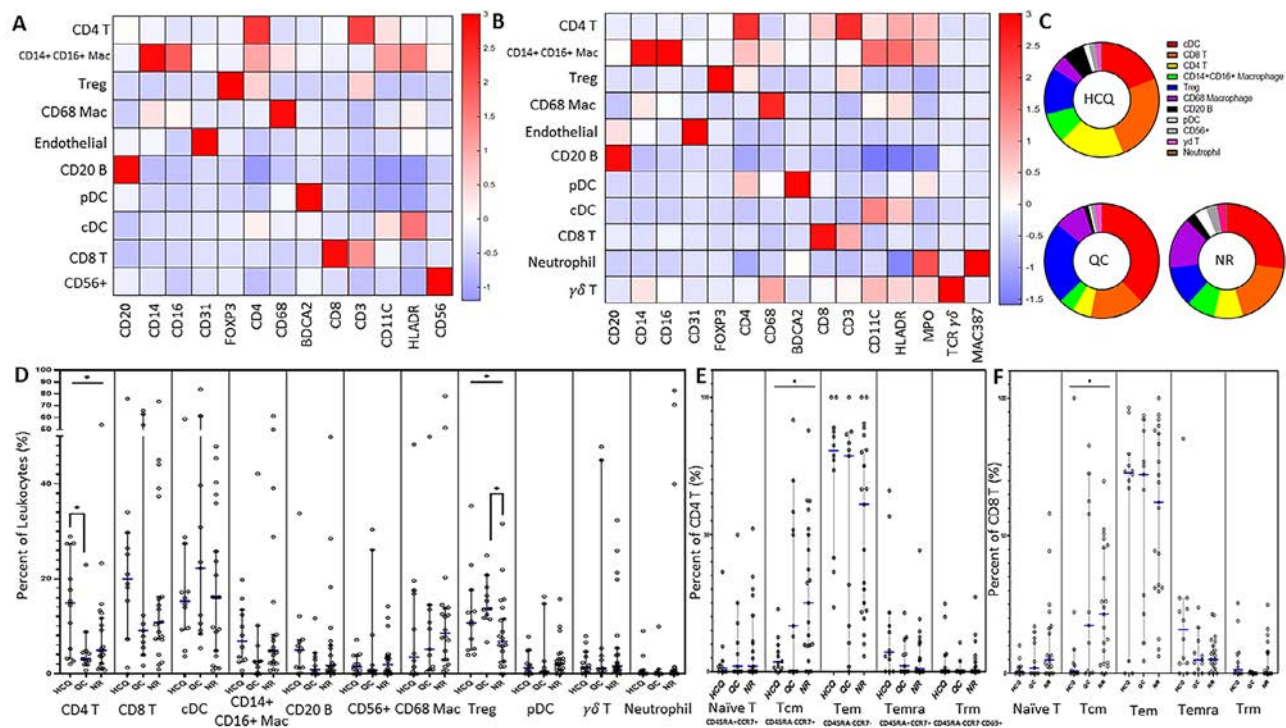
Figure 1. Immune cell composition of cutaneous lupus erythematosus (CLE) patients stratified by response to treatment with antimalarials. **A** and **B**, Heatmap showing cellular markers (horizontal axis) and immune cell clusters (vertical axis) in CLE patients, identified using Phenograph of cell cytometry panel 1 (**A**) and cell cytometry panel 2 (**B**). **C**, Relative composition of immune cell clusters in CLE patients responsive to treatment with hydroxychloroquine (HCQ), patients responsive to treatment with quinacrine (QC), and patients who did not respond to treatment with antimalarials (NR). **D**, Differences in the distribution of each immune cell cluster as a percentage of leukocytes in HCQ responders, QC responders, and nonresponders. CD4+ T cells were significantly increased in HCQ responders relative to QC responders ($P < 0.05$). Treg cells were significantly decreased in nonresponders relative to QC responders ($P < 0.05$). **E**, Distribution of CD4+ T cell subsets as a percentage of total CD4+ T cells, revealing differences in the proportion of central memory T (Tcm) cells ($P < 0.05$), with a trend toward increased Tcm cells in nonresponders. **F**, Distribution of CD8+ T cell subsets as a percentage of total CD8+ T cells. Proportions of Tcm cells were significantly different between treatment groups ($P < 0.05$) and there was a trend toward increased Tcm cells in nonresponders. Symbols represent individual patients; bars show the median and interquartile range. * $P < 0.05$. Mac = macrophage; pDC = plasmacytoid dendritic cell; cDC = conventional dendritic cell; Tem = effector memory T cell; Temra = terminally differentiated effector memory T cell; Trm = tissue-resident memory T cell.

their antimalarial response group (HCQ responder, QC responder, or nonresponder) (Figures 2C and D). There was a significant difference in the relative expression levels of phosphorylated stimulator of interferon genes (pSTING) and IFNκ between the 3 groups, with a significant increase in markers of both pathways in the QC responder group compared to the HCQ responder group ($P < 0.05$) (Figure 2C). Proinflammatory phosphorylation of JAK3 was increased in HCQ responders compared to QC responders ($P < 0.05$) (Figure 2D).

Using network analysis, we found that the numbers of Treg cells in QC responders (and to a lesser extent Treg cells in HCQ responders) were negatively correlated with the majority of proinflammatory pathways (Figures 2F and E and Supplementary Figure 2, available at http://onlinelibrary.wiley.com/doi/10.1002/art.42235). In contrast, Treg cells from nonresponders were found to have little to no association with such pathways (Figure 2G and Supplementary Figure 2). The CLASI-A score was found to be positively correlated with the expression levels of proinflammatory pSTAT5 in HCQ

responders (r = 0.816, $P < 0.05$), but no significant correlation was seen in QC responders or nonresponders (Supplementary Figure 3, available at http://onlinelibrary.wiley.com/doi/10.1002/art.42235). Analysis of intracellular markers identified differential inflammation marker expression between treatment response groups at the cell-type level (Supplementary Table 1, available at http://onlinelibrary.wiley.com/doi/10.1002/art.42235).

Low expression of type I IFNs in pDCs of CLE patients. Upon examination of the intracellular staining heatmaps (as shown in Figures 2A and B), we noticed that pDCs demonstrated relatively low expression of many inflammation markers, including all type I IFNs. Moreover, the numbers of pDCs were not found to be correlated with any of the global pathways (Supplementary Figure 4A, available at http://onlinelibrary.wiley.com/doi/10.1002/art.42235) or other cell counts. Only 8.5% of pDCs (interquartile range [IQR] 0.0–22.22) were IFNα+ (Supplementary Figure 4B). Across all biopsy samples from CLE
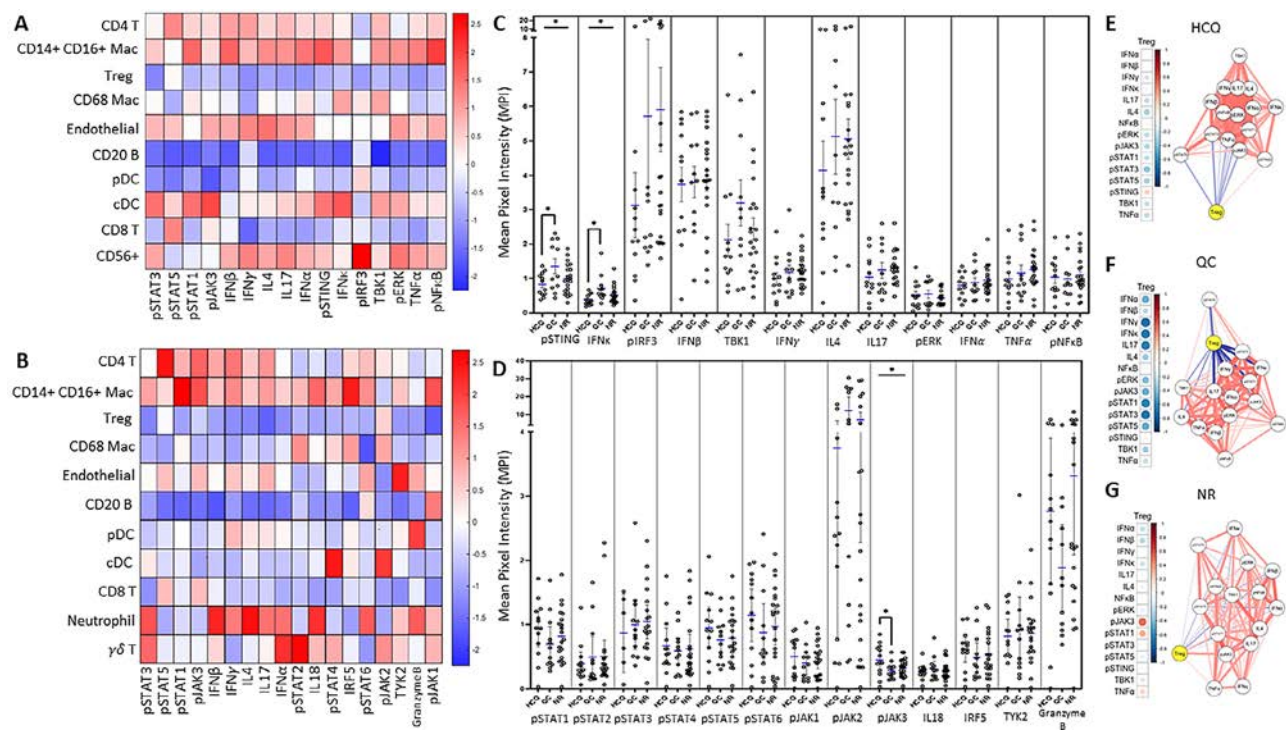
Figure 2. Global and cell-type specific intracellular inflammatory pathway expression in CLE patients stratified by antimalarial response. **A** and **B**, Heatmaps of activated intracellular pathways (horizontal axis) among immune cell clusters (vertical axis) in panel 1 (**A**) and in panel 2 (**B**). **C** and **D**, Differential pathway expression among CLE patients in each treatment group, assessed in IMC panel 1 (**C**) and panel 2 (**D**), with results expressed as the mean pixel intensity (MPI). Data in **C** show increased expression of phosphorylated stimulator of interferon genes (pSTING) and interferon-κ (IFNκ) in QC responders relative to HCQ responders ($P < 0.05$). Data in **D** show increased expression of pJAK3 in HCQ responders relative to QC responders ($P < 0.05$). **E–G**, Correlation networks showing correlations between activated pathway markers and Treg cell counts in HCQ responders (**E**) compared to QC responders (**F**) and nonresponders (**G**). The Treg cell counts of QC responders (and to a lesser extent HCQ responders) were negatively associated with the majority of pathways in panel 1. Treg cell counts of nonresponders displayed little to no association with panel 1 pathways. In **C** and **D**, symbols represent individual patients; bars show the median and interquartile range. * = $P < 0.05$. IL-4 = interleukin-4; pIRF3 = phosphorylated interferon regulatory factor 3; TBK1 = TANK-binding kinase 1; TNF = tumor necrosis factor (see Figure 1 for other definitions).

patients, pDCs were the second lowest contributor of absolute IFNα+ cells (median IFNα+ cell count 1 [IQR 0–4.5]) (B lymphocytes being the lowest contributor) (Supplementary Figure 4C). Conventional DCs and macrophages were the largest contributors to both relative and absolute cell counts of IFNα+ cells in CLE patients. Only 16.7% of pDCs were positive for IFNβ, compared to 60.7% of CD14+CD16+ macrophages. Plasmacytoid DCs were also low contributors of IFNβ+ cells (median 1 [IQR 0–7]) (B lymphocytes again being the lowest). These results suggest that pDCs are not in fact major producers of type I IFNs in CLE patients. These results also do not reveal a clear regulatory role for pDCs, as they were not found to be correlated with any other cell types or markers in the skin.

Using a weighted score accounting for cell count and MPI contributions of type I IFNs, we observed keratinocytes as collective producers of IFNα and IFNβ (Supplementary Figures 4D and E, available at http://onlinelibrary.wiley.com/doi/10.1002/art.42235). Myeloid lineage cells such as CD68+ macrophages, CD14+CD16+ macrophages, and cDCs made the greatest contributions to the production of IFNκ, with keratinocytes being

the second highest contributor (Supplementary Figure 4F). Overall, the immune infiltrate collectively contributes the most type I IFNs, followed by epidermal sources.

Epidermal expression of cytokines and activation of inflammation pathways. The average MPI of key pathways in the epidermis for each patient is shown in Supplementary Figure 1, available at http://onlinelibrary.wiley.com/doi/10.1002/art.42235. Phosphorylation of NF-κB differed significantly between treatment response groups ($P < 0.05$), with a trend toward decreased phosphorylation of NF-κB in QC responders in the post hoc test. Unlike in the dermis, we did not observe a difference in levels of epidermal IFNκ and pSTING among the HCQ responder, QC responder, and nonresponder groups.

Strong correlations in marker expression between all epidermal and dermal pathways were identified (Supplementary Figure 1B). This is further represented by a heatmap of intracellular marker expression in the epidermis and the dermis of each CLE patient (Supplementary Figures 1C and D). There was

marked overlap in staining patterns between the dermis and epidermis, suggesting that the inflammation patterns were highly concordant between these layers.

Increased pSTING and IFNκ in QC responders. Given the up-regulation of pSTING and IFNκ in the QC responder group, we sought to identify colocalization. When both markers were visualized simultaneously, there was demonstrable overlap, suggesting that IFNκ is likely produced in the same cells with increased activation of pSTING (Figures 3A–C). Moreover, we found that pSTING staining intensity and IFNκ staining intensity were positively correlated (r = 0.676) (Figure 3D). The highest degree of staining of both pSTING and IFNκ was seen in cDCs (Figure 3A). In patients with CLE, the number of cDCs in skin biopsy samples was positively correlated with the degree of IFNκ (r = 0.571) and pSTING (r = 0.429) staining (Figure 3E).

To confirm that there are not 2 distinct populations of cDCs, we used FlowJo to visualize IFNκ and pSTING produced by cDCs and identified few single-positive events (results not shown). Levels of CD11c in cDCs and IFNκ in cDCs were also shown to be correlated, although this was expected given the relative expression profile of cDCs in our PhenoGraph-generated heatmap.

We then wanted to confirm whether cDCs positive for pSTING and IFNκ were the cells driving increased expression of these markers in QC responders. Expression of pSTING (P < 0.01) and IFNκ (P < 0.05) in cDCs was significantly increased in QC responders compared to HCQ responders (Figure 3F). To confirm that cDCs were indeed producing IFNκ, we performed mRNA in situ hybridization. We confirmed colocalization of CD11c and IFNκ using IMC (Supplementary Figure 5, available at http://onlinelibrary.wiley.com/doi/10.1002/art.42235), with colocalization of the CD11c mRNA (ITGAX) and IFNκ mRNA observed in QC responder skin (Figure 3G). Furthermore, network analysis showed a high correlation between numbers of cDCs and expression of pSTING/IFNκ in both QC responder and nonresponder patients, with the formation of a correlation triangle indicating stronger associations with each other than with any other pathway (Figures 3I and J). Single-cell staining networks revealed
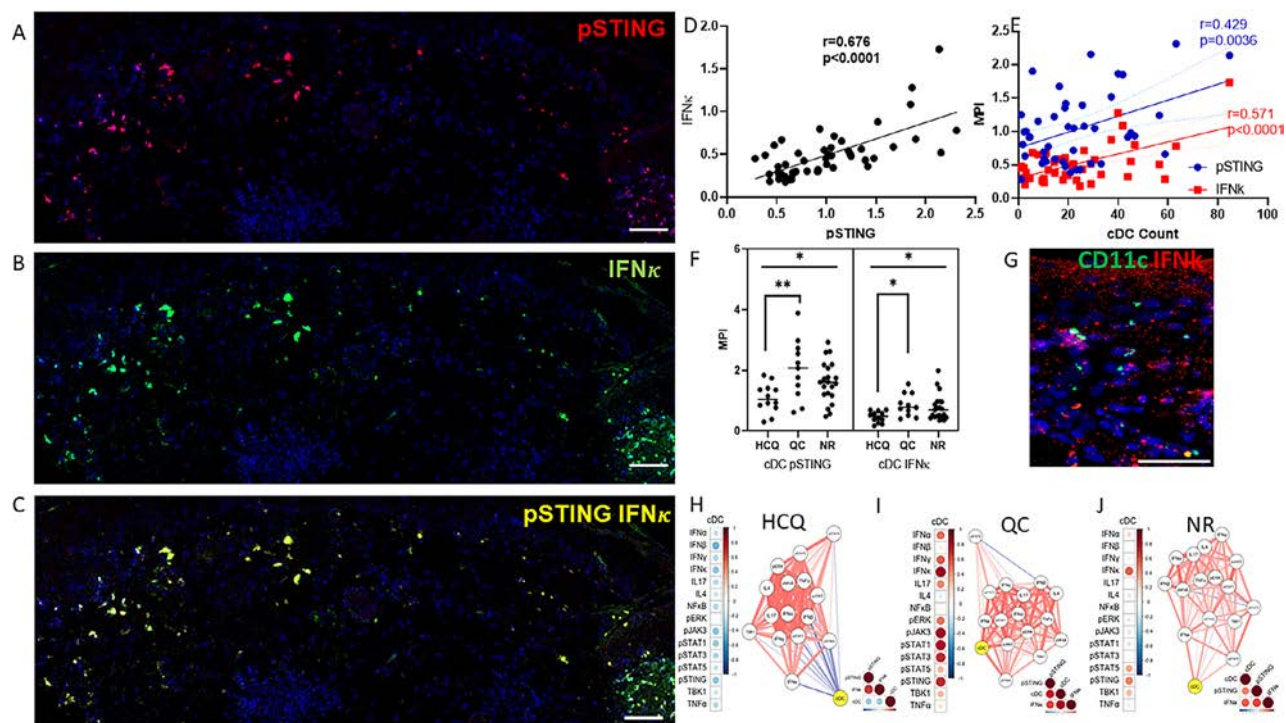

Figure 3. Increased colocalized expression of pSTING and IFNκ increased in cutaneous lupus erythematosus (CLE) patients who responded to treatment with QC. **A–C,** Images generated by imaging mass cytometry displaying staining for phosphorylated stimulator of interferon genes (pSTING) (red) (**A**), interferon-κ (IFNκ) (green) (**B**), and colocalization of pSTING and IFNκ (yellow) (**C**). **D–F,** The staining intensity of pSTING and IFNκ (mean pixel intensity) in conventional dendritic cells (cDCs) from CLE patients was assessed for correlation with each other (**D**) and with the cDC count (**E**), and levels of pSTING and IFNκ expression in cDCs were compared between the hydroxychloroquine (HCQ) responder, quinacrine (QC) responder, and nonresponder (NR) groups (**F**). Symbols represent individual patients; bars show the median and interquartile range. * = P < 0.05; ** = P < 0.01. **G,** In situ hybridization analyses of the skin of CLE patients, showing colocalization of expression of ITGAX (CD11c) mRNA (green) and IFNκ mRNA (red). Epidermal IFNκ mRNA is also visible. **H–J,** Correlation network analysis showing negative associations between cDC level and all panel 1 pathways in HCQ responders (**H**) and strong positive correlations between cDC counts and expression levels of pSTING and IFNκ in QC responders (**I**) and nonresponders (**J**). The triangle cluster formed by the cDC, pSTING, and IFNκ circles indicate that they are more strongly associated with each other than with any other pathways in panel 1. Bars in **A–C** = 100 μm; bar in **G** = 50 μm. IL-4 = interleukin-4; TBK1 = TANK-binding kinase 1; TNF = tumor necrosis factor.

cDCs to be the cell type most closely correlated to overall pSTING and IFNκ levels in QC responder patients (Supplementary Figure 2, available at http://onlinelibrary.wiley.com/doi/10.1002/art.42235). Previous studies have highlighted the dominant role of keratinocytes in the production of IFNκ in CLE, and in the present study we found no difference between levels of IFNκ produced by cDCs and levels of IFNκ produced in the epidermal layer ($P = 0.12$).

Neighborhood analysis and antimalarial nonresponder patient clustering. To determine spatial differences and cellular interactions, we performed neighborhood analysis of patients stratified by antimalarial response, with interactions classified as either significant interactions, significant avoidances, or nonsignificant interactions (Figures 4A–C). CD8+ T cells and γδ T cells interacted in HCQ responders and QC responders but not in nonresponder patients, with a significant negative correlation between the CLASI-A score and numbers of γδ T cells observed only in nonresponder patients ($P < 0.05$) (Supplementary Figure 3, available at http://onlinelibrary.wiley.com/doi/10.1002/art.42235). Similarly, Treg cells interacted with cDCs in HCQ

responders and QC responders but not in nonresponder patients. CD4+ T cells interacted significantly with cDCs in HCQ responders and QC responders, but avoided cDCs in nonresponders. CD14+CD16+ macrophages interacted with endothelial cells in nonresponders, but not in HCQ responders and QC responders. CD8+ T cells interacted with pDCs in nonresponders but not in HCQ responders and QC responders.

Hierarchical patient level clustering within treatment response groups. Given the heterogeneity in immune cell composition among CLE patients, and in particular antimalarial nonresponding patients, we clustered patients according to patterns of expression in each pathway using ClustVis (Figure 4D) (12). We found that nonresponder patients could be differentiated into 3 distinct groups by pathway expression profile. Group 1 expressed IFNα, IFNγ, pSTAT1, pJAK1, pJAK3, IL-4, and IL-17. Group 2 expressed pSTAT3, pSTAT4, pSTAT5, and TANK-binding kinase 1. Group 3 expressed phosphorylated interferon regulatory factor 3 (pIRF3), granzyme B, IRF5, pSTAT2, pERK, and IL-18. Clustering based on cellular composition, global pathway expression, and cellular pathway expression
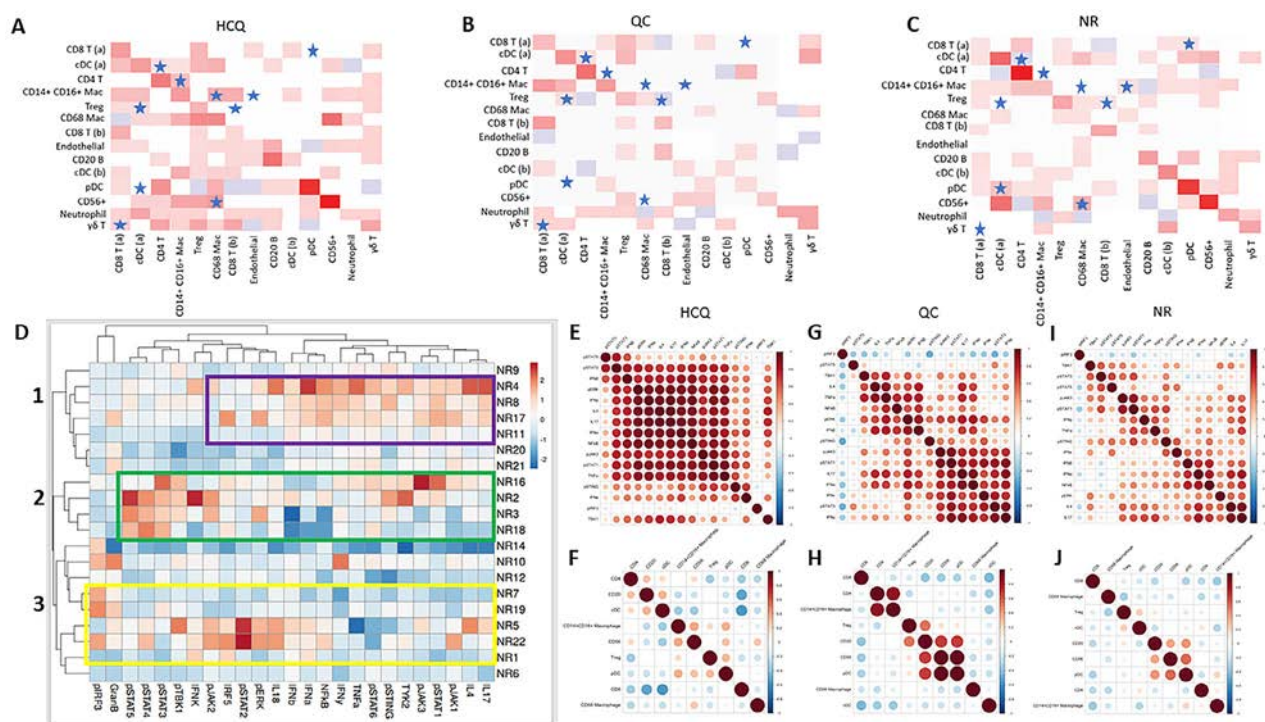

Figure 4. Neighborhood analysis of CLE patients stratified by antimalarial response and unsupervised nonresponder patient clustering. **A–C**, Neighborhood analysis heatmaps representing significant cellular interactions (red squares), significant cellular avoidances (blue squares), and insignificant cellular interactions (white squares) in CLE patients responsive to treatment with HCQ (**A**), CLE patients responsive to treatment with QC (**B**), and CLE patients who did not respond to treatment with antimalarials (**C**). Blue stars highlight differences in key spatial interactions between treatment groups. **D**, Unbiased hierarchical clustering analyses (constructed with ClustVis) of pathway expression profiles in 21 individual CLE patients in the nonresponder (NR) group, showing 3 distinct profiles (purple, green, and yellow boxes). **E–J**, Correlation matrices of intracellular markers and inflammation pathways by treatment response group. pIRF3 = phosphorylated interferon regulatory factor 3; GranB = granzyme B; TBK1 = TANK-binding kinase 1; IFN = interferon; IL-4 = interleukin-4; TNF = tumor necrosis factor; pSTING = phosphorylated stimulator of interferon genes (see Figure 1 for other definitions).

similarly revealed that nonresponder patient groups could be stratified by global and cellular expression of pSTAT3, pSTAT4, and pSTAT5 versus pSTAT2, pIRF3, and granzyme B, with differential pJAK2 expression compared to the remainder of the cohort (Supplementary Figure 6, available at http://onlinelibrary.wiley.com/doi/10.1002/art.42235).

In the QC responder group, we identified a CD8+ T cell–dominant subgroup and a separate cDC-dominant subgroup, both of which included only 3 patients (Supplementary Figure 7A, available at http://onlinelibrary.wiley.com/doi/10.1002/art.42235). Nonresponders demonstrated a CD14+CD16+ macrophage–dominant subgroup (n = 4), a cDC-dominant subgroup (n = 6), and a CD8+ T cell–dominant subgroup (n = 5) (Supplementary Figure 7B). In the HCQ responder group, we identified a large subgroup of CD8+ T cell–dominant patients (Supplementary Figure 7C). This subgroup also demonstrated the highest degree of overall pathway activity, suggesting an important role for cytotoxic T cells in those patients.

Correlation of inflammation pathways within treatment groups but not in antimalarial nonresponders. A correlation matrix of intracellular markers demonstrated positive correlation of pathway expression of many markers among HCQ responders (Figure 4E). This may suggest coregulation or common activators of these markers in patients who respond to treatment with HCQ. Responders to treatment with QC demonstrated 2 distinct groups of inflammation markers: one group of markers regulated by TNFα, pNF-κB, and IFNβ, and the other group of markers regulated by pJAK3, pSTAT1, pSTAT3, IFNα, and IFNκ, each with strong positive correlations (Figure 4G). When evaluating antimalarial nonresponders, we found no correlation between notable groups of pathways (Figure 4I). This may be driven by pathway independence within each patient or marked heterogeneity among nonresponders overall.

For each treatment group, we performed a correlation matrix of cell counts. For HCQ responders and nonresponders (Figures 4F and J), we found minimal correlation with the leukocyte count in CLE patients. In QC responders, cell counts for 2 groups of cells showed positive correlation (Figure 4H). The data showed a positive correlation of CD4+ T cells with CD14+CD16+ macrophages. We also found a second grouping of correlated cells including pDCs, CD56+ NK cells, and CD20+ B cells.

DISCUSSION

Although antimalarials are used as first-line systemic therapy for CLE, treatment response is often unpredictable, with many patients requiring coadministration of a second antimalarial or immunosuppressive drugs (13). Accuracy in predicting treatment response can vary due to the multifactorial nature of CLE pathogenesis, and prediction is currently limited by clinical applications utilizing low-dimensional histology and cytometry. In this study, we used markers of inflammation known to be active in CLE to characterize the immunologic profiles of CLE patients who responded to treatment with HCQ (HCQ responders), patients who responded to treatment with HCQ and QC (QC responders), and patients who did not respond to treatment with antimalarials (nonresponders).

Of the 12 immune cell populations identified, numbers of CD4+ T cells and numbers of Treg cells differed significantly between the 3 treatment response groups. It was found that the treatment-naive skin of patients who later responded to treatment with HCQ contained an expanded CD4+ T cell compartment relative to QC responders. CD4+ T cell pathogenesis may play a greater role in the inflammatory process in HCQ responders as CD4+ T cells may be more susceptible to the therapeutic effects of HCQ. The nonresponder group demonstrated decreased numbers of Treg cells and increased numbers of Tcm cells, suggesting a dysregulation of immune tolerance leading to refractoriness. Treg cells in nonresponders were also weakly associated with other inflammation markers compared to Treg cells in the HCQ responders and the QC responders, suggesting defective regulation of the Treg cell pathway.

Previous studies have identified defects in the Treg cells of SLE patients and decreased Treg cell counts in CLE patients; however, conflicting data exists given the limited markers and differing definitions of Treg cell phenotypes (14). In the present study we identified Treg cells using a multitude of markers, including CD3, CD4, FoxP3, and CD25, which were clustered without supervision. These decreased Treg cell counts in nonresponders may represent defects in trafficking or peripheral induction. Alternatively, this difference may be driven by an increase in the proportions of Treg cells in QC responders. Treg cells may be recruited to the skin of QC responders in response to certain inflammatory signals up-regulated in QC responders, such as IFNκ.

IL-2 is a cytokine critical for Treg cell survival and maintenance in the peripheral immune system, and production of IL-2 is often found to be decreased in SLE patients (15). Low-dose IL-2 therapy has been shown to increase the numbers of Treg cells and ameliorate skin lesions in small SLE clinical trials (16,17). Nonresponder patients with low Treg cell counts may respond to Treg cell–mediated treatment, such as IL-2 therapy or adoptive Treg cell therapy, as an effective strategy to restore autologous immune tolerance, rather than profound immunosuppression. An increase in Tcm cells in antimalarial nonresponders may have detrimental consequences as Tcm cells are known to circulate throughout the immune system and initiate a robust and rapid inflammatory response through T helper cell and B cell support (18). Antimalarials may not be sufficient to suppress this extensive Tcm cell response in nonresponders, because HCQ is known to have differential effects on effector T cell subtypes compared to naive T cells (19).

Of the JAK/STAT pathways, pJAK3 expression was increased in HCQ responders compared to QC responders.

JAK3 is activated by cytokines of the common γ-chain family (including IL-2, IL-4, IL-7, IL-9, IL-15, and IL-21), which may be inhibited by HCQ through transcriptional regulation and p38 MAPK inhibition (20,21). Patients who respond to treatment with HCQ may also respond to novel selective JAK3 inhibitors currently undergoing clinical trials, or to the existing nonselective JAK1/JAK3 inhibitor tofacitinib with the advantage of selective targeting and possibly reduced side effects of HCQ multipathway suppression (22,23).

Patients who responded to treatment with a combination of HCQ and QC had increased levels of IFNκ and pSTING, with trends in increased numbers of cDCs. The STING pathway is activated through the detection of cytosolic DNA, leading to the production of type I IFNs. This pathway is implicated in various autoimmune diseases, particularly in SLE when anti–double-stranded DNA antibodies are present (24). Ultraviolet irradiation induces the production of epidermal IFNκ in CLE patients and is thought to be a major contributor to the initial pathogenesis of the disease (25). STING gene silencing in human keratinocytes leads to a significant reduction in IFNκ production (26). The overlap and correlation of pSTING and IFNκ found through the use of IMC and fluorescence in situ hybridization, suggest a common, targetable pathway within the cDCs of QC responders. Furthermore, network analysis revealed pSTING and IFNκ to be among the pathways most strongly correlated with the number of cDCs, suggesting that the 2 markers are predominantly expressed or regulated by cDCs. In patients receiving treatment with HCQ, the addition of QC has several advantages, as QC has been shown to alternatively suppress type I IFNs when compared to other antimalarials, and QC may inhibit activation of the STING pathway as well as the ultimate production of IFNκ in select patients (27,28). In silico drug library screening identified QC as an inhibitor of STING expression and as a stronger inhibitor of IFNβ expression compared to HCQ (29). This inhibition was cooperative, further reinforcing the use of QC as an adjuvant in select patients with increased STING expression. Given the scarcity of QC in the US, these patients may benefit from treatment with alternative STING inhibitors or from the reintroduction of QC (30,31). This study also highlights the significant differences between HCQ responders and QC responders, reinforcing the need for QC availability.

Our correlation matrices demonstrated many positively correlated intracellular markers in HCQ responders and QC responders. Our data did not reveal correlation among cell types. Patients mainly converge on a pathway level, despite having noticeable differences in cell infiltrates, highlighting greater utility of pathway targeting for precision medicine. The current, evidence-based approach to treatment of CLE is to add QC to the treatment regimen of those patients who do not adequately respond to treatment with HCQ (31). These patients benefit from combination therapy, rather than QC alone. It is possible that each group of correlated inflammation markers in QC responders

may be amenable to treatment with either HCQ or QC. Different subsets of nonresponder pathway correlations demonstrate heterogeneity of inflammation in these patients and support the need for personalized therapy.

IMC analysis also allows for single-cell pathway comparison. Multiplexed images may be segmented in order to create cellular outlines based on surface markers or nuclear expansion, allowing for software-assisted extrapolation of intracellular antigen expression within cellular borders (32). Using this technology, we identified multiple single-cell differences between the treatment response groups. Increased expression of IFNγ may be affected by treatment with HCQ, as multiple studies have shown inhibition of IFNγ expression by HCQ in vitro, and our data show increased expression of IFNγ in the neutrophils and cDCs of HCQ responders (33–35). The STAT1 pathway is activated by IFNγ, and gain-of-function mutations have identified a relative deficiency in IL-17 expression. In patients who respond to treatment with HCQ, increased IFNγ production may stimulate expression of STAT1, leading to compounding effects such as an observed increase in pSTAT1 in the endothelium, resulting in activation and up-regulation of adhesive molecules (36). Similarly in HCQ responders, CD68+ macrophage–expressed pSTAT1 may be increased in response to IFNγ signaling, promoting an M1 phenotype (37). Nonresponders demonstrated increased CD4+ T cell–expressed IRF5, which may contribute to HCQ refractoriness as HCQ is known to inhibit Toll-like receptor 7, Toll-like receptor 9, and downstream IRF7-mediated IFN-1, although little is known about the effects of HCQ on IRF5-mediated cytokine and autoantibody production (38–40). The effects of CD4+ T cell–expressed IRF5 may be overcome with novel cell-penetrating peptides in order to prevent homodimerization in patients who do not respond to treatment with antimalarials (41).

B cell–expressed JAK2 is known to enhance cell adhesion and survival, possibly contributing to the production of autoantibodies in QC responders (42). Novel JAK2 inhibitors such as ruxolitinib, fedratinib, and baricitinib may serve as substitutes for QC in patients who do not respond to treatment with HCQ (43). In nonresponder patients, endothelial cells and CD8+ T cells showed increased expression of pSTAT3, which may be responsive to mycophenolate mofetil, as that medication has been shown to reduce the effects of STAT3 and Th17 in SLE patients (43). Of the type I IFNs compared in this study, expression of IFNα was increased in the CD8+ T cells of nonresponders, suggesting a difference in antimalarial responsiveness based on the cell type in which type I IFNs are expressed. Little is known about the production of type I IFNs by cytotoxic T cells; further research may elucidate novel targetable pathways for CLE patients whose disease is refractory to antimalarial treatment.

Differences among treatment response groups also extended to interactions between immune cells. Treg cells in nonresponder patients did not interact with cDCs, suggesting a deficiency in tolerance as they were also decreased in number.

Moreover, γδ T cells routinely monitor skin integrity and possess suppressive functions through the production of insulin-like growth factor 1 and transforming growth factor β. In nonresponders, γδ T cells did not interact with cytotoxic CD8+ T cells; however, this interaction was present in HCQ responders and QC responders, suggesting another deficiency in the immune response mechanisms of patients who do not respond to treatment with antimalarials (44,45). The negative correlation of γδ T cells with CLASI scores that we observed exclusively in nonresponders further supports this finding. Nonresponder patients also demonstrated fewer interactions between CD4+ T cells and cDCs, but an increased number of interactions between CD14+CD16+ macrophages and endothelium, indicating that infiltration had occurred, and increased number of interactions between pDCs and CD8+ T cells, suggesting that there was cytotoxic augmentation through local type I IFNs.

Our data also demonstrated that differences in the activation of inflammatory pathways and cytokines in the epidermis may have been different between the 3 treatment response groups, with a trend toward decreased phosphorylation of NF-κB in QC responders. The overall inflammation profile of the epidermis and inflammation profile of the dermis overlapped across all treatment groups, encouraging noninvasive techniques for the diagnosis of CLE, such as tape stripping (46). Sampling of keratinocytes may in fact yield information regarding the inflammation profile of the dermis, making the performance of skin biopsy unnecessary (47).

Treatment response prediction historically involves clinical data from randomized controlled trials that identify differences between treatment groups; however, such groups are often heterogeneous, and a single patient may not conform to either group on an individual level. Given the heterogeneity of the immune infiltrate among our groups of CLE patients, we implemented an unbiased patient clustering system using ClustVis (12). Nonresponder patients stratified into 3 groups according to pathway expression, highlighting diverse pathophysiologic patterns driven by either IFNγ, IL-4, IL-17, pJAK1, and pJAK3, or by pSTAT3, pSTAT4, and pSTAT5, or by pSTAT2, pIRF3, and granzyme B. Such individual differences may guide the ultimate selection of treatment, given the wide array of immunosuppressives and the known differences in pathway suppression. CLE patients may benefit greatly from personalized medicine approaches such as those that determine patient-specific targetable disease features.

We also identified a surprising paucity of type I IFN+ pDCs in our CLE patients, with the major producers being myeloid lineage cells. Our data demonstrated a relatively low MPI of type I IFN+ pDCs. The absolute counts and percentages of IFNα+ and IFNβ+ pDCs were also minimal. These results cut across a decade-long paradigm that places type I IFNs produced by pDCs at the center of lupus pathogenesis (48). The prominent role of type I IFNs in LE is well established (49,50). Several in vivo studies have shown that IFNα production, in response to CpG challenge, is exclusively dependent on pDCs (51–53). It is also well known that pDCs are

capable of producing type I IFNs abundantly and rapidly, producing over 1,000 times more type I IFNs than other cell types under appropriate stimulation (54,55). Naturally, it seems logical to assume that pDCs play a crucial role in autoimmune connective tissue diseases such as LE.

However, these results do not entirely contradict the findings in the current literature on the pathophysiologic processes of lupus. Recently, Psarras et al implicated a largely exhausted and unimportant role for pDCs in the pathogenesis of LE (56). These findings represent a crucial junction in the understanding of pDC biology and their role in autoimmunity. Indeed, previous studies have demonstrated decreased circulating pDCs in SLE patients (48,57). Some have hypothesized that type I IFN–producing pDCs were instead present in the end organs such as the skin and kidneys (49). Our results suggest that pDCs are not, in fact, major drivers of type I IFN production in the setting of CLE, and that myeloid cell lineages are the major contributors of type I IFNs. A subset of NK cells also express type I IFNs; however, like pDCs, they are relatively scarce in tissue. Given the success of anti–blood dendritic cell antigen 2 (58) therapy in patients with LE and the recent and promising initial success of VIB7734 (59), a monoclonal antibody directed against immunoglobulin-like transcript 7 (another pDC-specific marker), pDCs likely play an important role for some CLE patients. Ultimately, we believe these results highlight the complex and unclear role pDCs play in the pathogenesis of LE. Studies to confirm these findings and elucidate the role of pDCs in CLE are currently under way by our group.

This study was limited by sample size and the use of markers determined to be critical to CLE pathogenesis and is not all-inclusive. Cell clustering is limited by the resolution of IMC, and thus may cluster overlapping cells that were ultimately refined manually. A lack of multiple hypothesis testing limits the conclusions that can be drawn from this discovery pilot study; however, key findings were confirmed by manual identification of IMC images and fluorescence in situ hybridization exploration. By using IMC analysis for CLE patients stratified by antimalarial response, we were able to identify significant differences in their immune profiles. These differences will guide future therapies and encourage a more personalized approach to treatment, one that combines clinical, histopathologic, and immunologic sources of data.

AUTHOR CONTRIBUTIONS

All authors were involved in drafting the article or revising it critically for important intellectual content, and all authors approved the final version to be published. Dr. Vazquez had full access to all of the data in the study and takes responsibility for the integrity of the data and the accuracy of the data analysis.
Study conception and design. Patel, Vazquez, Werth.

Acquisition of data. Patel, Vazquez, Werth.
Analysis and interpretation of data. Patel, Vazquez, Chin, Keyes, Yan, Diaz, Grinnell, Sharma, Li, Feng, Sprow, Dan, Werth.

REFERENCES

1. Fabbri P, Cardinali C, Giomi B, Caproni M. Cutaneous lupus erythematosus: diagnosis and management. Am J Clin Dermatol 2003;4: 449–65.

2. Klein R, Moghadam-Kia S, Taylor L, Coley C, Okawa J, LoMonico J, et al. Quality of life in cutaneous lupus erythematosus. J Am Acad Dermatol 2011;64:849–58.

3. Chang AY, Ghazi E, Okawa J, Werth VP. Quality of life differences between responders and nonresponders in the treatment of cutaneous lupus erythematosus. JAMA Dermatol 2013;149:104–6.

4. Patel J, Borucki R, Werth VP. An update on the pathogenesis of cutaneous lupus erythematosus and its role in clinical practice. Curr Rheumatol Rep 2020;22:69.

5. Walling HW, Sontheimer RD. Cutaneous lupus erythematosus: issues in diagnosis and treatment. Am J Clin Dermatol 2009;10:365–81.

6. Kalia S, Dutz JP. New concepts in antimalarial use and mode of action in dermatology. Dermatol Ther 2007;20:160–74.

7. Wozniacka A, Carter A, McCauliffe DP. Antimalarials in cutaneous lupus erythematosus: mechanisms of therapeutic benefit. Lupus 2002;11:71–81.

8. Zeidi M, Kim HJ, Werth VP. Increased myeloid dendritic cells and TNF-α expression predicts poor response to hydroxychloroquine in cutaneous lupus erythematosus. J Invest Dermatol 2019;139: 324–32.

9. Sontheimer RD, Thomas JR, Gilliam JN. Subacute cutaneous lupus erythematosus: a cutaneous marker for a distinct lupus erythematosus subset. Arch Dermatol 1979;115:1409–15.

10. Hochberg MC. Updating the American College of Rheumatology revised criteria for the classification of systemic lupus erythematosus [letter]. Arthritis Rheum 1997;40:1725.

11. Albrecht J, Taylor L, Berlin JA, Dulay S, Ang G, Fakharzadeh S, et al. The CLASI (Cutaneous Lupus Erythematosus Disease Area and Severity Index): an outcome instrument for cutaneous lupus erythematosus. J Invest Dermatol 2005;125:889–94.

12. Metsalu T, Vilo J. ClustVis: a web tool for visualizing clustering of multivariate data using Principal Component Analysis and heatmap. Nucleic Acids Res 2015;43:W566–70.

13. Borucki R, Werth VP. An evidence-based approach to refractory cutaneous lupus erythematosus. Arthritis Rheumatol 2020;72: 1777–85.

14. Miyara M, Amoura Z, Parizot C, Badoual C, Dorgham K, Trad S, et al. Global natural regulatory T cell depletion in active systemic lupus erythematosus. J Immunol 2005;175:8392–400.

15. Furtado GC, de Lafaille MA, Kutchukhidze N, Lafaille JJ. Interleukin 2 signaling is required for CD4(+) regulatory T cell function. J Exp Med 2002;196:851–7.

16. Humrich JY, von Spee-Mayer C, Siegert E, Alexander T, Hiepe F, Radbruch A, et al. Rapid induction of clinical remission by low-dose interleukin-2 in a patient with refractory SLE. Ann Rheum Dis 2015; 74:791–2.

17. Von Spee-Mayer C, Siegert E, Abdirama D, Rose A, Klaus A, Alexander T, et al. Low-dose interleukin-2 selectively corrects regulatory T cell defects in patients with systemic lupus erythematosus. Ann Rheum Dis 2016;75:1407–15.

18. Raphael I, Joern RR, Forsthuber TG. Memory CD4(+) T cells in immunity and autoimmune diseases [review]. Cells 2020;9:531.

19. Van Loosdregt J, Spreafico R, Rossetti M, Prakken BJ, Lotz M, Albani S. Hydroxychloroquine preferentially induces apoptosis of CD45RO+ effector T cells by inhibiting autophagy: a possible mechanism for therapeutic modulation of T cells. J Allergy Clin Immunol 2013;131:1443–6.

20. Chen M, Cheng A, Chen YQ, Hymel A, Hanson EP, Kimmel L, et al. The amino terminus of JAK3 is necessary and sufficient for binding to the common gamma chain and confers the ability to transmit interleukin 2-mediated signals. Proc Natl Acad Sci U S A 1997;94:6910–5.

21. Roldan EQ, Biasiotto G, Magro P, Zanella I. The possible mechanisms of action of 4-aminoquinolines (chloroquine/hydroxychloroquine) against Sars-Cov-2 infection (COVID-19): a role for iron homeostasis? Pharmacol Res 2020;158:104904.

22. Robinson MF, Damjanov N, Stamenkovic B, Radunovic G, Kivitz A, Cox L, et al. Efficacy and safety of PF-06651600 (Ritlecitinib), a novel JAK3/TEC inhibitor, in patients with moderate-to-severe rheumatoid arthritis and an inadequate response to methotrexate. Arthritis Rheumatol 2020;72:1621–31.

23. Farmer LJ, Ledeboer MW, Hoock T, Arnost MJ, Bethiel RS, Bennani YL, et al. Discovery of VX-509 (decernotinib): a potent and selective janus kinase 3 inhibitor for the treatment of autoimmune diseases. J Med Chem 2015;58:7195–216.

24. Decout A, Katz JD, Venkatraman S, Ablasser A. The cGAS-STING pathway as a therapeutic target in inflammatory diseases. Nat Rev Immunol 2021:1–22.

25. Sarkar MK, Hile GA, Tsoi LC, Xing X, Liu J, Liang Y, et al. Photosensitivity and type I IFN responses in cutaneous lupus are driven by epidermal-derived interferon kappa. Ann Rheum Dis 2018;77: 1653–64.

26. Sunthamala N, Thierry F, Teissier S, Pientong C, Kongyingyoes B, Tangsiriwatthana T, et al. E2 proteins of high risk human papillomaviruses down-modulate STING and IFN-κ transcription in keratinocytes. PLoS ONE 2014;9:e91473.

27. Cardoso EC, Pereira NZ, Mitsunari GE, Oliveira LM, Ruocco RM, Francisco RP, et al. TLR7/TLR8 activation restores defective cytokine secretion by myeloid dendritic cells but not by plasmacytoid dendritic cells in HIV-infected pregnant women and newborns. PLoS ONE 2013;8:e67036.

28. Alves P, Bashir MM, Wysocka M, Zeidi M, Feng R, Werth VP. Quinacrine suppresses tumor necrosis factor-α and IFN-α in dermatomyositis and cutaneous lupus erythematosus. J Investig Dermatol Symp Proc 2017;18:S57–63.

29. An J, Woodward JJ, Sasaki T, Minie M, Elkon KB. Cutting edge: antimalarial drugs inhibit IFN-β production through blockade of cyclic GMP-AMP synthase-DNA interaction. J Immunol 2015;194: 4089–93.

30. Thim-Uam A, Prabakaran T, Tansakul M, Makjaroen J, Wongkongkathep P, Chantaravisoot N, et al. STING mediates lupus via the activation of conventional dendritic cell maturation and plasmacytoid dendritic cell differentiation. iScience 2020;23:101530.

31. Chang AY, Piette EW, Foering KP, Tenhave TR, Okawa J, Werth VP. Response to antimalarial agents in cutaneous lupus erythematosus: a prospective analysis. Arch Dermatol 2011;147:1261–7.

32. Schapiro D, Jackson HW, Raghuraman S, Fischer JR, Zanotelli VR, Schulz D, et al. histoCAT: analysis of cell phenotypes and interactions in multiplex image cytometry data. Nat Methods 2017;14:873–6.

33. Da Silva JC, Mariz HA, da Rocha LF Jr, de Oliveira PS, Dantas AT, Duarte AL, et al. Hydroxychloroquine decreases Th17-related cytokines in systemic lupus erythematosus and rheumatoid arthritis patients. Clinics (Sao Paulo) 2013;68:766–71.

34. Van den Borne B, Dijkmans B, De Rooij H, Le Cessie S, Verweij C. Chloroquine and hydroxychloroquine equally affect tumor necrosis factor-alpha, interleukin 6, and interferon-gamma production by peripheral blood mononuclear cells. J Rheumatol 1997;24:55–60.

35. Jeong JY, Choi JW, Jeon KI, Jue DM. Chloroquine decreases cell-surface expression of tumour necrosis factor receptors in human histiocytic U-937 cells. Immunology 2002;105:83–91.

36. Sikorski K, Chmielewski S, Przybyl L, Heemann U, Wesoly J, Baumann M, et al. STAT1-mediated signal integration between IFNγ and LPS leads to increased EC and SMC activation and monocyte adhesion. Am J Physiol Cell Physiol 2011;300:C1337–44.

37. Kim HS, Kim DC, Kim HM, Kwon HJ, Kwon SJ, Kang SJ, et al. STAT1 deficiency redirects IFN signalling toward suppression of TLR response through a feedback activation of STAT3. Sci Rep 2015;5: 1–15.

38. Manni M, Gupta S, Ricker E, Chinenov Y, Park SH, Shi M, et al. Regulation of age-associated B cells by IRF5 in systemic autoimmunity. Nat Immunol 2018;19:407–19.

39. Savitsky DA, Yanai H, Tamura T, Taniguchi T, Honda K. Contribution of IRF5 in B cells to the development of murine SLE-like disease through its transcriptional control of the IgG2a locus. Proc Natl Acad Sci U S A 2010;107:10154–9.

40. Takaoka A, Yanai H, Kondo S, Duncan G, Negishi H, Mizutani T, et al. Integral role of IRF-5 in the gene induction programme activated by Toll-like receptors. Nature 2005;434:243–9.

41. Banga J, Srinivasan D, Sun CC, Thompson CD, Milletti F, Huang KS, et al. Inhibition of IRF5 cellular activity with cell-penetrating peptides that target homodimerization. Sci Adv 2020;6:eaay1057.

42. Montresor A, Toffali L, Mirenda M, Rigo A, Vinante F, Laudanna C. JAK2 tyrosine kinase mediates integrin activation induced by CXCL12 in B-cell chronic lymphocytic leukemia. Oncotarget 2015;6: 34245–57.

43. Davis RR, Li B, Yun SY, Chan A, Nareddy P, Gunawan S, et al. Structural insights into JAK2 inhibition by ruxolitinib, fedratinib, and derivatives thereof. J Med Chem 2021;64:2228–41.

44. Toulon A, Breton L, Taylor KR, Tenenhaus M, Bhavsar D, Lanigan C, et al. A role for human skin-resident T cells in wound healing. J Exp Med 2009;206:743–50.

45. Yang J, Weinberg RA. Epithelial-mesenchymal transition: at the crossroads of development and tumor metastasis. Dev Cell 2008; 14:818–29.

46. Berekméri A, Tiganescu A, Alase AA, Vital E, Stacey M, Wittmann M. Non-invasive approaches for the diagnosis of autoimmune/autoinflammatory skin diseases-a focus on psoriasis and lupus erythematosus [review]. Front Immunol 2019;10:1931.

47. Merola JF, Wang W, Wager CG, Hamann S, Zhang X, Thai A, et al. RNA tape sampling in cutaneous lupus erythematosus discriminates affected from unaffected and healthy volunteer skin. Lupus Sci Med 2021;8:e000428.

48. Blomberg S, Eloranta ML, Cederblad B, Nordlin K, Alm GV, Rönnblom L. Presence of cutaneous interferon-α producing cells in patients with systemic lupus erythematosus. Lupus 2001;10:484–90.

49. Rönnblom L, Leonard D. Interferon pathway in SLE: one key to unlocking the mystery of the disease. Lupus Sci Med 2019;6: e000270.

50. Crow MK, Ronnblom L. Type I interferons in host defence and inflammatory diseases. Lupus Sci Med 2019;6:e000336.

51. Cisse B, Caton ML, Lehner M, Maeda T, Scheu S, Locksley R, et al. Transcription factor E2-2 is an essential and specific regulator of plasmacytoid dendritic cell development. Cell 2008;135:37–48.

52. Asselin-Paturel C, Brizard G, Pin JJ, Brière F, Trinchieri G. Mouse strain differences in plasmacytoid dendritic cell frequency and function revealed by a novel monoclonal antibody. J Immunol 2003;171: 6466–77.

53. Kumagai Y, Takeuchi O, Kato H, Kumar H, Matsui K, Morii E, et al. Alveolar macrophages are the primary interferon-alpha producer in pulmonary infection with RNA viruses. Immunity 2007;27:240–52.

54. Cella M, Jarrossay D, Facchetti F, Alebardi O, Nakajima H, Lanzavecchia A, et al. Plasmacytoid monocytes migrate to inflamed lymph nodes and produce large amounts of type I interferon. Nat Med 1999;5:919–23.

55. Liu YJ. IPC: professional type 1 interferon-producing cells and plasmacytoid dendritic cell precursors. Annu Rev Immunol 2005;23: 275–306.

56. Psarras A, Alase A, Antanaviciute A, Carr IM, Yusof MY, Wittmann M, et al. Functionally impaired plasmacytoid dendritic cells and non-haematopoietic sources of type I interferon characterize human autoimmunity. Nat Commun 2020;11:6149.

57. Farkas L, Beiske K, Lund-Johansen F, Brandtzaeg P, Jahnsen FL. Plasmacytoid dendritic cells (natural interferon- α/β-producing cells) accumulate in cutaneous lupus erythematosus lesions. Am J Pathol 2001;159:237–43.

58. Furie R, Werth VP, Merola JF, Stevenson L, Reynolds TL, Naik H, et al. Monoclonal antibody targeting BDCA2 ameliorates skin lesions in systemic lupus erythematosus. J Clin Invest 2019;129:1359–71.

59. Karnell JL, Wu Y, Mittereder N, Smith MA, Gunsior M, Yan L, et al. Depleting plasmacytoid dendritic cells reduces local type I interferon responses and disease activity in patients with cutaneous lupus. Sci Transl Med 2021;13:eabf8442.

AMERICAN COLLEGE
of RHEUMATOLOGY
Empowering Rheumatology Professionals

BRIEF REPORT

In Vivo Generation of SSA/Ro Antigen–Specific Regulatory T Cells Improves Experimental Sjögren's Syndrome in Mice

Junji Xu,[1] Ousheng Liu,[2] Dandan Wang,[2] Fu Wang,[2] Dunfang Zhang,[2] Wenwen Jin,[2] Alexander Cain,[2] Andrew Bynum,[2] Na Liu,[2] Yichen Han,[2] and WanJun Chen[2] (iD)

Objective. Sjögren's syndrome (SS) is a systemic autoimmune disease, and T cells play an important role in the initiation and perpetuation of the disease. In this study, we developed an immunotherapy for NOD/LtJ mice with SS-like symptoms by combining a transient depletion of CD4+ T cells with the administration of autoantigen-specific peptide Ro480.

Methods. NOD/LtJ mice were treated with single anti-CD4 monoclonal antibody (mAb) followed 2 days later by a series of 6 intraperitoneal injections of Ro480–494 every other day. Salivary flow rates were determined pre- and posttreatment once a week. Mice were euthanized 6 weeks after the initial anti-CD4 mAb treatment, salivary glands (SGs) were collected for analyses of histologic disease scores and inflammatory cell infiltration, polymerase chain reaction determination of genes was conducted, and flow cytometry analysis including major histocompatibility complex class II tetramer staining of immune cells was performed. In addition, adoptive transfer of Treg cells was administrated to investigate the function of the newly generating Treg cells in vivo.

Results. The combination of anti-CD4 mAb with autoantigen-specific peptide Ro480 generated SSA/Ro antigen–specific Treg cells in vivo, which can suppress interferon-γ production of CD4+ T cells and inflammation infiltration in SGs and maintain the function of SGs.

Conclusion. Our findings provide a new approach to generating antigen-specific Treg cells in vivo for SS treatment, which may have implications for potential therapy for patients with SS.

INTRODUCTION

Primary Sjögren's syndrome (SS) is a systemic autoimmune disease characterized by lymphocytic infiltration of the exocrine glands such as salivary glands (SGs) and lacrimal glands (1). The primary pathophysiology of SS includes concurrent mechanisms of dysregulated innate and adaptive immunity involving cell-mediated and humoral disease processes, characterized by lymphocytic infiltrates and destruction of the SGs and lacrimal glands and systemic production of autoantibodies to the ribonucleoprotein particles SSA/Ro and SSB/La (2).

The roles of T cells in the initiation and perpetuation of SS have been reported for decades. Activated T cells contribute to the pathogenesis by producing proinflammatory cytokines, including interferon-γ (IFNγ), and by inducing B cell activation. T cells may also be involved in a loss of self-tolerance; considerable evidence supports the notion that regulatory Treg cells are impaired in SS patients (3). Accumulated evidence indicates that manipulation of CD4+CD25+FoxP3+ Treg cells holds promise for developing immunotherapy for autoimmune and inflammatory diseases (4–6).

Treg cells are instrumental in the induction and maintenance of immunologic tolerance (4). Transforming growth factor β

[1]Junji Xu, DDS, PhD: Mucosal Immunology Section, National Institute of Dental and Craniofacial Research, NIH, Bethesda, Maryland, and Department of Periodontology, School of Stomatology, Capital Medical University, Beijing, China (current address); [2]Ousheng Liu, DDS, PhD, Dandan Wang, MD, PhD, Fu Wang, DDS, PhD, Dunfang Zhang, PhD, Wenwen Jin, MS, Alexander Cain, DDS, Andrew Bynum, MS, Na Liu, PhD, Yichen Han, MD, PhD, WanJun Chen, MD: Mucosal Immunology Section, National Institute of Dental and Craniofacial Research, NIH, Bethesda, Maryland.

(TGFβ) induces FoxP3 gene expression in T cell receptor (TCR)–stimulated CD4+CD25– naive T cells, which mediates their transition toward a Treg cell phenotype with potent immunosuppressive potential (7). TGFβ can be produced by phagocytes, such as macrophages exposed to apoptotic cells, which induces CD4+FoxP3+ Treg cells in culture and also contributes to immune tolerance in vivo (8). Previously, we developed an approach to suppress experimental autoimmune encephalomyelitis and type 1 diabetes mellitus in animals by induction of respective autoantigen-specific Treg cells in vivo, which is accomplished with a combination of transient B cell depletion or immune cell apoptosis with single- and low-dose gamma irradiation, in addition to autopeptide administration (9). However, it is unknown whether this therapy is beneficial for SS.

In the present study, we show that induction of apoptotic T cells with a single injection of anti-CD4 antibody followed by administration of autoantigenic peptide Ro480 significantly suppresses SS-like symptoms in NOD/LtJ mice, which was achieved by the generation of the autoantigen-specific Treg cells in vivo. Our findings may have implications for the development of similar immunotherapy for patients with SS.

MATERIALS AND METHODS

Animals. Female NOD/LtJ mice (n = 45) were purchased from The Jackson Laboratory and maintained under specific pathogen–free conditions. The experiments were approved by the Animal Care and Use Committees of National Institute of Dental and Craniofacial Research, National Institutes of Health, performed in accordance with the guiding principles in the care and use of animals. Data sampling, evaluation, and presentation complied with the Animals in Research: Reporting In Vivo Experiments guidelines.

Antibodies and peptides used in vivo. Anti-CD4 (clone Gk1.5) was purchased from Bio X Cell. Peptides Ro480–494 (amino acid sequence AIALREYRKKMDIPA), Ro274–290 (QEMPLTALLRNLGKMT), and ovalbumin (OVA) 323–339 (ISQAVHAAHAEINEAGR) was synthesized and purchased from GenScript Inc.

Cell isolation and adoptive transfer of Treg cells. CD4+ T cells, CD4+CD25+ T cells, and CD4+CD25– T cells were isolated from spleens via either positive or negative selection using magnetic-activated cell sorting isolation kits following protocols of the manufacturer (Miltenyi Biotec). Briefly, CD4+CD25– T cells were isolated using a Treg cell isolation kit (Miltenyi Biotec). Non-CD4+ T cells were isolated via negative selection using a Treg cell isolation kit (purity of cell separation was >90% each) and used as antigen-presenting cells (APCs) after irradiation with 3,000 rads of gamma irradiation (Gammacell 1000; Best Theratronics). For adoptive transfer, splenic Treg cells

were isolated from anti-CD4 mAb and OVA–treated or anti-CD4 and Ro480–treated NOD/LtJ mice using a Treg cell isolation kit, and Treg cells were transferred to naive NOD/LtJ mice at a dose of 2×10^5 cells per mouse by intraperitoneal injection.

In vitro cell cultures, proliferation assays, and cytokine assays. Splenocytes were cultured at 37°C in 5% CO^2 for 3 days with either soluble CD3-specific antibody (anti-CD3; 0.5 μg/ml) or peptide (Ro480; 50 μg/ml as indicated). After 3 days of culture supernatant, cells were collected for cytokine assays and determination of T cell proliferation. We quantified the following cytokines in culture supernatants by enzyme-linked immunosorbent assay: IFNγ, interleukin-4 (IL-4), and IL-17a (all from BioLegend). Cell proliferation was determined by Ki-67 staining.

Salivary flow rate measurement. For the saliva flow rate test, mice were weighed and mild anesthesia was induced with ketamine and xylazine (20 mg/ml; Sigma) injected intraperitoneally (1 μl/g). Salivary secretion was stimulated using 0.1 ml/kg body weight of a pilocarpine (50 mg/ml). Animals were positioned with a 75-mm hematocrit tube placed in the oral cavity, and whole saliva was collected into preweighed 0.75 ml Eppendorf tubes for 10 minutes.

Histologic staining and analysis. SGs were collected and fixed in 10% formalin, embedded in paraffin, cut into 5-μm sections, and stained with hematoxylin and eosin (H&E). Anti–aquaporin 5 (anti–AQP-5) monoclonal antibodies (mAb) (Abcam) and anti–sodium, potassium, and chloride cotransporter 1 (anti-NKCC1) mAb (Santa Cruz Biotechnology) were used for immunofluorescence staining, and images were obtained using a Leica TCS SP8 microscope. For H&E staining, the counts and area of inflammatory focus (containing >50 lymphocytes per 4-mm^2 tissue) was calculated per field at 200× magnification. Three entire SG sections for each animal were counted, with an average of 10 fields, by an expert of histopathology (FW) in a blinded manner.

Flow cytometry analysis. SGs were digested with collagenase type II (4 mg/ml)/Dispase type II (4.67 mg/ml; both from Worthington) combined in Hanks' balanced salt solution for 15 minutes at 37°C. Single-cell suspension was stained with the following antibodies: IL-17a (clone ebio17B7), CD4 (clone RM4-4 and RM4-5), CD8β (clone H35-17.2), CD19 (clone 1D3), FoxP3 (clone FJK-16s), Ki-67 (clone SolA15), IFNγ (clone XMG1.2), IL-4 (clone 11B11), IL-10 (clone JES5-16E3), and KLRG1 (clone 2F1). I-A^b major histocompatibility complex (MHC) class II tetramer complexes that were refolded with synthetic peptides Ro480, Ro274, and OVA323 and subsequently conjugated with allophycocyanin were customized and synthesized (Helixgen, Ltd. and MBL, Inc). Fixation/permeabilization

buffer solution (eBioscience) was used for intranuclear staining. For intracellular cytokine staining, cells were stimulated with phorbol myristate acetate (50 ng/ml; Sigma), ionomycin (250 ng/ml; Sigma), and GolgiPlug (1:1,000 dilution; BD PharMingen) at 37°C for 4 hours, followed by fixation with the fixation/permeabilization buffer solution (BD Biosciences). Stained cells were analyzed on an LSRFortessa (BD Biosciences), and data were analyzed with FlowJo software.

Statistical analysis. All data show a normal distribution and are presented as the mean ± SEM of 3 independent experiments. We used an α level of 0.05 for all statistical tests. The mice salivary flow rates were statistically analyzed with repeated

measurement; other data were analyzed with one-way analysis of variance.

RESULTS

Suppression of SS-like symptoms in NOD/LtJ mice by anti-CD4 mAb and autopeptide Ro480. First, we tested the hypothesis of inducing a specific immune tolerance by the combination of anti-CD4 mAb followed by the administration of a known self peptide, Ro480 (10), in a mouse model of SS to induce the generation of SSA/Ro antigen–specific Treg cells. Since NOD/LtJ mice spontaneously develop SS-like symptoms, including inflammation and dysfunction in SGs, from 7–8 weeks
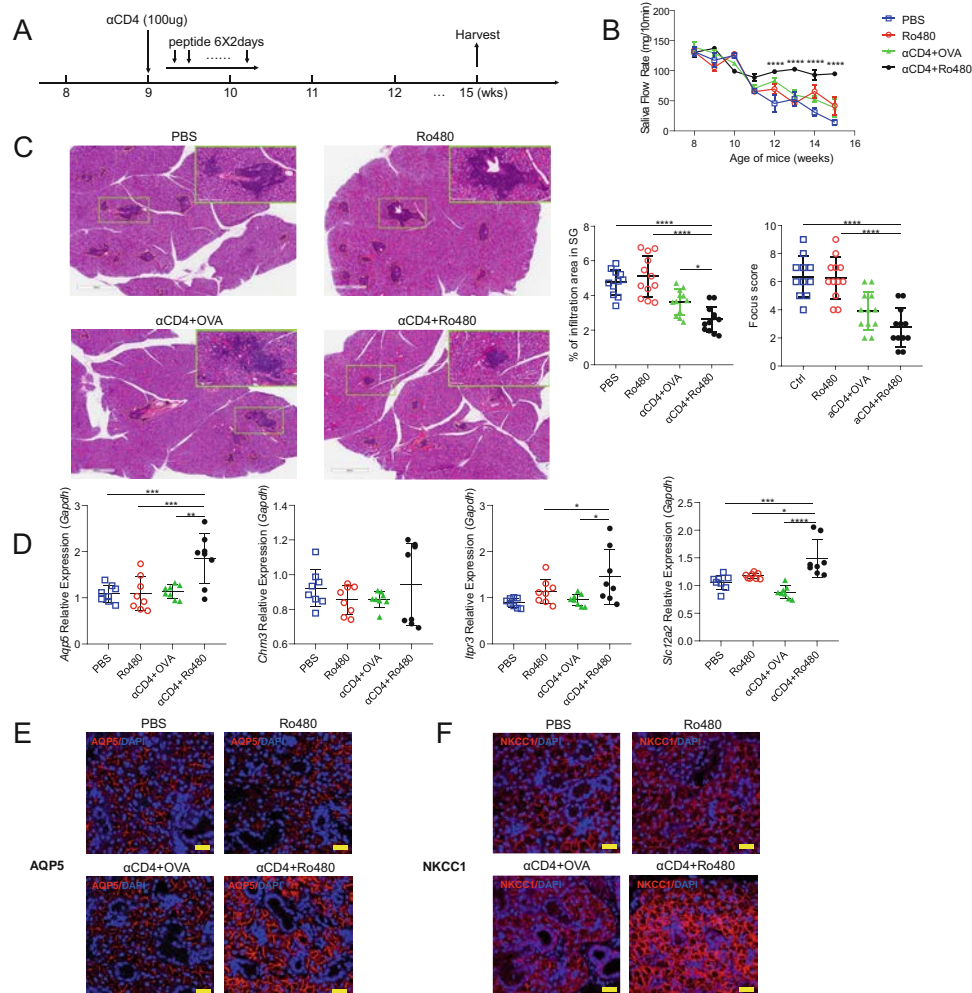
Figure 1. Therapeutic effects of combined anti-CD4 (αCD4) and self peptide treatment in animals with Sjögren's syndrome–like symptoms. **A**, NOD/LtJ mice (9 weeks old; n = 9–12) were treated with 100 μg anti-CD4 monoclonal antibody (mAb), followed by 6 intraperitoneal injections of peptide Ro480–494 injection every other day from 2 days after anti-CD4 mAb treatment (anti-CD4 + Ro480). Mice were euthanized at 15 weeks of age. **B**, Salivary flow rates during the observation are shown. **C**, Formalin-fixed sections of the salivary glands (SGs) of representative mice in each group were stained with hematoxylin and eosin (left), and both the percentage of infiltration area and focus scores of SGs were analyzed (right). Bars = 600 μm. **Inset**, higher-magnification views of the boxed areas. **D**, Expression levels of *Aqp5*, *Chm3*, *Itpr3*, and *Slc12a2* were assessed in the SGs by real-time reverse transcriptase–polymerase chain reaction. **E** and **F**, Immunofluorescence staining was conducted to detect aquaporin 5 (AQP5) (**E**) and sodium, potassium, and chloride cotransporter 1 (NKCC1) (**F**) in the SGs. Bars = 25 μm. In **B**, **C**, and **D**, bars show the mean ± SEM. * = P < 0.05; ** = P < 0.01; *** = P < 0.001; **** = P < 0.0001. PBS = phosphate buffered saline; OVA = ovalbumin.

of age, we used 9-week-old NOD/LtJ mice as the SS model. The depleting efficiency with a single dose of anti-CD4 mAb was checked at different time points (see Supplementary Figure 1, on the *Arthritis & Rheumatology* website at https://onlinelibrary. wiley.com/doi/10.1002/art.42244). NOD/LtJ mice were treated with a single intraperitoneal injection of 100 μg anti-CD4 mAb, followed by 6 intraperitoneal injections of peptide Ro480–494 (50 μg per mouse; amino acid sequence AIALREYRKKMDIPA; anti-CD4 + Ro480) every other day from 2 days after anti-CD4 mAb treatment (Figure 1A). We also included groups treated with phosphate buffered saline (PBS; control), Ro480 only, or anti-CD4 mAb combined with peptide OVA323–229 (anti-CD4 + OVA; 50 μg/mouse) as treatment controls.

We monitored the treated mice for ≥6 weeks and found that only the anti-CD4 + Ro480–treated group maintained their salivary flow rates, whereas the other 3 groups showed significantly reduced salivary secretion (Figure 1B). The H&E staining showed that the anti-CD4 + Ro480–treated group had much fewer and smaller inflamed infiltrations in SGs compared to other groups (Figure 1C). Real-time reverse transcriptase–polymerase chain reaction (RT-PCR) analysis revealed that anti-CD4 + Ro480 treatment protected critical SG secreting function–related gene expressions, such as water channel AQP5 (*Aqp5*), calcium channel (*Itpr3*), and NKCC1 (*Slc12a2*), but did not affect the expression of muscarinic acetylcholine receptor M3 (*Chrm3*) (Figure 1D). Immunofluorescence staining for AQP5 (Figure 1E) and NKCC1 (Figure 1F) also showed the same trend.

Taken together, these data indicate that treatment with anti-CD4 + Ro480 suppresses SS-like symptoms in NOD/LtJ mice. Another self antigen peptide (Ro274) was also used as a treatment and showed similar but weaker treatment effects (data not shown).

Reduction of IFNγ in CD4+ T cells in SGs via anti-CD4 + Ro480 treatment. We next studied the underlying mechanisms by which anti-CD4 + Ro480 treatment suppressed SS-like symptoms. We examined cytokine production of T cells in the SGs. We isolated CD4+ and CD8+ T cells from the SGs and analyzed their cytokine profiles with flow cytometry. CD4+ T cells in the SGs produced mainly IFNγ but only background levels of IL-17a (Figure 2A), suggesting that IFNγ is a dominant inflammatory cytokine. CD4+ T cells from mice in the anti-CD4 + Ro480–treated group produced significantly less IFNγ compared to the anti-CD4 + OVA–treated group (Figure 2A), while no difference was found for IL-17a production (Figure 2A). IFNγ production in CD8+ T cells in the anti-CD4 + Ro480–treated group also showed a trend toward decreasing levels compared to other groups, although not statistically significant, and CD8+IL-17a+ T cells were also negligible in all the groups (Figures 2C and D). Anti-CD4 + Ro480 treatment could also significantly suppress B cells in SGs and autoantibodies in serum (Supplementary Figure 2, https://onlinelibrary.wiley.com/doi/10.1002/art.42244). Furthermore, we examined cytokine production of T cells in the spleen and draining lymph nodes of SGs, and no significant differences were observed (data not shown).
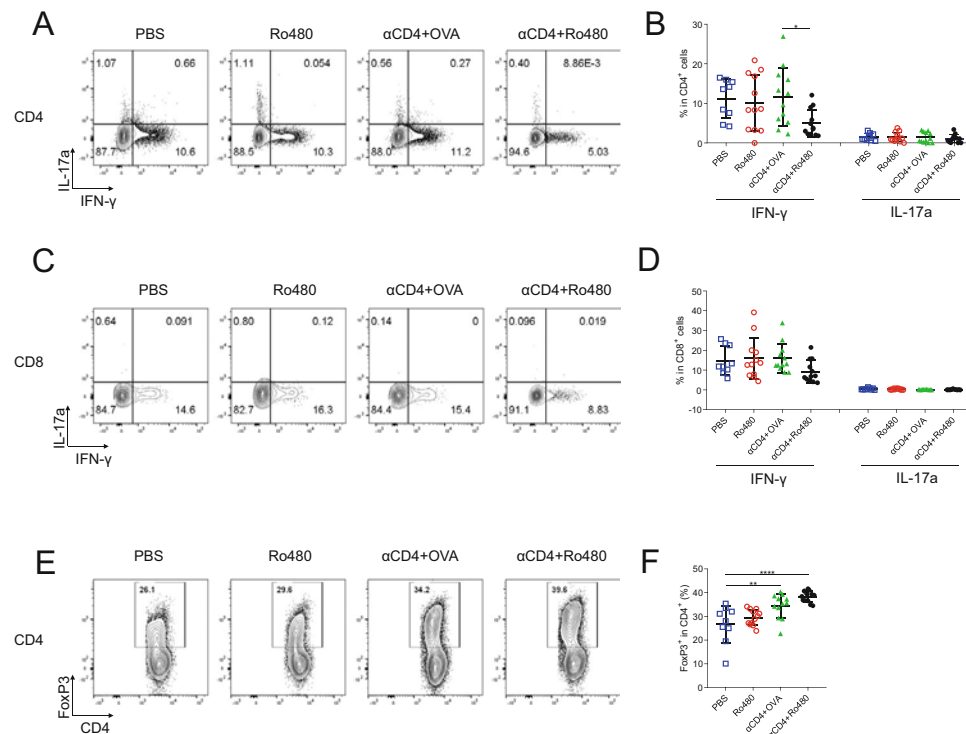

Figure 2. Flow cytometry analysis of T cells in the SGs after treatment. Representative flow cytometry plots and percentages of interleukin-17–positive (IL-17+) and interferon-γ–positive (IFNγ+) cells among CD4+ T cells (**A** and **B**) and among CD8+ T cells (**C** and **D**), and FoxP3+ cells among CD4+ T cells (**E** and **F**) in the SGs of mice in each treatment group. Bars show the mean ± SEM. * = P < 0.05; ** = P < 0.01; **** = P < 0.0001. See Figure 1 for other definitions. Color figure can be viewed in the online issue, which is available at http://onlinelibrary.wiley.com/doi/10.1002/art.42244/abstract.

These data indicate that anti-CD4 + Ro480 treatment suppresses IFNγ production of CD4+ T cells in the SGs, which may have therapeutic effects on SS.

Generation of antigen-specific Treg cells in vivo via anti-CD4 + Ro480 treatment. To investigate the underlying mechanisms responsible for the IFNγ reduction in the anti-CD4 + Ro480 group, we studied CD4+FoxP3+ regulatory Treg cells in the SGs, because Treg cells remain a key factor in suppressing Th1 cells (9). Surprisingly, both anti-CD4 + OVA and anti-CD4 + Ro480 groups had significantly higher frequencies of Treg cells in the SGs compared to the untreated (PBS) control group (Figures 2E and F). We also assessed IL-10 and KLRG1 expression in Treg cells from SGs and detected no significant difference in IL-10 production, but both anti-CD4 + OVA and anti-CD4 + Ro480 treatments were observed to up-regulate KLRG1 expression (Supplementary Figure 3, https://onlinelibrary.wiley.com/doi/10.1002/art.42244).

Since only the anti-CD4 + Ro480 group but not the anti-CD4 + OVA group showed suppressed IFNγ production, we hypothesized that the SSA/Ro antigen–specific Treg cells were generated in the anti-CD4 + Ro480 group. We developed an in vitro system to determine the presence of Ro480-specific Treg cells (Supplementary Figure 4, https://onlinelibrary.wiley.com/doi/10.1002/art.42244). We isolated CD4+ T cells as well as their CD4+CD25– (non–Treg cell responder) cells and CD4+CD25+ (Treg cell) subsets from the spleens of NOD/LtJ mice after therapy and examined the antigen-specific T cell proliferation and cytokine production by stimulation with peptide Ro480 and splenic APCs isolated from the PBS-treated controls. Since Treg cells require specific TCR stimulation to suppress effector T cells (11,12), if Ro480-specific Treg cells are generated and serve as a suppressor, decreased CD4+ T cell responses to peptide Ro480 may be presented. Consistent with this hypothesis, splenic CD4+ T cells from anti-CD4 + Ro480–treated mice showed significantly decreased CD4+ T cell proliferation to peptide Ro480 compared to the other 3 groups (Supplementary Figures 5A and B, https://onlinelibrary.wiley.com/doi/10.1002/art.42244). On the other hand, the same CD4+ T cells and subpopulations showed no significant alterations of Ki-67+ T cells in response to anti-CD3 antibody stimulation, indicating no difference in their proliferation to pan-TCR stimulation among these groups (Supplementary Figures 5C and D).

To prove that the newly generated Treg cells were antigen-specific, we administrated the customized I-Ab/Ro480 MHC class II tetramer complexes for fluorescence-activated cell sorting. Significantly more Ro480-specific Treg cells were detected
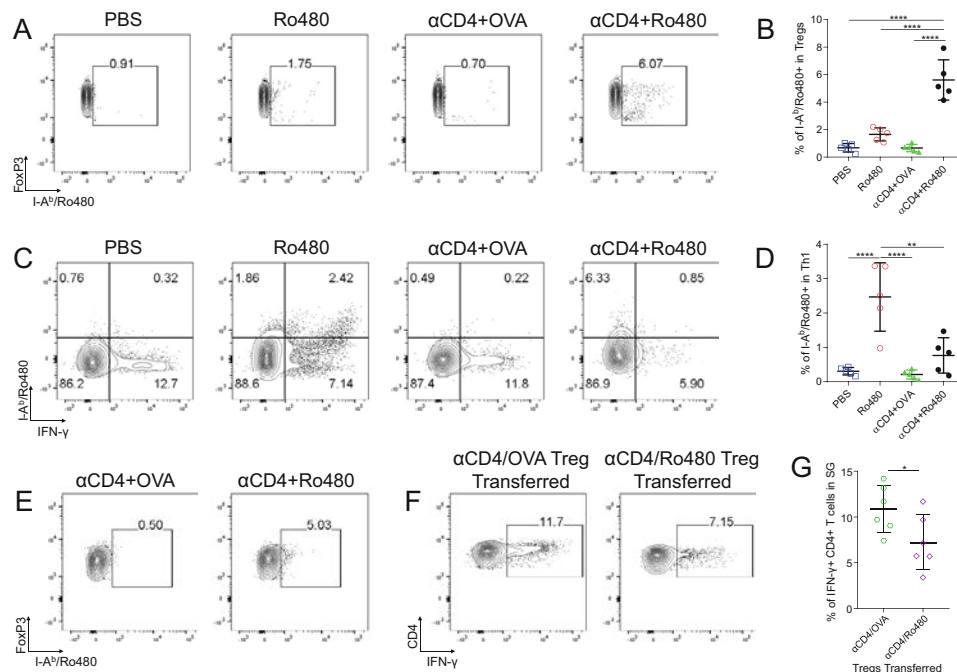

Figure 3. Ro480-specific CD4+FoxP3+ Treg cells and CD4+ interferon-γ–positive (IFNγ+) Th1 cells in SGs from mice in each treatment group, detected by major histocompatibility complex class II tetramer staining. **A** and **B**, Anti-CD4 + Ro480 treatment generated significantly higher levels of Ro480-specific Treg cells in the SGs compared to other treatments. **C** and **D**, Ro480-only treatment generated significantly higher levels of Ro480-specific CD4+IFNγ+ Th1 cells compared to other treatments. **E**, Anti-CD4 + Ro480 treatment generated significantly higher levels of Ro480-specific Treg cells than anti-CD4 + OVA treatment in the spleens of NOD/LtJ mice. **F** and **G**, Adoptive transfer of Treg cells from mice treated with anti-CD4 + Ro480 for 1 week significantly decreased the CD4+IFN-γ+Th1 cells in the SGs from NOD/LtJ mice compared to adoptive transfer of Treg cells from mice treated with anti-CD4 + OVA. In **B**, **D**, and **G**, bars show the mean ± SEM. * = $P < 0.05$; ** = $P < 0.01$; **** = $P < 0.0001$. See Figure 1 for other definitions.

in the SGs from anti-CD4 + Ro480–treated mice compared to those treated with PBS, Ro480 alone, or anti-CD4 + OVA (Figures 3A and B). Furthermore, the highest number of Ro480-specific CD4+IFNγ+ T cells were detected in mice treated with only Ro480, and anti-CD4 + Ro480 treatment significantly reduced these Ro480-specific Th1 cells (Figures 3C and D). The Ro480-specific Treg cells were also detected in spleens from anti-CD4 + Ro480–treated mice (Figure 3E). To investigate the function of newly generated Treg cells by anti-CD4 + Ro480 treatment in vivo, we adoptive-transferred splenic Treg cells from anti-CD4 + OVA–treated or anti-CD4 + Ro480–treated mice to naive NOD/LtJ mice (2×10^5 cells per mouse; intraperitoneal injection). The CD4 + IFNγ+ Th1 cells in the SGs from recipient mice were assessed 1 week after Treg adoptive transfer and were compared to those treated with Treg cells from anti-CD4 + OVA–treated mice. Mice treated with Treg cells from anti-CD4 + Ro480–treated mice showed significant suppression in the frequency of CD4+IFNγ+ T cells (Figures 3F and G).

To further investigate whether other peptides could generate the antigen-specific Treg cells for SS treatment, we also treated the NOD/LtJ mice with anti-CD4 mAb and Ro274 (anti-CD4 + Ro274). We found that anti-CD4 + Ro274 treatment could also improve saliva flow rate but not as much as Ro480 (Supplementary Figures 6A–C, https://onlinelibrary.wiley.com/doi/10.1002/art.42244). Moreover, we found that anti-CD4 + Ro274 treatment generated fewer antigen-specific Treg cells than anti-CD4 + Ro480 treatment (Supplementary Figures 6D and E), which might be the cause of its reduced treatment effects. Taken together, these data indicate that Ro480 antigen–specific Treg cells were generated in anti-CD4 + Ro480–treated mice, which are responsible for the suppression of Th1 cells in SS.

DISCUSSION

In this study, we generated SSA/Ro antigen–specific Treg cells in NOD/LtJ mice with SS-like symptoms and evaluated the treatment effects. First, we found that the combination of anti-CD4 mAb with autopeptide Ro480 can suppress inflammation infiltration in SGs and maintain salivary flow rates, which both reflect SS-like symptoms. Second, anti-CD4 + Ro480 treatment suppresses IFNγ production of CD4+ T cells in the SGs. Finally and importantly, we demonstrated that anti-CD4 + Ro480 treatment generates antigen-specific Treg cells in vivo, which may be a main underlying mechanism of the suppression of Th1 cells and consequently for therapeutic effects on SS symptoms in NOD mice. The findings here extend the list of our discovered experimental approaches to generate antigen-specific Treg cells in vivo to suppress autoimmune diseases (9,13).

CD4 depletion treatment for autoimmune diseases has been undertaken and assessed for decades, with conflicting findings and undetermined effects (14,15). In the present study, we used a combination of CD4 T cell depletion and an injection of SG-specific autoantigen peptide Ro480 to induce antigen-specific Treg cells in NOD mice with SS-like symptoms, using the presence of autoantigens and TGFβ produced by phagocytes upon uptake of apoptotic CD4+ T cells. This treatment blocked the development of SS, which further supports the concept that antigen-specific Treg cell generation can be accomplished in mice with ongoing and established autoimmune diseases (14,15). This has further advanced the path to development of similar therapy for human patients with autoimmune diseases including SS.

Our data showed that both anti-CD4 + OVA and anti-CD4 + Ro480 treatment up-regulated Treg cells in the SGs, but only anti-CD4 + Ro480 treatment significantly suppressed IFNγ production compared to the anti-CD4 + OVA treatment group. Despite the clear evidence that the Ro480 autoantigen–specific Treg cells are generated and suppress Th1 inflammation and SS, the mechanisms by which Ro480-specific Treg cells inhibit IFNγ production in CD4+ T cells remain to be elucidated. The importance of TCR signaling for Treg cell survival and function have been studied for many years (2,5). Recently, a study showed that antigen-specific Treg cells can form strong interactions with dendritic cells (DCs), resulting in selective inhibition of the binding of naive T cells to DCs. Moreover, the strong interaction of this Treg cell can remove the complex of cognate peptide and MHC class II from the surface of the DC, reducing the capacity for antigen presenting (11). It will be important to study whether these aforementioned mechanisms are involved in the regulatory activity of Ro480-specific Treg cells induced in our setting, and whether local and systemic effects of Ro480-specific Treg cells are similar in future studies.

In conclusion, we have successfully generated SSA/Ro antigen–specific Treg cells in vivo in NOD/LtJ mice via induction of a transient CD4+ T cell apoptotic depletion plus an administration of low doses of autoantigenic peptides. The understanding and optimization of this process will help us to "reprogram" the dysregulated immune responses in patients with SS to develop more specific immunotherapy.

AUTHOR CONTRIBUTIONS

All authors were involved in drafting the article or revising it critically for important intellectual content, and all authors approved the final version to be published. Dr. Xu had full access to all of the data in the study and takes responsibility for the integrity of the data and the accuracy of the data analysis.
Study conception and design. Xu, D. Wang, Zhang, Chen.
Acquisition of data. Xu, O. Liu, D. Wang, F. Wang, Jin, Cain, Bynum, N. Liu, Han.
Analysis and interpretation of data. Xu, O. Liu, D. Wang.

REFERENCES

1. Fox RI. Sjogren's syndrome. Lancet 2005;366:321–31.

2. Garcia-Carrasco M, Fuentes-Alexandro S, Escarcega RO, Salgado G, Riebeling C, Cervera R. Pathophysiology of Sjogren's syndrome. Arch Med Res 2006;37:921–32.

3. Christodoulou MI, Kapsogeorgou EK, Moutsopoulos NM, Moutsopoulos HM. Foxp3+ T-regulatory cells in Sjogren's syndrome: correlation with the grade of the autoimmune lesion and certain adverse prognostic factors. Am J Pathol 2008;173:1389–96.

4. Bluestone JA, Abbas AK. Natural versus adaptive regulatory T cells [review]. Nat Rev Immunol 2003;3:253–7.

5. Littman DR, Rudensky AY. Th17 and regulatory T cells in mediating and restraining inflammation. Cell 2010;140:845–58.

6. Sakaguchi S, Miyara M, Costantino CM, Hafler DA. FOXP3+ regulatory T cells in the human immune system [review]. Nat Rev Immunol 2010;10:490–500.

7. Chen W, Jin W, Hardegen N, Lei KJ, Li L, Marinos N, et al. Conversion of peripheral CD4+CD25- naive T cells to CD4+CD25+ regulatory T cells by TGF-β induction of transcription factor Foxp3. J Exp Med 2003;198:1875–86.

8. Perruche S, Zhang P, Liu Y, Saas P, Bluestone JA, Chen W. CD3-specific antibody-induced immune tolerance involves transforming growth factor-β from phagocytes digesting apoptotic T cells. Nat Med 2008;14:528–35.

9. Kasagi S, Zhang P, Che L, Abbatiello B, Maruyama T, Nakatsukasa H, et al. In vivo-generated antigen-specific regulatory T cells treat autoimmunity without compromising antibacterial immune response. Sci Transl Med 2014;6:241ra78.

10. Scofield RH, Asfa S, Obeso D, Jonsson R, Kurien BT. Immunization with short peptides from the 60-kDa Ro antigen recapitulates the serological and pathological findings as well as the salivary gland dysfunction of Sjogren's syndrome. J Immunol 2005;175:8409–14.

11. Akkaya B, Oya Y, Akkaya M, Al Souz J, Holstein AH, Kamenyeva O, et al. Regulatory T cells mediate specific suppression by depleting peptide-MHC class II from dendritic cells. Nat Immunol 2019;20: 218–31.

12. Chen W, Wahl SM. TGF-β: the missing link in CD4+CD25+ regulatory T cell-mediated immunosuppression. Cytokine Growth Factor Rev 2003;14:85–9.

13. Kasagi S, Wang D, Zhang P, Zanvit P, Chen H, Zhang D, et al. EBioMedicine 2019;44:50–9.

14. Jabs DA, Prendergast RA. Autoimmune ocular disease in MRL/Mp-lpr/lpr mice is suppressed by anti-CD4 antibody. Invest Ophthalmol Vis Sci 1991;32:2718–22.

15. Rep MH, van Oosten BW, Roos MT, Ader HJ, Polman CH, van Lier RA. Treatment with depleting CD4 monoclonal antibody results in a preferential loss of circulating naive T cells but does not affect IFN-γ secreting TH1 cells in humans. J Clin Invest 1997;99:2225–31.

Corrigendum

In the article by Chen et al in the September 2015 issue of *Arthritis & Rheumatology* ("Leptin and neutrophil-activating peptide 2 promote mesenchymal stem cell senescence through activation of the phosphatidylinositol 3-kinase/Akt pathway in patients with systemic lupus erythematosus" [pages 2383–2393]), the Western blot images in the bottom panels of Figure 2C (representing GAPDH) were incorrect due to the mistaken images being inadvertently inserted during the assembly of Figure 2. The bottom panels of Figure 2C have been updated with the correct data. These errors do not affect the results or conclusions of this article. The corrected Figure 2 is reproduced below.

AMERICAN COLLEGE
of RHEUMATOLOGY
Empowering Rheumatology Professionals
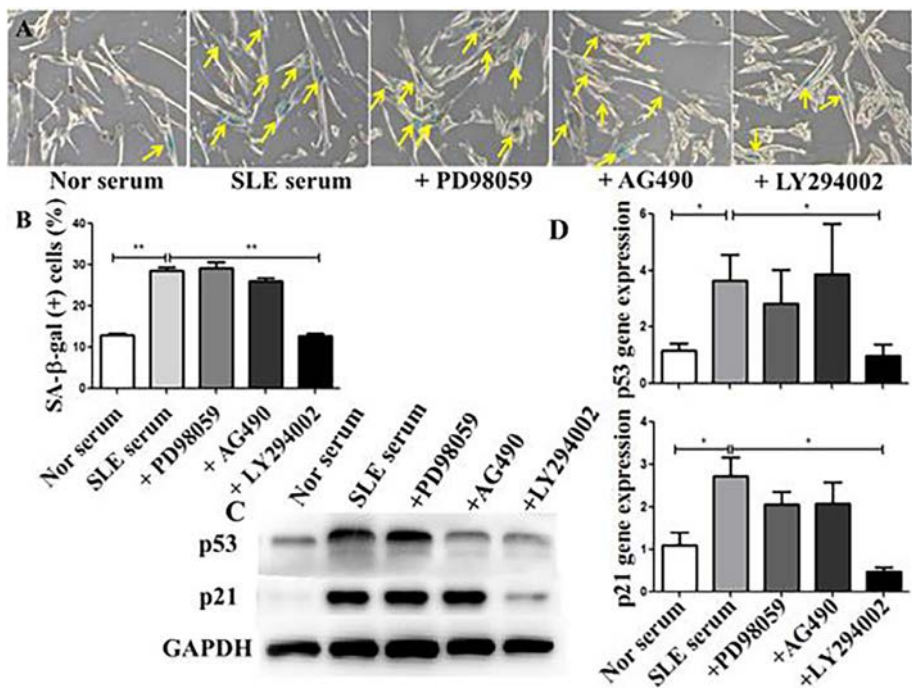
Machine Learning for the Identification of a Common Signature for Anti–SSA/Ro 60 Antibody Expression Across Autoimmune Diseases

Nathan Foulquier,[1] Christelle Le Dantec,[1] Eleonore Bettacchioli,[1] Christophe Jamin,[2] Marta E. Alarcón-Riquelme,[3] and Jacques-Olivier Pers[2] (iD)

Objective. Anti-Ro autoantibodies are among the most frequently detected extractable nuclear antigen autoantibodies, mainly associated with primary Sjögren's syndrome (SS), systemic lupus erythematosus (SLE), and undifferentiated connective tissue disease (UCTD). This study was undertaken to determine if there is a common signature for all patients expressing anti–Ro 60 autoantibodies regardless of their disease phenotype.

Methods. Using high-throughput multiomics data collected from the cross-sectional cohort in the PRECISE Systemic Autoimmune Diseases (PRECISESADS) study Innovative Medicines Initiative (IMI) project (genetic, epigenomic, and transcriptomic data, combined with flow cytometry data, multiplexed cytokines, classic serology, and clinical data), we used machine learning to assess the integrated molecular profiling of 520 anti–Ro 60+ patients compared to 511 anti–Ro 60– patients with primary SS, patients with SLE, and patients with UCTD, and 279 healthy controls.

Results. The selected clinical features for RNA-Seq, DNA methylation, and genome-wide association study data allowed for a clear distinction between anti–Ro 60+ and anti–Ro 60– patients. The different features selected using machine learning from the anti–Ro 60+ patients constituted specific signatures when compared to anti–Ro 60– patients and healthy controls. Remarkably, the transcript Z score of 3 genes (*ATP10A*, *MX1*, and *PARP14*), presenting with overexpression associated with hypomethylation and genetic variation and independently identified using the Boruta algorithm, was clearly higher in anti–Ro 60+ patients compared to anti–Ro 60– patients regardless of disease type. Our findings demonstrated that these signatures, enriched in interferon-stimulated genes, were also found in anti–Ro 60+ patients with rheumatoid arthritis and those with systemic sclerosis and remained stable over time and were not affected by treatment.

Conclusion. Anti–Ro 60+ patients present with a specific inflammatory signature regardless of their disease type, suggesting that a dual therapeutic approach targeting both Ro-associated RNAs and anti–Ro 60 autoantibodies should be considered.

INTRODUCTION

Anti-Ro autoantibodies are among the most frequently detected extractable nuclear antigen (ENA) autoantibodies and are mainly associated with primary Sjögren's syndrome (SS). These autoantibodies are also frequently observed in systemic lupus erythematosus (SLE) and undifferentiated connective tissue disease (UCTD) (1,2). Additionally, anti-Ro autoantibodies have been reported in other autoimmune diseases such as systemic sclerosis (SSc), mixed connective tissue disease (MCTD), rheumatoid arthritis (RA), and myositis (3).

Anti-Ro autoantibodies include reactivity against 2 autoantigens (Ro 52 and Ro 60) encoded by separate genes and are

[1]Nathan Foulquier, PhD, Christelle Le Dantec, PhD, Eleonore Bettacchioli, PharmD: B Lymphocytes, Autoimmunity and Immunotherapies Laboratory, UMR 1227, Université de Brest, INSERM, Brest, France; [2]Christophe Jamin, PhD, Jacques-Olivier Pers, DDS, PhD: B Lymphocytes, Autoimmunity and Immunotherapies Laboratory, UMR 1227, Université de Brest, INSERM, and University Hospital of Brest, Brest, France; [3]Marta E. Alarcón-Riquelme, MD, PhD: Department of Medical Genomics, GENYO Centre for Genomics and Oncological Research, Granada, Spain.

Author disclosures are available at https://onlinelibrary.wiley.com/action/downloadSupplement?doi=10.1002%2Fart.42243&file=art42243-sup-0001-Disclosureform.pdf.

Address correspondence to Jacques-Olivier Pers, DDS, PhD, Université de Brest, INSERM, B Lymphocytes, Autoimmunity and Immunotherapies Laboratory, UMR 1227, Brest, France. Email: pers@univ-brest.fr.

Submitted for publication December 24, 2021; accepted in revised form May 17, 2022.

found in distinct cellular compartments (4). Ro 52 is a type I interferon (IFN)– and type II IFN–inducible protein (5,6) and is a negative regulator of proinflammatory cytokine production (7). Ro 60 antigen binds to ~100 nucleotide noncoding RNAs called human Y RNA (8) and acts as a quality checkpoint for RNA misfolding with molecular chaperones for defective RNA (9).

Findings from previous studies have shown variation in clinical manifestations or outcomes according to the presence or absence of anti-Ro autoantibodies. Thus, SLE subjects with anti–Ro 60 antibodies have an increased prevalence of skin disease, photosensitivity, and nephritis, along with elevated expression of IFN-inducible genes in immune cells and tissue samples (10). In primary SS, patients with both anti–Ro 60 and Ro 52 antibodies were distinguished by a higher prevalence of markers of B cell hyperactivity and glandular inflammation (11). Those patients also had earlier disease onset and presented with more systemic extraglandular manifestations, such as leukopenia, hypergammaglobulinemia, and major salivary gland swelling (12). Recently, 2 subgroups of patients with primary SS were defined according to HLA association, Ro 60/SSB antibodies, and clinical manifestations. The Ro 60/SSB antibody–positive subgroup was younger at disease onset and diagnosis and more frequently presented with anemia, leukopenia, hypergammaglobulinemia, purpura, major salivary gland swelling, lymphadenopathy, and lymphoma. These results confirmed an overall more severe disease phenotype in patients who were Ro 60/SSB antibody–positive compared to patients negative for both anti–Ro 60 and anti-SSB antibodies (13). Anti–Ro 60 reactivity alone strongly correlated with oral ulcers, a characteristic manifestation of SLE, while the combination of anti–Ro 60 and anti–Ro 52 was significantly more prevalent in patients with interstitial kidney disease and sicca syndrome symptoms (14).

Due to the presence of anti–Ro 60 antibodies in different autoimmune diseases and the reported clinical manifestations that characterize this expression, the question remains of if there is a common signature for all patients expressing anti–Ro 60 autoantibodies that would allow physicians to consider a suitable therapy regardless of disease phenotype.

Using algorithms derived from machine learning, the present study was undertaken to determine the precise signature of anti–Ro 60+ patients in diseases where this autoantibody is the most frequently observed (primary SS, SLE, and UCTD) using high-throughput multiomics data collected in the PRECISE Systemic Autoimmune Diseases (PRECISESADS) study Innovative Medicines Initiative Joint Undertaking project (genetic, epigenomic, and transcriptomic data, combined with flow cytometry data, multiplexed cytokines, classic serology, and clinical data). In this study, we performed integrated molecular profiling of 520 anti–Ro 60+ patients compared to 511 anti–Ro 60– patients and 279 healthy controls. We then observed whether this signature was also present in the 41 of 725 anti–Ro 60+ patients with other autoimmune diseases such as MCTD, RA, and SSc, all from the same PRECISESADS cohort. See Appendix A for a list of members of the PRECISESADS Clinical Consortium and members of the PRECISESADS Flow Cytometry Consortium.

PATIENTS AND METHODS

Patient population. The present study was conducted in 1,755 patients (367 with primary SS, 508 with SLE, 156 with UCTD, 307 with RA, 327 with SSc, and 90 with MCTD) and 279 healthy controls included in the European multicenter cross-sectional study of the PRECISESADS IMI consortium (15). Classification criteria were the 2010 American College of Rheumatology (ACR)/European Alliance of Associations for Rheumatology (EULAR) RA classification criteria (16), the 1997 update of 1982 ACR SLE criteria (17), 2013 ACR/EULAR SSc classification criteria (18), or the American–European Consensus Group primary SS classification criteria (19) with at least the presence of anti-Ro and/or a positive focus score on minor salivary gland biopsy, MCTD using the Alarcon-Segovia criteria (20), and UCTD in patients with clinical features of systemic autoimmune diseases that did not fulfill any of the above criteria or any other systemic autoimmune disease criteria for at least 2 years (with the presence of nonspecific antibodies, antinuclear antibodies [ANAs] ≥1:160). Patients fulfilling 3 of 4 SLE classification criteria and patients with early SSc (21) were not classified as having UCTD. Recruitment occurred between December 2014 and October 2017 involving 19 institutions in 9 countries (Austria, Belgium, France, Germany, Hungary, Italy, Portugal, Spain, and Switzerland).

The PRECISESADS study adhered to the standards set by International Council for Harmonisation Guidelines for Good Clinical Practice and the ethics principles that have their origin in the 2013 Declaration of Helsinki. Informed consent was obtained from each patient prior to inclusion in the study. This study protocol was approved the Ethics Review Boards of the 19 participating institutions. Protection of the confidentiality of records that could identify included subjects was ensured as defined according to the European Union Directive 2001/20/EC and the applicable national and international requirements relating to data protection in each participating country. The cross-sectional cohort study and inception cohort study are registered on ClinicalTrials.gov (clinicalTrials.gov identifiers: NCT02890121 and NCT02890134, respectively). The anti–Ro 60+ signature identified using machine learning was validated using the transcriptome of 106 patients in the PRECISESADS inception study (ClinicalTrials.gov identifier: NCT02890134), who were followed up and had samples collected at the time of recruitment and at 6 and/or 14 months. Of note, patients in the inception cohort were diagnosed within less than a year and had not received high doses of immunosuppressants, cyclophosphamide, or belimumab at least 3 months prior to recruitment. For time points 6 and 14 months, patients could receive any standard of care therapy prescribed by their physician. Healthy controls were individuals not receiving

Table 1. Demographic and clinical characteristics of the healthy controls, patients with primary SS, those with SLE, and those with UCTD according to anti–Ro 60 expression (anti–Ro 60+ patients compared to anti–Ro 60– patients)*

Characteristic	Value	Characteristic	Value
Healthy controls		Steroid usage *(cont'd).*	
No. of patients	279	Yes	
Age, mean ± SD years	52 ± 9	Anti–Ro 60–	16 (26)
Sex, female	262 (94)	Anti–Ro 60+	62 (20)
Sex, male	17 (6.1)	P	0.3
Ethnicity		Antimalarials	
American Indian/Alaska Native	0 (0)	No	
Asian	2 (0.7)	Anti–Ro 60–	37 (61)
Black/African American	0 (0)	Anti–Ro 60+	194 (63)
Caucasian/White	277 (99)	Yes	
Native Hawaiian/Other Pacific Islander	0 (0)	Anti–Ro 60–	24 (39)
Other	0 (0)	Anti–Ro 60+	112 (37)
Obesity†	16 (5.8)	P	0.7
Smoking‡	38 (14)	Immunosuppressants	
Primary SS		No	
No. of patients	367	Anti–Ro 60–	47 (77)
Anti–Ro 60–	61	Anti–Ro 60+	264 (86)
Anti–Ro 60+	306	Yes	
Age, mean ± SD years		Anti–Ro 60–	14 (23)
Anti–Ro 60–	59 ± 13	Anti–Ro 60+	42 (14)
Anti–Ro 60+	57 ± 13	P	0.067
P§	0.3	Biologics**	
Sex, female		No	
Anti–Ro 60–	57 (93)	Anti–Ro 60–	10 (100)
Anti–Ro 60+	293 (96)	Anti–Ro 60+	29 (100)
Sex, male		Yes	
Anti–Ro 60–	4 (6.6)	Anti–Ro 60–	0 (0)
Anti–Ro 60+	13 (4.2)	Anti–Ro 60+	0 (0)
P	0.5	P	>0.9
Ethnicity		PhGA, mean ± SD score††	
American Indian/Alaska Native		Anti–Ro 60–	30 ± 18
Anti–Ro 60–	0 (0)	Anti–Ro 60+	24 ± 19
Anti–Ro 60+	0 (0)	P	0.007
Asian		ESSDAI, mean ± SD score‡‡	
Anti–Ro 60–	0 (0)	Anti–Ro 60–	4 ± 6
Anti–Ro 60+	2 (0.7)	Anti–Ro 60+	5 ± 5
Black/African American		P	0.11
Anti–Ro 60–	0 (0)	ESSPRI, mean ± SD score§§	
Anti–Ro 60+	1 (0.3)	Anti–Ro 60–	5.59 ± 2.29
Caucasian/White		Anti–Ro 60+	4.71 ± 2.33
Anti–Ro 60–	61 (100)	P	0.029
Anti–Ro 60+	299 (98)	SLE	
Native Hawaiian/Other Pacific Islander		No. of patients	508
Anti–Ro 60–	0 (0)	Anti–Ro 60–	333
Anti–Ro 60+	0 (0)	Anti–Ro 60+	175
Other		Age, mean ± SD years	
Anti–Ro 60–	0 (0)	Anti–Ro 60–	46 ± 14
Anti–Ro 60+	4 (1.3)	Anti–Ro 60+	45 ± 13
P	>0.9	P	0.6
Obesity§		Sex, female	
Anti–Ro 60–	7 (12)	Anti–Ro 60–	302 (91)
Anti–Ro 60+	37 (12)	Anti–Ro 60+	163 (93)
P	>0.9	Sex, male	
Smoking¶		Anti–Ro 60–	31 (9.3)
Anti–Ro 60–	7 (12)	Anti–Ro 60+	12 (6.9)
Anti–Ro 60+	29 (10.0)	P	0.3
P	0.6	Ethnicity	
Disease duration, mean ± SD years#		American Indian/Alaska Native	
Anti–Ro 60–	9 ± 8	Anti–Ro 60–	0 (0)
Anti–Ro 60+	10 ± 8	Anti–Ro 60+	0 (0)
P	0.2	Asian	
Steroid usage		Anti–Ro 60–	3 (0.9)
No		Anti–Ro 60+	1 (0.6)
Anti–Ro 60–	45 (74)		
Anti–Ro 60+	244 (80)		

(Continued)

Table 1. (*Cont'd*)

Characteristic	Value	Characteristic	Value
Ethnicity *(cont'd).*		UCTD	
Black/African American		No. of patients	156
Anti–Ro 60–	3/333 (0.9)	Anti–Ro 60–	117
Anti–Ro 60+	9/175 (5.1)	Anti–Ro 60+	39
Caucasian/White		Age, mean ± SD years	
Anti–Ro 60–	318 (95)	Anti–Ro 60–	47 ± 12
Anti–Ro 60+	162 (93)	Anti–Ro 60+	46 ± 12
Native Hawaiian/Other Pacific Islander		P	0.6
Anti–Ro 60–	0 (0)	Sex, female	
Anti–Ro 60+	1 (0.6)	Anti–Ro 60–	108 (92)
Other		Anti–Ro 60+	36 (92)
Anti–Ro 60–	9 (2.7)	Sex, male	
Anti–Ro 60+	2 (1.1)	Anti–Ro 60–	9 (7.7)
P	0.010	Anti–Ro 60+	3 (7.7)
Obesity¶¶		P	>0.9
Anti–Ro 60–	23 (7.2)	Ethnicity	
Anti–Ro 60+	15 (8.8)	American Indian/Alaska Native	
P	0.5	Anti–Ro 60–	1 (0.9)
Smoking##		Anti–Ro 60+	0 (0)
Anti–Ro 60–	60 (19)	Asian	
Anti–Ro 60+	30 (18)	Anti–Ro 60–	0 (0)
P	0.8	Anti–Ro 60+	1 (2.6)
Disease duration, mean ± SD years		Black/African American	
Anti–Ro 60–	14 ± 10	Anti–Ro 60–	1 (0.9)
Anti–Ro 60+	12 ± 9	Anti–Ro 60+	0 (0)
P	0.079	Caucasian/White	
Steroid usage		Anti–Ro 60–	113 (97)
No		Anti–Ro 60+	38 (97)
Anti–Ro 60–	179 (54)	Native Hawaiian/Other Pacific Islander	
Anti–Ro 60+	77 (44)	Anti–Ro 60–	0 (0)
Yes		Anti–Ro 60+	0 (0)
Anti–Ro 60–	154 (46)	Other	
Anti–Ro 60+	98 (56)	Anti–Ro 60–	2 (1.7)
P	0.037	Anti–Ro 60+	0 (0)
Antimalarials		P	0.6
No		Obesity#	
Anti–Ro 60–	112 (34)	Anti–Ro 60–	17 (15)
Anti–Ro 60+	45 (26)	Anti–Ro 60+	6 (15)
Yes		P	>0.9
Anti–Ro 60–	221 (66)	Smoking§§§	
Anti–Ro 60+	130 (74)	Anti–Ro 60–	17 (15)
P	0.066	Anti–Ro 60+	6 (15)
Immunosuppressants		P	>0.9
No		Disease duration, mean ± SD years¶¶¶	
Anti–Ro 60–	234 (70)	Anti–Ro 60–	6 ± 6
Anti–Ro 60+	111 (63)	Anti–Ro 60+	7 ± 8
Yes		P	>0.9
Anti–Ro 60–	99 (30)	Steroid usage	
Anti–Ro 60+	64 (37)	No	
P	0.12	Anti–Ro 60–	78 (67)
Biologics***		Anti–Ro 60+	38 (97)
No		Yes	
Anti–Ro 60–	27 (100)	Anti–Ro 60–	39 (33)
Anti–Ro 60+	17 (100)	Anti–Ro 60+	1 (2.6)
Yes		P	<0.001
Anti–Ro 60–	0 (0)	Antimalarials	
Anti–Ro 60+	0 (0)	No	
P	>0.9	Anti–Ro 60–	62 (53)
PhGA, mean ± SD score†††		Anti–Ro 60+	23 (59)
Anti–Ro 60–	19 ± 18	Yes	
Anti–Ro 60+	21 ± 17	Anti–Ro 60–	55 (47)
P	0.067	Anti–Ro 60+	16 (41)
SLEDAI, mean ± SD score‡‡‡		P	0.5
Anti–Ro 60–	4 ± 6		
Anti–Ro 60+	5 ± 5		
P	0.2		

(Continued)

Table 1. (*Cont'd*)

Characteristic	Value	Characteristic	Value
Immunosuppressants		Biologics (*cont'd*).	7 (100)
No		Anti–Ro 60+	
Anti–Ro 60–	100 (85)	Yes	
Anti–Ro 60+	38 (97)	Anti–Ro 60–	4 (15)
Yes		Anti–Ro 60+	0 (0)
Anti–Ro 60–	17 (15)	*P*	0.6
Anti–Ro 60+	1 (2.6)	PhGA, mean ± SD score****	
P	0.045	Anti–Ro 60–	26 ± 21
Biologics###		Anti–Ro 60+	18 ± 15
No		*P*	0.12
Anti–Ro 60–	23 (85)		

* Except where indicated otherwise, values are the number (%) of patients. Significance was determined by Wilcoxon's rank sum test, Fisher's exact test, or Pearson's chi-square test. SS = Sjögren's syndrome; SLE = systemic lupus erythematosus; UCTD = undifferentiated connective tissue disease; PhGA = physician global assessment of disease activity; ESSDAI = European Alliance of Associations for Rheumatology (EULAR) Sjögren's Syndrome Disease Activity Index; ESSPRI = EULAR Sjögren's Syndrome Patient Reported Index.
† Data were missing from 1 patient.
‡ Data were missing from 10 patients.
§ Data were missing from 3 patients and 10 patients who were anti–Ro 60– and anti–Ro 60+, respectively.
¶ Data were missing from 4 patients and 15 patients who were anti–Ro 60– and anti–Ro 60+, respectively.
# Data were missing from 1 patient each who was anti–Ro 60– and anti–Ro 60+.
** Data were missing from 51 patients and 277 patients who were anti–Ro 60– and anti–Ro 60+, respectively.
†† Data were missing from 2 patients and 26 patients who were anti–Ro 60– and anti–Ro 60+, respectively.
‡‡ Data were missing from 15 patients and 112 patients who were anti–Ro 60– and anti–Ro 60+, respectively.
§§ Data were missing from 17 patients and 167 patients who were anti–Ro 60– and anti–Ro 60+, respectively.
¶¶ Data were missing from 12 patients and 15 patients who were anti–Ro 60– and anti–Ro 60+, respectively.
Data were missing from 21 patients and 11 patients who were anti–Ro 60– and anti–Ro 60+, respectively.
*** Data were missing from 306 patients and 158 patients who were anti–Ro 60– and anti–Ro 60+, respectively.
††† Data were missing from 16 patients and 15 patients who were anti–Ro 60– and anti–Ro 60+, respectively.
‡‡‡ Data were missing from 159 patients and 96 patients who were anti–Ro 60– and anti–Ro 60+, respectively.
§§§ Data were missing from 2 patients who were anti–Ro 60–.
¶¶¶ Data were missing from 1 patient who was anti–Ro 60–.
Data were missing from 90 patients and 32 patients who were anti–Ro 60– and anti–Ro 60+, respectively.
**** Data were missing from 5 patients and 2 patients who were anti–Ro 60– and anti–Ro 60+, respectively.

long-term medication, without any inflammatory autoimmune, allergic, or infectious condition, and without a history of autoimmune disease, particularly thyroid disease or other diseases that may modify cellular profiles in blood.

Determination of autoantibodies, ANAs, free light chains, and complement fractions. For all samples collected between March 2016 and June 2019, all autoantibodies were determined at a single center (University Hospital of Brest). Anti-ENA (comprising Sm, U1 RNP, Scl-70, Ro 52, Ro 60, and SSB) and specific autoantibodies anti–Ro 52 and anti–Ro 60, anti–cyclic citrullinated peptide 2 (anti-CCP2), IgG and IgM anti-β_2GPI, IgG, and IgM anticardiolipin [aCL], anti–double-stranded DNA (anti-dsDNA), and anticentromere autoantibody levels were determined using a chemiluminescent IDS-iSYS immunoanalyser (Immunodiagnostic Systems). Rheumatoid factor (RF) was determined regardless of the isotypes measured by turbidimetry using SPA$_{PLUS}$ (Binding Site), as well as C3 and C4 complement fractions and kappa and lamba free light chains. Samples from all patients and healthy controls were tested. See Supplementary Methods for more details regarding sample and data collection (available on the *Arthritis & Rheumatology* website at http://onlinelibrary.wiley.com/doi/10.1002/art.42243). Autoantibodies and RF distribution were described according to

concentration level (negative, low, medium, or elevated/high), and the proportion and the concentration across anti–Ro 60+ patients and anti–Ro 60– patients in each disease were compared using Fisher's exact test. Complements C3 and C4 and circulating free light chains have been described in continued concentrations expressed in gm/liter and mg/liter respectively, and Kruskal-Wallis testing was used to compare the concentration level across the anti–Ro 60+ patients and anti–Ro 60– patients in each disease. Anti–Ro 60 autoantibody–positive samples were also classified according to their degree of positivity. Patients with positive samples with concentrations between 10 and 640 arbitrary units (AU)/ml were considered anti–Ro 60^{low} patients, whereas those with samples with a concentration > 640 AU/ml were considered anti–Ro 60^{high} patients.

ANA detection was performed using an in-house technique on HEp-2 cells (ATCC strain CCL23). Each sample was systematically tested at 5 successive dilutions (1:80, 1:160, 1:320, 1:640, 1:1,280), and the threshold of positivity was set at 1:160, according to international recommendations [22]. Information regarding current or past presence of hypergammaglobulinemia was collected in each center at the time of inclusion and defined as, within 12 weeks, a serum IgG value greater than the upper limit of normal and/or gammaglobulin values >20%.

Clinical data. Clinical data obtained from 520 anti–Ro 60+ patients (306 with primary SS, 175 with SLE, and 39 with UCTD), 511 anti–Ro 60– patients (61 with primary SS, 333 with SLE, and 117 with UCTD), and 279 healthy controls were collected using an electronic case report form. Clinical data included patient's age, sex, ethnicity, disease duration, the physician global assessment of disease activity (PhGA), fulfillment of Systemic Lupus Erythematosus Disease Activity Index (SLEDAI) (23) for SLE, fulfillment of EULAR Sjögren's Syndrome Disease Activity Index (ESSDAI) (24) for primary SS, and current use of treatments.

Other available data. High-dimensional omics genotypes, RNA-Seq data, DNA methylation data, and the proportions of relevant cell types using custom flow cytometry marker panels were analyzed in whole blood samples. Additional information, such as cytokine levels, chemokine levels, and inflammatory mediator expression levels were obtained from serum samples. All of these parameters are described in greater detail in the Supplementary Methods (http://onlinelibrary.wiley.com/doi/10.1002/art.42243), and repartition of patients with a full data set per omic type and across diseases is shown in Supplementary Table 1.

Dimensionality reduction. Our strategy for dimensionality reduction was driven by artificial intelligence approaches involving machine learning. Patients were first grouped according to their disease (primary SS, SLE, or UCTD). We then separately considered each of the data sets describing these patients (RNA-Seq, DNA methylation, GWAS, and flow cytometry associated with cytokine expression). For each of these data sets, we performed a Boruta analysis (25) to discriminate between anti–Ro 60+ patients and anti–Ro 60– patients in order to extract features that significantly distinguish the 2 groups within each data set. The Boruta algorithm was used to create an extended data set by adding copies of each feature in the original data set. Values of the duplicated features were then shuffled, and the resulting features were called "shadow features." The random permutation of modality within these features lead to the removal of any preexisting correlation with the target variable, in our case, anti–Ro 60 positivity. Once shadow features were generated, a random forest classifier was run on the whole data set and Z scores were computed for all clinical features (real and shadow). Shadow features were then sorted according to their Z score, and the maximum score was stored in memory as a threshold. The algorithm marked each non-shadow feature with a Z score above this threshold. Finally, Boruta findings indicated the clinical features that had Z scores that were significantly lower than the shadow features with maximum Z scores. These features were considered unimportant and were removed from the data set before removing all shadow features and returning a clean data set.

We ran the Boruta algorithm for 300 iterations with a maximum depth set to 5. Extracted features were run on a linear discriminant analysis (LDA), which was only used to visually assess the distinction between anti–Ro 60+ patients, anti–Ro 60– patients, and healthy controls. No classification metrics were computed using LDA.

RESULTS

Specific biologic and clinical features of anti–Ro 60+ patients. We compared the characteristics of the 279 anti–Ro 60– healthy controls and 520 anti–Ro 60+ patients (306 with primary SS, 175 with SLE, and 39 with UCTD) to the 511 anti–Ro 60– patients (61 with primary SS, 333 with SLE, and 117 with UCTD) (Table 1). Regarding the antibody profile, compared to anti–Ro 60– patients, anti–Ro 60+ patients from the 3 diseases had significantly increased levels of ANAs, kappa and lambda free light chains, RF, anti–Ro 52, and anti-SSB antibodies (Figure 1 and Supplementary Table 2). Both anti–Ro 52 autoantibody levels and anti-SSB autoantibody levels were also significantly increased in anti–Ro 60^{high} patients compared to anti–Ro 60^{low} patients. Past and/or present hypergammaglobulinemia was more common in anti–Ro 60+ patients regardless of the disease (Supplementary Figure 1A, http://onlinelibrary.wiley.com/doi/10.1002/art.42243). No difference in terms of the disease activity score (ESSDAI, SLEDAI, PhGA) was observed between anti–Ro 60–patients and anti–Ro 60+ patients (Supplementary Figure 1B). However, in those with primary SS, anti–Ro 60+ patients had lower EULAR Sjögren's Syndrome Patient Reported Index (ESSPRI) (26) scores, and the higher the anti–Ro 60 scale, the lower the ESSPRI score and its components (dryness, fatigue, and pain) (Supplementary Figure 1C, http://onlinelibrary.wiley.com/doi/10.1002/art.42243).

Identification of a specific signature common to anti–Ro 60+ patients in the different omics data sets using machine learning. We used the Boruta algorithm (25) with all data sets to extract features that significantly contributed to the prediction of which patients were anti–Ro 60+ according to the different omics (RNA-Seq, DNA methylation, GWAS, and cytokine expression associated with cell subset distribution). A total of 923 features were selected from RNA-Seq variables, 64 features were selected from DNA methylation variables, 5,749 features were selected from GWAS variables (Supplementary Tables 3–5 respectively, http://onlinelibrary.wiley.com/doi/10.1002/art.42243), and 8 features were selected from the association of cytokine expression levels and cell subset distribution. An LDA for each omics is shown in Figure 2. We considered the combined analysis of patients with primary SS, patients with SLE, and patients with UCTD within the framework of the Boruta results. Features were selected from disease data sets to capture the maximum amount of discriminating information. We then considered the combination
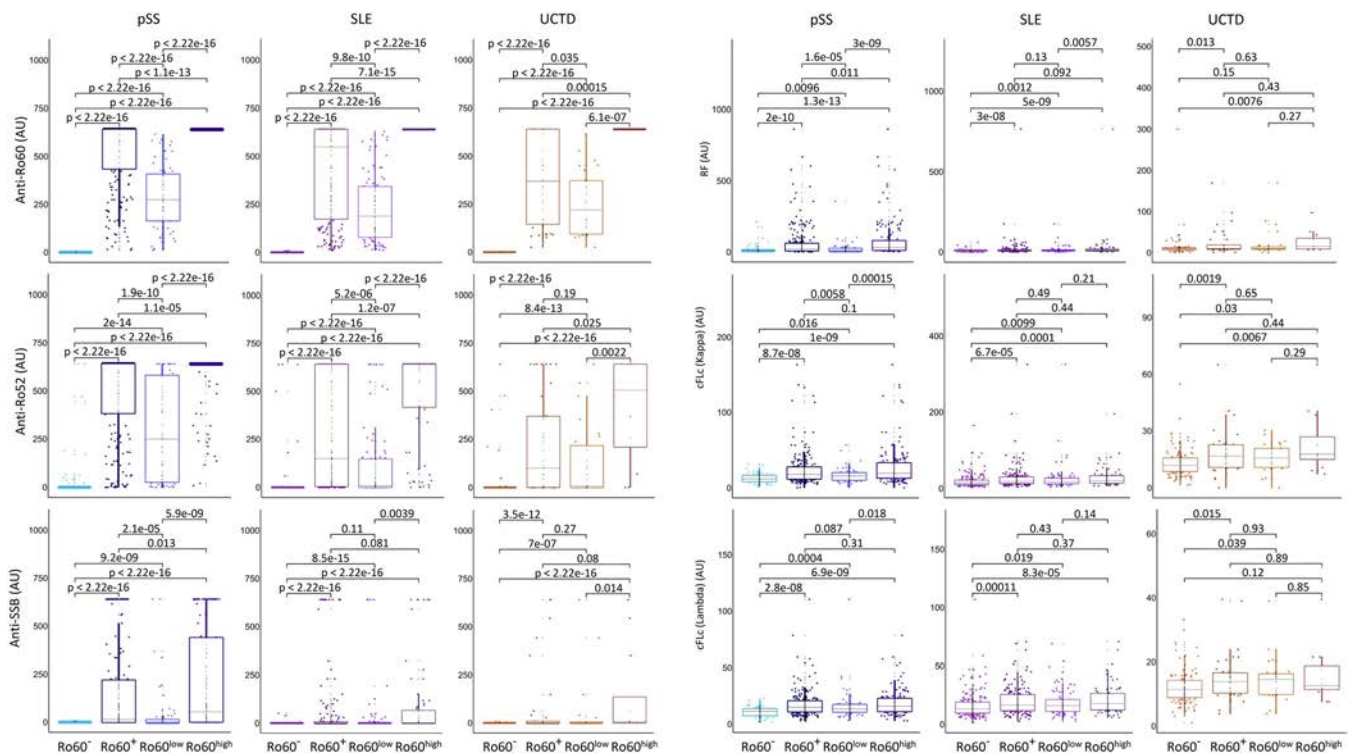
Figure 1. Serologic distributions in patients with primary Sjögren's syndrome (pSS), those with systemic lupus erythematosus (SLE), and those with undifferentiated connective tissue disease (UCTD). The presence of anti–Ro 52, anti–Ro 60, anti-SSB antibodies, rheumatoid factor (RF), and circulating free light chains (cFLc) were measured in serum samples from 520 anti–Ro 60+ patients (306 with primary SS, 175 with SLE, and 39 with UCTD) and 511 anti–Ro 60– patients (61 with primary SS, with 333 SLE, and 117 with UCTD) from the same center using an automated chemiluminescent IDS-iSYS immunoanalyser. Turbidimetry was used for the detection of RF and circulating free light chains (kappa and lambda). Anti–Ro 60+ patients were divided in 2 groups: anti–Ro 60^{low} patients (samples with concentrations between 10 and 640 arbitrary units [AU]/ml) and anti–Ro 60^{high} patients (samples with concentrations >640 AU/ml). Statistical significance was determined by 2-tailed pairwise Wilcoxon's rank sum test. Results are shown as box plots, in which each box represents the interquartile range, lines inside the box represent the median, and lines outside the box represent the 10th and 90th percentiles; symbols represent individual samples. Color figure can be viewed in the online issue, which is available at http://onlinelibrary.wiley.com/doi/10.1002/art.42243/abstract.

of Boruta results for primary SS, SLE, and UCTD to generate the final signature. Of note, selected features for RNA-Seq and GWAS data clearly distinguished between anti–Ro 60+ patients and anti–Ro 60– patients. Remarkably, even if data from healthy controls were not used for feature selection, their integration into the different LDA based on the Boruta algorithm–identified features that discriminate between anti–Ro 60+ patients and anti–Ro 60– patients, resulted in a separation from patients. These results demonstrate that the different features selected using machine learning from the anti–Ro 60+ patients constitute specific signatures when compared to anti–Ro 60– patients and healthy controls.

Characterization and pathway analysis of the transcriptomic signature found in anti–Ro 60+ patients. The 923 transcripts identified using machine learning to discriminate anti–Ro 60+ patients (Figure 2A) were analyzed using Reactome (27). The 25 most relevant pathways are shown in Supplementary Table 6 (http://onlinelibrary.wiley.com/doi/10.1002/art.42243). Anti–Ro 60+ patients were enriched in genes involved in IFN signaling (type

I and II), cytokine signaling, activation of C3 and C5, antiviral response by IFN-stimulated genes, and interleukin-10 (IL-10) signaling.

To further understand the IFN signature, we analyzed IFN-annotated modules previously described as strongly up-regulated in SLE (28,29). The different type I and type II IFN Z scores were increased in anti–Ro 60+ patients regardless of the disease (Figure 3).

Characterization and pathway analysis of the DNA methylation signature found in anti–Ro 60+ patients. The 37 genes associated with the 64 CpGs identified using machine learning to discriminate anti–Ro 60+ patients (Figure 2B) were analyzed using Reactome. Interestingly, the most relevant pathways were the same as those previously found in the transcriptome analysis, such as type I and type II IFN signaling, cytokine signaling in the immune system, and antiviral response by IFN-stimulated genes (Supplementary Table 7, http://onlinelibrary.wiley.com/doi/10.1002/art.42243).

Among these 37 differentially methylated genes, 33 methylated genes were also found using the Boruta algorithm in the RNA-Seq analysis. The interaction networks of these 33 common genes,
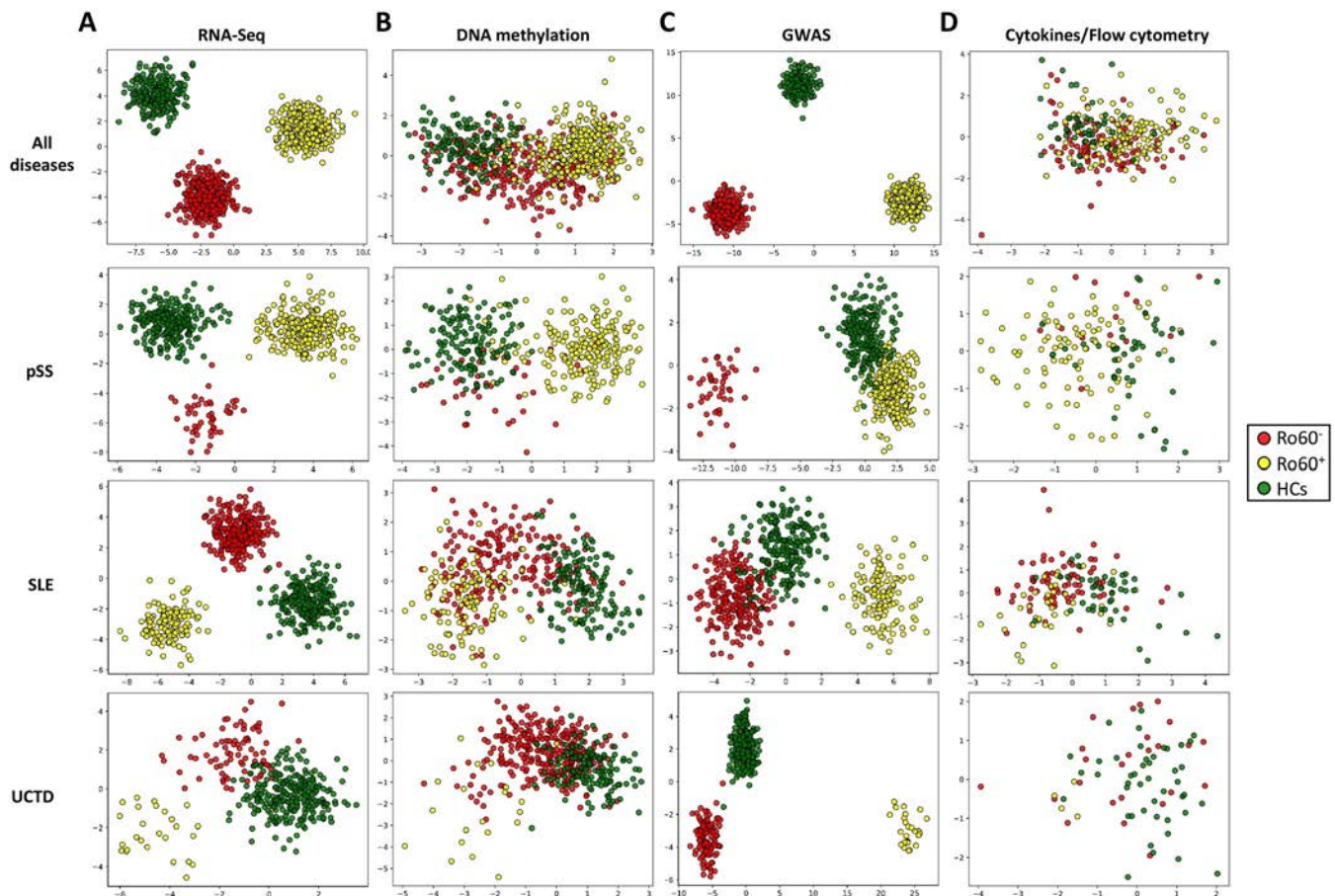
Figure 2. Identification of specific signatures common to anti–Ro 60+ patients in different omics data sets using machine learning. Linear discriminant analysis of features selected with the Boruta algorithm, assessed among all 3 diseases combined or separately among patients with SLE, those with UCTD, and those with primary SS. A total of 923 features were selected from RNA-Seq data (**A**), 64 features were selected from methylation data (**B**), 5,749 features were selected from genome-wide association study (GWAS) data (**C**), and 8 features were selected from flow cytometry distribution and cytokine expression data (**D**). Symbols represent individual samples from anti–Ro 60– patients, anti–Ro 60+ patients, and healthy controls (HCs). See Figure 1 for other definitions.

determined using STRING with a confidence cutoff of 0.4, revealed and confirmed the common IFN signature (Supplementary Figure 2, http://onlinelibrary.wiley.com/doi/10.1002/art.42243) (30). Of note, all transcripts were overexpressed in anti–Ro 60+ patients regardless of the disease, and global hypomethylation of CpGs was observed for all but 1 gene (*ISG15*). For 1 gene (*IFITM1*), up to 8 hypomethylated CpGs were assessed (Supplementary Figure 3, http://onlinelibrary.wiley.com/doi/10.1002/art.42243).

GWAS analysis of anti–Ro 60+ patients. Our machine learning approach identified 5,749 single-nucleotide polymorphisms (SNPs) that were able to discriminate anti–Ro 60+ patents from anti–Ro 60– patients (Figure 2C). Interestingly, 3 of these SNPs were located on genes previously indicated by the algorithm from the previous RNA-Seq and DNA methylation analyses (Figure 4A). The 3 corresponding genes were *ATP10A*, *MX1*, and *PARP14*. Remarkably, the transcript Z score of these 3 genes was clearly higher in anti–Ro 60+ patients compared to

anti–Ro 60– patients but was also higher in anti–Ro 60^{high} compared to anti–Ro 60^{low} patients when all diseases were merged (Figure 4B). The same was true in all the diseases and constituted a clear signature (Figure 4C). Given the strong association between anti–Ro 60 and anti–Ro 52/tripartite motif–containing protein 21 (TRIM21) antibodies, we considered that positivity for anti–Ro 52/TRIM21 may define the signature. We then divided patients with primary SS, patients with SLE, and patients with UCTD into 3 groups (anti–Ro 60–/anti–Ro 52–, anti–Ro 60+/anti–Ro 52–, and anti–Ro 60+/anti–Ro 52+) and assessed the anti–Ro 60 signature identified using the transcript Z score of the 3 genes (*ATP10A*, *MX1*, and *PARP14*). Z scores were higher in anti–Ro 60+/Ro 52– patients compared to anti–Ro 60–/anti–Ro 52– patients with primary SS and those with SLE. In contrast, the Z scores were only higher in anti–Ro 60+/anti–Ro 52+ primary SS patients compared to anti–Ro 60+/anti–Ro 52– patients with primary SS, and no significant difference was observed in SLE patients and UCTD patients (Supplementary Figure 4A, http://onlinelibrary.wiley.com/doi/10.1002/art.42243).
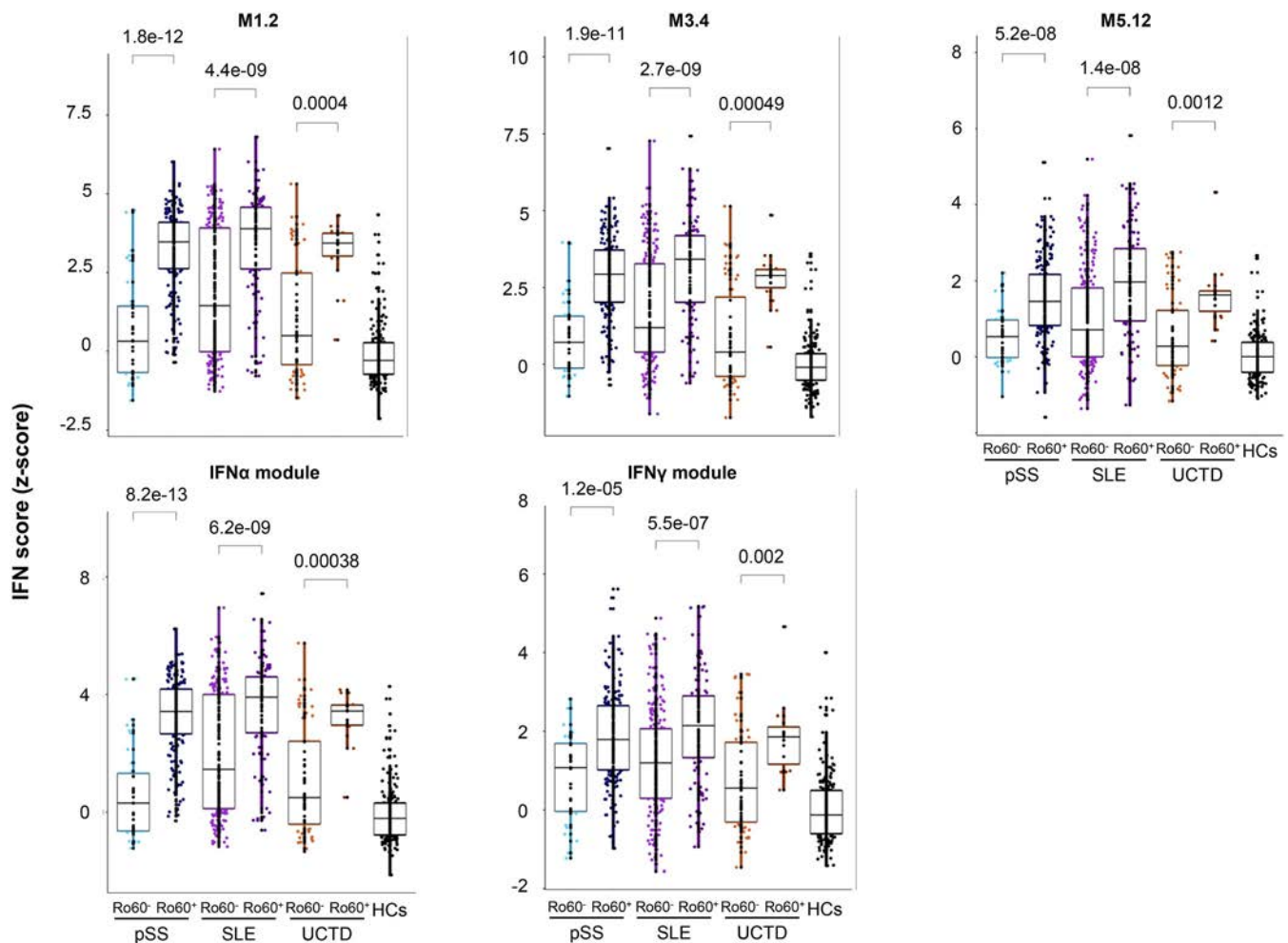
Figure 3. Anti–Ro 60+ patients have a higher interferon (IFN) signature regardless of the disease. IFN Z score analyses were performed with 411 anti–Ro 60+ patients (249 with primary SS, 136 with SLE, and 26 with UCTD) compared to 392 anti–Ro 60– patients (46 with primary SS, 267 with SLE, and 79 with UCTD) and 254 healthy controls. The genes from the M1.2 module (*IFI44*, *IFI44L*, *IFIT1*, and *MX1*) are induced by IFNα, while genes from both M1.2 and M3.4 (*ZBP1*, *IFIH1*, *EIF2AK2*, *PARP9*, and *GBP4*) are up-regulated by IFNβ. The genes from the M5.12 module (*PSMB9*, *NCOA7*, *TAP1*, *ISG20*, and *SP140*) are poorly induced by IFNα and IFNβ alone, while they are up-regulated by IFNγ. Moreover, transcripts belonging to M3.4 and M5.12 are only fully induced by a combination of type I and type II IFNs. Other modules identified genes preferentially induced by IFNα (*IFIT1*, *IFI44*, and *EIF2AK2*) or IFNγ (*IRF1*, *GBP1*, and *SERPING1*). Statistical significance was determined by 2-tailed pairwise Wilcoxon's rank sum test. Results are shown as box plots, in which each box represents the interquartile range, lines inside the box represent the median, and lines outside the box represent the 10th and 90th percentiles; symbols represent individual samples. HCs = healthy controls (see Figure 1 for other definitions). Color figure can be viewed in the online issue, which is available at http://onlinelibrary.wiley.com/doi/10.1002/art.42243/abstract.

We also considered that anti–Ro 60 positivity may just be a marker of B cell reactivity, given that the majority of anti–Ro 60– patients were ENA negative. We then assessed the transcript Z score of the 3 genes (*ATP10A*, *MX1*, and *PARP14*) in 5 groups of patients regardless of disease: patients without any autoantibodies, anti–Ro 60–/anti–Ro 52+ patients negative for any of the autoantibodies analyzed (anti-RNP, anti-Sm, anti-SSB, anti–Scl-70, anti-CCP, anti-dsDNA, antimyeloperoxidase, anti–proteinase 3, anti–CENP-B), anti–Ro 60–/anti–Ro 52+ patients who were positive for any other autoantibodies, anti–Ro 60–/anti–Ro 52– patients who were positive for any of the autoantibodies, and anti–Ro 60+ patients. Z scores were clearly higher in anti–Ro 60+ patients compared to all the other groups (Supplementary Figure 4B,

http://onlinelibrary.wiley.com/doi/10.1002/art.42243). All these data confirm that the determined signature is specific to anti–Ro 60+ patients and is not just a marker of B cell activation or due to the presence of any other autoantibody.

Characterization of the flow cytometry signature and cytokine expression in anti–Ro 60+ patients. Machine learning was used to identify 6 parameters among flow cytometry data and 2 parameters among cytokine expression data (assessed using Luminex-based quantitative assay) to discriminate anti–Ro 60+ patients from anti–Ro 60– patients (Figure 2D). The robustness of the 6 flow cytometry features was poor and was only associated with 1 disease (Supplementary Figure 5,
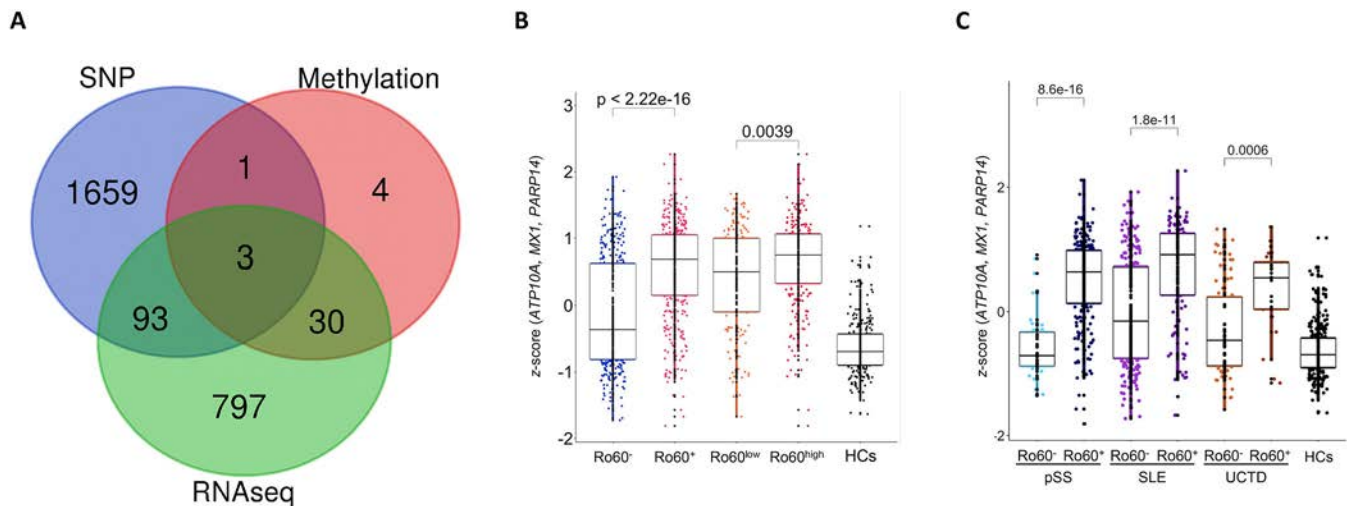
Figure 4. Three genes common to RNA-Seq data, DNA methylation data, and GWAS findings used to characterize anti–Ro 60+ patients. **A**, Venn diagram showing the number of overlapping genes according to the different omics data analyses conducted using machine learning (RNA-Seq, DNA methylation, and single-nucleotide polymorphisms [SNPs]) to discriminate anti–Ro 60+ patients from anti–Ro 60– patients. **B**, *ATP10/MX1/PARP14* Z score analyses in 803 patients and 254 healthy controls (HCs) according to anti–Ro 60 expression. **C**, *ATP10/MX1/PARP14* Z score analyses in 295 patients with primary SS, 403 patients with SLE, and 105 patients with UCTD and 254 healthy controls. Statistical significance was determined by 2-tailed pairwise Wilcoxon's rank sum test. Results are shown as box plots, in which each box represents the interquartile range, lines inside the box represent the median, and lines outside the box represent the 10th and 90th percentiles; symbols represent individual samples. See Figure 1 for other definitions. Color figure can be viewed in the online issue, which is available at http://onlinelibrary.wiley.com/doi/10.1002/art.42243/abstract.

http://onlinelibrary.wiley.com/doi/10.1002/art.42243). Interestingly however, cytokine expression in serum samples showed an increase of IFNγ-induced protein (CXCL10/IFNγ-inducible 10-kd protein) and down-regulation of IL-1 R2, the decoy receptor for cytokines belonging to the IL-1 family, in anti–Ro 60+ patients regardless of disease (Supplementary Figure 5).

Established common signature between anti–Ro 60+ patients with primary SS, those with SLE, or those with UCTD and patients with RA, those with SSc, or those with MCTD expressing anti–Ro 60 antibodies and showing stable antibody expression over time. To confirm the robustness of the identified signature, we observed whether this signature was also present in an independent cohort of 106 newly diagnosed patients with primary SS, those with SLE, or those with UCTD from the inception cohort of the PRECISESADS study, which provided an additional validation data set to test the generalization of our signature in patients whose samples were not used for the feature selection process. At inclusion (first time point), our study included 46 anti–Ro 60+ patients and 60 anti–Ro 60– patients. Again, using the 923 transcripts of the RNA-Seq signature, the LDA findings showed a clear separation between anti–Ro 60+ and anti–Ro 60– patients regardless of the disease (Supplementary Figure 6A). Furthermore, the Z scores for the 33 genes identified using the Boruta algorithm that were common to RNA-Seq and DNA methylation data were significantly increased in anti–Ro 60+ patients (Supplementary Figure 6B). This was also true with the Z scores for

the 3 genes (*ATP10A*, *MX1*, and *PARP14*) previously selected using the algorithm from the RNA-Seq, GWAS, and DNA methylation analyses (Supplementary Figure 6C).

Finally, the signature's robustness was also assessed in 724 patients with other autoimmune diseases, such as MCTD, RA, and SSc, all from the PRECISESADS cross-sectional cohort. A clear separation between anti–Ro 60+ patients (n = 40) and anti–Ro 60– patients (n = 684) using the representation space generated by the LDA is shown in Figure 5A. In all diseases except MCTD, anti–Ro 60+ patients had significantly increased Z scores for the 33 common genes (Figure 5B) and for the 3 genes constituting the signature (Figure 5C). We can therefore conclude that anti–Ro 60+ patients have a specific signature regardless of disease.

Additionally, we assessed the transcript Z scores of the 3 genes (*ATP10A*, *MX1*, and *PARP14*) in the inception cohort restricted to 86 patients (primary SS, SLE, UCTD, RA, SSc, and MCTD) who were followed up and had samples collected at 3 time points (recruitment, at 6 and/or 14 months). At the 6- and 14-month time points, patients could receive any standard of care therapy prescribed by their physician (Supplementary Table 8, http://onlinelibrary.wiley.com/doi/10.1002/art.42243). Anti–Ro 60+ patients remained positive and anti–Ro 60– patients remained negative over time (data not shown). We confirmed that the Z score remained stable in anti–Ro 60+ patients and anti–Ro 60– patients over time (Figure 5D). Overall, the signature identified for anti–Ro 60+ patients does not depend on treatment and is stable over time.
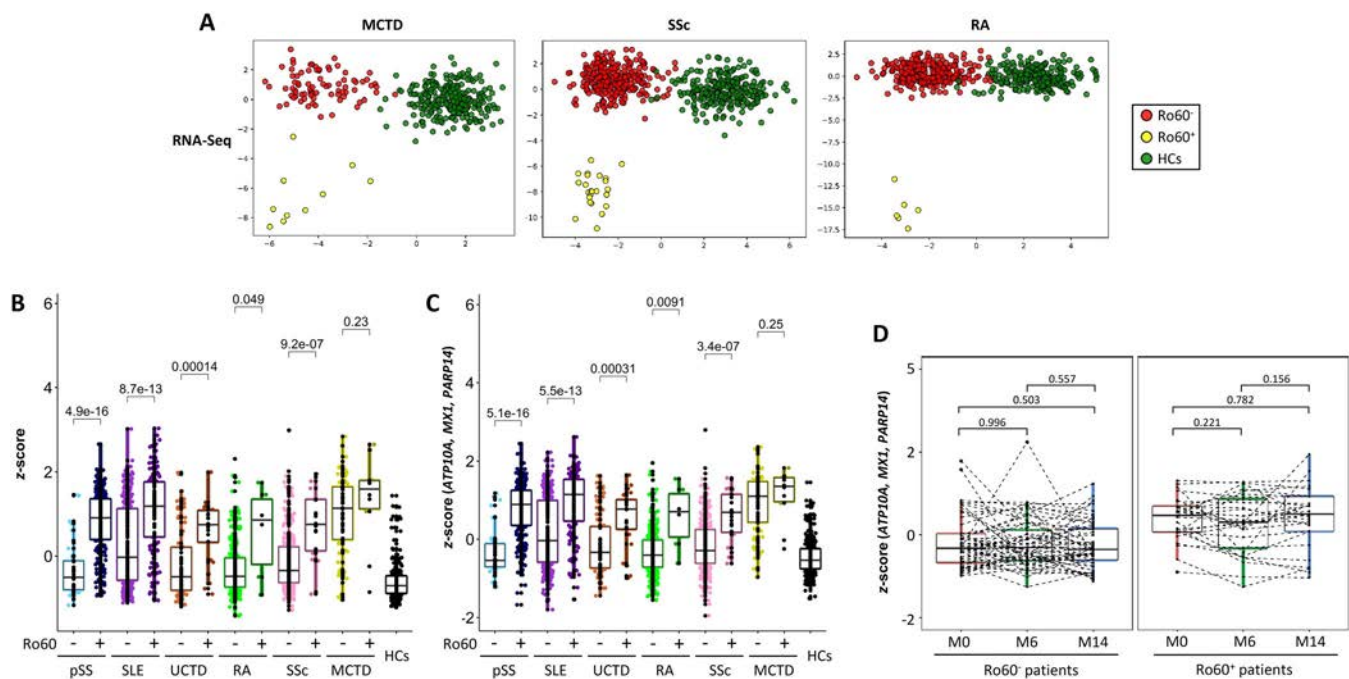
Figure 5. Confirmation of the established signature of anti–Ro 60+ patients common to patients with rheumatoid arthritis (RA), those with systemic sclerosis (SSc), or those with mixed connective tissue disease (MCTD) expressing anti–Ro 60 antibodies. **A**, Linear discriminant analysis of 923 features selected from RNA-Seq data (obtained using the Boruta algorithm in patients with SLE, UCTD, or primary SS), to discriminate anti–Ro 60+ patients from anti–Ro 60– patients with mixed connective tissue disease (MCTD), those with systemic sclerosis (SSc), and those with rheumatoid arthritis (RA). **B**, Z score analyses of the 33 genes, identified using the Boruta algorithm and common to RNA-Seq and methylome data, in 295 patients with primary SS, 403 patients with SLE, 105 patients with UCTD, 307 patients with RA, 327 patients with SSc, and 90 patients with MCTD, and 254 healthy controls (HCs). **C**, *ATP10/MX1/PARP14* Z score analyses in 295 patients with primary SS, 403 patients with SLE, 105 patients with UCTD, 307 patients with RA, 327 patients with SSc, and 90 patients with MCTD and 254 healthy controls. Statistical significance was determined by 2-tailed pairwise Wilcoxon's rank sum test. **D**, *ATP10/MX1/PARP14* Z score analyses in 86 patients from the inception cohort who were followed up and had samples collected at the time of recruitment (M0) and at month 6 (M6) and/or month 14 (M14). Patients were grouped as anti–Ro 60+ (n = 29) and anti–Ro 60– (n = 57) regardless of the disease (primary SS, SLE, UCTD, RA, SSc, or MCTD). Statistical significance was determined by pairwise *t*-test. Results are shown as box plots, in which each box represents the interquartile range, lines inside the box represent the median, and lines outside the box represent the 10th and 90th percentiles; symbols represent individual samples. Color figure can be viewed in the online issue, which is available at http://onlinelibrary.wiley.com/doi/10.1002/art.42243/abstract.

DISCUSSION

Our study demonstrates that anti–Ro 60+ patients have a specific signature regardless of disease. Anti–Ro 60+ patients compared to anti–Ro 60– patients presented with the same clinical and biologic characteristics as those previously described in the literature, such as hypergammaglobulinemia (12,13) and an association with other autoantibodies (anti–Ro 52, anti-SSB, and RF) (14). Anti–Ro 60 positivity was reported to be higher in the low symptom burden subgroups of patients with primary SS (31) in accordance with our observation that anti–Ro 60+ patients had a lower ESSPRI score.

Our study has some limitations. First, it could be argued that this was a cross-sectional study and it is assumed that single samples (cells and sera) were collected at an arbitrary time point during the disease course of different autoimmune diseases. However, in our inception cohort with a 14-month follow-up period, we demonstrated that the identified signature in anti–Ro 60+ patients remained stable over time and was not influenced by treatment. Second, virtually all subjects were Caucasian, and although common variants were expected to be old in evolution and shared across ethnicities, some risk loci show considerable ethnic differences in frequency and/or effect size.

The novelty of our study was our use of machine learning to identify a robust signature specific to anti–Ro 60+ patients through dimensionality reduction approaches, using high-throughput multi-omics data. Assessment of the signature's robustness occurred in 3 steps. First, we used discriminant features extracted from the different omics data sets to perform LDA. The new data representation spaces generated using the selected features through this analysis allowed for sufficient separation of anti–Ro 60+ patients and anti–Ro 60– patients in each of the 3 diseases studied (SLE, primary SS, and UCTD). Second, we considered the overlap of the selected features in RNA-Seq data and DNA methylation data and the overlap of the selected features in RNA-Seq data, DNA

methylation data, and GWAS data, narrowing down the original selection to 2 signatures composed of 33 genes and 3 genes, respectively. Both Z scores, generated by either the 33 genes or the 3 genes, were significantly different between anti–Ro 60+ patients and anti–Ro 60– patients in SLE, primary SS, and UCTD. Third, because we used a machine learning approach to identify the features, we assessed the possibility of overfitting by testing the validity of these signatures in patients whose samples were not used in the training process of the algorithm. Generalizability of the signature was evaluated by determining RNA-Seq features from another cohort of patients with primary SS, patients with SLE, and patients with UCTD and from RA patients, SSc patients, and MCTD patients. LDA findings consistently showed a clear distinction between anti–Ro 60+ patients and anti–Ro 60– patients.

Again, Z scores were significantly different between anti–Ro 60+ patients and anti–Ro 60– patients with RA and those with SSc but not for those with MCTD. Consequently, the discriminating properties of the representation space obtained through the computation of LDA, the statistical tests of distributions, and the generalizability to other diseases constituted strong indicators of the signature's robustness.

Reactome pathway analysis of the 33 differentially expressed and methylated genes showed a link between anti–Ro 60 antibodies and IFN signature, cytokine secretions, and IFN regulatory factor 7, which were associated with Toll-like receptor (TLR) signaling. The notable association between anti–Ro 60 autoantibodies and inflammation in autoimmune diseases led to the hypothesis that the RNA-binding properties of Ro 60 produce aberrant TLR signaling (32). Alu retroelements activate TLR-7 and TLR-8 as oligoribonucleotides and associate with Ro 60 in cell lines (33); consequently, inflammatory and IFN signatures associated with anti–Ro 60 autoantibodies may be due to the RNA-binding properties of Ro 60.

Remarkably, the transcript Z scores of 3 genes (ATP10A, MX1, and PARP14) were clearly higher in anti–Ro 60+ patients compared to anti–Ro 60– patients in all the diseases and constituted a clear signature. The first gene, ATP10A, encoded 1 of the 5 P4 ATPase that requires interaction with transmembrane protein 30A to exit from the endoplasmic reticulum to the plasma membrane. ATP10A was recently linked to autoimmunity, as one study demonstrated that methylation qualitative trait loci regulated the methylation of the ATP10A gene in blood samples from patients with primary SS (34). Since this enzyme mainly transports 2 aminophospholipids: phosphatidylserine and phosphatidylethanolamine, which may be the target of minor autoantibodies in antiphospholipid syndrome (APS) (35), it is reasonable to speculate that there is a link between the presence of antiphospholipid antibodies and the increase in ATP10A transcript. We re-ran the analysis excluding patients positive for the major autoantibodies found in APS (i.e., anti-β_2GPI and IgG and IgM aCLs) to exclude potential patients with secondary APS, and the signature that was identified persisted ($P = 4.2 \times 10^{-10}$) (data not shown).

Moreover, to our knowledge, no association with APS has been described in the literature to date. Thus, the signature carried by ATP10A appears to be specific to anti–Ro 60+ patients. Another GWAS study on cytokine responses found that genetic variants of ATP10A were associated with IFNα production (36). The second gene, PARP14, encoded for a member of poly(ADP-ribose) polymerase (PARP) family proteins which contain macrodomain binding proteins influencing many biologic processes (37). PARP-14 suppressed proinflammatory IFN/STAT1 signaling and activated the antiinflammatory IL-4/STAT6 pathway in primary human macrophages (38). PARP-14 also enhanced histone activation to promote transcription of type I IFN genes such as IFNB1 after lipopolysaccharide stimulation in RAW264.7 cells (39). Interestingly, PARP14 was identified as 1 of the 5 genes that can distinguish patients with primary SS from controls (40). The third gene, MX1, encoded the Mx dynamic, MX dynamin-like GTPase 1 or MxA, which participates in the cellular antiviral response by antagonizing the replication processes of several different RNA or DNA viruses. MX1 gene expression is induced by IFN via JAK1A/Tyk-2 followed by the activation of the STAT1/STAT2 pathway (41). Furthermore, MX1 protein levels were recently reported as a surrogate for the type I IFN gene scores in SLE (42). Consequently, these 3 overexpressed, hypomethylated, and mutated genes in anti–Ro 60+ patients were significantly associated with the IFN signature regardless of the autoimmune disease.

To control the IFN signature in anti–Ro 60+ patients with autoimmune diseases, a key challenge would be to break the continual turnover of Ro 60–specific clones that seems to drive lifelong Ro 60 humoral autoimmunity (43). This may entail a dual approach targeting both Ro 60–associated RNAs (including Alu transcripts and Y RNAs) and Ro 60–specific autoantibody clonotypes as suggested by Reed and Gordon (32).

AUTHOR CONTRIBUTIONS

All authors were involved in drafting the article or revising it critically for important intellectual content, and all authors approved the final version to be published. Dr. Pers had full access to all of the data in the study and takes responsibility for the integrity of the data and the accuracy of the data analysis.
Study conception and design. Pers.
Acquisition of data. Bettacchioli, Jamin, Alarcón-Riquelme.
Analysis and interpretation of data. Foulquier, Le Dantec.

REFERENCES

1. Aggarwal A. Role of autoantibody testing. Best Pract Res Clin Rheumatol 2014;28:907–20.

2. Radin M, Rubini E, Cecchi I, Foddai SG, Barinotti A, Rossi D, et al. Disease evolution in a long-term follow-up of 104 undifferentiated connective tissue disease patients. Clin Exp Rheumatol 2022;40:575–80.

3. Robbins A, Hentzien M, Toquet S, Didier K, Servettaz A, Pham BN, et al. Diagnostic utility of separate anti-Ro60 and anti-Ro52/TRIM21 antibody detection in autoimmune diseases. Front Immunol 2019; 10:444.

4. Schulte-Pelkum J, Fritzler M, Mahler M. Latest update on the Ro/SS-A autoantibody system. Autoimmun Rev 2009;8:632–7.

5. Strandberg L, Ambrosi A, Espinosa A, Ottosson L, Eloranta ML, Zhou W, et al. Interferon-α induces up-regulation and nuclear translocation of the Ro52 autoantigen as detected by a panel of novel Ro52-specific monoclonal antibodies. J Clin Immunol 2008;28: 220–31.

6. Rhodes DA, Ihrke G, Reinicke AT, Malcherek G, Towey M, Isenberg DA, et al. The 52 000 MW Ro/SS-A autoantigen in Sjögren's syndrome/systemic lupus erythematosus (Ro52) is an interferon-γ inducible tripartite motif protein associated with membrane proximal structures. Immunology 2002;106:246–56.

7. Yoshimi R, Chang TH, Wang H, Atsumi T, Morse HC, Ozato K. Gene disruption study reveals a nonredundant role for TRIM21/Ro52 in NF-κB-dependent cytokine expression in fibroblasts. J Immunol 2009;182:7527–38.

8. Lerner MR, Boyle JA, Hardin JA, Steitz JA. Two novel classes of small ribonucleoproteins detected by antibodies associated with lupus erythematosus. Science 1981;211:400–2.

9. Belisova A, Semrad K, Mayer O, Kocian G, Waigmann E, Schroeder R, et al. RNA chaperone activity of protein components of human Ro RNPs. RNA 2005;11:1084–94.

10. Kirou KA, Lee C, George S, Louca K, Peterson MG, Crow MK. Activation of the interferon-α pathway identifies a subgroup of systemic lupus erythematosus patients with distinct serologic features and active disease. Arthritis Rheum 2005;52:1491–503.

11. Armağan B, Robinson SA, Bazoberry A, Perin J, Grader-Beck T, Akpek EK, et al. Antibodies to both Ro52 and Ro60 may identify Sjögren's syndrome patients best suited for clinical trials of disease-modifying therapies. Arthritis Care Res (Hoboken) doi: 10.1002/acr.24597/abstract 2021. E-pub ahead of print.

12. Brito-Zerón P, Acar-Denizli N, Ng WF, Zeher M, Rasmussen A, Mandl T, et al. How immunological profile drives clinical phenotype of primary Sjögren's syndrome at diagnosis: analysis of 10,500 patients (Sjögren Big Data Project). Clin Exp Rheumatol 2018;36 Suppl: 102–12.

13. Thorlacius GE, Hultin-Rosenberg L, Sandling JK, Bianchi M, Imgenberg-Kreuz J, Pucholt P, et al. Genetic and clinical basis for two distinct subtypes of primary Sjögren's syndrome. Rheumatology (Oxford) 2021;60:837–48.

14. Zampeli E, Mavrommati M, Moutsopoulos HM, Skopouli FN. Anti-Ro52 and/or anti-Ro60 immune reactivity: autoantibody and disease associations. Clin Exp Rheumatol 2020;38 Suppl:134–41.

15. Barturen G, Babaei S, Català-Moll F, Martínez-Bueno M, Makowska Z, Martorell-Marugán J, et al. Integrative analysis reveals a molecular stratification of systemic autoimmune diseases. Arthritis Rheumatol 2021;73:1073–85.

16. Aletaha D, Neogi T, Silman AJ, Funovits J, Felson DT, Bingham CO III, et al. 2010 Rheumatoid arthritis classification criteria: an American College of Rheumatology/European League Against Rheumatism collaborative initiative. Arthritis Rheum 2010;62:2569–81.

17. Hochberg MC, for the Diagnostic and Therapeutic Criteria Committee of the American College of Rheumatology. Updating the American College of Rheumatology revised criteria for the classification of systemic lupus erythematosus [letter]. Arthritis Rheum 1997;40:1725.

18. Van den Hoogen F, Khanna D, Fransen J, Johnson SR, Baron M, Tyndall A, et al. 2013 classification criteria for systemic sclerosis: an American College of Rheumatology/European League Against Rheumatism collaborative initiative. Arthritis Rheum 2013;65:2737–47.

19. Vitali C, Bombardieri S, Jonsson R, Moutsopoulos HM, Alexander EL, Carsons SE, et al. Classification criteria for Sjögren's syndrome: a revised version of the European criteria proposed by the American-European Consensus Group. Ann Rheum Dis 2002;61: 554–8.

20. Alarcón-Segovia D, Cardiel MH. Comparison between 3 diagnostic criteria for mixed connective tissue disease. Study of 593 patients. J Rheumatol 1989;16:328–34.

21. LeRoy EC, Medsger TA. Criteria for the classification of early systemic sclerosis. J Rheumatol 2001;28:1573–6.

22. Sack U, Conrad K, Csernok E, Frank I, Hiepe F, Krieger T, et al. Autoantibody detection using indirect immunofluorescence on HEp-2 cells. Ann N Y Acad Sci 2009;1173:166–73.

23. Bombardier C, Gladman DD, Urowitz MB, Caron D, Chang DH, and the Committee on Prognosis Studies in SLE. Derivation of the SLEDAI: a disease activity index for lupus patients. Arthritis Rheum 1992; 35:630–40.

24. Seror R, Ravaud P, Bowman SJ, Baron G, Tzioufas A, Theander E, et al, on behalf of the EULAR Sjögren's Task Force. EULAR Sjögren's Syndrome Disease Activity Index: development of a consensus systemic disease activity index for primary Sjögren's syndrome. Ann Rheum Dis 2010;69:1103–9.

25. Kursa MB, Rudnicki WR. Feature selection with the Boruta package. J Stat Softw 2010;36:1–13.

26. Seror R, Ravaud P, Mariette X, Bootsma H, Theander E, Hansen A, et al, on behalf of the EULAR Sjögren's Task Force. EULAR Sjögren's Syndrome Patient Reported Index (ESSPRI): development of a consensus patient index for primary Sjögren's syndrome. Ann Rheum Dis 2011;70:968–72.

27. Fabregat A, Jupe S, Matthews L, Sidiropoulos K, Gillespie M, Garapati P, et al. The reactome pathway knowledgebase. Nucleic Acids Res 2018;46:D649–55.

28. Kirou KA, Lee C, George S, Louca K, Papagiannis IG, Peterson MG, et al. Coordinate overexpression of interferon-α–induced genes in systemic lupus erythematosus. Arthritis Rheum 2004;50:3958–67.

29. Chiche L, Jourde-Chiche N, Whalen E, Presnell S, Gersuk V, Dang K, et al. Modular transcriptional repertoire analyses of adults with systemic lupus erythematosus reveal distinct type I and type II interferon signatures. Arthritis Rheumatol 2014;66:1583–95.

30. Franceschini A, Szklarczyk D, Frankild S, Kuhn M, Simonovic M, Roth A, et al. STRING v9.1: protein-protein interaction networks, with increased coverage and integration. Nucleic Acids Res 2013;41: D808–15.

31. Tarn JR, Howard-Tripp N, Lendrem DW, Mariette X, Saraux A, Devauchelle-Pensec V, et al. Symptom-based stratification of patients with primary Sjögren's syndrome: multi-dimensional characterisation of international observational cohorts and reanalyses of randomised clinical trials. Lancet Rheumatol 2019;1:e85–94.

32. Reed JH, Gordon TP. Autoimmunity: Ro60-associated RNA takes its toll on disease pathogenesis. Nat Rev Rheumatol 2016;12:136–8.

33. Hung T, Pratt GA, Sundararaman B, Townsend MJ, Chaivorapol C, Bhangale T, et al. The Ro60 autoantigen binds endogenous retroelements and regulates inflammatory gene expression. Science 2015; 350:455–9.

34. Teruel M, Barturen G, Martínez-Bueno M, Castellini-Pérez O, Barroso-Gil M, Povedano E, et al. Integrative epigenomics in Sjögren's syndrome reveals novel pathways and a strong interaction

between the HLA, autoantibodies and the interferon signature. Sci Rep 2021;11:23292.

35. Alessandri C, Conti F, Pendolino M, Mancini R, Valesini G. New auto-antigens in the antiphospholipid syndrome. Autoimmun Rev 2011;10: 609–16.

36. Kennedy RB, Ovsyannikova IG, Pankratz VS, Haralambieva IH, Vierkant RA, Jacobson RM, et al. Genome-wide genetic associations with IFNγ response to smallpox vaccine. Hum Genet 2012;131:1433–51.

37. Fehr AR, Singh SA, Kerr CM, Mukai S, Higashi H, Aikawa M. The impact of PARPs and ADP-ribosylation on inflammation and host-pathogen interactions. Genes Dev. 2020;34:341–59.

38. Iwata H, Goettsch C, Sharma A, Ricchiuto P, Goh WW, Halu A, et al. PARP9 and PARP14 cross-regulate macrophage activation via STAT1 ADP-ribosylation. Nat Commun 2016;7:12849.

39. Caprara G, Prosperini E, Piccolo V, Sigismondo G, Melacarne A, Cuomo A, et al. PARP14 controls the nuclear accumulation of a sub-set of type I IFN-inducible proteins. J Immunol 2018;200:2439–54.

40. Yao Q, Song Z, Wang B, Qin Q, Zhang JA. Identifying key genes and functionally enriched pathways in Sjögren's Syndrome by weighted gene co-expression network analysis. Front Genet 2019;10:1142.

41. Haller O, Staeheli P, Kochs G. Protective role of interferon-induced Mx GTPases against influenza viruses [review]. Rev Sci Tech 2009;28: 219–31.

42. Chasset F, Ribi C, Trendelenburg M, Huynh-Do U, Roux-Lombard P, Courvoisier DS, et al. Identification of highly active systemic lupus ery-thematosus by combined type I interferon and neutrophil gene scores vs classical serologic markers. Rheumatology (Oxford) 2020;59: 3468–78.

43. Lindop R, Arentz G, Bastian I, Whyte AF, Thurgood LA, Chataway TK, et al. Long-term Ro60 humoral autoimmunity in primary Sjögren's syndrome is maintained by rapid clonal turnover. Clin Immunol 2013;148:27–34.

APPENDIX A: MEMBERS OF THE PRECISESADS CLINICAL CONSORTIUM AND FLOW CYTOMETRY CONSORTIUM

Members of the PRECISESADS Clinical consortium are as follows: Lorenzo Beretta, Barbara Vigone (Fondazione IRCCS Ca'Granda Ospe-dale Maggiore Policlinico di Milano, Milan, Italy); Jacques-Olivier Pers, Alain Saraux, Valérie Devauchelle-Pensec, Divi Cornec, Sandrine Jousse-Joulin (B Lymphocytes, Autoimmunity and Immunotherapies laboratory, UMR 1227, Université de Brest, INSERM and Centre Hospitalier Regional Universitaire Brest, Brest, France); Bernard Lauwerys, Julie Ducreux, Anne-Lise Maudoux (Université catholique de Louvain, Brussels, Belgium); Carlos Vasconcelos, Ana Tavares, Raquel Faria, Mariana Brandão, Ana Campar, António Marinho, Fátima Farinha, Isabel Almeida (Centro Hospitalar do Porto, Porto, Portugal); Esmeralda Neves (Centro Hospitalar e Universitário do Porto, Porto, Portugal); Miguel Ángel González-Gay, Ricardo Blanco Alonso, Alfonso Corrales Martínez (Hospital Universitario Marqués de Valdecilla and Universidad de Canta-bria, Santander, Spain); Ricard Cervera, Ignasi Rodríguez-Pintó, Gerard Espinosa (Hospital Clinic, Institut d'Investigacions Biomèdiques August Pi i Sunyer, Barcelona, Spain); Rik Lories, Ellen De Langhe (UZ Leuven, Leuven, Belgium); Nicolas Hunzelmann, Doreen Belz (Klinikum der Univer-sitaet zu Koeln, Cologne, Germany); Torsten Witte, Niklas Baerlecken (Medical University Hannover, Hannover, Germany); Georg Stummvoll, Michael Zauner, Michaela Lehner (Medical University Vienna, Vienna, Austria); Eduardo Collantes, Rafaela Ortega-Castro, Maria Angeles Aguirre-Zamorano, Alejandro Escudero-Contreras, Carmen Castro-Villegas, Yolanda Jiménez Gómez (Reina Sofia Hospital and University of Cordoba, Cordoba, Spain); Norberto Ortego, María Concepción Fernández Roldán (Hospital Universitario Clínico San Cecilio, Spain); Enrique Raya, Inmaculada Jiménez Moleón, Hospital Universitario Vir-gen a de las Nieves, Granada Spain); Enrique de Ramon, Isabel Díaz Quintero (Hospital Regional Universitario de Málaga, Málaga, Spain); Pier Luigi Meroni, Maria Gerosa, Tommaso Schioppo, Carolina Artusi (Università degli studi di Milano, Milan, Italy); Carlo Chizzolini, Aleksandra Dufour, Donatienne Wynar (University Hospital and School of Medicine, Geneva, Switzerland); Laszló Kovács, Attila Balog, Magdolna Deák, Márta Bocskai, Sonja Dulic, Gabriella Kádár (University of Szeged, Szeged, Hungary); Falk Hiepe, Velia Gerl, Silvia Thiel (Charite Universitätsmedizin Berlin, Berlin, Germany); Manuel Rodriguez Maresca, Antonio López-Berrio, Rocío Aguilar-Quesada, Héctor Navarro-Linares (Andalusian Public Health System Biobank, Granada, Spain); Yiannis Ioannou, Chris Chamberlain, Jacqueline Marovac (UCB Pharma PRECISESADS Project Office, Slough, UK); Marta Alarcón Riquelme, Tania Gomes Anjos (Center for Genomics and Oncological Research, Granada, Spain).

Members of the PRECISESADS Flow Cytometry Consortium are as follows: Christophe Jamin, Bénédicte Rouvière, Jacques-Olivier Pers (B Lymphocytes, Autoimmunity and Immunotherapies laboratory, UMR 1227, Université de Brest, INSERM, and Centre Hospitalier Regional Uni-versitaire Brest, Brest, France); Lucas Le Lann, Quentin Simon (B Lymphocytes, Autoimmunity and Immunotherapies laboratory, UMR 1227, Université de Brest, and INSERM, Brest, France); Concepción Marañón, Nieves Varela, Brian Muchmore (Center for Genomics and Oncological Research, Granada, Spain); Aleksandra Dufour, Montserrat Alvarez, Carlo Chizzolini (University Hospital and School of Medicine, Geneva, Switzerland); Jonathan Cremer, Ellen De Langhe (UZ Leuven, Leuven, Belgium); Nuria Barbarroja (Reina Sofia Hospital and University of Cordoba, Cordoba, Spain); Chary Lopez-Pedrera (Centro Hospitalar do Porto, Porto, Portugal); Velia Gerl, Laleh Khodadadi, Qingyu Cheng (Charite Universitätsmedizin Berlin, Berlin, Germany); Anne Buttgereit, Zuzanna Makowska (Bayer Pharma Aktiengesellschaft, Berlin, Germany); Aurélie De Groof, Julie Ducreux (Université catholique de Louvain, Brus-sels, Belgium); Elena Trombetta (Fondazione IRCCS Ca'Granda Ospedale Maggiore Policlinico di Milano, Milan, Italy); Tianlu Li, Damiana Alvarez-Errico (Bellvitge Biomedical Research Institute, Barcelona, Spain); Torsten Witte, Katja Kniesch (Medical University Hannover, Hannover, Germany); Nancy Azevedo, Esmeralda Neves (Centro Hospitalar and Universitário do Porto, Porto, Portugal); Maria Hernandez-Fuentes (UCB Pharma PRECISESADS Project Office, Slough, UK); Pierre-Emmanuel Jouve (AltraBio SAS, Lyon, France).

LETTERS

Pregnancy outcomes in women with psoriatic arthritis: comment on the article by Remaeus et al

To the Editor:

We read with considerable interest the findings presented in the study by Dr. Remaeus et al, who reported on the outcomes of antirheumatic treatment in pregnancy (1). Remaeus et al concluded that women with psoriatic arthritis (PsA) receiving antirheumatic treatment had a higher risk of their pregnancy resulting in preterm birth and caesarean delivery compared with women without PsA. The authors attributed this increased risk to antirheumatic treatment, especially treatment with biologic disease-modifying antirheumatic drugs (bDMARDs) during pregnancy.

The authors made some assumptions that we would like to challenge. We were particularly surprised that bDMARD therapy was used as a proxy for disease activity. Previous studies have demonstrated that disease burden improved with the use of bDMARDs. Ursin et al reported significantly lower disease activity in pregnant women with PsA who took tumor necrosis factor inhibitors (2). We also reported similar findings in a cohort of PsA patients (3). Furthermore, most of the published evidence in relation to pregnancy outcomes in patients with inflammatory arthritis point to better outcomes when the disease is well controlled at the time of conception and throughout pregnancy.

The authors suggested that the risk of spontaneous preterm birth could be up to 4-fold higher in pregnant women who took bDMARDs than in pregnant women not exposed to bDMARDs. However, this finding may reflect a selection bias in the study design that the authors have not recognized, as the underlying mechanisms, risk factors, and etiology of preterm birth are not completely understood; therefore, many confounders may have contributed to their results. It is unclear what the psoriasis status is in their study population and whether bDMARDs were prescribed for active psoriasis rather than PsA. Findings from a previous study suggested that psoriasis is associated with adverse maternal and fetal outcomes (4). Given the lack of data on disease activity and on other patient factors, such as metabolic syndrome, that are significantly associated with psoriasis, it is unclear to what extent preterm birth could be directly attributed to the effects of bDMARD treatment. Finally, the factors involved in rates of caesarean section that Remaeus et al described are even more varied and uncontrolled; thus, these data are virtually unusable.

In conclusion, we agree that disease activity and severity are important factors that should be optimally controlled in patients with PsA before they consider pregnancy. We disagree with the assumption that treatment with bDMARDs in PsA patients during pregnancy is a good surrogate for the clinical metrics reported in the study from Remaeus et al. The conclusion that bDMARDs are associated with adverse outcomes in PsA pregnancies is counterintuitive and potentially a dangerous message to this population.

Áine Gorman, MB, BCh, BAO
ainegorman1@gmail.com
Sonia Sundanum, MB, BCh, BAO
St. Vincent's University Hospital
Louise Moore, MSc
Our Ladies Hospice
Celine O'Brien, MSc
Fionnula McAuliffe, MD
The National Maternity Hospital
Douglas J. Veale, MD
St. Vincent's University Hospital
Dublin, Ireland

1. Remaeus K, Johansson K, Granath F, Stephansson O, Hellgren K. Pregnancy outcomes in women with psoriatic arthritis in relation to presence and timing of antirheumatic treatment. Arthritis Rheumatol 2022;74:486–95.
2. Ursin K, Lydersen S, Skomsvoll JF, Wallenius M. Psoriatic arthritis disease activity during and after pregnancy: a prospective multicenter study. Arthritis Care Res (Hoboken) 2019;71:1092–100.
3. Murray K, Moore L, McAuliffe F, Veale DJ. Reproductive health outcomes in women with psoriatic arthritis. Ann Rheum Dis 2019;78:850–2.
4. Bröms G, Haerskjold A, Granath F, Kieler H, Pedersen L, Berglind IA. Effect of maternal psoriasis on pregnancy and birth outcomes: a population-based cohort study from Denmark and Sweden. Acta Derm Venerol 2018;98:728–34.

Reply

To the Editor:

We thank Dr. Gorman et al for their interest in our study. We fully agree that it is counterintuitive that treatment with bDMARDs is associated with adverse pregnancy outcomes since low disease activity, irrespective of treatment, is associated with better outcomes in studies of, for example, rheumatoid arthritis (1). The use and timing of antirheumatic treatment as a measure of

disease activity and/or severity during pregnancy are not perfect measures; instead, information on a validated measure of disease activity would be ideal. Nevertheless, given the heterogeneity of the PsA diagnosis and the spectra of treatment strategies, we believe that assessing the impact of treatment exposure in detail provides important insights that augment the understanding of risks associated with a diagnosis of PsA.

In our study, we found that adverse outcomes were more common among pregnant women with PsA than among pregnant women without PsA and that the highest risks were seen among those who were treated with antirheumatic medications, especially bDMARDs, during pregnancy. Although the use of bDMARDs during pregnancy has lately become more widespread, in our cohort of PsA pregnancies, 11% of women took bDMARDs during pregnancy, indirectly suggesting that women continuing this treatment most probably had severe disease.

We do not attribute the increased risk of preterm birth and caesarean delivery to bDMARD treatment as such; however, we described an increased risk of adverse pregnancy outcomes in PsA patients who took bDMARDs compared with pregnancy outcomes in those without PsA. Our interpretation, as also expressed in our study, is that the increased risk of adverse outcomes in pregnancies with antirheumatic treatment is probably attributed to disease severity rather than an effect of the treatment itself.

We agree that the underlying mechanisms of spontaneous preterm birth in women with PsA are not fully understood. We also endorse that metabolic factors might be of importance, as explored in a previous study from our group (2). In our current study, we were able to take known risk factors for spontaneous preterm birth into account. Very few of the 921 pregnant women with PsA in our cohort had hypertension or diabetes before pregnancy, although more women with PsA than without PsA were categorized as obese. However, in distribution of women with PsA in terms of obesity, the lowest proportion of obesity was among those who were taking bDMARDs, indicating that metabolic syndrome was not the main explanation for the increased risk of preterm birth in this cohort.

In conclusion, our findings support that the risk of adverse pregnancy outcomes varies with presence, timing, and also type of antirheumatic treatment in women with PsA. The outcomes should not be interpreted as caused by the medications. It is of great importance to further elucidate the impact of maternal disease activity on pregnancy outcomes in PsA.

Katarina Remaeus, PhD [ORCID]
katarina.remaeus@ki.se
Kari Johansson, PhD
Fredrik Granath, PhD
Karolinska Institutet
Olof Stephansson, PhD
Karin Hellgren, PhD
Karolinska Institutet
  and Karolinska University Hospital
Stockholm, Sweden

1. Hellgren K, Secher AE, Glintborg B, Rom AL, Gudbjornsson B, Michelsen B, et al. Pregnancy outcomes in relation to disease activity and anti-rheumatic treatment strategies in women with rheumatoid arthritis. Rheumatology (Oxford) 2021. doi: https://doi.org/10.1093/rheumatology/keab894. E-pub ahead of print.
2. Remaeus K, Stephansson O, Johansson K, Granath F, Hellgren K. Maternal and infant pregnancy outcomes in women with psoriatic arthritis: a Swedish nationwide cohort study. BJOG 2019;126: 1213–22.

Revisiting the disease specificity and nomenclature of ficolin-1–positive monocyte-derived dendritic cells in diffuse cutaneous systemic sclerosis: comment on the article by Xue et al

To the Editor:

We read with great interest the article by Dr. Xue and colleagues (1) on the discovery of the expansion of ficolin-1–positive (FCN-1+) monocyte-derived dendritic cells (mo-DCs), which were reported to be correlated with the severity of skin disease in patients with diffuse cutaneous systemic sclerosis (dcSSc). Advances in single-cell technologies have enabled investigators to use high-resolution gene profiling and gene identification to understand cellular heterogeneity in tissue. In their study, Xue et al used single-cell RNA-sequencing analysis to identify a gene expression signature of the disease-specific FCN-1+ myeloid cell type in dcSSc skin. They illustrated that FCN-1+ cells belong to a single cluster that was best characterized by gene expression of *FCN1, EREG, S100A8*, and *THBS1*. In addition, the frequency of perivascular FCN-1+ myeloid cells was higher in dcSSc patients who had elevated modified Rodnan skin thickness (MRSS) scores than in patients with low MRSS scores or in skin from healthy donors. Thus, the authors proposed that FCN-1+ cells represent a dcSSc-specific myeloid population. Noteworthy, this cell population was mostly expanded in selected dcSSc patients (i.e., 2 of 12 patients), displaying a proinflammatory gene profile (2).

Interestingly, the gene expression profile of FCN-1+ cells was reminiscent of the inflammatory monocyte–like (Inf-Mo–like) cells reported in the inflamed colon of patients with Crohn's disease (CD) (3). Frequency of Inf-Mo–like cells was positively correlated with disease severity, as measured in CD patients by the simple endoscopic score for CD. Gene set enrichment analysis (4) further indicated that cluster E, which included Inf-Mo–like cells reported in inflamed CD colon (see Figure 6 in Chapuy et al [3]) was enriched in genes expressed by cluster 5 that comprise FCN-1+ cells in the skin of dcSSc patients. The normalized enrichment score was 1.650 with a false discovery rate q value of 0.0275, and the core genes enriched included *EREG, S100A9, THBS1 FCN1, TIMP1, IL1RN, SAMSN1, C5RA1, OLR1, CD300E, APOBEC3A, FPR1, SERPINA1*, and *GK*. Thus, we note the

shared gene expression profile and potential similar function between skin FCN-1+ cells in dcSSc patients and colonic Inf-Mo–like cells in CD patients. In Xue et al, bulk RNA-sequencing analysis of dcSSc skin highlighted the expression of *TREM1*, which was also in the list of discriminating genes identified in cluster E in the colon of CD patients ($\log_2$ fold change >1.2, area under the curve >0.75) (3). Interestingly, colonic Inf-Mo–like cells promoted autologous Th17/Th1 responses in an interleukin-1b–dependent manner; in cluster 5, which was enriched in FCN-1+ myeloid cells, *IL1B* displayed differential gene expression in dcSSc skin.

The precise nature and classification of FCN-1+ myeloid cells in skin and Inf-Mo–like cells in the colon remain unclear. A consensus appears to have been reached regarding their monocyte origin. Whether these 2 CD163-negative cell types that share a molecular signature can be classified as mo-DCs, Inf-Mo–like cells, inflammatory macrophages, or inflammatory DCs warrants further clarification (5). A trajectory analysis of skin FCN-1+ cells by Xue et al suggested that these cells are closely related to mo-DCs, whereas Inf-Mo–like cells in inflamed colon did not fulfill criteria to be classified as DCs. Ginhoux and colleagues argue in favor of developing detailed transcriptomic cell atlases that would integrate cellular heterogeneity and status of tissue in health and disease (6). This strategy might enable a common nomenclature to be proposed for mononuclear phagocytes. Furthermore, cells displaying a shared molecular signature with FCN-1+ cells were observed in skin blisters after acute inflammation (7), suggesting that these cells are not dcSSc-specific but characterize the cellular infiltrate in inflamed skin.

We suggest that meta-analyses across different tissue (e.g., joints, heart, lungs), particularly in chronic skin inflammatory disorders that include psoriasis and atopic dermatitis, are needed before a pathogenic role or disease specificity can be attributed to a particular monocyte-derived cell type.

Author disclosures are available at https://onlinelibrary.wiley.com/action/downloadSupplement?doi=10.1002%2Fart.42247&file=art42247-sup-0001-Disclosureform.pdf.

Marika Sarfati, MD, PhD
m.sarfati@umontreal.ca
*Centre de Recherche du Centre Hospitalier
  de l'Université de Montréal*
Laurence Chapuy, MD, PhD
Research Institute-McGill University Health Center
Heena Mehta, PhD
*Centre de Recherche du Centre Hospitalier
  de l'Université de Montréal
Montréal, Quebec, Canada*

1. Xue D, Tabib T, Morse C, Yang Y, Domsic RT, Khanna D, et al. Expansion of Fcγ receptor IIIa–positive macrophages, ficolin 1–positive monocyte-derived dendritic cells, and plasmacytoid dendritic cells associated with severe skin disease in systemic sclerosis. Arthritis Rheumatol 2022;74:329–41.

2. Assassi S, Swindell WR, Wu M, Tan FD, Khanna D, Furst DE, et al. Dissecting the heterogeneity of skin gene expression patterns in systemic sclerosis. Arthritis Rheumatol 2015;67:3016–26.

3. Chapuy L, Bsat M, Sarkizova S, Rubio M, Therrien A, Wassef E, et al. Two distinct colonic CD14+ subsets characterized by single-cell RNA profiling in Crohn's disease. Mucosal Immunol 2019;12:703–19.

4. Subramanian A, Tamayo P, Mootha VK, Mukherjee S, Ebert BL, Gillette MA, et al. Gene set enrichment analysis: a knowledge-based approach for interpreting genome-wide expression profiles. Proc Natl Acad Sci U S A 2005;102:15545–50.

5. Chapuy L, Sarfati M. Single-cell protein and RNA expression analysis of mononuclear phagocytes in intestinal mucosa and mesenteric lymph nodes of ulcerative colitis and Crohn's disease patients. Cells 2020; 9:813.

6. Ginhoux F, Guilliams M, Merad M. Expanding dendritic cell nomenclature in the single-cell era. Nat Rev Immunol 2022;22:67–8.

7. Chen YL, Gomes T, Hardman CS, Vieira Braga FA, Gutowska-Owsiak D, Salimi M, et al. Re-evaluation of human BDCA-2+ DC during acute sterile skin inflammation. J Exp Med 2020;217: jem.20190811.

Reply

To the Editor:

We thank Dr. Sarfati and colleagues for their thoughtful comments on our recent description of myeloid cell phenotypes in dcSSc skin. Our previous biomarker articles, in which we reported strong correlations between macrophage gene expression and presentation of systemic sclerosis clinical disease in skin and lung (1,2), led us to better understand the specific myeloid population(s) potentially driving disease. In our single-cell RNA-sequencing study discussed by Sarfati et al, we highlighted not only the increase in certain myeloid populations in dcSSc skin but also reemphasized the tremendous heterogeneity of intensity of inflammatory infiltrates in dcSSc skin. Our description of the myeloid populations as "specific" to skin in patients with SSc was in contrast to myeloid populations in normal skin (3). We did not mean to suggest that FCN-1+ cells are seen only in dcSSc skin. We appreciate the analyses of Sarfati et al, in which they showed a very similar population of cells expanded in intestinal tissue from patients with CD that might also be expanded in other skin diseases.

Regarding the naming of these cells, we agree that these names are provisional. Although our trajectory analysis suggested that FCN-1+ cells are most closely related to mo-DCs, such relationships are better defined experimentally. Single-cell RNA sequencing has created significant challenges with regard to naming the plethora of new cell types being discovered; in addition, these discoveries raise questions about how to define and distinguish discrete cell phenotypes and states. The current bioinformatics algorithms alone are not convincing methods for defining progenitor relationships. Experimental solutions, such as the study of the effects of genetic deficiencies (4) or lineage tracing by mitochondrial mutations (5,6), can provide more direct insights (7). However, the plasticity of myeloid cells and the nimble alterations in their phenotype in response
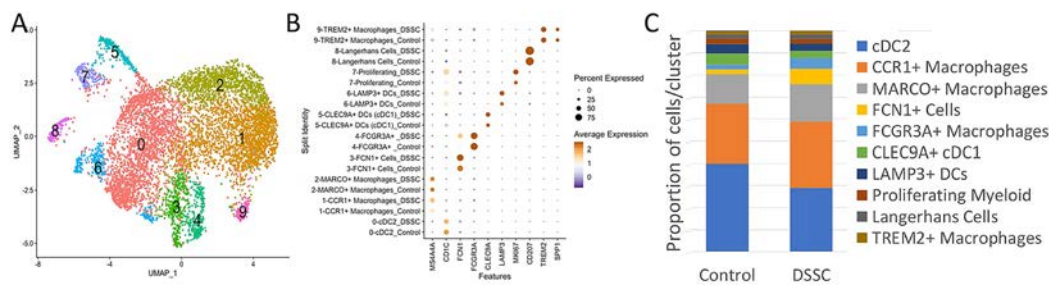
Figure 1. Myeloid cells from Gur et al (8) show the same expanded myeloid cell populations in SSc skin as described in Xue et al. **A**, Uniform Manifold Approximation and Projection (UMAP) clustering analysis of myeloid cells from 45 patients with diffuse cutaneous systemic sclerosis (dcSSc; or DSSC) and 39 healthy control subjects. Myeloid population cluster identities are numbered as indicated in **B**. **B**, Gene marker expression in each designated cell subset from the skin of patients with dcSSc from Gur et al (8) similar to our recent description of myeloid cells in SSc skin. **C**, Expansion of ficolin-1–positive (FCN1+) cells and Fcγ receptor IIIa–positive (FCGR3A+) macrophages compared with other cell subsets in the skin of patients with dcSSc. TREM-2 = triggering receptor expressed on myeloid cells 2; LAMP-3 = lysosome-associated membrane protein 3; DCs = dendritic cells; CLEC9A = C-type lectin domain containing 9A; cDC1 = type 1 conventional DCs; MARCO = macrophage receptor with collagenous structure.

to various soluble mediators and environmental stimuli may make lineage tracing of these cells particularly complex.

A recent study by Gur et al (8), in which an expanded cell population, referred to as nonclassical, CD16+ monocytes, was described but not characterized in detail, confirmed our key observations of altered myeloid populations in dcSSc skin. Upon reanalysis of the myeloid cells in the data set from Gur et al using Uniform Manifold Approximation and Projection (UMAP) clustering, we found cell populations similar to cell populations described in our article (Figures 1A–C). In particular, we observed that myeloid populations expressing markers FCN1 and Fcγ receptor IIIa (FCGR3A) were expanded. Similar to that reported in our previous article, FCN-1+ cells expressed only low levels of FCGR3A (CD16), with UMAP clustering immediately adjacent to the cDC2 dendritic cell population.

In contrast to our data, in which expanded FCGR3A-positive cells clustered adjacent to macrophages, the FCGR3A-expressing macrophages in the Gur et al data set cluster were adjacent to the cells expressing FCN1. Unlike the FCGR3A+ cells that we previously described, we observed that the FCGR3A+ cells in the study by Gur et al did not express MS4A4A, a macrophage marker that we have previously found to be associated with disease severity in the skin of patients with dcSSc (2).

We agree that the presence of increased numbers of FCN-1+ mo-DCs, or for that matter FCGR3A-expressing macrophages or plasmacytoid DCs, in dcSSc skin does not prove a pathogenic role. Inflammatory cells represent a relatively small proportion of cells in dcSSc skin, making their extraction for functional studies challenging. Although the processes driving vascular injury and fibrosis in systemic sclerosis remain uncertain, aberrant myeloid cells remain leading candidates.

Robert Lafyatis, MD [iD]
lafyatis@pitt.edu
Tracy Tabib, MS
University of Pittsburgh School of Medicine
Pittsburgh, PA

1. Christmann RB, Sampaio-Barros P, Stifano G, Borges CL, de Carvalho CR, Kairalla R, et al. Association of Interferon- and transforming growth factor β-regulated genes and macrophage activation with systemic sclerosis-related progressive lung fibrosis. Arthritis Rheumatol 2014;66:714–25.

2. Rice LM, Ziemek J, Stratton EA, McLaughlin SR, Padilla CM, Mathes AL, et al. A longitudinal biomarker for the extent of skin disease in patients with diffuse cutaneous systemic sclerosis. Arthritis Rheumatol 2015;67:3004–15.

3. Xue D, Tabib T, Morse C, Lafyatis R. Transcriptome landscape of myeloid cells in human skin reveals diversity, rare populations and putative DC progenitors. J Dermatol Sci 2020;97:41–9.

4. Cytlak U, Resteu A, Pagan S, Green K, Milne P, Maisuria S, et al. Differential IRF8 transcription factor requirement defines two pathways of dendritic cell development in humans. Immunity 2020;53:353–70.e8.

5. Ludwig LS, Lareau CA, Ulirsch JC, Christian E, Muus C, Li LH, et al. Lineage tracing in humans enabled by mitochondrial mutations and single-cell genomics. Cell 2019;176:1325–39.e22.

6. Xu J, Nuno K, Litzenburger UM, Qi Y, Corces MR, Majeti R, et al. Single-cell lineage tracing by endogenous mutations enriched in transposase accessible mitochondrial DNA. Elife 2019;8:e45105.

7. Abyzov A, Vaccarino FM. Cell lineage tracing and cellular diversity in humans. Annu Rev Genomics Hum Genet 2020;21:101–16.

8. Gur C, Wang SY, Sheban F, Zada M, Li B, Kharouf F, et al. LGR5 expressing skin fibroblasts define a major cellular hub perturbed in scleroderma. Cell 2022;185:1373–88.e20.

Concerns regarding the title and abstract conclusion in a recent genome-wide association study on Behçet's disease: comment on the article by Su et al

To the Editor:

In a recent genome-wide association study (GWAS) among Chinese patients with Behçet's disease (BD), Dr. Su and colleagues underline in the title and in the conclusion of their abstract that "this GWAS study identified a novel set of genetic variants

that are associated with susceptibility to uveitis in BD" (1). However, we found no data in their study that suggested what they had observed was specifically linked to BD-related uveitis since no patients with BD without uveitis were studied. Although this absence of data on BD patients without uveitis is brought up as a study limitation at the end of the Discussion, we simply want to highlight this important concern.

Author disclosures are available at https://onlinelibrary.wiley.com/action/downloadSupplement?doi=10.1002%2Fart.42268&file=art42268-sup-0001-Disclosureform.pdf.

Muhammed Abdulkerim Sahin, MD 🔵
md.abdulkerim@gmail.com
Sinem Nihal Esatoglu, MD
Division of Rheumatology
Department of Internal Medicine
Cerrahpasa Medical School
Istanbul University-Cerrahpasa
Istanbul, Turkey

1. Su G, Zhong Z, Zhou Q, Du L, Ye Z, Li F, et al. Identification of novel risk loci for Behçet's disease–related uveitis in a Chinese population in a genome-wide association study. Arthritis Rheumatol 2022;74: 671–81.

Reply

To the Editor:

Drs. Sahin and Esatoglu raised a concern regarding the title and the abstract conclusion of our recently published study, in which we described the presentation of a novel set of genetic variants that are associated with susceptibility to uveitis in BD. The authors' concern was that these findings could not be stated as linked to BD-related uveitis since no BD patients without uveitis were studied.

We are grateful for Sahin et al's interest in our study and for raising this concern. We agree that, with no control group of BD patients without uveitis, the expression "Behçet's disease–related uveitis" is not precise. The reason that we used this expression is to bring attention to the fact that all of the BD patients included in our study had uveitis and that the new loci identified may not be generalized to all BD types. We thank Sahin et al for highlighting this issue.

Guannan Su, PhD
Peizeng Yang, MD, PhD 🔵
peizengycmu@126.com
The First Affiliated Hospital of Chongqing Medical University
Chongqing Key Laboratory of Ophthalmology
and Chongqing Eye Institute
and Chongqing Branch of National Clinical Research Center
for Ocular Diseases
Chongqing, China

A methodologic problem and a conceptual issue related to the new 2022 antineutrophil cytoplasmic antibody–related vasculitis criteria sets: comment on criteria sets approved by the American College of Rheumatology Board of Directors and the European Alliance of Associations for Rheumatology Executive Committee

To the Editor:

We would like to raise a concern with the methodology of the 3 new classification criteria sets for antineutrophil cytoplasmic antibody (ANCA)–associated vasculitides, which were approved by the American College of Rheumatology (ACR) Board of Directors and the European Alliance of Associations for Rheumatology (EULAR) Executive Committee (1–3). We further learned that approval of the criteria sets was based on validation of independent data sets. We disagree. At stage 5 of the criteria development methodology, the recruited patients, after a rigorous selection process by vasculitis experts, were randomized into the development and validation sets. Unfortunately, this randomization had in fact ensured that the validation sets were not independent of the development sets. The similar features between the development and validation sets are reflected in the almost identical paired area under the curve results for discriminating between eosinophilic granulomatosis with polyangiitis, granulomatosis with polyangiitis, and microscopic polyangiitis classification criteria, as depicted in Supplementary Materials 12A–C (https://onlinelibrary.wiley.com/doi/abs/10.1002/art.41982) (1).

We propose that there is also an important conceptual issue related to these 3 criteria sets. First, although the use of well-structured and expertly analyzed records of clinical experience is helpful as disease recognition guidelines, we maintain that there are shortcomings to the separation of these guidelines into "classification for research" and "diagnostic criteria" categories (4). Each well-planned observational or interventional human research project requires patient selection criteria tailored to the main hypothesis and outcome measure of that study, instead of attempts to use generic, all-purpose disease classification criteria, which are in vogue. Well-prepared disease recognition guidelines, instead of disease criteria, will surely be helpful in this tailoring. Second, the same disease recognition guidelines will also be extremely useful in diagnosing our patients as long as 2 important caveats are considered: the prevalence of the particular disease in our practice setting and the total transparency with our patients that the art or science of medicine is probabilistic. We suspect this "decriterization" that we propose here might not be well-received by drug licensing authorities, third-party payors, and perhaps the drug industry. However, this should not deter us from reminding and advising these groups of the inherent and all-important probabilistic aspect of our trade.

Hasan Yazici, MD [ID]
hasan@yazici.net
Academic Hospital
Istanbul, Turkey
Yusuf Yazici, MD
NYU Grossman School of Medicine
New York, NY

1. Grayson PC, Ponte C, Suppiah R, Robson JC, Craven A, Judge A, et al. 2022 American College of Rheumatology/European Alliance of Associations for Rheumatology classification criteria for eosinophilic granulomatosis with polyangiitis. Arthritis Rheumatol 2022;74:386–92.

2. Robson JC, Grayson PC, Ponte C, Suppiah R, Craven A, Judge A, et al. 2022 American College of Rheumatology/European Alliance of Associations for Rheumatology classification criteria for granulomatosis with polyangiitis. Arthritis Rheumatol 2022;74:393–9.

3. Suppiah R, Robson JC, Grayson PC, Ponte C, Craven A, Khalid S, et al. 2022 American College of Rheumatology/European Alliance of Associations for Rheumatology classification criteria for microscopic polyangiitis. Arthritis Rheumatol 2022;74:400–6.

4. Yazici H, Yazici Y. Criteria for Behçet's disease with reflections on all disease criteria. J Autoimmun 2014;48-49:104–7.

Reply

To the Editor:

Drs. Yazici and Yazici question a specific aspect of the methodology used to develop and validate the 2022 ACR/EULAR classification criteria for ANCA-associated vasculitides. They state concerns with the fact that patients recruited into the Diagnostic and Classification Criteria in Vasculitis (DCVAS) study were included into either a set of patients used to develop the criteria or an independent set of patients used to validate the criteria. They argue that this methodology constitutes "randomization," resulting in 2 groups that are not truly independent but rather are perfectly balanced in terms of potential confounding differences. We disagree with this argument because it confuses "random sampling" with "random assignment." For the DCVAS project, we went to great efforts to recruit 6,991 study participants from 136 sites from around the world. When deriving the classification criteria, we randomly sampled patients from this diverse and representative study population for inclusion into a development set or a validation set. Not every patient with ANCA-associated vasculitis in the cohort was included in either the development or validation set. Random sampling ensures that the study results are generalizable to the population at large, and the use of completely different sets of patients ensures that the development and validation sets are indeed independent. In contrast to random sampling, random assignment occurs after participants are selected for a study, whereby all study participants are randomly assigned either to receive an intervention or to act as a control.

The alternative to our approach of random sampling within the large DCVAS study cohort would be to validate the criteria in a set of patients not recruited through the DCVAS project. While we welcome independent investigators from around the world to validate the new criteria in other study populations, it is unlikely that another data set would represent as broad a spectrum of patients as the DCVAS study cohort. Rather, it is highly likely that these types of data sets would be prone to selection bias.

We also contend that, although the performance characteristics of the new criteria were similar in the development and validation sets, it does not mean, as suggested by Yazici and Yazici, that the development and validation sets were not independent. Rather, these results emphasize that the criteria are highly valid.

Finally, Yacizi and Yazici expressed concerns that classification criteria are "generic" and "in vogue." We respectfully disagree with both of these points. Classification criteria ensure that a study population is homogeneous for inclusion to research trials. Homogeneity is important to ensure that research studies are more easily comparable. Use of classification criteria in a research study in no way precludes investigators from developing additional study-specific selection criteria, a common practice and application of such criteria. Notably, classification criteria have been used to facilitate research in rheumatology for more than 50 years.

We anticipate that the new 2022 ACR/EULAR classification criteria for ANCA-associated vasculitides will support the conduct of successful research for decades to come.

Peter C. Grayson, MD, MSc [ID]
National Institute of Arthritis and Musculoskeletal
*   and Skin Diseases*
National Institutes of Health
Bethesda, MD
Cristina Ponte, MD, PhD [ID]
Department of Rheumatology
Hospital de Santa Maria
Centro Hospitalar Universitário Lisboa Norte
*   and Rheumatology Research Unit*
*   Instituto de Medicina Molecular*
*   Universidade de Lisboa*
Lisbon, Portugal
Joanna C. Robson, MBBS, PhD [ID]
Centre for Health and Clinical Research
University of the West of England
*   and University Hospitals*
*   and Weston NHS Foundation Trust*
Bristol, UK
Ravi Suppiah, MBChB, MD, FRACP
Te Whatu Ora - Health New Zealand
Auckland, New Zealand
Andrew Judge, PhD
Oxford NIHR Biomedical Research Centre
University of Oxford
Oxford, UK

Andrew Hutchings, MSc
London School of Hygiene and Tropical Medicine
London, UK
Anthea Craven, BSc
Sara Khalid, DPhil
Raashid A. Luqmani, DM
Oxford NIHR Biomedical Research Centre
Nuffield Department of Orthopaedics Rheumatology
  and Musculoskeletal Sciences
University of Oxford
Oxford, UK
Richard A. Watts, MD [iD]
Oxford NIHR Biomedical Research Centre
Nuffield Department of Orthopaedics Rheumatology
  and Musculoskeletal Sciences

University of Oxford
Oxford, UK
  and Norwich Medical School
  University of East Anglia
Norwich, UK
Peter A. Merkel, MD, MPH [iD]
pmerkel@upenn.edu
Division of Rheumatology
Department of Medicine
Division of Epidemiology
Department of Biostatistics, Epidemiology,
  and Informatics
University of Pennsylvania
Philadelphia, PA

GENERAL INFORMATION

TO SUBSCRIBE

Institutions and Non-Members

Email:	wileyonlinelibrary.com	Volumes 74, 2022:	
Phone:	(201) 748-6645	Institutional Print Only:	**Arthritis & Rheumatology and Arthritis Care & Research:**
Write:	Wiley Periodicals LLC		$2,603 in US, Canada, and Mexico
	Attn: Journals Admin Dept UK		$2,603 outside North America
	111 River Street	Institutional Online Only:	$2,495 in US, Canada, Mexico, and outside North America
	Hoboken, NJ 07030	Institutional Print and Online Only:	$2,802 in US, Canada, and Mexico; $2,802 outside North America

For submission instructions, subscription, and all other information visit: wileyonlinelibrary.com.

Arthritis & Rheumatology accepts articles for Open Access publication. Please visit https://authorservices.wiley.com/author-resources/Journal-Authors/open-access/hybrid-open-access.html for further information about OnlineOpen.

Wiley's Corporate Citizenship initiative seeks to address the environmental, social, economic, and ethical challenges faced in our business and which are important to our diverse stakeholder groups. Since launching the initiative, we have focused on sharing our content with those in need, enhancing community philanthropy, reducing our carbon impact, creating global guidelines and best practices for paper use, establishing a vendor code of ethics, and engaging our colleagues and other stakeholders in our efforts.
Follow our progress at www.wiley.com/go/citizenship.

Access to this journal is available free online within institutions in the developing world through the HINARI initiative with the WHO. For information, visit www.healthinternetwork.org.

Disclaimer

The Publisher, the American College of Rheumatology, and Editors cannot be held responsible for errors or any consequences arising from the use of information contained in this journal; the views and opinions expressed do not necessarily reflect those of the Publisher, the American College of Rheumatology and Editors, neither does the publication of advertisements constitute any endorsement by the Publisher, the American College of Rheumatology and Editors of the products advertised.

Members:

American College of Rheumatology/Association of Rheumatology Professionals

For membership rates, journal subscription information, and change of address, please write:

American College of Rheumatology
2200 Lake Boulevard
Atlanta, GA 30319-5312
(404) 633-3777

ADVERTISING SALES AND COMMERCIAL REPRINTS

Sales:	Kathleen Malseed, National Account Manager	**Production:**	Patti McCormack
	E-mail: kmalseed@pminy.com		E-mail: pmccormack@pminy.com
	Phone: (215) 852-9824		Phone: (212) 904-0376
	Pharmaceutical Media, Inc.		Pharmaceutical Media, Inc.
	30 East 33rd Street, New York, NY 10016		30 East 33rd Street, New York, NY 10016